1-1-2011

Examination of UV-Cross-Linkable Di-Block Copolymer Strategy for Functionalized Reaction Surface on Microelectrode Arrays

Libo Hu
Washington University in St. Louis

WASHINGTON UNIVERSITY IN ST. LOUIS

Department of Chemistry

Dissertation Examination Committee:
Kevin D. Moeller, Chair
Kendall J. Blumer
Sophia E. Hayes
James W. Janetka
Joshua A. Maurer
John-Stephen A. Taylor

Examination of UV-Cross-Linkable Di-Block Copolymer Strategy for Functionalized Reaction Surface on Microelectrode Arrays

by

Libo Hu

A dissertation presented to the
Graduate School of Arts and Sciences
of Washington University in
partial fulfillment of the
requirements for the degree
of Doctor of Philosophy

December 2011

St. Louis, Missouri

Abstract

Microarrays are powerful tools for high-throughput screening of small molecule libraries. Our group is using a microelectrode array variant on these efforts that allows us to construct and screen the libraries in a rapid, cost effective fashion. In this approach, the small molecules are attached to polymer-coated microelectrodes, which can be used to detect ligand-receptor interactions as they happen by means of impedance. Impedance experiment work by monitoring the current associated with a redox couple in solution. When a protein binds a ligand on the array, it sterically prevents the redox couple from reaching the electrode surface and thus causes a reduction in the current being measured.

In order to realize the construction of a library and measurement of the electrochemical impedance on the array, the polymer coating applied on the array needs to be stable for long periods of time, stable to washing the array, compatible with the array-based reactions, compatible with electrochemical impedance experiments, and relatively inert with respect to its non-specific binding with receptors. This work makes progress towards this goal by first exploring the Pd(0) chemistry on the array, identifying the incompatibility of palladium chemistry with the agarose coating that was being used on the surface of the arrays, and the designing and synthesizing new polymer coatings for microelectrode arrays.

Three different block copolymers were made to investigate the compatibility of the polymers with the array-based reactions and signaling experiments. All three types of polymers consisted of a PCEMA block for UV-cross-linking reactions to improve the stability of the coating. The prototype polymer PBrSt-b-CEMA used 4-bromostyrene as the second block for functionalization purpose. It was proven to be a very versatile

polymer which was stable, and compatible with all the electrochemical experiments conducted on the array. As a result this coating was extensively utilized in the study of the behavior of signaling experiments on the array. The major drawback of this polymer was its non-specific binding to proteins at higher protein concentrations. In order to fix this problem, a second polymer PCEMA-b-PEGMA with PEG as side chains was made in the hope that PEG would reduce non-specific binding to the surface. Unfortunately the polymer was not stable enough as coating for the array. Finally, a copolymer with boronic acid functionality, PCEMA-b-BoSt was made in order to test the versatility of the boronic acid as a starting material for building other functionalities. The boronic acid derived polymer performs better than the previous coating in terms of array-based reactions. However, it was found to be incompatible with the electrochemical impedance experiments.

Acknowledgements

First I would like to express my sincere gratitude for the help and support from my advisor, Dr. Kevin Moeller. I thank him for giving me the freedom to explore the science I was interested in while at the same time always being there for help when I was in trouble. I do not believe I could walk out of the many frustrations during graduate school without him. He serves as a role model for me both as a scientist and as a family man. The lessons I learned from him extend far beyond what words can describe here.

My committee members, Dr. John-Stephen Taylor and Dr. Josh Maurer, both gave helpful ideas that directed the course of this research. I am thankful for their assistance in our yearly meetings, which made me a better scientist. I appreciate Dr. Sophia Hayes, Dr. Kendall Blumer and Dr. James Janetka for their willingness to bring their perspectives to my work by serving on my defense committee.

I thank all my wonderful group members, previous and current, for making the Moeller lab a pleasant place to work in. I am also thankful to Dr. Karen Wooley and her group members for helping me initiate my project.

I would also like to thank Dr. Karl Maurer from CustomArray for providing the arrays and the techniques, as well as the many helpful discussions during the course of my research.

I thank my parents and my beloved wife for their patience and unconditional support during this time. Their love gave me inspiration and was my driving force. This work would not be possible without them by my side.

Finally, I would like to thank National Science Foundation and Syngenta for their financial support.

Table of Contents

List of Figures

List of Schemes

Abbreviations

2,4-DNP	2,4-Dinitrophenylhydrazine
AFM	atomic force microscopy
AIBN	2,2′-azobis(2-methylpropionitrile)
ATRP	atom transfer radical polymerization
BoSt	4-stryeneboronic acid
BrSt	4-bromostyrene
BSA	bovine serum albumin
CAN	cerium ammonium nitrate
CDI	1,1'-Carbonyldiimidazole
CEA	2-cinnamoyloxyethyl acrylate
CEMA	2-cinnamoyloxyethyl methacrylate
CRP	conventional radical polymerization
CV	cyclic voltammetry /cyclic voltammogram
DMAP	4-dimethylaminopyridine
DMF	N, N’-dimethylformamide
DMSO	dimethyl sulfoxide
DCC	N,N'-dicyclohexyl carbodiimide
DCU	N,N'-dicyclohexyl urea
EDC	N-(3-dimethylaminopropyl)-N-ethyl carbodiimide
ELISA	enzyme-linked immunosorbent assay
ESI-MS	electrospray ionization mass spectrometry
EtOAc	ethyl acetate

EtOH	ethanol
Fc	ferrocene
F-P-T	freeze pump thaw
FT-IR	Fourier transform infrared spectroscopy
GPC	gel permeation chromatography
HEA	2-hydroxyethyl acrylate
HEMA	2-hydroxyethyl methacrylate
HRMS	high resolution mass spectrometry
i	initiator
LC-MS	liquid chromatography mass spectrometry
LRMS	low resolution mass spectrometry
LRP	living radical polymerization
MeCN	acetonitrile
MEK	methyl ethyl ketone
MeOH	methanol
MMA	methyl methacrylate
NHS	N-hydroxysuccinimide
NMP	nitroxide-mediated radical polymerization
NMR	nuclear magnetic resonance spectroscopy
PBA	phenyl boronic acid
pBoSt	pinacol 4-styreneboronic ester
PBoSt	poly(4-styreneboronic acid)
PBrSt	poly(4-bromostyrene)

PBS	phosphate buffer saline
PCEMA	poly(2-cinnamoyloxyethyl methacrylate)
PEG	polyethylene glycol
PEGMA	polyethylene glycol methacrylate
PEO	polyethylene oxide
PHEMA	poly(2-hydroxyethyl methacrylate)
PMDETA	N,N,N',N',N-Pentamethyldiethylenetriamine
PMMA	poly(methyl methacrylate)
Pn	growing polymer chain
PpBoSt	poly(pinacol 4-styreneboronic ester)
PPEGMA	poly(polyethylene glycol methacrylate)
PSt	polystyrene
RAFT	reversible addition-fragmentation chain transfer polymerization
St	styrene
TBAB	tetrabutylammonium bromide
TFA	trifluoroacetic acid
THF	tetrahydrofuran
TMS	trimethylsilyl
TOF-SIMS	time of flight secondary ionization mass spectrometry
UV	ultraviolet
VB_{12}	vitamin B_{12}

Chapter 1

Introduction

1.1 Introduction to addressable libraries and microelectrode arrays

The explosion of interest in combinatorial chemistry in the pharmaceutical industry since the 1990s had brought forth the evolution of molecular libraries on multiple platforms.[1] Among these, microarrays excel as a platform for investigating biological interactions due to their small size, minimal requirements for the amount of biological material needed, and high library density.[2] Addressable microarrays take these advantages even further by correlating the identities of the library members to the spatial arrangement of the array, offering the advantage of evaluating the performance of each library member as a "pure" individual entity.[3]

Since the earliest attempt of combinatorial synthesis, the solid-phase peptide synthesis invented by Bruce Merrifield,[4] the physical size of molecular libraries has been shrinking from vials of polymer beads to the size of a dime or even smaller.[5] The advancement of electronics and micro-contact printing technology has led to high density microarrays. Several different types of microarrays have been developed, such as small molecule microarrays,[6] DNA/RNA microarrays,[7] protein microarrays,[8] glycoarrays,[9] cellular microarrays[10] and even tissue microarrays.[11] These microarrays play active roles in the high-throughput screening of biological assays, the method of choice for current drug discovery efforts and related fields. The arrays are fabricated using different technologies to immobilize the library members onto the array. Taking

DNA microarrays as an example, the array may be fabricated by printing with fine-pointed pins onto glass slides,[12] photolithography using pre-made masks,[13] ink-jet printing[14] or electrochemistry on microelectrode arrays.[15] Detection methods vary accordingly, such as fluorescence microscopy, chemiluminescence labeling, or electrochemical signaling. Among these different methods, CombiMatrix has been taking advantage of microelectrode arrays and electrochemistry to build DNA microarrays, as well as antibody microarrays for diagnostic purpose.[16] Our group has been working to broaden the synthetic chemistry available for use on the CombiMatrix arrays so that the arrays can be used to support addressable libraries of more diverse origins.

While the small size of microelectrode arrays brings the advantage of high library density and low compound loadings, it raises a series of challenges as well. First of all, how do we confine each member of a library to a specific location on the array? Since we are using a microelectrode array and the electrodes themselves provide a handle by each site on the array, it would be natural to think we should use electrochemistry to realize this goal. But how can this be accomplished? Secondly, how do we know the compounds that are supposed to be on certain areas of the array are actually there and have the correct structures? In other words, how do we do quality control on a molecular library built on an array? Third, how reliable is this method? How reproducible are the results from different arrays and how many times can an array be reused? The goal of the research below was aimed at answering these questions.

1.2 Microelectrode array specifications

The microelectrode arrays obtained from CombiMatrix generally fall into one of two types. Arrays with a lower density of electrodes typically have 1,024 electrodes in a 1 cm^2 area. They are abbreviated as 1-K arrays in the discussion that follows (Figure 1.1a). The diameter of the round platinum electrode is 92 μm and the distances between the electrodes (rectangular cell) are 245.3 μm and 337.3 μm respectively (Figure 1.1b). Arrays with a higher density of electrodes have 12,544 electrodes in a 1 cm^2 area. They are abbreviated as 12-K arrays in the discussion that follows ((Figure 1.2a). The diameter of the round platinum electrode is 44 μm and the distance between the electrodes (square cell) is 33 μm (Figure 1.2b).

a) b)

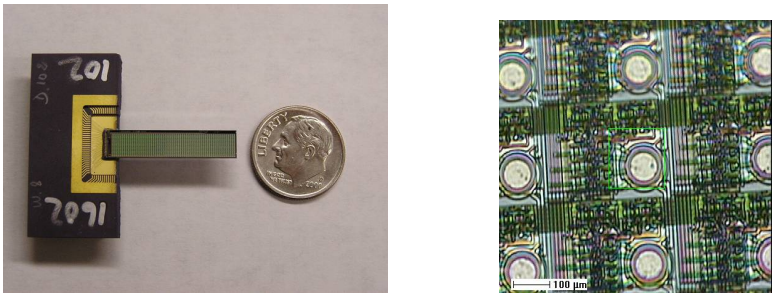

Figure 1.1 a) The 1-K array. b) Blowup image of the electrodes on the 1-K array.

a) b)

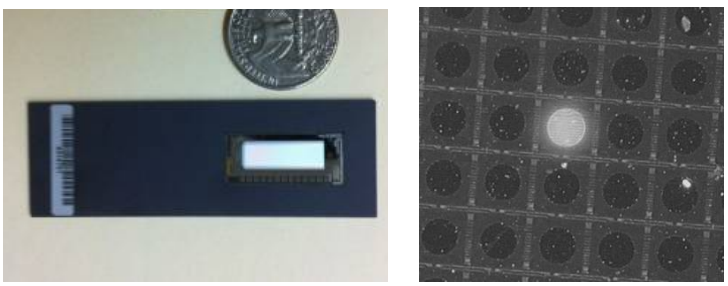

Figure 1.2 a) The 12-K array slide. b) Blowup image of the electrodes on the 12-K array.

The fabrication process of the array was done by layering the circuits and electrodes beneath a passivation layer made of a ceramic corrosion-resist material called silicon nitride (Si_3N_4). The passivation layer above the electrodes was cut with laser to remove the silicon nitride protection so that the electrodes were exposed and the circuits were protected. This processing leaves a well-like structure on the array surface with the electrodes in the well, as demonstrated by an AFM image of the 12-K array (Figure 1.3a). The depth of the well is around 500 nm. Also, the circuit-layering process left groove-like structures on the surface (Figure 1.3b). The grooves measure around 4 μm wide and 200 nm deep on average and were not smoothed out after the fabrication process.

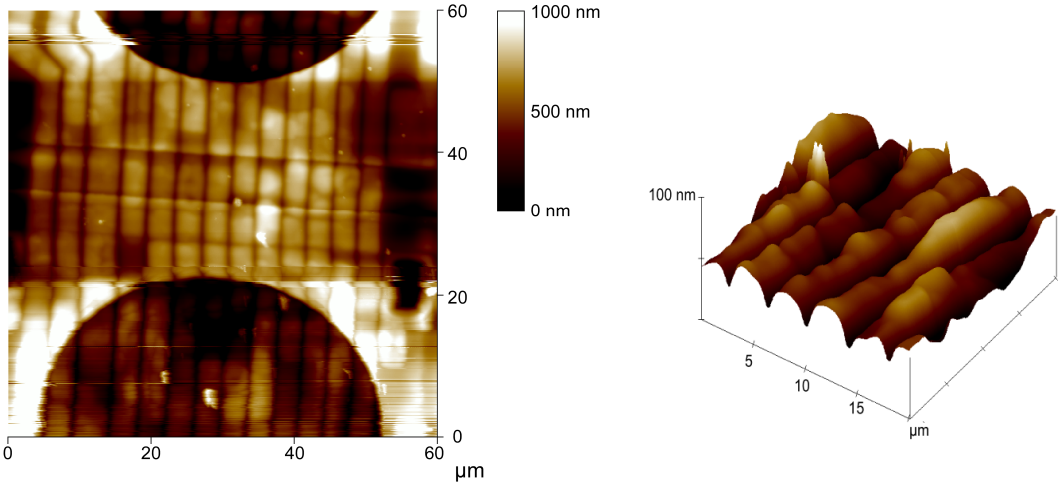

Figure 1.3 a) AFM image of two electrodes and the area in between on 12-K array. b) The groove structure on the array surface.

1.3 Fundamentals of running array-based reactions

To give one an idea of the general procedure for running an array-based reaction, it is best to use an example. For this example, let us look at a Pd(0)-catalyzed Heck reaction[17] run on the array (Scheme 1.1).

Scheme 1.1

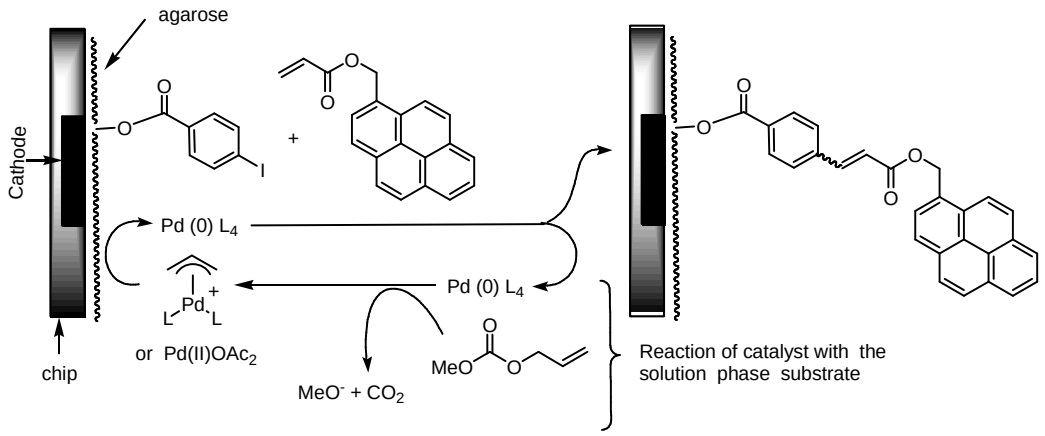

As mentioned in Section 1.2, the arrays are coated with a passivation layer. This layer does not provide the functionality needed to attach organic molecules to the surface of the electrodes. Hence, all reactions run on an array start with the array being coated with a layer that provides the functional groups needed for attaching molecules to the surface. In the case of the Heck reaction illustrated in Scheme 1.1, the array was coated with agarose. The agarose provides free hydroxyl groups as the functionality needed for further modification. Next, a substrate is attached to the coating on the array next to the electrodes. In the case of the Heck reaction, 4-iodobenzoic acid was placed on the array using a base-catalyzed esterification reaction. The base was generated by reducing vitamin-B_{12} at the electrodes in the

array.[18] This reaction was conducted at each electrode in the array. While site-selectivity for the esterification was not needed here, the reaction can be done site-selectively. [19]

Once the substrate for the Heck reaction was placed onto the array, the array was inserted into the Heck reaction solution mixture which contains three main components; the olefin coupling partner, the Pd(II)-precursor to the Pd(0)-catalyst needed for the reaction, and a "confining agent". The role of the solution-phase acrylate coupling partner is self-explanatory. The Pd(II)-reagent was added to the solution because it is catalytically inactive in terms of the Heck reaction. Hence, it does not catalyze the Heck reaction anywhere on the array. The reaction works by using the electrodes in the array as cathodes to reduce the Pd(II) in the solution into Pd(0). The Pd(0) then catalyzes a Heck reaction between the immobilized aryl iodide on the array and the solution-phase olefin. Since the Pd(0) generated was not destroyed after the catalytic cycle, it was free to migrate to undesired areas of the array. Hence, the reaction needs a "confining agent" to be site-selective. Confining agents are solution-phase reagents that destroy the reactive reagent or catalyst being generated at the electrodes. In this case, the Pd(0)-catalyst generated at the electrodes is oxidized back to Pd(II) by the confining agent before it can migrate to remote sites on the array. In the reaction shown, the confining agent is allyl methyl carbonate. Allyl methyl carbonate reacts with any Pd(0) in solution to generate a dormant π-allyl-Pd(II) species. In this way, the reaction was confined to only the electrodes selected for the reduction.

The identification of an appropriate confining agent is one of the most important steps in developing any array-based reaction. The requirements for the confining agent are quite simple. First, it must efficiently destroy the reactive species generated at the microelectrodes. Second, it should not undergo side reactions with either of the surface bound substrate for the reaction, the solution-phase substrate, or the surface coating on the array. As a result of the second requirement, it is easy to imagine that not one confining agent is going to fit all reactions, even if the reactive species generated from the microelectrodes are the same. For example, consider the Pd(0)-catalyzed allylation reaction[20] shown in Scheme 1.2.

Scheme 1.2

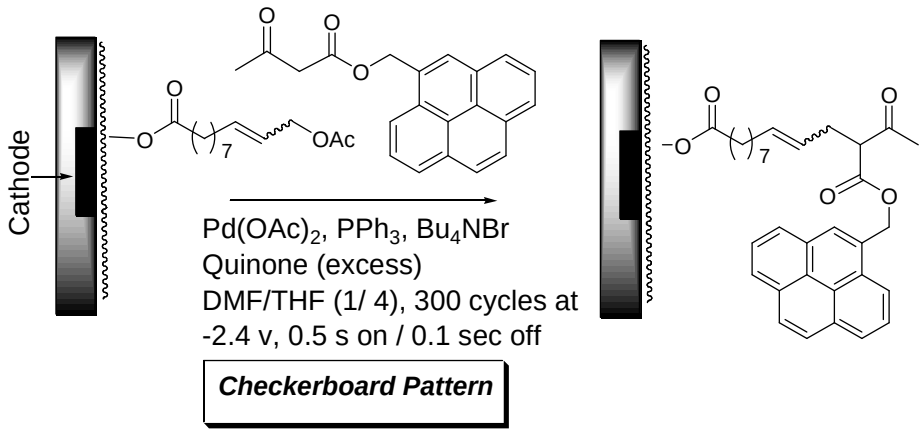

In this case, the surface-bound substrate is an allylic acetate that during the reaction undergoes π-allyl palladium formation. A solution phase nucleophile then adds to the reactive intermediate generated. For such a reaction, allyl methyl carbonate cannot be used as the confining agent because the π-allyl palladium species generated from its reaction with the catalyst would also undergo a reaction with the solution phase

nucleophile. This reaction would regenerate the catalyst and confinement would be lost. As a result, quinone was used as the confining agent for the array-based allylation reaction. Of course, quinone is a viable substrate in the Heck reaction so it would not be a suitable choice as the confining agent for the Heck reaction.

1.4 Experimental setups for array-based reactions

To run an array-based reaction, a computer program is needed to control the potential applied, the reaction time, as well as the electrodes used for the reaction. For both 1-K and 12-K arrays, only positive potentials can be applied between the working electrode and counter electrode. This means that the counter electrode is always the negative electrode. The potential for the cell is measured as a drop between the working and counter electrode. As a result, when doing an oxidation reaction, a platinum wire in the case of 1-K array and a platinum cap in the case of 12-K array is used as the counter electrode and the array itself used as the working electrode. When doing a reduction reaction, the platinum wire or cap is used as the "working" electrode and the array used as "counter" electrode. As a two electrode system, it does not matter which role (working or counter) the array plays, since the current passing from both electrodes will be identical. The more important thing in such context is whether reduction or oxidation is happening on the microelectrodes. As long as we can control the array to serve as a cathode or anode, then we can control the nature of the reactions that are triggered by the electrolysis.

Taking the 12-K instrument as an example, the instrument has 6 terminals

(Figure 1.4). One of the terminals, the white one, is connected to an internal bipolar potentiostat. In principle, it can be used to apply both positive and negative potentials to an electrode. However, reactions that use this terminal to apply a negative potential to the array are often problematic so this terminal is rarely used. A second terminal is also not needed for our current discussion. The most recent arrays developed have the counter electrode built into the array as part of the grid surrounding the working electrodes on the array. The orange terminal is used when these arrays are employed to make a connection to that counter electrode. Since the majority of the synthetic reactions we will be talking about here use a setup where the array is imbedded into a slide (Figure 1.2a, see the discussion below) and then covered with a cap that contains a Pt-counter electrode, the use of this orange terminal will not be discussed further here. That leaves four terminals of concern. One (the blue terminal) is hooked to a positive potentiostat and can be used to apply a positive potential to an electrode. One (the black terminal) is a ground and is connected to the cathode. The potential drop across the cell reflects the potential difference between these two electrodes. The third terminal of importance here (the yellow one) is connected to the Pt-cap, and the fourth (the red terminal) is connected to the microelectrodes in the array. The reactions are run by connecting the positive blue terminal to either the red (array) or yellow (cap) terminals and then black terminal to the alternative. For example, to run a reduction on the array (Figure 1.5a) the positive blue terminal is connected to the Pt-electrode on the cap through the yellow terminal and the negative black terminal is connected to the array through the red terminal. To run an oxidation on the array (Figure 1.5b), the

positive blue terminal is connected to the array through the red terminal and the negative black terminal is connected to the Pt-electrode on the cap through the yellow terminal.

A very similar setup is used to run reactions on a 1-K array with the only difference being that the 1-K arrays are not imbedded into slides (Figure 1.1a). Instead they are simply placed into a reaction solution along with a remote Pt-wire that serves as the counter electrode (see the discussion below). The setups are very easy to use, and therefore often represent the method of choice for exploring a new array-based synthetic method.

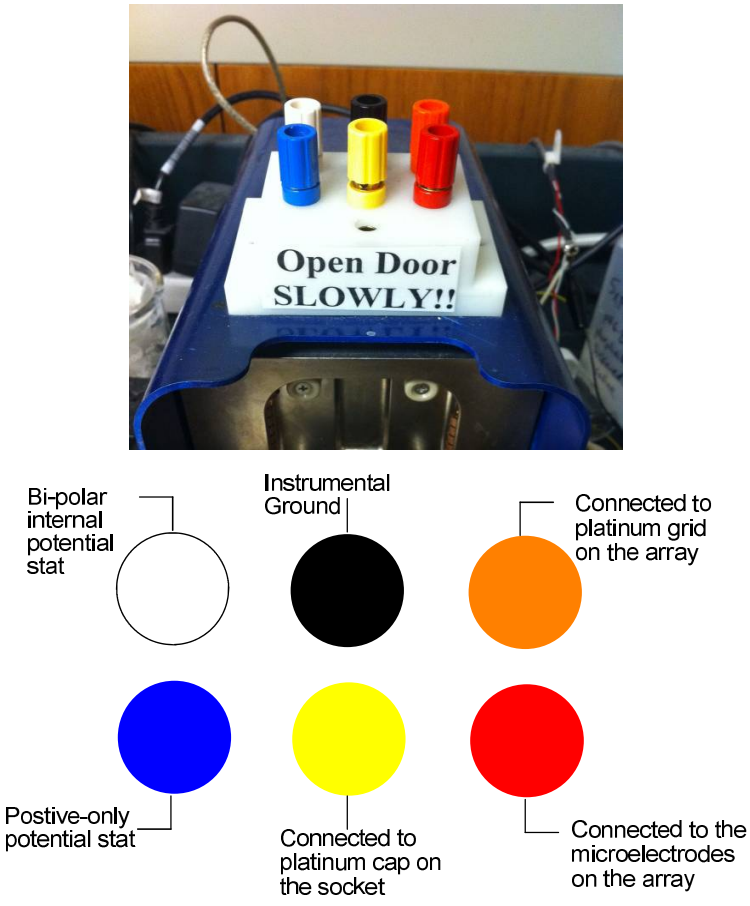

Figure 1.4 The 6 terminals on the 12 K instrument and their functions.

a) b)

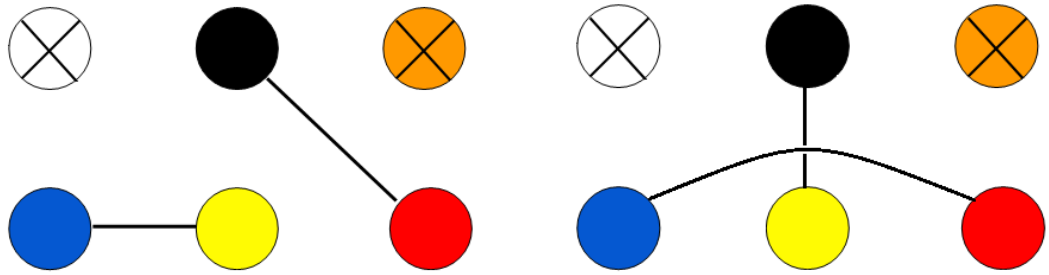

Figure 1.5 The connections for a) reduction reactions and b) oxidation reactions.

With regard to reaction time, 1-K array and 12-K array use different terms. With the 1-K array, the reactions are run with an on-and-off cycle. In the reactions, the selected electrodes are turned on for a set period of time and then turned off for a period of time. The combination is called one cycle. The total reaction time is controlled by setting the number of cycles that are performed. The cycling of the electrodes in this way is important. When the electrodes are turned on, the reactive reagent is generated and the desired reaction happens. When the electrodes are turned off the charged species being generated at the electrodes has time to diffuse away from the electrodes. This reduces the resistance to the current that builds up at an electrode. In a bulk electrolysis setup, this is handled by stirring. If it is not, then the resistance at the surface of the electrode will become large enough to interfere with current flow through the cell. From our previous experience, turning the electrodes on for 0.5 second and off for 0.1 second typically provides the optimal reaction conditions.

Different from the 1-K array term “cycle”, the 12-K array uses the term

“pause” to describe reaction time. Generally, 1 pause equals 1 second in reaction time so 60 pauses will be 1 minute. On 12-K array, the potential at the electrode can be applied continuously without causing a problem. This is due to the closeness of the counter electrode in the cap to the array. 12-K arrays are essentially undivided cells (For the 1-K arrays the Pt-wire is located a long way from the array. Such reactions are essentially divided cells). In an undivided cell, the products generated at the cathode can interact with the products generated at the anode. In this way, the charges generated at each electrode are neutralized and no buildup of resistance occurs in the cell. Because of the smaller electrodes utilized in a 12-K array, the arrays are less tolerant of high potential differences (faster current rates). Hence, the reactions typically employ lower potential differences and longer reaction times than the 1-K arrays.

For 1-K reactions, the reaction solution is made in a 1.5 mL eppendorf tube. The array is then inserted into a socket that is used to control which electrodes in the array are utilized (Figure 1.6a). The array is then submerged in the solution in the eppendorf tube so that the microelectrodes in the array are fully immersed in the solution (Figure 1.6b). The counter electrode is then inserted into the solution, and the reaction conducted by using a PC to activate selected electrodes in the array. The PC utilizes proprietary software available from CustomArray for addressing the array.

a) b)

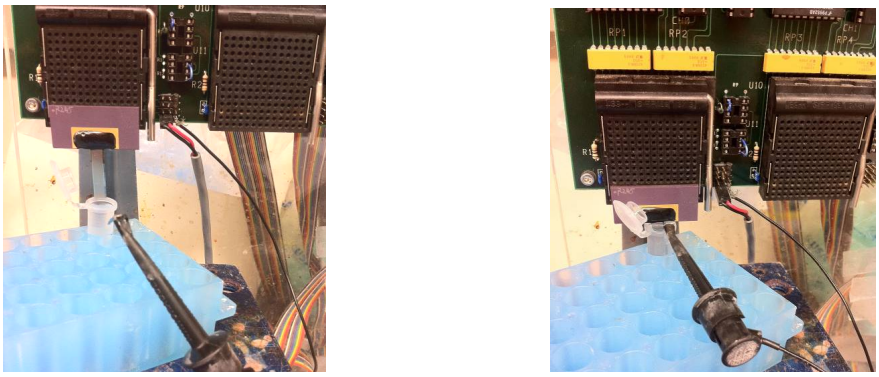

Figure 1.6 The 1-K reaction setup with the chip a) before and b) after inserted into the reaction solution mixture.

For 12-K reactions, the setup is somewhat more complex. As mentioned above, the 12-K slide is imbedded in a ceramic slide as shown in Figure 1.7a. The slide is then fitted with a cap that contains a Pt-electrode sputtered onto its surface. The cap is separated from the slide with a rubber ring that provides a seal for the space in between the array and the cap. The setup is held together with two blue clips as illustrated in Figure 1.7b. The platinum-electrode on the cap is connected to the yellow terminal on the power supply (Figure 1.4) with the use of a yellow wire.

a) b)

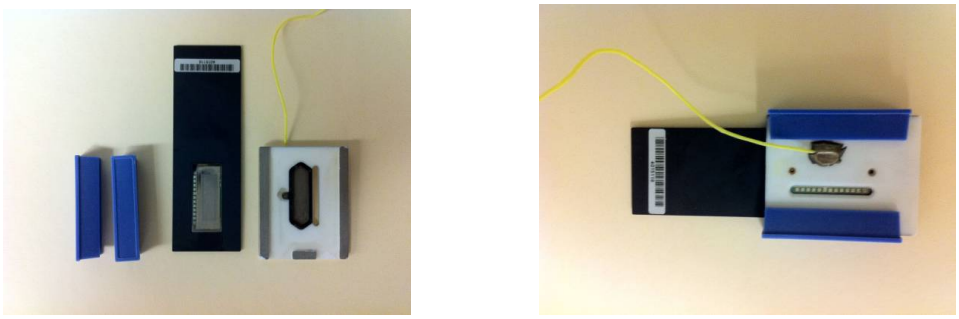

Figure 1.7 The 12-K array slide a) before and b) after inserted into the cap.

The reaction is then run by flowing the reaction medium (slightly more than 100 μL) into the space between the array and the cap. This is done by injecting the solution into the chamber through the bottom hole in the cap with the use of a pipet. A clear version of the cap is shown in Figure 1.8 so that the setup can be more clearly seen.

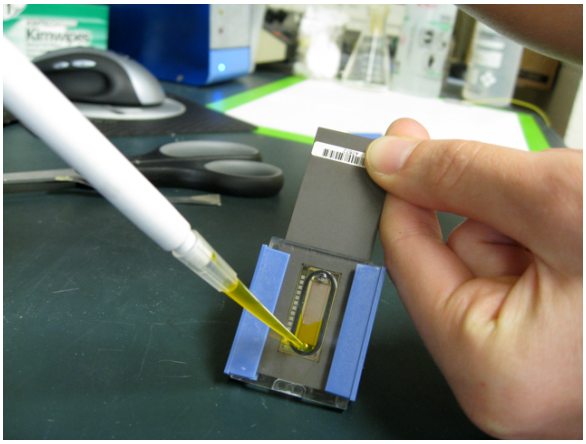

Figure 1.8 A clear cap showing the solution filling up the reaction chamber.

After this step, the two holes on the socket are sealed with two pieces of adhesive silver foil, and the array-socket complex is inserted into the instrument (ElectraSense®) shown in Figure1.9. The yellow wire from the socket is led through a small hole in the instrument to connect with the yellow terminal, and then the gate where the array rests on is closed. Pins on the instrument make contact with pads on the array resulting in a connection between the power supply and the array. The pins are connected to the red terminal on the power supply. After that, the terminals are connected as described above in the discussion of Figures 1.5a and 1.5b. As with the 1-K array, selected electrodes on the array are turned on using a PC and proprietary software. The control of the computer programs is discussed in the appendixes.

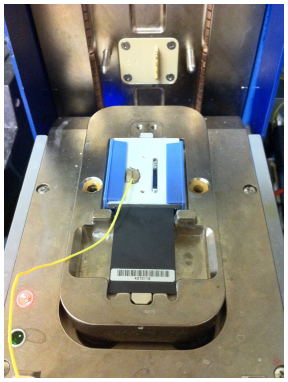

Figure 1.9 The array-cap complex inserted into the ElectraSense® instrument.

1.5 Fundamentals of electrochemical signaling experiments

Of course the arrays are not only used for synthetic reactions. They are also used to monitor binding events between small molecules on the surface of the electrodes and solution-phase receptors. The details of these experiments will be covered in Chapter 4. However, a brief introduction to the topic that focuses on the experimental setup is appropriate here.

The signaling studies conducted are electrochemical impedance experiments. They monitor the current associated with an iron-species in solution. This current falls off at any given electrode in the array when a solution-phase receptor binds a molecule on the surface of that electrode (Figure 1.10).[21] In effect, the binding event increases the resistance to the current at the electrode (an increase in impedance). A picture of how the impedance experiment works is provided in Figure 1.11. The current monitored at the electrodes in the array result from the oxidation of the iron species at the array followed by reduction of the oxidized product at the auxiliary electrode. The binding of a receptor to a molecule on the surface, blocks the oxidation reaction and causes a decrease in current at the electrode. This decrease in current can

be detected using cyclic voltammetry. Of course, at electrode modified with non-binding ligands, no current drop occurs. The current drop at the electrode with the binding event relative to the background current provides an indication of the binding event. By sweeping the concentration of the solution-phase receptor, a binding curve can be generated for the interaction. This provides an opportunity to measure relative binding data for various ligands on the surface of the array.

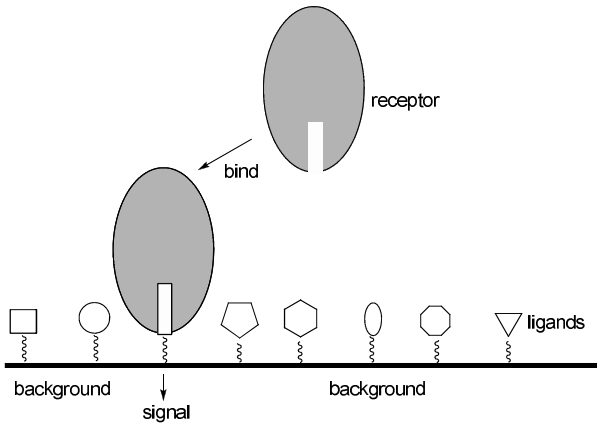

Figure 1.10 A receptor binds to a specific ligand in a library of ligands.

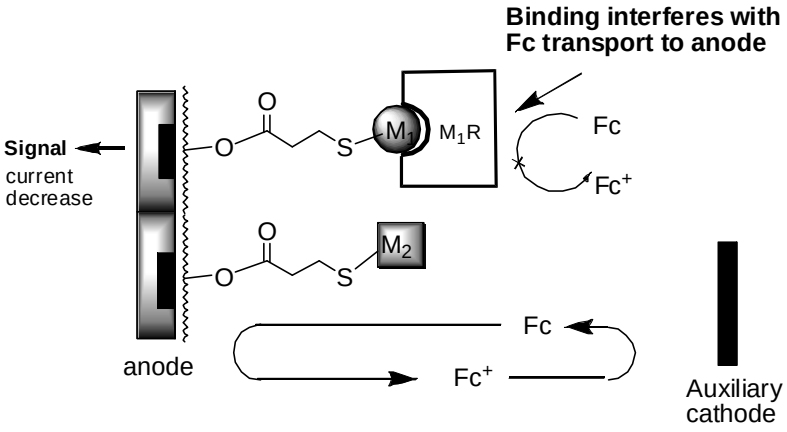

Figure 1.11 Mechanism of electrochemical impedance generated by a binding event.

1.6 Experimental setup for electrochemical signaling experiments

The experimental setup for the signaling experiment is similar to an array-based reaction on the 12-K array. However, for the impedance experiments an external potentiostat is needed to run the analytical electrochemical method since the 12-K instrument ElectraSense® does not have the ability to sweep potential and measure current at the same time. For this reason, we employ a BAS 100B Electrochemical Analyzer to conduct cyclic voltammetry studies on the arrays. Since the internal potentiostats in the ElectraSense instrument are not used, the connection of array to the power supply is different from that used in the preparative experiments. A cable is used to connect the external power supply to the array. This cable has four differently-colored clips (Figure 1.12). The black clip is connected to the working electrode, the red to the counter electrode and the white to a reference electrode. The off-white clip that is separated from the group of three is connected to instrumental ground. These connections are illustrated in Figure 1.13. The setup uses the microelectrodes (red terminal) in the array as the working electrode, the platinum cap (yellow terminal) as the counter and reference electrode, and the black terminal as the ground.

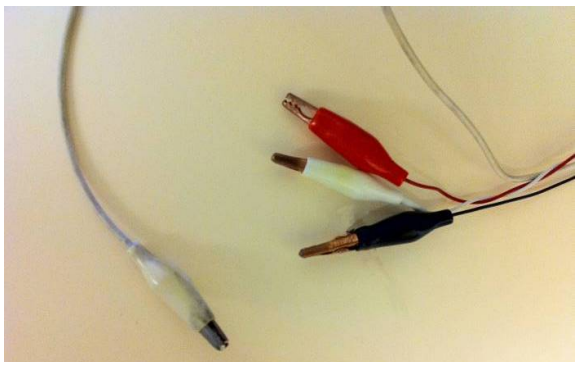

Figure 1.12 The four clips on the cable connecting to the BAS potential stat.

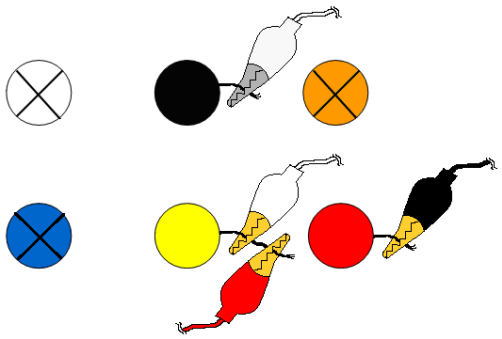

Figure 1.13 The connection between the clips and the terminals for CV setup.

The protocol in the 12-K software used in the signaling experiment is different from the reaction protocols as well. This change is also detailed in the appendixes.

1.7 Progress in the microelectrode array project

Since the initiation of the array project in 2004, our group has made a lot of progress toward the development of site-selective synthetic strategies on the array, characterization of the products generated on the arrays, and signaling strategies for monitoring biological interactions on the microelectrode arrays.

Our earliest work on the arrays focused on exploring site-selective transition-metal-catalyzed reactions on the arrays. The idea was to generate reactive reagents on the arrays by juggling the oxidation states of the metals. The first attempts to use the electrodes in the arrays as cathodes focused on the development of Pd(0)-catalyzed reactions like the Heck reaction (Scheme 1.1).[17] As discussed above, the reactions employed a π-allyl Pd(II) complex as the dormant species in the solution above the array and then used the microelectrodes as cathodes to generate the Pd(0)-species. An oxidant was used in solution as the confining agent. With the

success of Heck reaction, the scope of Pd(0) chemistry was expanded to Suzuki reaction[22] and allylation reactions of 1,3-dicarbonyl compounds.[20] The reactions mediated with other metals via site-selective reduction reactions were also explored. For example, the Cu(I)-catalyzed click reaction of an acetylene and an azide was carried out in a site-selective fashion on a microelectrode array (Scheme 1.3).[23] Recently, this scope of these reactions has been expanded to include a series of couplings between aryl- and vinyl halide and different nucleophiles.[24]

Scheme 1.3

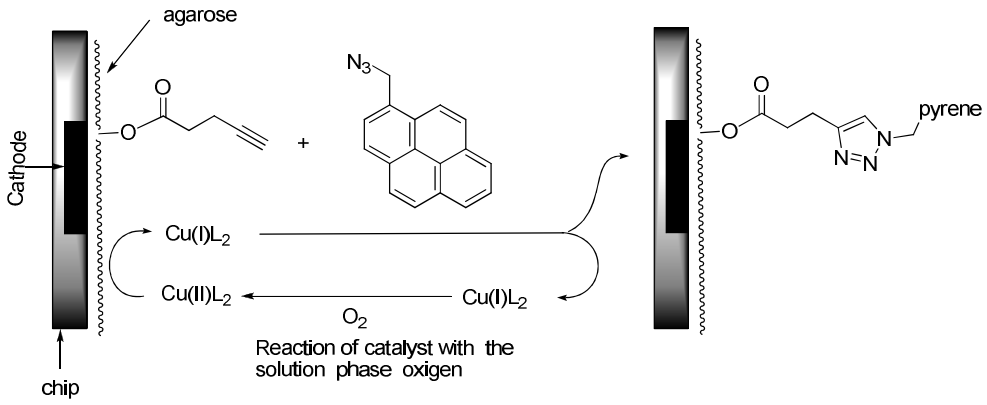

The microelectrodes in the arrays could also be used as anodes to conduct oxidation reactions. This work is particularly effective if the active oxidation state of the transition metal is higher than that of the dormant state. The first successful example of a reaction using the array as anodes was the Pd(II)-mediated Wacker oxidation (Scheme 1.4).[18] This reaction used a triarylamine species as the electron transfer mediator to oxidize a solution-phase Pd(0) species and generate the necessary Pd(II)-oxidant. The Pd(II)-species then oxidized the alkene substrate to a ketone.

Ethyl vinyl ether was used as a solution phase confining agent. It underwent a Wacker oxidation of its own to reduce any Pd(II)-oxidant that migrated away from the selected electrode. In addition to Pd(II), we have successfully used cerium ammonium nitrate (CAN)[25] and Sc(III)[26] on the arrays. In both cases, the electrodes in the array were used as anodes.

Scheme 1.4

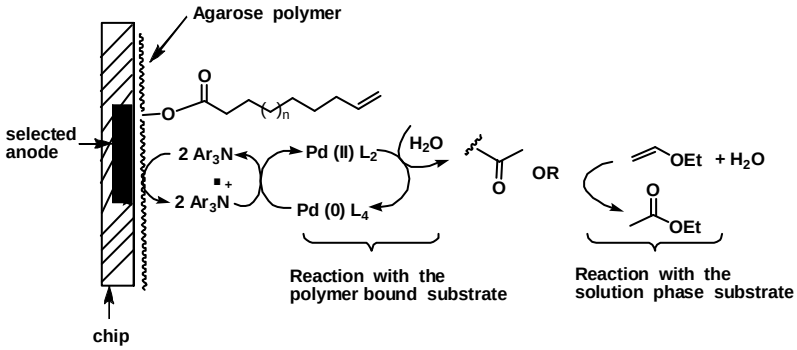

Our group has also made progress in characterizing the products generated on the arrays. These efforts allow for quality control of a molecular library built on the array. The first method used for characterizing molecules on the arrays was time-of-flight secondary ionization mass spectrometry (TOF-SIMS). With the use of a mass-cleavable linker,[23,27] the structures of the molecules on the array could be determined. However, this method for characterization destroyed the array. This was problematic in that we needed a method for characterizing the molecules on the array that preserved our ability to conduct further experiments on the array. For this reason, acid-cleavable "safety-catch" linkers have been developed for use on the arrays (Scheme 1.5).[28] The linkers can be cleaved by the site-selective generation of acids at

the electrodes in the array. The resulting solution above the array can then be analyzed by LC-MS to obtain information on the molecules cleaved from the array. This method is useful for characterizing not only the composition of the molecules synthesized, but also their stereochemistry. Besides the above mentioned linkers, fluorescent linkers have also been developed for the arrays. These linkers are used to determine the quality of the arrays themselves.[29]

Scheme 1.5

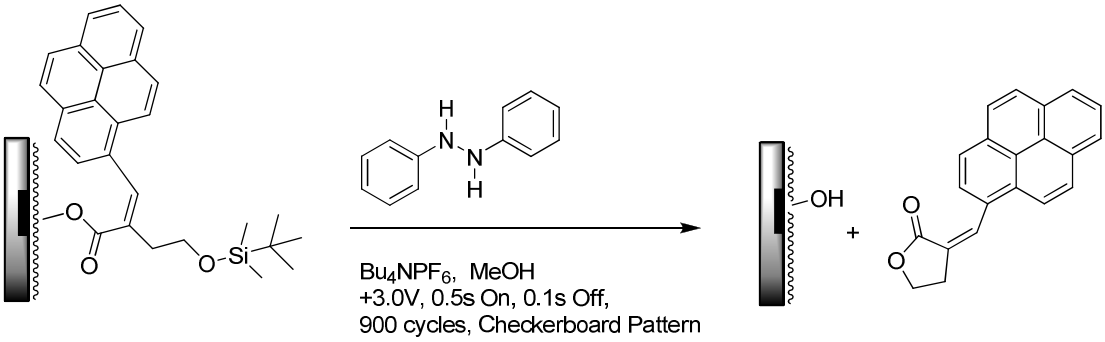

Finally, we have been making great progress on the development of the electrochemical impedance experiments described above.[19,30] The details of these progresses will be covered in Chapter 4 of this thesis.

1.8 Aims of this project

One of the key elements of all of this work that has been ignored in the discussion above is the nature of the polymer surface coating the array. The polymer coating for the array serves as the matrix for everything else that happens. Therefore, the performance of the polymer coating has a significant impact on the outcome of all

array-based reactions and signaling experiments. The ideal coating needs to be stable for long periods of time, stable to washing the array, compatible with the array-based reactions, compatible with electrochemical impedance experiments, and relatively inert with respect to its non-specific binding with receptors. In this regard, the agarose coating that we have used extensively in our initial studies is a failure. It barely meets more than one of the requirements stated above.[25] Hence, to realize our goal of using microelectrode arrays to build and analyze addressable molecular libraries, the development of an new coating for the arrays was urgently needed.

As a result, the main focus of the work reported in this thesis is the exploration of new UV-cross-linkable di-block copolymers as coatings for the microelectrode arrays.

The specific objectives that will be undertaken in this work are 1) broadening the scope of Pd(0) chemistry on the array,[22,31] which will be used to test the performance of the polymer coatings developed later, 2) synthesizing a series of UV-cross-linkable di-block copolymers and testing their performance as coatings for microelectrode arrays,[32] and 3) study the signaling behavior on these block copolymer coatings and establish structure-property relationship.[33]

Reference and Notes

1. For general review on molecular libraries, see: (a) Thompson, L. A.; Ellman, J. A. *Chem. Rev.* **1996**, *96*, 555. (b) Terrett, N. K.; Gardner, M.; Gordon, D. W.; Kobylecki, R. J.; Steele, J. *Tetrahedron* **1995**, *51*, 8135.

2. For general review on small molecule microarrays, see: Duffner, J. L.; Clemons, P. A.; Koehler, A. N. *Curr. Opin. Chem. Biol.* **2007**, *11*, 74.

3. For a general review on addressable libraries, see: Pirrung, M. C. *Chem. Rev.* **1997**, *97*, 473.

4. Merrifield, R. B. *J. Am. Chem. Soc.* **1963**, *85*, 2149.

5. Lipshutz, R. J.; Fodor, S. P. A.; Gingeras, T. R.; Lockhart, D. J. *Nat. Genet.* **1999**, *21*, 20.

6. Wu, H.; Ge, J.; Uttamchandani, M.;Yao, S. Q. *Chem. Commun.* **2011**, *47*, 5664.

7. Brown, P. O.; Botstein, D. *Nat. Genet.* **1999**, *21*, 33.

8. Templin, M. F.; Stoll, D.; Schrenk, M.; Traub, P. C.; Vohringer, C. F.; Joos, T. O. *Trends Biotechnol.* **2002**, *20*, 160.

9. Laurent, N.; Voglmeir, J.; Flitsch, S. L. *Chem. Commun.* **2008**, 4400.

10. Yarmush, M. L.; King, K. R. *Annu. Rev. Biomed. Eng.* **2009**, *11*, 235.

11. Kallioniemi, O.; Wagner, U.; Kononen, J.; Sauter, G. *Hum. Mol. Genet.* **2001**, *10*, 657.

12. George. R. A. *Method. Enzymol.* **2006**, 4*10*, 121.

13. Beier, M.; Hoheisel, J. D. *Chemtracts* **2000**, *13*, 487.

14. Theriault, T. P.; Winder, S. C.; Gamble, R. C. *DNA Microarrays* **1999**, 101.

15. Neugebauer, S.; Zimdars, A..; Liepold, P.; Gebala, M.; Schuhmann, W.; Hartwich, G. *ChemBioChem* **2009**, *10*, 1193.

16. (a) Wojciechowski, J.; Danley, D.; Cooper, J.; Yazvenko, N.; Taitt, C. R. *Sensors* **2010**, *10*, 3351. (b) Dill, K.; Montgomery, D. D.; Ghindilis, A. L.; Schwarzkopf, K. R.; Ragsdale, S. R.; Oleinikov, A. V. *Biosens. Bioelectron.* **2004**, *20*, 736.

17. Tian, J.; Maurer, K.;Tesfu, E.; Moeller, K. D. *J. Am. Chem. Soc.* **2005**, *127*, 1392.

18. Tesfu, E.; Maurer, K.; Ragsdale, S. R.; Moeller, K. D. *J. Am. Chem. Soc.* **2004**, *126*, 6212.

19. Stuart, M.; Maurer, K.; Moeller, K. D. *Bioconjugate Chem.* **2008**, *19*, 1514.

20. Tian, J.; Maurer, K.; Moeller, K. D. *Tetrahedron Lett.* **2008**, *49*, 5664.

21. Murata, M.; Gonda, H.; Yano, K.; Kuroki, S.; Suzutani, T.; Katayama, Y. *Bioorg. Med. Chem. Lett.* **2004**, *14*, 137.

22. Hu, L.; Maurer, K.; Moeller, K. D. *Org. Lett.* **2009**, *11*, 1273.

23. Bartels, J. L.; Lu, P.; Walker, A.; Maurer, K.; Moeller, K. D. *Chem. Commun.* **2009**, 5573.

24. Bartels, J.; Lu, P.; Maurer, K.; Walker, A. V.; Moeller, K. D. *Langmuir* **2011**, *27*, 11199.

25. Kesselring, D.; Maurer, K.; Moeller, K. D. *J. Am. Chem. Soc.* **2008**, *130*, 11290.

26. Bi, B.; Maurer, K.; Moeller, K. D. *Angew. Chem., Int. Ed.* **2009**, *48*, 5872.

27. Chen, C.; Nagy, G.; Walker, A. V.; Maurer, K.; McShea, A.; Moeller, K. D. *J. Am. Chem. Soc.* **2006**, *128*, 16020.

28. Bi, B.; Maurer, K.; Moeller, K. D. *J. Am. Chem. Soc.* **2010**, *132*, 17405.

29. Takamasa, T.; Bi, B.; Hu, L.; Maurer, K.; Moeller, K. D. manuscript submitted.

30. Tesfu, E.; Roth, K.; Maurer, K.; Moeller, K. D. *Org. Lett.* **2006**, *8*, 709.

31. Hu, L.; Stuart, M.; Tian, J.; Maurer, K.; Moeller, K. D. *J. Am. Chem. Soc.* **2010**, *132*, 16610.

32. Hu, L.; Bartels, J. L.; Bartels, J. W.; Maurer, K.; Moeller, K. D. *J. Am. Chem. Soc.* **2009**, *131*, 16638.

33. Manuscript in draft.

Chapter 2

The Advancement of Palladium(0) Chemistry on Microelectrode Arrays

2.1 Introduction to palladium(0) chemistry on microelectrode arrays

As discussed in Chapter 1, microelectrode arrays hold great promise as analytical platforms for detecting ligand-receptor interactions in "real-time".[1-3] This promise is based on electrochemical impedance experiments that can be used to monitor the molecules (Figure 2.1).[3] The impedance experiments work by cycling a redox couple between oxidation at the array and reduction at a remote electrode. The current for this process is measured at each microelectrode in the array. When a receptor binds a molecule on the array, a drop-off in this current is recorded at the associated microelectrode. For example, when a receptor that recognizes and binds to M1 (Figure 2.1), the current at the corresponding microelectrode drops relative to the current at the neighboring microelectrode. For this to work, the molecules being probed must be selectively located next to only the microelectrode being used to monitor them. If any M1 is located next to the microelectrode used to monitor M2, then differentiating the binding of M1 and M2 to the receptor becomes impossible.

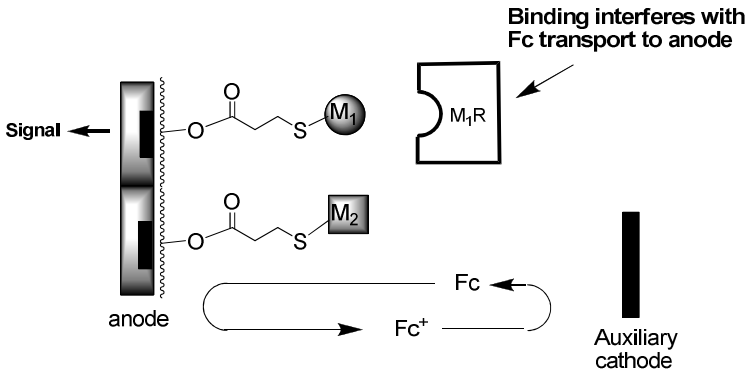

Figure 2.1 Plan for signaling on a microelectrode array.

Hence, to use the arrays as analytical tools we need to develop "site-selective" reactions that allow us to first functionalize and then conduct syntheses next to any single microelectrode or pattern of microelectrodes in an array. These reactions must be carefully confined to the region of the array immediately surrounding a selected electrode without any migration of reagents to the neighboring electrodes, even when the array has a density of 12,544 microelectrodes/cm^2. Given these constraints, traditional synthetic protocols become impossible. One cannot simply buy a reagent and then add it to the surface of an array next to only one microelectrode. Instead, strategies must be developed for making reagents on the arrays proximal to selected microelectrodes and then confining the reagents to those, and only those, locations. To do this, one needs to take advantage of the microelectrodes themselves for initiating the synthetic reactions. With this in mind, we have begun moving traditional synthetic methods to the microelectrode array platform by taking advantage of a competitive reaction strategy.[4-8] To this end, the microelectrodes on the array are used to generate a reactive chemical reagent or catalyst. At the same time, a confining agent is added to the solution above the array in order to destroy whatever reagent or catalyst is being

generated. By balancing the rate at which the reagent or catalyst is generated relative to the rate at which it is consumed in solution, the distance the reagent or catalyst can migrate away from the electrode where it is generated can be controlled. Different molecules are then placed at different locations on the array by utilizing a new set of microelectrodes for generating the desired chemical reagent (Scheme 2.1).

Scheme 2.1

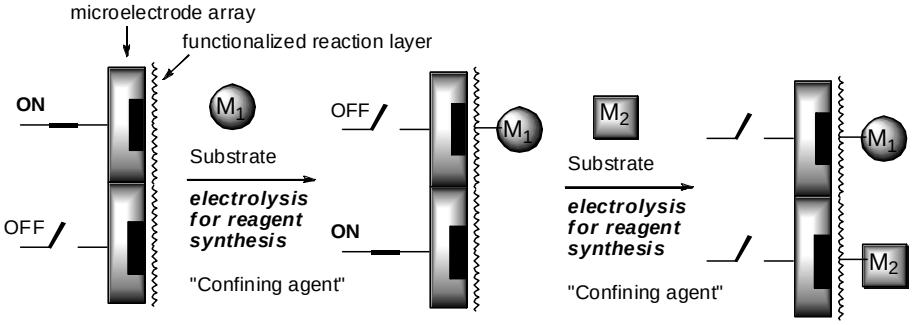

Due to the tremendous synthetic versatility of Pd(0) catalysts, we have been working to develop them as tools for synthesis on the arrays.[9] Particularly attractive is the potential that Heck and Suzuki-type reactions hold as strategies for coupling new molecules to the surface of an array. The Heck reaction (highlight again here in Scheme 2.2) was used as the example for how an array-based reaction can be conducted in Chapter 1.[9a] The success of this strategy can be seen in Figure 2.2.

Scheme 2.2

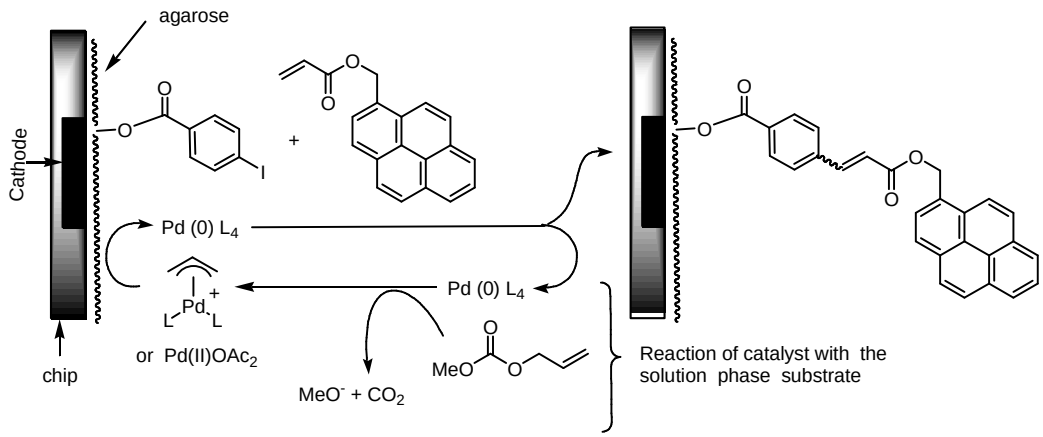

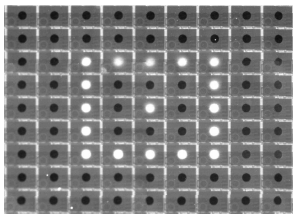

Figure 2.2 A "confined" Heck-reaction on a 1-K array.

The figure shows a 1-K array (1024 microelectrodes/cm^2) with a dot in a box pattern of microelectrodes used as cathodes (-2.4 V relative to a Pt counter electrode for 300 cycles of 0.5 s on and 0.1 s off) to accomplish the reaction illustrated in Scheme 2.2. Following this reaction, a different pattern could be placed on the same array by simply repeating the reaction while using a new set of electrodes for the reduction of Pd(II). Interestingly, the Heck reactions worked beautifully with either the aryl iodide or the acrylate derivative on the surface of the array. The “inverse” Heck reaction (acrylate on the surface) worked in spite of the aryl palladium intermediate for the reaction being generated in solution where it would be free to migrate.[10] Apparently, the Heck reaction on the surface is fast enough to prevent the migration. Overall, the

reaction was extremely attractive because it enabled the placement of molecules by any electrode in the microelectrode array.

Although the reactions worked well and confinement was easy to obtain, there was an underlying problem with reactions requiring longer reaction times. As the reaction time increased, the intensity of fluorescence from the selected microelectrodes decreased (Figure 2.3).

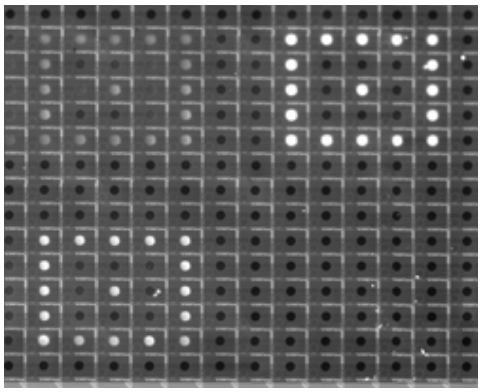

Figure 2.3 Fluorescence image of Heck reaction: -2.4 V, time on 0.5 second, time off 0.1 second, allyl methyl carbonate confined. Lower right: methyl acrylate substrate for 6 min as blank comparison; upper right: 1-pyrenemethyl acrylate, reaction running 3 min; lower left: 1-pyrenemethyl acrylate, reaction running 6 min; upper left: 1-pyrenemethyl acrylate, reaction running 12 min.

In this image, an array is shown with four experiments run on its surface. The first is shown in the lower right portion of the array. It utilized methyl acrylate instead of the pyrene-derived substrate for the Heck reaction and served as a control showing no fluorescence. The second experiment is shown in the upper right. This experiment was identical to the one illustrated in Figure 2.2. The reduction was run for 300 cycles. In the third experiment, shown in the lower left, the reduction was run for 600 cycles. In the fourth, shown in the upper left, the reduction was run for 1200 cycles. Clearly,

the intensity of the fluorescence decreased with increasing reaction time. At the time, we wondered if the methoxide generated from the reaction of the confining agent with the Pd(0)-catalyst was cleaving either the ester linkage between the molecule on the surface of the array and the agarose polymer or the acrylate ester. These initial findings left us with three questions: Were the conditions developed for initiating Pd(0)-catalyzed reactions general? Did all Pd(0)-catalyzed reactions have the problem associated with longer reaction times? How could the decrease of material on the surface of the array with greater reaction time be stopped? In this chapter of the thesis, these three questions will be answered. As we will see, the answers lead to the need for a new polymer surface.

2.2 Development of the Suzuki-reaction on microelectrode arrays

The Suzuki reaction offers a potentially powerful strategy for placing molecules onto arrays. Hence, it was selected as a test for examining the generality of site-selective Pd(0)-catalyst formation (Scheme 2.3).[9b]

Scheme 2.3

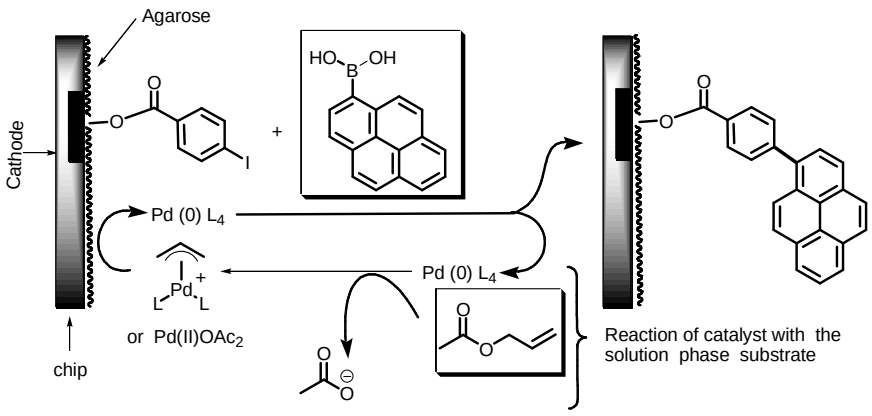

Efforts to conduct a site-selective Suzuki reaction began with the placement of 4-iodobenzoic acid proximal to every microelectrode in an array. Two changes to the previously studied Heck reaction were made. First, the acrylate substrate for the Heck reaction was replaced with a pyrenylboronic acid nucleophile. Second, in an attempt to avoid any complications with the generation of methoxide during the reaction, the allyl methyl carbonate was replaced with allyl acetate as the confining agent. Allyl acetate reacts with Pd(0) to generate the π-allylpalladium(II) species and acetate anion. The result would be a significantly less basic solution than when the carbonate is used. The electrochemical part of the reaction was kept identical to the earlier Heck reaction with the selected electrodes (a checkerboard pattern) held at -2.4 V *vs*. the remote Pt-electrode for 0.5 s followed by 0.1 s off. This was continued for 300 cycles. The image generated is shown in Figure 2.4a.

a) b)

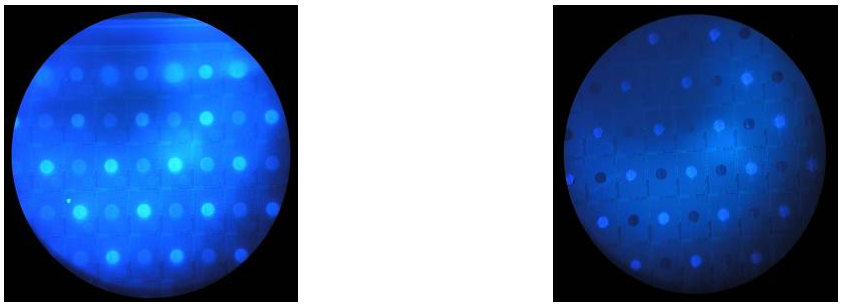

Figure 2.4 Fluorescence image of a site-selective Suzuki reaction (a) checkerboard pattern run at -2.4 V vs. a remote Pt-electrode, (b) checkerboard pattern run at -1.7 V.

The checkerboard pattern can be clearly seen, but the confinement of the reaction was not perfect. Weaker fluorescent spots can be observed by the microelectrodes not

utilized for the reaction. This loss of confinement is consistent with the Suzuki reaction being significantly faster than the Heck reaction. To address this issue, either the rate of Pd(0) catalyst generation at the electrodes needs to be decreased or the rate of catalyst destruction in solution needs to be increased. In this case, the former approach was chosen. The potential at the selected microelectrodes was reduced to -1.7 V, thereby reducing the current flow through the electrolysis cell and the rate at which Pd(0) was generated. This change led to complete confinement of the reaction to the selected microelectrodes (Figure 2.4b).

The Suzuki reaction could also be confined nicely with air as the solution-phase oxidant. However, since the oxidation of Pd(0) with air is slower than the reaction between Pd(0) and allyl acetate, the rate at which Pd(0) was generated had to be reduced even further. In the experiment illustrated in Figure 2.5, the Suzuki reaction was run at a single microelectrode in an array.

a) b) c)

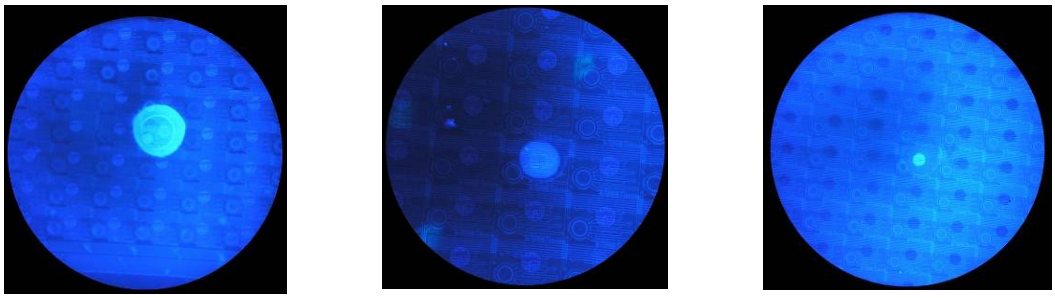

Figure 2.5 Fluorescence image of air confined Suzuki reaction run at a) -2.4 V, b) -1.7 V, and c) -1.4 V relative to a remote Pt-electrode.

Air was bubbled through the reaction mixture prior to the electrolysis. As can be seen in Figure 2.5a, when the reaction was run at -2.4 V relative to the remote Pt electrode,

confinement was completely lost. As the current was reduced and the rate of Pd(0) generation decreased, confinement was regained. When the voltage at the selected microelectrode was set at -1.4 V, the reaction was nicely confined to the single electrode being used. Confinement of the Suzuki reaction could also be gained by increasing the concentration of the confining agent. A nice example of this approach is illustrated in Figure 2.6.

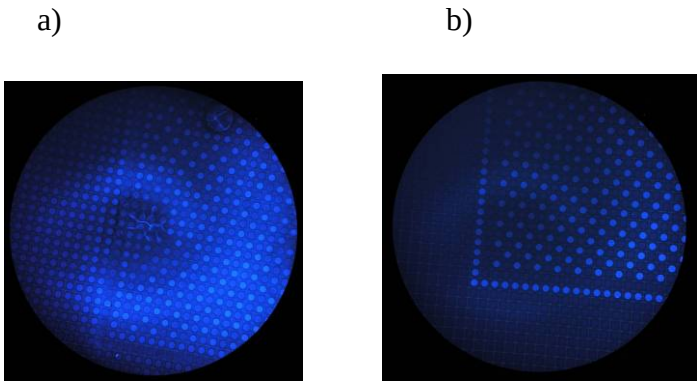

Figure 2.6 Fluorescence image of site-selective Suzuki reaction on 12-K chip (a) checkerboard pattern run with 1-K-conditions (b) checkerboard pattern run with double the amount of confining reagent.

In this experiment, a 12-K array (12, 544 microelectrodes/cm^2) was used. Initially, the experiment was run in a fashion identical to that used successfully on the 1-K array with allyl acetate as the confining agent (Figure 2.6a). In other words, the reaction was run at a voltage of -1.7 V *vs*. the remote Pt-electrode. The pattern selected for the electrolysis was a checkerboard inside of a box. Although the pattern can be seen on the right-hand side of the image, the reaction was not confined to the selected electrodes. To bring the reaction back into confinement (Figure 2.6b), the amount of

allyl acetate was doubled from a concentration of 0.54 *M* for the experiment illustrated in Figure 2.6a to 1.08 *M* for the experiment illustrated in Figure 2.6b.

Both of the previous examples illustrate the nature of the competition that leads to site selectivity on the arrays. Every site-selective reaction on a microelectrode array involves this balancing of the rate at which a reagent or catalyst is generated at the electrodes with the rate at which it is destroyed in the solution above the array.

An inverse-Suzuki reaction having the nucleophile on the surface of the array and the aryl bromide in solution could also be confined to selected microelectrodes in an array (Scheme 2.4).

Scheme 2.4

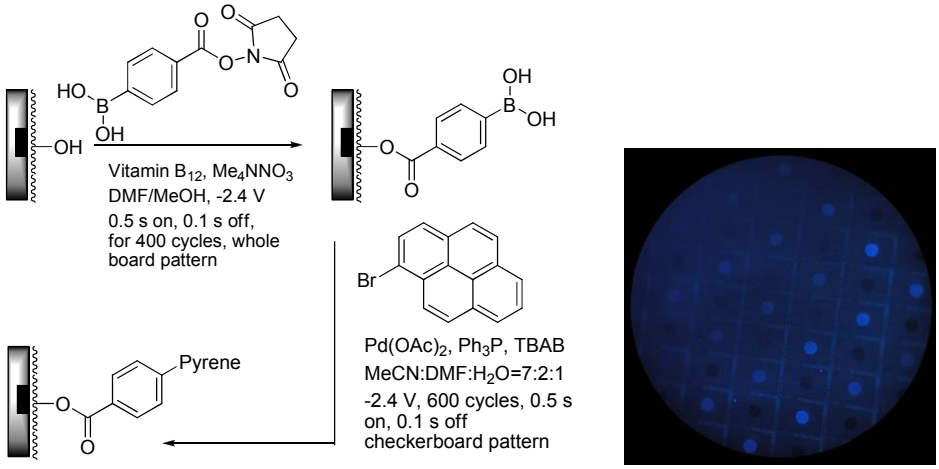

To this end, a phenylboronic acid was placed next to each microelectrode in a 1-K array. This was accomplished by using a base-catalyzed esterification reaction as illustrated.[5,7-9] Once the boronic acid was in place, the array was treated with a solution containing 1-bromopyrene and $Pd(OAc)_2$. Allyl acetate was used as the

confining agent. A checkerboard pattern of microelectrodes was then selected as cathodes for reducing the Pd(II) species and generating the catalyst. The reaction was confined to the selected electrodes, even when the microelectrodes were held at -2.4 V relative to the remote Pt-electrode. In this case, the reaction on the surface of the array was fast enough, relative to migration of the pyrenyl Pd(II) species away from the selected electrode, to allow confinement even with the more rapid generation of Pd(0). It is noteworthy that the unevenness of the fluorescent image in the picture shown above was due to a problem associated with the microscope, not the reaction itself. If the upper left spots were moved into the center of the field they would be of the same fluorescent intensity. This is the same with Figure 2.6 as well.

With the Suzuki reaction in place, we utilized it to probe the generality of observation made with the Heck reaction concerning the relationship between spot fluorescent intensity and reaction time. Would extended reaction times also lead to a decrease in the intensity of fluorescence in the Suzuki reaction? To address this question, the reaction outlined in Scheme 2.3 was repeated at three different microelectrodes on a 1-K array, varying the reaction time at each of the sites (Figure 2.7).

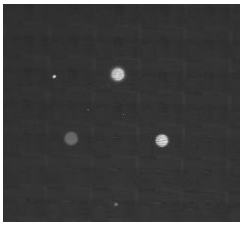

Spot	Relative intensity*
200	100 ± 8
400	187 ± 11
600	204 ± 8

Figure 2.7 Fluorescence image of Suzuki reaction: -1.7 V, time on 0.5 second, time off 0.1 second, 200, 400, 600 cycles, allyl acetate confined. Lower left: reaction

running 2 min; lower right: reaction running 4 min; upper middle: reaction running 6 min.

Following the reactions, the amount of fluorescence relative to background was measured for each site. The setup for the reactions was identical. The array was coated with agarose, 4-iodobenzoic acid was placed by each of the microelectrodes on the array, a voltage of -1.7 V *vs*. the remote Pt electrode was applied to each of the selected electrodes for 0.5 s followed by 0.1 s with the electrode turned off, and allyl acetate was used as the confining agent. The reactions at the three different microelectrodes were run for 200 (2 min), 400 (4 min), and 600 (6 min) cycles, respectively. After 600 cycles, the reaction began to lose confinement, a very curious observation that initially defied explanation. From the experiment, it was clear that the Suzuki reactions were very fast and approach saturation of the surface after only 6 min. During the time of the experiment before loss of confinement, there did not appear to be a loss in fluorescence at the reaction sites. But how did the reaction lose confinement? With a large excess of confining agent being used, the rate of Pd(0) generation at the electrode relative to the rate of Pd(0) destruction by the confining agent in solution should not vary significantly as the reaction progressed. With this question in mind, we began revisiting the Heck reaction for more information.

2.3 Time dependence control experiments on Heck reaction

The result highlighted in Figure 2.7 led to questions about how the change from allyl methyl carbonate to allyl acetate as the confining agent influenced the

reaction. The change was made to try and stop the loss of fluorescence from the surface of the array with time. Was the change successful or was the difference observed with the Suzuki-reactions due to the change in the reaction conducted? To answer this question, the Heck reaction was repeated using allyl acetate as the confining agent. Everything else was kept the same as the reaction outlined in Figure 2.2 (electrode voltage of -2.4 V relative to a remote Pt electrode, etc.). As in the Suzuki time trial, three microelectrodes in a 1-K array were selected for use (Figure 2.8).

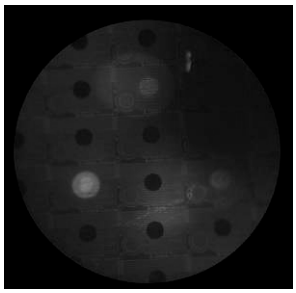

Figure 2.8 Fluorescence image of Heck reaction run at -2.4 V for 0.5 second followed by 0.1 second with the electrode off. The reaction was run for 300, 600, and 900 cycles with allyl acetate as the confining agent. Lower left: reaction time = 3 min; lower right: reaction time = 6 min; upper middle: reaction time = 9 min**.**

The three reactions were run for 300, 600, and 900 cycles. As in the earlier Heck reaction, the most intense spot was obtained for the reaction run for 300 cycles (lower left). As the reaction ran longer, the fluorescent spot indicating product grew less intense. Clearly, the change in confining agent did not alter the reaction. The methoxide generated when allyl methyl carbonate was used was not the reason for the decrease in product intensity with time. An inverse-Heck reaction appeared to show similar behavior (Figure 2.9), although in this case the decrease in intensity was small

enough to preclude a definitive conclusion.

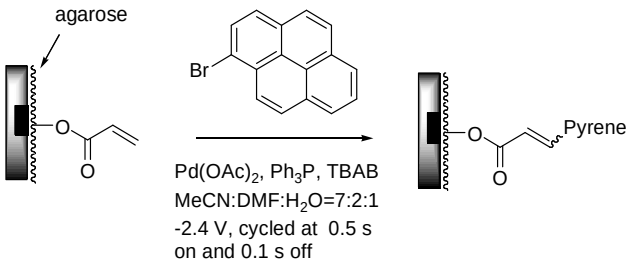

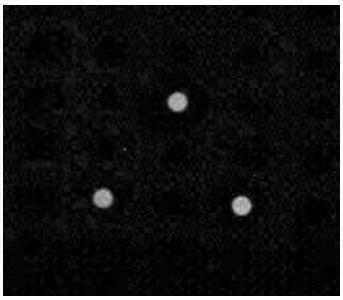

Spot	Relative intensity with green filter	Relative intensity with blue filter
300	100 ± 9	100 ± 2
600	210 ± 15	116 ± 2
900	197 ± 10	95 ± 2

Figure 2.9 Fluorescence image of "Inverse-Heck" reaction -2.4 V Time on 0.5 second, time off 0.1 second 300, 600, 900 cycles, allyl acetate confined Lower left: reaction running 3 min; Lower right: reaction running 6 min; Upper middle: reaction running 9 min.

The reaction was slower, leading to an increase in intensity from 3 to 6 min of reaction time. This increase dropped off at the 9-min mark (900 cycles), but again the effect was small. The reaction could not be continued past 900 cycles because of decomposition of the agarose polymer coating the surface of the array.

Interestingly, when the product was independently synthesized, placed on the array, and then exposed to the reaction conditions, the image shown in Scheme 2.5 was obtained.

Scheme 2.5

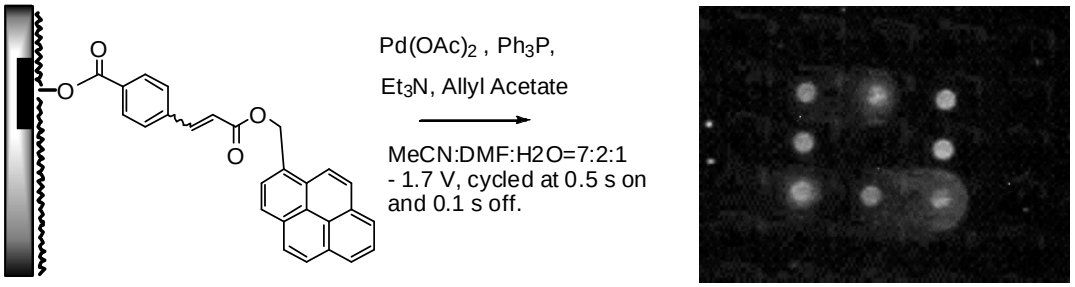

The product was placed in a box pattern on the array. After the Heck reaction conditions were applied to the array, the box pattern was still evident, but the fluorescence had begun migrating away from the microelectrodes. Like the Suzuki reaction, confinement was being lost. Since the only fluorophore in the reaction was the product placed by the microelectrodes, the loss of confinement in this experiment provided evidence that the product from the reaction was being cleaved from the surface of the array and then migrating to other locations.

2.4 The truth of the "Heck Reaction Story"

A much clearer picture of what was happening with the Heck reaction came to light when the reaction was utilized for placing a peptide substrate onto the array (Scheme 2.6) by Dr. Melissae Stuart.[11] As in the earlier experiments, the microelectrode array was coated with an agarose polymer and then 4-iodobenzoic acid placed by each microelectrode in the central region of a 12-K array using a base-catalyzed esterification reaction.[5,7-9] The Heck reaction was then conducted in a checkerboard pattern by using the conditions described above. The only change in the reaction was the olefin substrate used for the transformation. In this case, an

unactivated olefin was used for the Heck reaction to avoid polymerization of the peptide triggered by the N-terminal amine. Although Heck reactions are slower with unactivated olefins, 4-pentenoic acid derivatives are known to undergo the reaction.[12]

Scheme 2.6

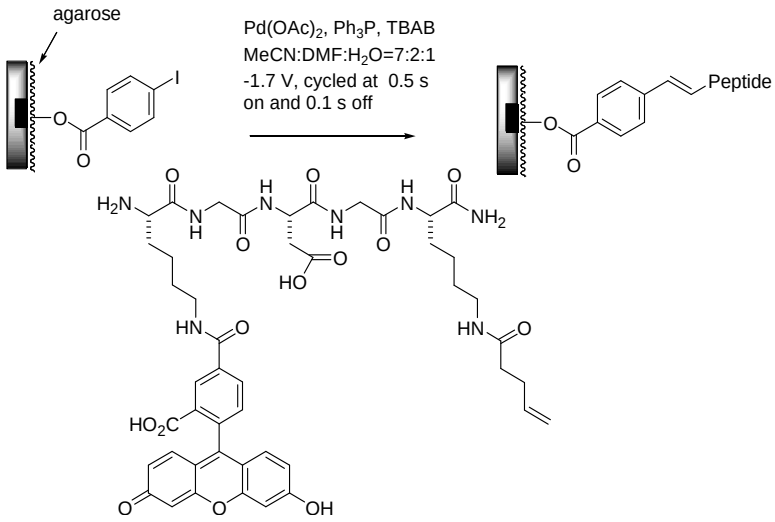

Surprisingly, this Heck-reaction could not be confined at all (Figure 2.10). The product was added to every microelectrode in the array where the iodobenzoic acid had been placed.

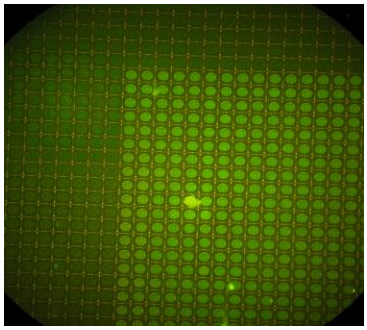

Figure 2.10 Heck reaction using a peptide substrate.

The result surprised us since we know that Pd(0) is confined under these conditions (see Figure 2.2 above). Attempts to place the peptide on an array using an inverse-Heck reaction met with the same loss of confinement (Figure 2.11).

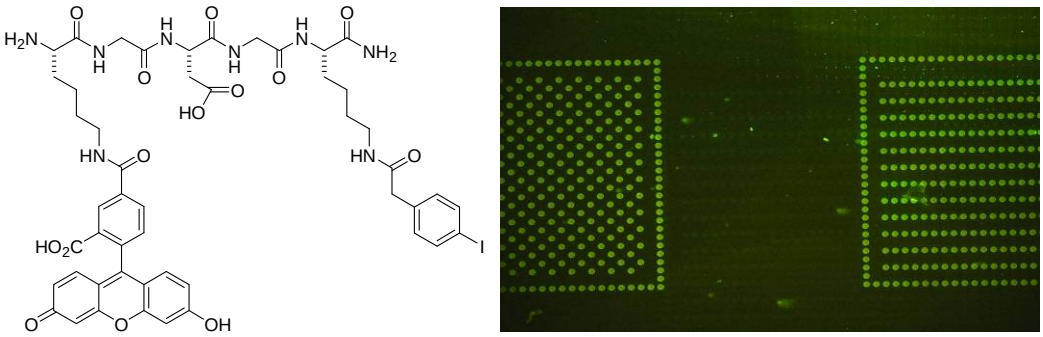

Figure 2.11 Inverse Heck reaction using a peptide substrate.

In this experiment, acrylate was placed on a 12-K array in two patterns, one a checkerboard within a box and one a series of lines in a box. The peptide was functionalized with an aryl iodide, as shown in the Figure. The inverse-Heck reaction was then performed using only the microelectrodes in the lines within a box pattern. The image shows that the peptide was not only placed by the microelectrodes used for Pd(0) generation but also by each of the microelectrodes in the unused checkerboard within a box pattern. There was no evidence of confinement, even though once again we know Pd(0) is confined under these conditions (Scheme 2.4).

Clearly, a side reaction was placing the peptide on the array. For the inverse-Heck reaction it was easy to suggest a Michael-type reaction between the amine nucleophile at the N-terminus of the peptide and the acrylate on the surface of

the array. However, no such possibility exists for the Heck reaction illustrated in Scheme 2.6. Suggestions that the reaction was catalyzing an addition of the amine nucleophile to the aryl iodide were ruled out with solution-phase control reactions showing that this reaction does not occur.

An alternative explanation was that placing the initial reaction substrates on the agarose surface using an ester linkage generated leaving groups on the anomeric carbons of the sugar. The Pd(II)-precursor for the reaction could then serve as a Lewis acid to generate oxonium ions on the surface of the array and trigger the addition of the N-terminus of the peptide to the agarose coating on the array. Such a reaction would only occur at sites having been functionalized with the initial substrate, giving rise to the patterns seen in Figure 2.11.

To test this idea, a control experiment was performed by Dr. Stuart by taking advantage of the chemistry developed earlier for conducting site-selective Pd(II)-reactions on the arrays.[4] The experiment started by taking an agarose-coated array and functionalizing the sugars by each of the microelectrodes with a benzoyl group (Scheme 2.7). The functionalized array was then treated with a solution of $Pd(OAc)_2$, ethyl vinyl ether, a triarylamine, triphenylphospine, triethylamine, and tetra-n-butylammonium bromide in a DMF, acetonitrile, water mixture. The ethyl vinyl ether was used as a confining agent to rapidly reduce any Pd(II) in solution by means of a Wacker oxidation. The triethylamine was present to scavenge the protons generated during this oxidation. Previous site-selective Wacker oxidations have shown this method to be extremely effective for confining Pd(II) on an array to only

regions surrounding microelectrodes used as anodes.[4b] Pyrenemethylamine was then added to the solution above the array and selected microelectrodes (a checkerboard pattern) were used to oxidize Pd(0) and generate Pd(II).

Scheme 2.7

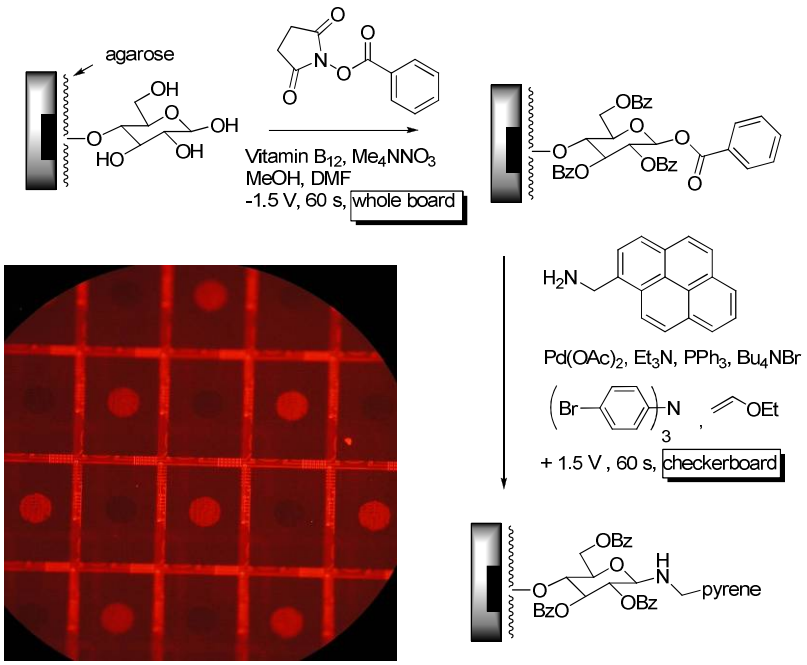

As can be seen in the image shown, the amine nucleophile was added to the functionalized agarose surface by each of the microelectrodes selected for Pd(II) generation. Clearly, Pd(II) catalyzes the addition of amine nucleophiles to the functionalized agarose, an observation that explains the lack of confinement shown in Figures 2.10 and 2.11. In these previous "Pd(0)- experiments", the whole array was covered with a Pd(II) species that was then reduced at selected electrodes. Hence, a Pd(II)-catalyzed reaction would occur everywhere on the array.

Although it is tempting to suggest that a Pd(II)-catalyzed addition can be

used to add peptides to an array using a lysine side chain, the addition reaction proved to be reversible. When an array covered with agarose was functionalized with the benzoyl groups in two regions and then the pyrenylmethylamine placed on one of the patterns using the site-selective generation of Pd(II), a fluorescence image of the array showed fluorescence only by the pattern of microelectrodes selected for the Pd(II) reaction (the benzoyl group on the anomeric carbon is essential for oxonium ion formation and nucleophilic addition to the surface). However, when the array was re-exposed to the reaction conditions minus the pyrenylmethylamine and the second pattern used to generate Pd(II), the image of the array showed fluorescence at the second pattern. With no fluorescent amine nucleophile in solution, the fluorescence observed at the second pattern must have originated from the first pattern. This led to a conclusion that the attachment was not stable enough for use in generating isolated patterns of molecules on the arrays.

In the end, we concluded that both the loss of confinement during some Pd(0)-catalyzed reactions on the arrays and the decreasing amount of product by the selected microelectrodes in others were the result of the sugar-based surface being not stable to the Pd(II) solutions used, which led to the major project of developing new polymeric surfaces for microelectrode arrays in the next chapter.

2.5 Solution to the unstable surface

To make the story complete, results from the next chapter are included here to further support the conclusion that the problem with the Pd-reactions was the stability

of the agarose surface. The polymer we developed consists of a methacrylate block functionalized with a cinnamoyl group and a 4-bromo-substituted polystyrene block (Figure 2.12).[13]

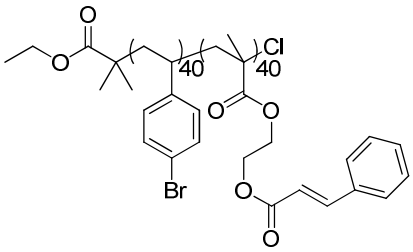

Figure 2.12 Diblock copolymer as coating the microelectrode arrays.

The block copolymer is applied onto the array as a soluble polymer first and then the cinnamoyl groups are photo cross-linked in order to make the surface stable and insoluble. The bromo-substituted polystyrene block is used to provide attachment points for fixing molecules to the surface of the arrays. Using this polymer, substrates are attached to the surface in a manner that cannot be readily cleaved. Hence, if the issues with the Heck reaction are due to cleavage of the product from the surface of the array, then they should not be a problem when the diblock copolymer is employed as the porous reaction layer. This proved to be the case (Figure 2.13).

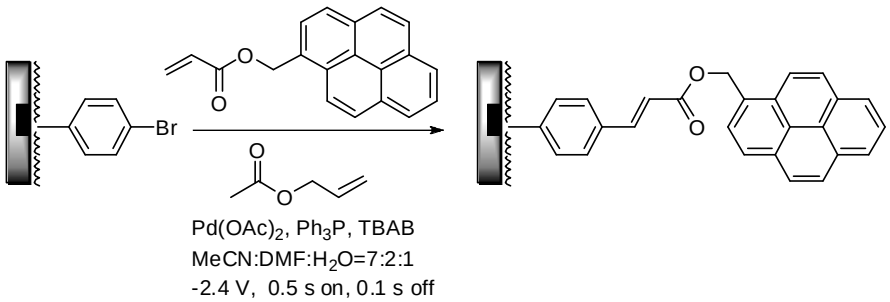

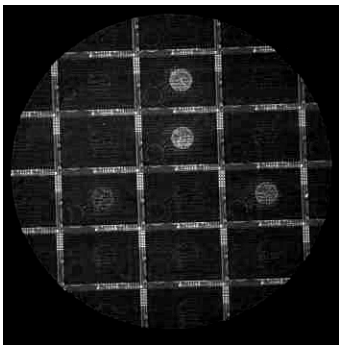

Spot	Relative intensity*
300	100 ± 5
600	118 ± 3
900	235 ± 10
1800	296 ± 9

Figure 2.13 Fluorescence image of Heck reactions run on the PBrSt-b-CEMA surface. The reactions were run by cycling selected electrodes on at -2.4 V for 0.5 s and then off for 0.1 s. Lower left: reaction run time = 3 min (300 cycles); lower right: reaction run time = 6 min (600 cycles); upper middle: reaction run time = 9 min (900 cycles); middle: reaction run time = 18 min (1800 cycles).

When the Heck reaction was repeated, varying the number of cycles used for the electrolysis, the intensity of product fluorescence by the selected electrodes continued to increase with increasing reaction time. There was no decrease in intensity, even after an 18-min reaction. Previous reactions could not be conducted for this length of time because of agarose decomposition (delamination from the surface). A nearly identical result was obtained when the same experiment was repeated using the Suzuki reaction.

2.6 Conclusion

Two different Pd(0)-catalyzed reactions have been conducted site-selectively on microelectrode arrays: the Heck and Suzuki reactions. It was found that the Suzuki reaction is faster and requires either lower currents to reduce the rate of Pd(0) generation or greater amounts of a solution-phase oxidant to maintain confinement of the reaction. Although both reactions proceeded well at short reaction times, in the

initial studies both had problems when the reactions were run for longer periods. In the case of the Heck reaction, the product was cleaved from the surface of the array with longer reaction time, and for the Suzuki reaction confinement on the array was lost with time. The use of a peptide substrate containing an N-terminal amine shed light on the chemistry involved with these changes. When an agarose-coated array was functionalized with substrates using an ester linkage, Pd(II) catalyzed the formation of oxonium ions on the surface of the array. This allowed for addition of the amine nucleophile to the agarose on the array, a reaction that could be accomplished site-selectively by controlling the synthesis of Pd(II). With this knowledge, a non-sugar-based porous reaction layer was used to coat and functionalize the array. Using this more stable surface, both the Heck and Suzuki reactions showed normal behavior with longer reaction times, leading to greater amounts of product on the array with no loss of confinement. The use of Pd(0) on the microelectrode arrays is quickly becoming one of the main synthetic tools available for developing addressable molecular libraries.

2.7 Experimental procedure

General experimental procedures

Materials

All materials were used as purchased from Aldrich without further purification unless

otherwise indicated.

Characterization

Fluorescence microscopy was carried out with an Olympus IX70-S1F2 microscope connected to an Olympus BH2-RFL-T3 burner and an Olympus CAMEDIA C-5060 camera. Exposure time usually ranges from 1/3 s to 2.5 s. The filters used are listed below:

Position	Manufacturer	Catalog#	Color	Data
WB	Chroma Technology	31057 Pyrene C61722	Blue	Ex. = 360 ± 40 nm Mirror = 400 nm Em. = 480 ± 60 nm
Blank #1	Chroma Technology	UN31004 Texas Red/Cy3.5 C52285	Red	Ex. =560 ± 40 nm Mirror = 595 nm Em. = 630 ± 60 nm
Blank #2	Omega Optical	XF105-2(BX19)	Yellow	Ex. =500 ± 25 nm Mirror = 525 nm Em. = 530 nm
WG	Olympus	U-MWG	Red	Ex. =510 – 550 nm Mirror = 570 nm Em. = 590 nm

^{1}H and ^{13}C NMR spectra were recorded by using Varian Mercury 300 spectrometer with $CDCl_3$ as solvent.

FT-IR spectra were obtained using a Perkin Elmer Spectrum BS FT-IR System spectrophotometer.

Images used for fluorescence quantification: Images were taken with an EXFO X-CITE lamp at 50% power and a FITC filter with excitation wavelengths of 465-495 nm and emission at 515-555 nm. The images are 12-bit with 3x3 or 4x4 binning and exposure time of 300 ms to 1 sec.

Sample procedure for coating arrays with agarose:

The microelectrode arrays were coated with a spin-coater MODEL WS-400B-6NPP/ LITE. The chip was inserted into a socket in the spinner and adjusted to be horizontal, and then three drops of 0.03 g/mL agarose solution in 9:1 DMF/water were added onto the chip in order to cover the entire electrode area. The chip was then spun 2000 rpm for 45 s. The coating was allowed to dry for 2 h before use.

Sample procedure for coating arrays with block copolymer:

The microelectrode arrays were coated with a spin-coater MODEL WS-400B-6NPP/ LITE. The chip was inserted into a socket in the spinner and adjusted to be horizontal, and then three drops of 0.03 g/mL block copolymer solution in 1:1 xylene/THF were

added onto the chip in order to cover the entire electrode area. The chip was then spun 1000 rpm for 40 s. The coating was allowed to dry for 15 min and subjected to irradiation using a 100 W Hg lamp for 20 min before use.

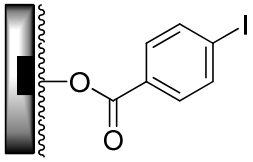

Example coupling of the succinimidyl 4-iodobenzoate to the agarose polymer:

To a 1.7 mL Eppendorf tube was added a DMF solution (100 μL) of succinimidyl 4-iodobenzoate (6.9 mg) and a MeOH (1.5 mL) solution of vitamin B_{12} (2.8 mg) and Bu_4NNO_3 (12.2 mg). The mixed solution was vortexed for a few seconds and then the chip immediately inserted. Selected cathodes were turned on at –2.4 V relative to a remote platinum counter electrode using a 0.5 sec on and 0.1 sec off pulse sequence for 600 cycles. Following that, the chip was repeatedly washed with EtOH and then used for further reactions. For the 12-K microelectrode arrays, the array was coated with agarose and then submerged in the solution prepared above. Selected electrodes were used as cathodes by pulsing them at a voltage of –1.7 V relative to a remote platinum cap for 150 seconds. The array was then repeatedly washed with ethanol before examination using a fluorescence microscope.

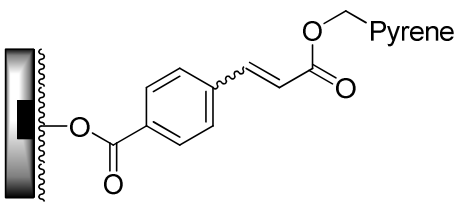

Example of the Heck reaction on chip:

$Pd(OAc)_2$ (0.18 mg), 0.63 mg of PPh_3, 20.0 mg of Bu_4NBr, 5.0 mg of pyrene-1-methyl acrylate, 28.0 μL of Et_3N, and 100 μL of allyl methyl carbonate were dissolved in a 2:7:1 DMF/MeCN/H_2O solution (1.5 mL). The chip loaded with aryl iodide was submerged in this mixed solution and selected cathodes were pulsed at a voltage of -2.4 V relative to a remote platinum counter electrode for 0.5 sec on and 0.1 sec off. After allowing the reaction to proceed for 3 min, the chip was repeatedly washed with EtOH and prepared for pyrene-based fluorescent analysis. The reaction condition using allyl acetate as confining agent is identical to the above procedure except that 100 μL allyl acetate was used as the confining agent instead of allyl methyl carbonate. For the 12-K microelectrode arrays, the array was loaded with iodobenzoate and then submerged in the solution prepared above. Selected electrodes were used as cathodes at a voltage of –1.7 V relative to a remote platinum cap for 150 seconds. The array was then repeatedly washed with ethanol before examination using a fluorescence microscope.

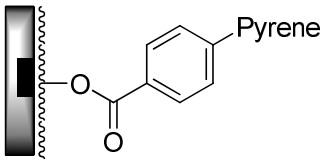

Example of the Suzuki reaction on chip:

$Pd(OAc)_2$ (0.18 mg), 0.63 mg of PPh_3, 20.0 mg of Bu_4NBr, 5.0 mg of pyrene-1-boronic acid, 28.0 μL of Et_3N and 100 μL of allyl acetate were dissolved in a 2:7:1 DMF/MeCN/H_2O solution (1.5 mL). The chip loaded with aryl iodide was

submerged in this mixed solution and selected cathodes were pulsed at a voltage of –1.7 V relative to a remote platinum counter electrode for 0.5 sec on and 0.1 sec off. After 3 min, the chip was repeatedly washed with EtOH and prepared for pyrene-based fluorescent analysis. For the 12-K microelectrode arrays, the array loaded with iodobenzoate was submerged in the solution prepared above except for the amount of confining agent used being doubled. Selected electrodes were used as cathodes at a voltage of –1.7 V relative to a remote platinum cap for 150 seconds. The array was then repeatedly washed with ethanol before examination using a fluorescence microscope.

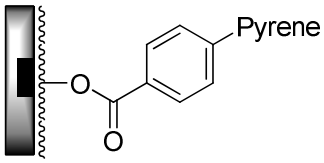

Example of the Suzuki reaction on chip with air as confining agent:

$Pd(OAc)_2$ (0.18 mg), 0.63 mg of PPh_3, 20.0 mg of Bu_4NBr, 5.0 mg of pyrene-1-boronic acid, and 28.0 μL of Et_3N were dissolved in a 2:7:1 DMF/MeCN/H_2O solution (1.5 mL). Air was then bubbled through the mixture for 1 min. The chip loaded with aryl iodide was submerged in this mixed solution and selected cathodes were pulsed at a voltage of –1.4 V relative to a remote platinum counter electrode for 0.5 sec on and 0.1 sec off. After conducting the electrolysis for 3 min, the chip was repeatedly washed with EtOH and prepared for pyrene-based fluorescent analysis.

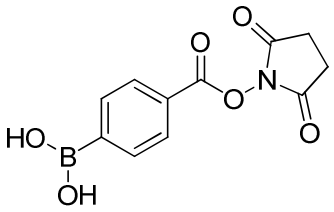

4-((2,5-dioxopyrrolidin-1-yloxy)carbonyl)phenylboronic acid (1)

A 25 mL round bottom flask was charged with 4-carboxyphenylboronic acid (0.083 g, 0.50 mmol), N-hydroxy-succinimite (0.069 g, 0.60 mmol), and a solution of N,N'-dicyclohexyl-carbodiimide (DCC) (0.144 g, 0.7 mmol) in 10 mL DMF was slowly added into the flask. The resulting solution was stirred for overnight. The reaction solution was added with water and extracted three times with diethyl ether. The organic extracts were combined and washed with water and brine, and dried over $MgSO_4$ and then concentrated in *vacuo*. The crude material was then chromatographed through a silica gel column using a solvent of 30% hexane in ethyl acetate as an eluant to afford 0.074 g desired product (74%) as colorless crystal. ^{1}H NMR (300MHz, THF) δ 8.21 (dd, J_1=7.8 Hz, J2=31.5, 2H), 8.02(dd, J_1=7.8 Hz, J2=31.5, 2H), 7.55(s, 1H), 2.84(s, 4H); ^{13}C NMR (75MHz, THF) δ (170.2, 163.1, 135.4, 135.3, 130.1, 129.9, 128.1, 127.8, 26.5); FT-IR (neat) cm-1(3367.7, 2256.9, 2129.2, 1768.7, 1733.8, 1649.7, 1408.5, 1376.6, 1210.5, 1047.6, 1025.2, 998.0, 827.0, 765.5, 632.7) ; LRMS: m/z (ESI^+) 303.2, 286.0, 226.2, 225.7, 225.1; HRMS (ESI^+) ($[M+Na]^+$) calc. 286.0493, Found 286.0500.

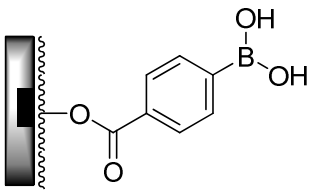

Example coupling of boronic acid substituted succinimide ester to agarose polymer:

To a 1.7 mL Eppendorf tube was added a DMF solution (100 μL) of the 4-boronic acid substituted succinimide ester (6.9 mg) and a MeOH (1.5 mL) solution of vitamin B_{12} (2.8 mg) and Bu_4NNO_3 (12.2 mg) were added respectively. The mixed solution was vortexed for a few seconds and then the chip was immediately inserted into this solution. Selected cathodes were turned on at –2.4 V relative to a remote platinum counter electrode using 0.5 sec on and 0.1 sec off pulse sequence for 400 cycles. Following that, the chip was repeatedly washed with EtOH and used for the Suzuki reaction.

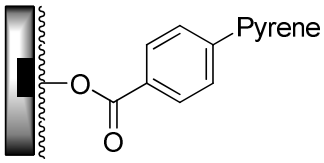

Example of the inversed Suzuki reaction on chip:

$Pd(OAc)_2$ (0.18 mg), 0.63 mg of PPh_3, 20.0 mg of Bu_4NBr, 5.0 mg of 1-bromopyrene, 28.0 μL of Et_3N and 100 μL allyl acetate were dissolved in a 2:7:1 DMF/MeCN/H_2O solution (1.5 mL). The chip loaded with aryl boronic acid was submerged in this mixed solution and selected cathodes were pulsed at a voltage of –2.4 V relative to a remote platinum counter electrode for 0.5 sec on and 0.1 sec off. Following the reaction for 6 minutes, the chip was repeatedly washed with EtOH and prepared for pyrene-based fluorescent analysis.

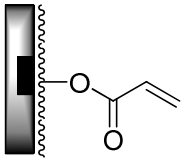

Example coupling of the succinimidyl acrylate to agarose polymer

To a tube of 1.7 mL, a DMF solution (100 μL) of succinimidyl acrylate (6.9 mg) and a MeOH (1.5 mL) solution of vitamin B_{12} (2.8 mg) and Bu_4NNO_3 (12.2 mg) were added respectively. The mixed solution was vortexed for a few seconds and then the chip was inserted into this solution immediately. Selected cathodes were turned on at –2.4 V relative to a remote platinum counter electrode using 0.5 sec on and 0.1 sec off pulse system for 600 cycles. Following that, the chip was repeatedly washed with EtOH and used for further reaction.

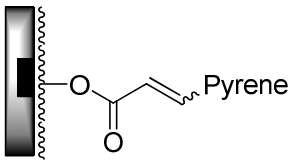

Example of the inversed Heck reaction on chip

0.18 mg $Pd(OAc)_2$, 0.63 mg PPh3, 20.0 mg Bu_4NBr, 5.0 mg 1-bromopyrene, 28.0 μL Et_3N and 100.0 μL allyl acetate were dissolved in a 2:7:1 DMF/MeCN/H_2O solution (1.5 mL). The chip loaded with acrylate was submerged in this mixed solution and selected cathodes were pulsed at a voltage of –2.4 V relative to a remote platinum counter electrode for 0.5 sec on and 0.1 sec off. Following the reaction for 6 minutes, the chip was repeatedly washed with EtOH and prepared for pyrene-based fluorescent analysis.

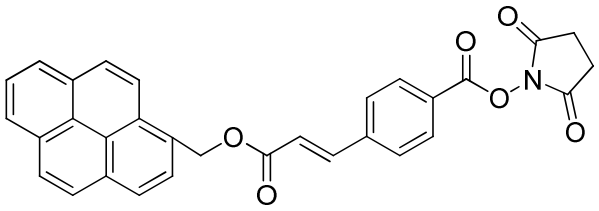

(E)-2,5-dioxopyrrolidin-1-yl 4-(3-oxo-3-(1-pyrenemethoxy)prop-1-enyl)benzoate

A 250 mL round-bottom flask was charged with 1-pyrenemethyl acrylate (0.823 g, 2.88 mmol), 4-iodobenzoic acid (0.694 g, 2.80 mmol), Bu_4NBr (1.805 g, 5.60 mmol) and $Pd(OAc)_2$ (0.189 g, 0.84 mmol) under argon. Then a mixture of 100 mL DMF, 12 mL Et_3N, 12 mL H_2O was degassed with argon for 2 min and injected into the flask. The resulting solution was stirred over night at room temperature. The reaction was quenched with 1 *M* HCl and product was extracted with ethyl acetate and washed with brine to remove DMF. Due to the difficulty of purification of the formed acid, the crude product was directly used as the starting material for the next coupling step. The crude unpurified acid product was dissolved in 30 mL DMF along with N-hydroxy-succinimite (0.386 g, 3.36 mmol) and N,N'-dicyclohexyl- carbodiimide (DCC) (0.809 g, 3.92 mmol). The mixture was stirred for 24 h at room temperature. The reaction mixture was then filtered, extracted with ethyl acetate, and washed with brine. The crude product was then chromatographed through a silica gel column using a solvent of 30% hexane in ethyl acetate as the eluant to afford 0.278 g desired product (20% for two steps total) which could be recrystallized in ethyl acetate/ methanol to give a light yellow crystal. ^1H NMR (300MHz, $CDCl_3$) δ 8.33 (d, J=9.0 Hz, 1H), 8.13 (m, 10H), 7.72 (d, J= 15.9 Hz, 1H), 7.56 (d, J=8.1 Hz, 2H), 6.59 (d,

J=15.9, 1H), 5.98 (s, 2H), 2.87 (s, 4H); ^{13}C NMR (75MHz, $CDCl_3$) δ 169.1, 166.1, 161.2, 143.0, 140.3, 131.8, 131.1, 130.9, 130.6, 129.5, 128.5, 128.3, 128.1, 127.8, 127.3, 126.1, 126.0, 125.5, 125.4, 124.8, 124.6, 124.5, 122.8, 121.3, 65.1, 25.6); FT-IR (neat) cm^{-1}(3324.2, 2926.5, 2849.3, 1768.7, 1737.9, 1624.2, 1414.0, 1366.0, 1311.4, 1240.9, 1166.7, 1068.9, 997.2, 847.3, 729.2, 642.2) ; LRMS: m/z (ESI^+) 526.1, 537.4, 542.1, 543.1; HRMS (ESI^+) ($[M+Na]^+$) calc. 526.1267, Found 526.1244.

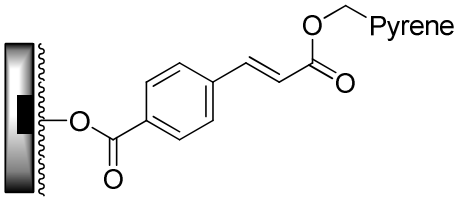

Example of the azobenzene coupling reaction on chip:

Activated ester **1** (6.9 mg), 32.2 mg of Bu_4NBr, and 1.5 mg of azobenzene were dissolved in 1.5 mL of MeCN in an eppendorf tube. The chip was pre-washed with water and ethanol and then directly inserted (before drying) into the solution prepared above. Selected cathodes were pulsed at a voltage of -2.0 V relative to a remote platinum counter electrode for 0.5 sec on and 0.1 sec off. After 3 min, the chip was repeatedly washed with EtOH and prepared for further reactions using the Heck-conditions.

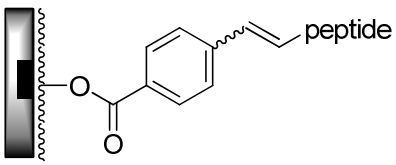

Example of the Heck reaction on 12-K chip using a peptide substrate:

The procedure for conducting a site-selective Heck reaction on a 12-K array was followed, except 100 μL of a 10 mM solution of peptide in H_2O was used as the solution-phase substrate instead of the 1-pyrenemethyl acrylate.

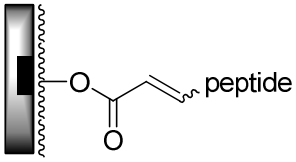

Example of the inversed Heck reaction on 12-K chip using a peptide substrate:

A solution of 8.2 mg succinimidyl acrylate was dissolved in 100 μL DMF in a 1.7 mL Eppendorf tube. To this solution was added 1.5 mL of MeOH containing 2.77 mg Vitamin B_{12} and 13.6 mg of tetramethylammonium nitrate. The array was exposed to 100 μL of the reaction solution and selected electrodes in a large block were applied a voltage of -1.5 V relative to a remote platinum cap for 60 sec. The chip was washed with ethanol and water and let to dry. For the Pd reaction, a solution was prepared containing 100 μL of a 10 mM solution of the peptide in water, 0.18 mg of $Pd(OAc)_2$, 0.63 mg of PPh_3, 20.0 mg of Bu_4NBr, 28.0 μL of Et_3N in a 1.7 mL Eppendorf tube. A 2:7:1 DMF/MeCN/H_2O solution (1.5 mL) was added to the tube. The array was exposed to 100 μL of this solution and selected electrodes in a checkerboard pattern were applied a voltage of -1.2 V relative to a remote platinum cap for 60 sec. The chip was washed with ethanol, water and, ethanol and then visualized with a fluorescence microscope.

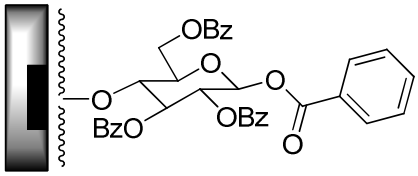

Example coupling of the succinimidyl benzoate to agarose polymer:

To a 1.7 mL Eppendorf tube was added a DMF solution (100 μL) of succinimidyl benzoate (6.9 mg) and a MeOH (1.5 mL) solution of vitamin B_{12} (2.8 mg) and Bu_4NNO_3 (12.2 mg). The mixed solution was vortexed for a few seconds and then the chip immediately inserted into this solution. Selected cathodes were turned on at –2.4 V relative to a remote platinum counter electrode using a 0.5 sec on and 0.1 sec off pulse sequence for 600 cycles. Following that, the chip was repeatedly washed with EtOH and used in subsequent reactions.

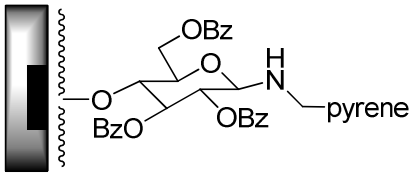

Example of Pd(II) catalyzed addition of an amine under Wacker oxidation condition:

$Pd(OAc)_2$ (32 μg) and 1.39 μg of tris-(4-bromophenyl) amine were dissolved in 1.6 mL of 0.5 *M* tetraethyl ammonium p-toluenesulfonate solution of MeCN: H_2O (7:1). Ethyl vinyl ether (83 μL) was added and the solution was vortexed for 3 min. The chip was inserted into this solution and selected electrodes were pulsed at +2.4 volts relative to a remote platinum counter electrode for 0.5 sec and 0 volt for 0.5 sec. The cycles were repeated for 300 cycles. Then the chip was washed with ethanol and

water and ethanol and visualized with a fluorescence microscope.

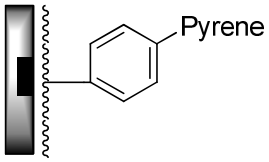

Example of the Suzuki reaction on the block copolymer:

A mixture of 0.18 mg $Pd(OAc)_2$, 0.63 mg PPh_3, 20.0 mg Bu_4NBr, 15.0 mg pyrene-1-boronic acid, 28.0 μL Et_3N and 100.0 μL allyl acetate was dissolved in a 2:7:1 solution of DMF/MeCN/H_2O (1.5 mL). For the 1-K microelectrode arrays, the array coated with the block copolymer was submerged in the solution, and then selected electrodes used as cathodes by pulsing them at a voltage of –2.0 V relative to a remote platinum counter electrode for 0.5 sec on and 0.1 sec off. After 3 min, the chip was repeatedly washed with acetone and DMF and prepared for pyrene-based fluorescent analysis.

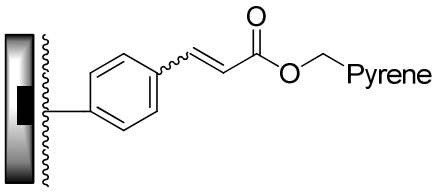

Example of the Heck reaction on the block copolymer:

A solution of 0.18 mg $Pd(OAc)_2$, 0.63 mg PPh_3, 20.0 mg Bu_4NBr, 15.0 mg pyrene-1-methyl acrylate, 28.0 μL Et_3N and 100 μL allyl acetate was dissolved in a 2:7:1 solution of DMF/MeCN/H_2O (1.5 mL). For the 1-K microelectrode arrays, the array was coated with the block copolymer, submerged in the solution made above,

and then selected electrodes used as cathodes by pulsing them at a voltage of –2.0 V relative to a remote platinum counter electrode for 0.5 sec on and 0.1 sec off. After 3 min, the array was repeatedly washed with acetone and DMF and then examined with the use of a fluorescence microscope.

in THF
8.276
8.250
8.171
8.146
8.081
8.060
8.054
7.976
7.949
7.548
3.580
2.836
1.721
1.293
3.89
0.72
4.00
ppm

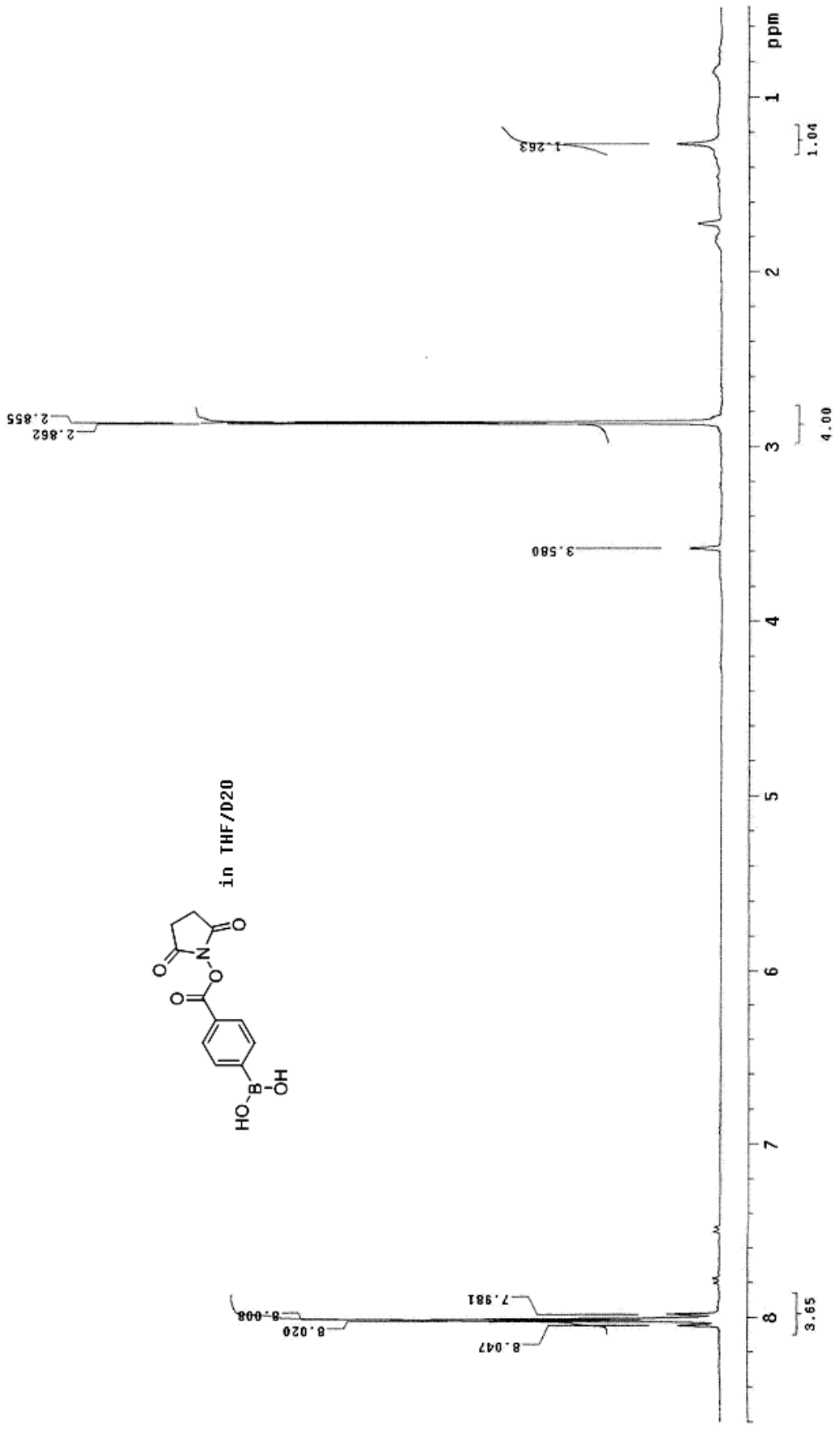
in THF/D20
8.047
8.020
8.008
7.981
3.580
2.862
2.855
1.263
ppm
3.65
4.00
1.04

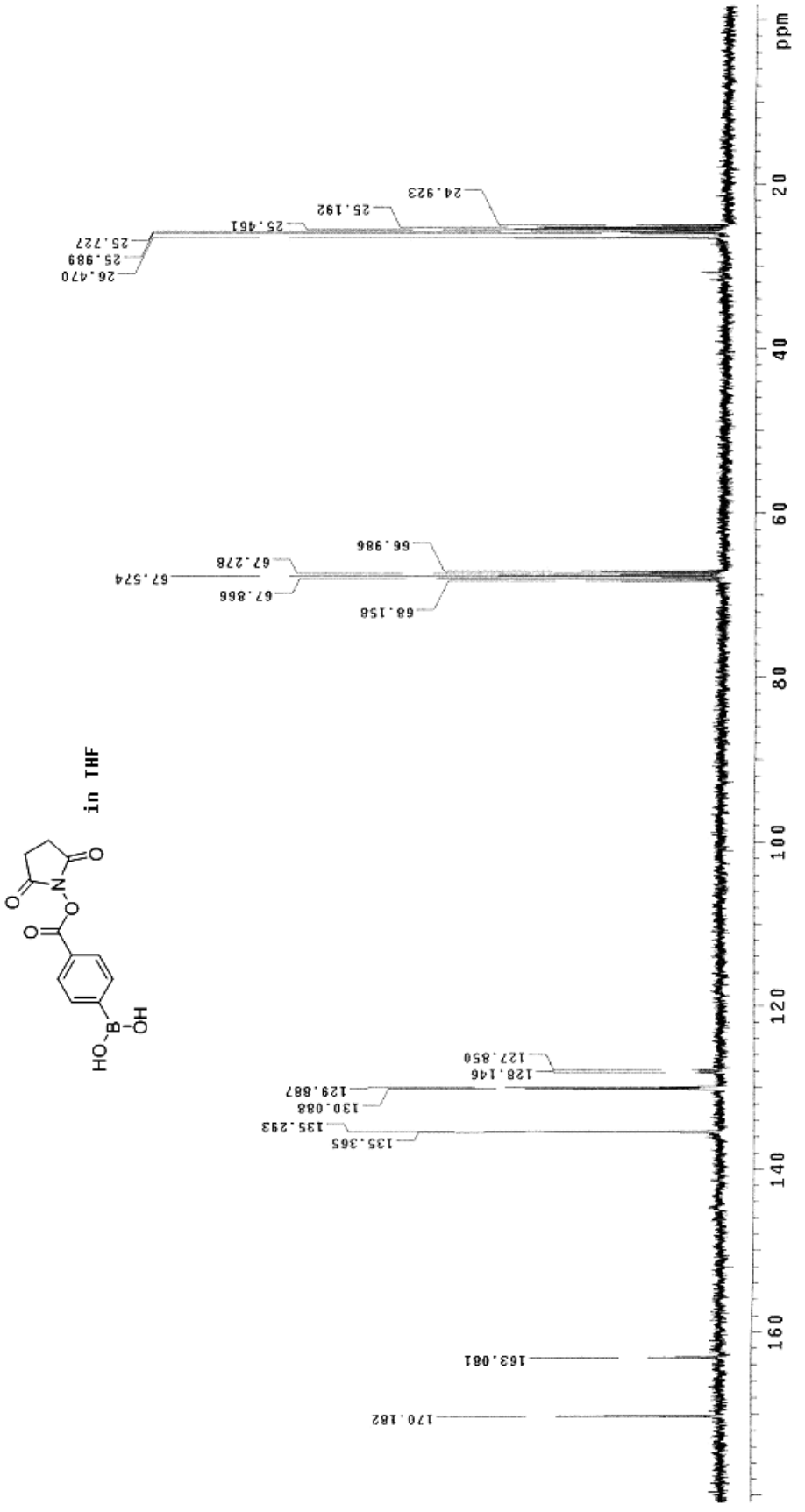
in THF
170.182
163.061
135.365
135.293
130.088
129.887
128.146
127.850
68.158
67.866
67.574
67.278
66.986
26.470
25.989
25.727
25.461
25.192
24.923
ppm
20
40
60
80
100
120
140
160

8.344
8.312
8.235
8.223
8.209
8.201
8.197
8.171
8.123
8.096
8.092
8.082
8.074
8.064
8.052
8.026
7.745
7.692
7.578
7.551
7.254
6.620
6.567
5.983
2.871
ppm
10.17
1.92
1.29
0.94
2.00
4.23

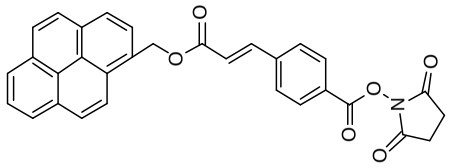
O
O
O
O
O
N
O
O

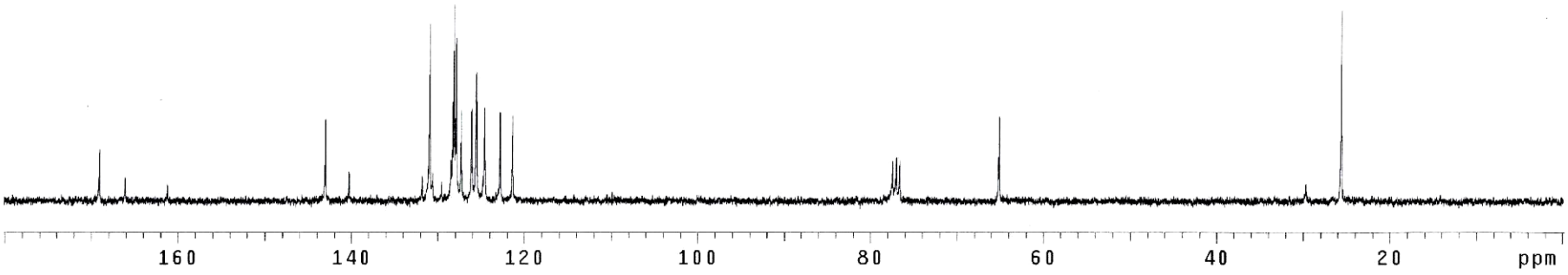
160
140
120
100
80
60
40
20
ppm

Reference and Notes

1. For a description of the chips used here, see: Dill, K.; Montgomery, D. D.; Wang, W.; Tsai, J. C. *Anal. Chim. Acta* **2001**, *444*, 69.

2. For alternative approaches, see: (a) Sullivan, M. G.; Utomo, H.; Fagan, P. J.; Ward, M. D. *Anal. Chem.* **1999**, *71*, 4369. (b) Zhang, S.; Zhao, H.; John, R. *Anal. Chim. Acta* **2000**, *421*, 175. (c) Hintsche, R.; Albers, J.; Bernt, H.; Eder, A. *Electroanalysis* **2000**, *12*, 660.

3. For real time signaling on an array, see: (a) Tesfu, E.; Roth, K.; Maurer, K.; Moeller, K. D. *Org. Lett.* **2006**, *8*, 709. (b) Stuart, M.; Maurer, K.; Moeller, K. D. *Bioconjugate Chem.* **2008**, *19*, 1514.

4. For Pd(II) reactions, see: (a) Tesfu, E.; Roth, K.; Maurer, K.; Moeller, K. D. *Org. Lett.* **2006**, *8*, 709. (b) Tesfu, E.; Maurer, K.; Ragsdale, S. R.; Moeller, K. D. *J. Am. Chem. Soc.* **2004**, *126*, 6212. (c) Tesfu, E.; Maurer, K.; McShae, A.; Moeller, K. D. *J. Am. Chem. Soc.* **2006**, *128*, 70.

5. For examples of the site-selective generation of base, see ref 2b and the work of Maurer et al. [Maurer, K.; McShea, A.; Strathmann, M.; Dill, K. *J. Comb. Chem.* **2005**, *7*, 637].

6. For the site-selective generation of acid, see: Kesselring, D.; Maurer, K.; Moeller, K. D. *Org. Lett.* **2008**, *10*, 2501.

7. For the use of CAN in a site-selective fashion, see: Kesselring, D.; Maurer, K.; Moeller, K. D. *J. Am. Chem. Soc.* **2008**, *130*, 11290.

8. For the site-selective use of Sc(III), see: Bi, B.; Maurer, K.; Moeller, K. D. *Angew. Chem., Int. Ed.* **2009**, *48*, 5872.

9. (a) Tian, J.; Maurer, K.;Tesfu, E.; Moeller, K. D. *J. Am. Chem. Soc.* **2005**, *127*, 1392. (b) Hu, L.; Maurer, K.; Moeller, K. D. *Org. Lett.* **2009**, *11*, 1273.

10. Tang, F.; Chen, C.; Moeller, K. D. *Synthesis* **2007**, 3411.

11. Hu, L.; Stuart, M.; Tian, J.; Maurer, K.; Moeller, K. D. *J. Am. Chem. Soc.* **2010**, *132*, 16610.

12. Lambert, J. D.; Rice, J. E.; Hong, J.; Hou, Z.; Yang, C. S. *Bioorg. Med. Chem. Lett.* **2005**, *15*, 873.

13. Hu, L.; Bartels, J. L.; Bartels, J. W.; Maurer, K.; Moeller, K. D. *J. Am. Chem. Soc.*

2009, *131*, 16638.

Chapter 3

The Development of New Polymeric Coatings for Microelectrode Arrays

3.1 Introduction to polymer coatings for microelectrode arrays

As mentioned in the last chapter, microelectrode arrays hold great promise as platforms for monitoring ligand-receptor binding events in "real-time". For this reason, we have been developing the synthetic tools necessary for site-selectively building and placing molecules by the Pt-microelectrodes in an active-semiconductor array. Key to this work is coating the arrays with a porous reaction layer that allows for the attachment of substrates or completed library members to the surface of the arrays proximal to the microelectrodes. To date, both agarose[1] and sucrose[2] have been used for this purpose. Both approaches have significant weaknesses. In the case of agarose, the polymer coating is unstable. It delaminates from the surface of the array with time, dissolves in a variety of solvents, and reacts with a number of the reagents used to perform site-selective syntheses.[3] For this reason, agarose is mainly used as a "practice-polymer" for studying new reactions on the arrays. The use of a sucrose-based coating solves these problems by providing a stable surface for generating functionalized arrays. However, like agarose the sucrose-coating provides a polyhydroxylated surface on the array. This surface limits the use of the microelectrode arrays for monitoring the behavior of small molecules that are synthesized by constructing core scaffolds and then diversifying the scaffolds through

the use of protected amine and alcohol functional groups. In addition, preparing a stable sucrose surface requires special cleaning and handling of the microelectrode array performed in a clean room.

With these things in mind, we sought to develop a new approach to coating the arrays that would allow for customization of the surface. Any porous reaction layer developed needs to be chemically inert, stable to multiple reaction steps and washings, functionalized in a manner that allows for site-selective modification proximal to the microelectrodes in the array, and porous enough to allow for both electrochemically mediated synthetic reactions[1,2] and electrochemical impedance experiments[2a,4]. In addition, preparation of the coating needs to be general so that it can be tailored for specific uses in the future. To this end, it appeared that a UV-cross-linkable di-block copolymer like the one illustrated in Figure 3.1 might be ideal.[5]

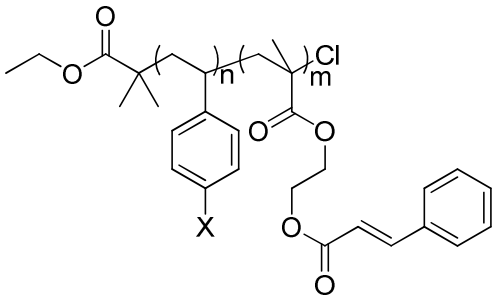

X = Cl, Br, I, $B(OH)_2$, $B(OR)_2$, OTf, OH, NH_2, etc

Figure 3.1 Di-block copolymer strategy with a functionalized block for attachment of the substrates and a UV-cross-linkable block for attachment to the array surface.

One block in the polymer could be used to fix the polymer to the surface of the array, and the second used to provide attachment points for substrates to the resulting

surface. To fix the polymer to the surface of the array, the first bock of the polymer was designed to employ of the cinnamoyl-substituted polymethacrylate (PCEMA) strategy developed by Guojun Liu and co-workers.[6] This chemistry takes advantage of the photochemical dimerization of the cinnamoyl groups to provide stability to the coating. The key question for this strategy was whether the resulting nonconductive, cross-linked copolymer would be porous enough to allow for both the electrochemically mediated reactions needed for placing molecules on the surface proximal to the microelectrodes and the electrochemical impedance experiments needed for monitoring ligand-receptor interactions on the arrays.[7]

To fix molecules to the surface of the array, the second block utilized a 4-substituted styrene starting material. This provided a handle on the surface so that Heck, Suzuki, and Cu(I)-catalyzed reactions[8] could all be used to add functional groups to the array.

3.2 Surface conditions on the microelectrode

Before applying any coating to the microelectrode array surface, it is important to know the surface properties of the microelectrode. The shape of the electrodes, the material that the electrodes are made of, the smoothness of the electrode surface, and other properties may all affect the overall performance of the coatings.

To begin, we currently use one of two types of microelectrode arrays. The 1-K arrays have a density of 1,024 electrodes/ cm^{-2}, and the 12-K arrays have a density of

12,544 electrodes/cm^2. The diameter of an electrode in a 1-K array is around 92 μm, and the distances between the electrodes are 245 and 337 μm since the individual cells are rectangular. The diameter of an electrode in a 12-K array is around 44 μm, and the distance between the electrodes is 33 μm, as the cells are square. So the surface of the array is comprised of both electrodes and the regions between the electrodes. Two questions arise about such a setup: what is the nature of the surface in between the electrodes and is the surface of the electrode smooth or uneven with the surface between the electrodes elevated or recessed relative to the electrodes?

The answers to these questions lie in the fabrication process of the microelectrode arrays. The array was fabricated by layering different layers of materials on top of one another, including the matrix, the circuit, the electrodes and a protective layer. The last two steps of the layering have the most impact on the surface. They are accomplished by first putting the platinum electrodes down onto the array and then covering the whole array with a passivation layer made from a ceramic, corrosion-resistant material, namely silicon nitride. The silicon nitride immediately above the electrode is then removed with a laser to expose the platinum electrode. The area in between the electrodes remains protected by silicon nitride. Thus, to answer the first question, the material on top of the electrode should mainly be platinum. However, a small amount of silicon nitride residue most likely remains on top of the platinum electrode. With respect to the second question, the electrode surface is at a level lower than the surrounding silicon nitride surface. This can be observed in an AFM image of the array (Figure 3.2). Since only 12-K array is capable of performing

electrochemical signaling experiments, only the 12-K array surface was investigated in this manner.

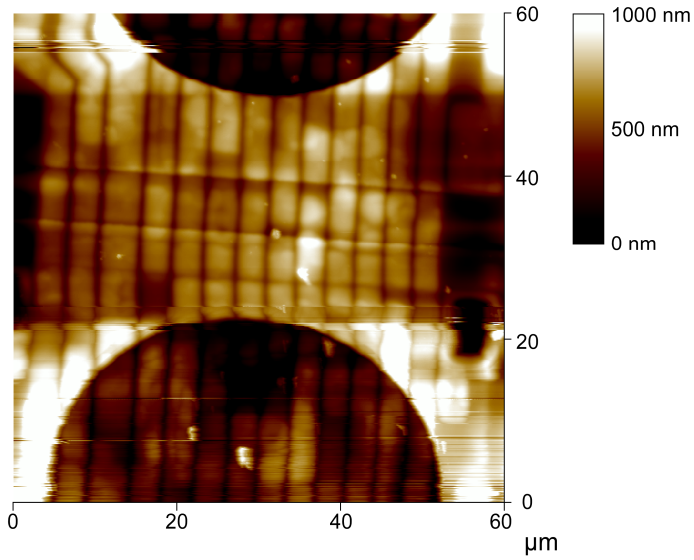

Figure 3.2 AFM image of the electrode surface and the areas in between the electrodes on a 12-K microelectrode array slide.

Based on the AFM image, it can be estimated that the depth of the well in which the electrodes reside is around 0.5 μm. This is a very important piece of information for coating applications, as the thickness of coatings could range from a few nanometers to a few micrometers. If the coating is very thin, say less than 50 nm thick, then the height difference between the inside and the outside of the well would still persist after the coating is applied. In contrast, if the coating is very thick, greater than 5 micrometers, then the coating will fill in the well and even out the surface. Either way, the coating conditions will become more complicated when the polymer surface is spin-coated onto the array. Spin-coated surfaces are inherently thinner at the center of the spinner than towards the edges.

Although there are potential problems that could arise from these issues, the key properties of any surface used are electrochemical. Do the differences caused by the unevenness of the surface have negative effect on the uniformity of the reactions over the array as well as the reproducibility of electrochemical signaling experiments? If the answer to this question is no, then the differences across the array will not matter.

Another detail about the AFM image shown above is the straight lines that cut across the entire array including the surface of the electrode. These lines indicate a finer secondary structure associated with the surface of the array. This is better seen with an image showing a higher magnification of the surface (Figure 3.3a), as well as a 3D-image of the surface (Figure 3.3 b) which clearly shows grooves on the surface of the array. The average depth of the groove is around 200 nm, while the average width of each "hill" is 3 μm. So the groove is actually not as steep as the figure shows. According to information obtained from CombiMatrix, the uneven surface is caused by the wiring of the circuit during manufacture process. This unevenness can be removed and the surface made more even, but such efforts did not improve the electrochemical performance of the microelectrode array. Hence, further processing of the array was skipped in order to reduce fabrication costs. As with the presence of the wells associated with the electrodes, the grooves on the array do pose problems for coating the arrays. Fortunately, the variations did not influence the performance of the surfaces as we will see later.

a) b)

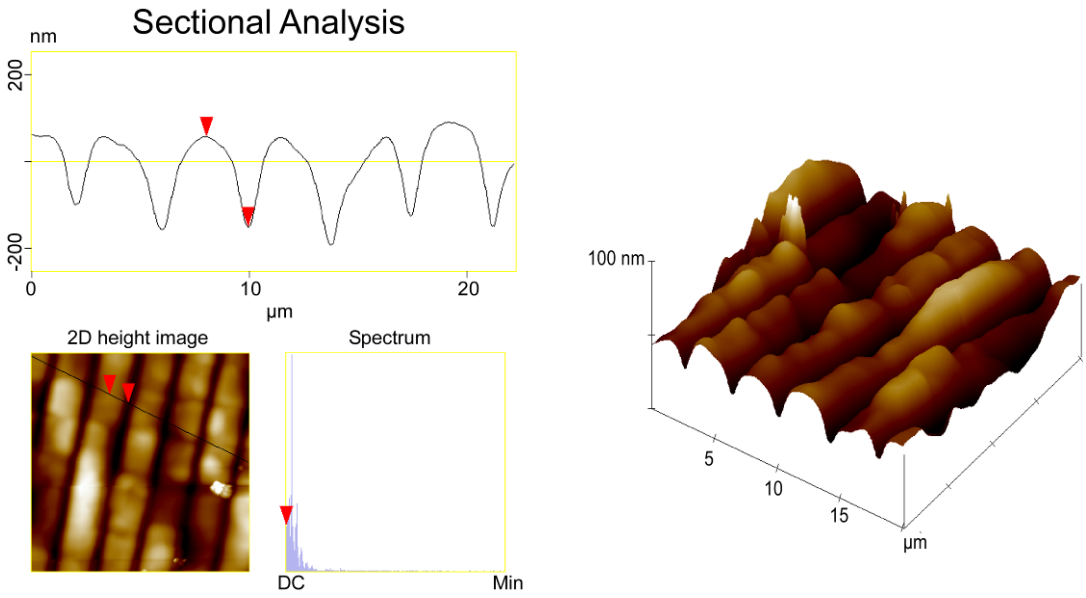

Figure 3.3 a) Magnified image of the surface inside the electrode "well". The uneven surface is caused by the wiring of the circuit during manufacture process. b) A 3D-image of the electrode surface.

3.3 Background information on the PSt-b-CEMA di-block copolymer

The idea of using a UV-cross-linkable di-block copolymer originated from Guojun Liu's work[5] and their use of a di-block copolymer comprised of a polystyrene (PSt) block and a poly(2-cinnamoyloxyethyl methacrylate) (PCEMA) block. This PSt-b-PCEMA block copolymer has several properties that make it a perfect candidate for coating an array. First, although not mentioned in the original paper,[5] the PCEMA block can be cross-linked[6] by a photo [2+2] cycloaddition (Scheme 3.1) to form a very stable polymer network. This polymer is insoluble in most solvents and should therefore stay on the array once the crosslinking step has been completed. Second, when a solvent mixture is used that is comprised of one solvent that dissolves both blocks and one solvent that dissolves only one block, the block copolymer will

form a polymer brush structure on the surface. The insoluble block (to the second solvent) is placed next to the surface and the soluble block exposed to the solution (Figure 3.4). For our purposes, such a system can be used to place the PCEMA block of the di-block copolymer next to the surface. This would leave the functionalized styrene block of the polymer exposed to the solution so that it will be easier to attach the substrates.

Scheme 3.1

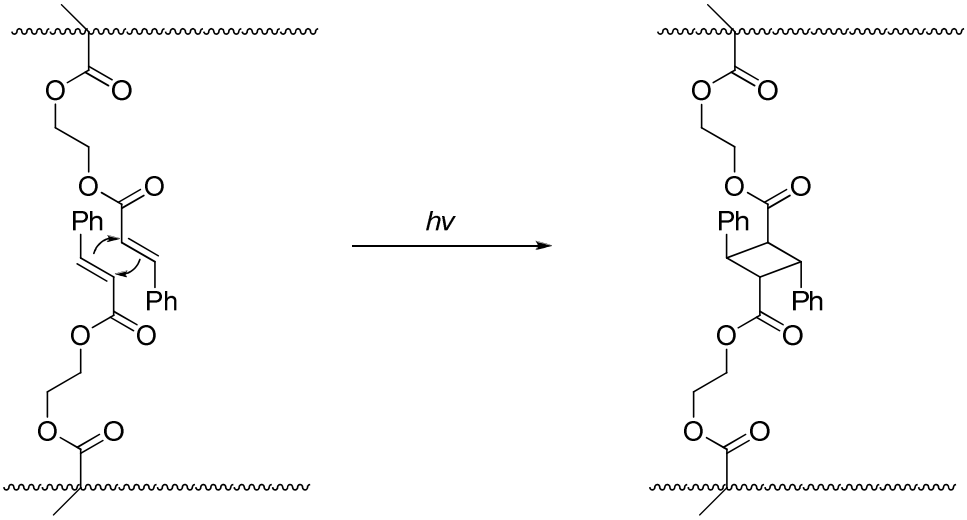

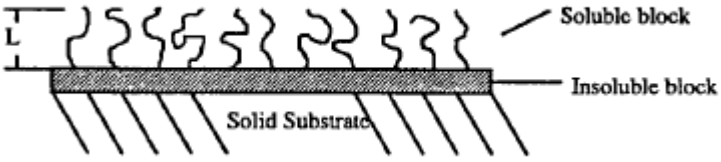

Figure 3.4 Brush structure formed by using a mixed-solvent solution of di-block copolymer, image courtesy of *Macromolecules*, ACS Publication.

However, there were also some drawbacks associated with the synthesis of the PSt-b-CEMA block copolymer in this paper. First of all, the block copolymer was

synthesized with anionic polymerization, which is notorious for its extreme sensitivity to moisture and impurities. Second, a TMS protected 2-hydroxyethyl methacrylate (HEMA) monomer was used instead of HEMA itself, (Scheme 3.2) so that the free hydroxyls would not terminate the anionic polymerization. This approach not only increased the steps needed to make the final CEMA block, but also raised the cost of the HEMA monomer greatly.

Scheme 3.2

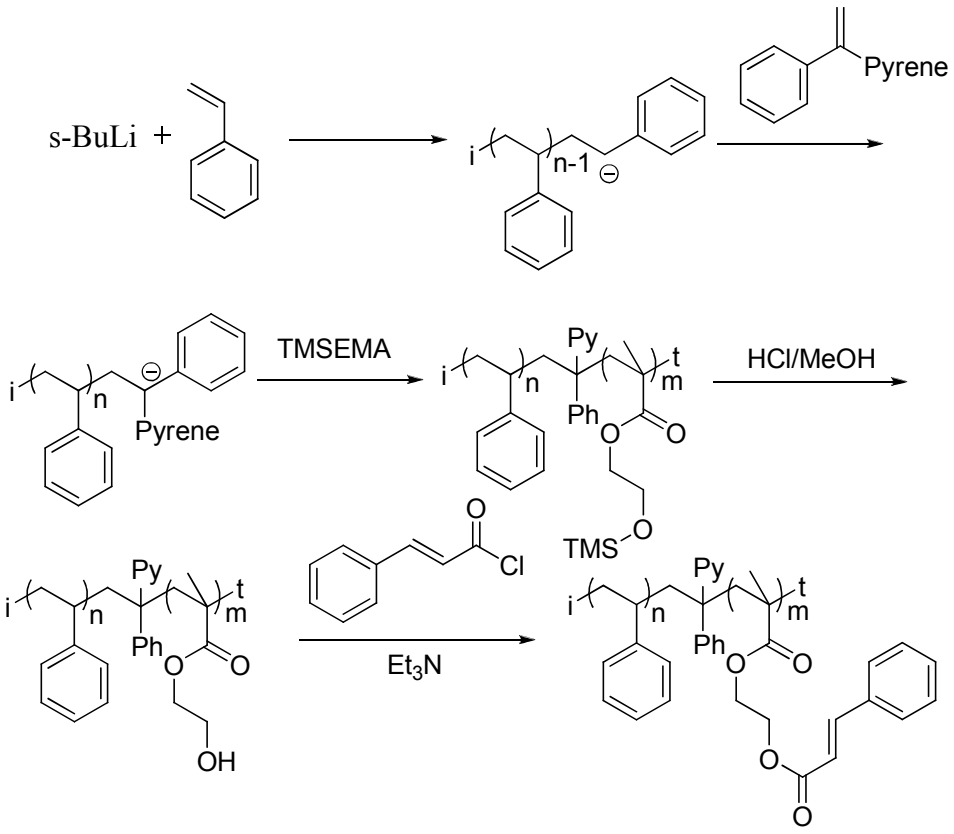

To take advantage of this block copolymer, there were several questions that needed to be answered. First, will the block copolymer form a brush structure on the surface of the array, and is such a structure really necessary for our needs? Second, is

there a better way to make the polymer instead of anionic polymerization? Third, will a new method for synthesizing the polymer allow HEMA to be used directly in the polymerization as a monomer or will it still need to be protected?

The first question could not be answered in a simple manner. As mentioned in Section 3.2, the array surface is not smooth. Even if the block copolymer can form a brush structure on the surface, it will not change the uneven nature of the surface because such brush structures typically involveare only a single layer of self-assembled polymer. So how effective will the surface coating be? This is a question that can only be answered by testing it.

Fortunately, the second question is simple to answer. Back in the early 1990s, living radical polymerization techniques were still at infancy, so the controlled polymerizations of vinyl type monomers were still dominated by cationic and anionic polymerization. However, about the same time Liu's paper was published, Wang and Matyjaszewski reported the first atom transfer radical polymerization (ATRP),[9] which started a large effort to capitalize on "living" radical polymerizations. More than a decade later, "living" polymerization techniques, including ATRP, RAFT and NMP have become the predominant methods to synthesize the vinyl-type block copolymers. Since styrene and methacrylates are substituted vinyl monomers, there was little doubt when we started that the desired PSt-b-CEMA block copolymer could be made by living radical polymerization. Compared to anionic polymerization, living radical polymerization has a lot of advantages. The most important of these is its tolerance of impurities and water. A number of the living radical polymerizations can actually be

accomplished in water.[10] Since the use of ultra pure monomers and ultra dry solvents is not required for living radical polymerization, the reactions are significantly easier to perform.

To answer the third question, a brief search in the literature revealed that HEMA can be polymerized directly as an unprotected monomer both with ATRP[11] and RAFT approaches.[12] Since living polymerizations, especially RAFT polymerizations are quite tolerant of functional groups,[13,14] a wide range of monomers with unprotected functional groups such as the hydroxyls in the HEMA case, as well as amino groups and carboxylic[14a] acid groups can be used.

3.4 A Brief Introduction to "Living" Radical Polymerizations (LRPs)

Radical polymerization has been one of the most widely used processes for the commercial production of high-molecular-weight polymers. Its predominant role in the production of vinyl type polymers is due to its tolerance of functional groups, different reaction conditions and impurities, and ease of operation. However, there are two major drawbacks of conventional radical polymerization (CRP). First, it is very difficult to precisely control the molecular weight, as well as the molecular weight distribution of the product polymer with CRP. Second, the ability to make different polymer structures like block copolymers, brush copolymers, star-shaped polymers and so on is very limited due to its irreversible termination mechanism.

However, this situation greatly improved when living radical polymerization (LRPs) techniques appeared in the mid-1990s.[13,14] The most utilized LRP techniques

are Nitroxide Mediated Polymerization (NMP), Atom Transfer Radical Polymerization (ATRP), and Reversible Addition-Fragmentation chain-Transfer radical polymerization (RAFT). Although mechanistically different, all living radical polymerizations employ the same concept in their development, the usage of reversible termination/capping.

The mechanistic differences between conventional and living polymerization are illustrated in Scheme 3.3. The most important difference is that with CRP the growing polymer chain is terminated irreversibly by radical recombination, radical disproportionation, or chain-transfer (Scheme 3.4). With a living radical polymerization the growing polymer chain is terminated reversibly.

Scheme 3.3

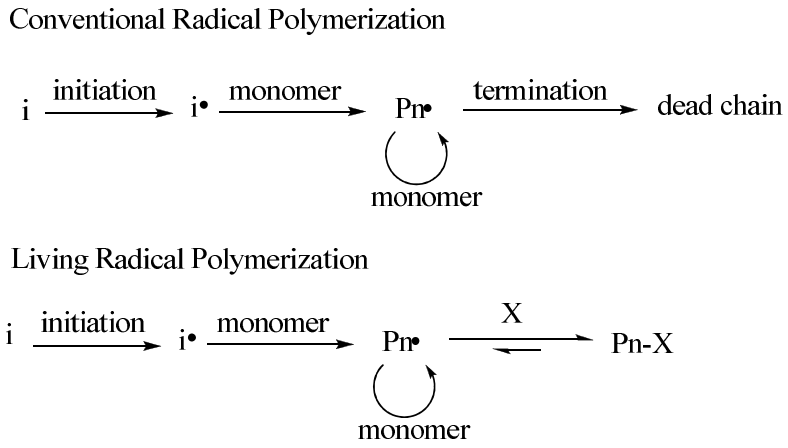

Scheme 3.4

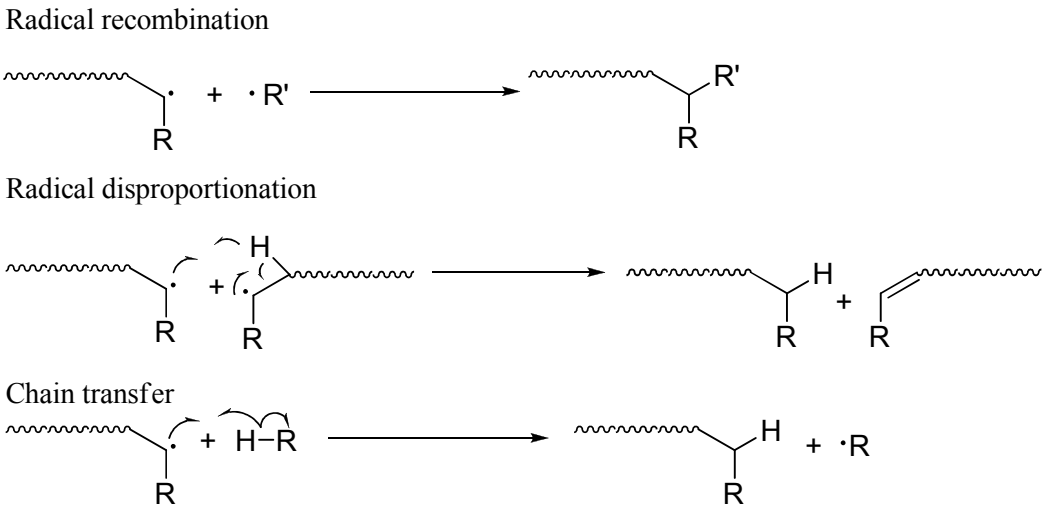

By predominantly keeping the growing polymer chain in a dormant capped state, living polymerization techniques greatly reduce the concentration of active radicals in the reaction mixture. This reduces the rate of irreversible termination events illustrated in Scheme 3.3. Two advantages are gained. First, since the radical concentration is low, the rate of initiation is usually much faster than the rate of propagation, so all polymer chains start to grow at about the same time and grow at a similar rate, resulting in a much narrower molecular weight distribution. With CRP, propagation is faster than initiation, thus when a chain is initiated, it will propagate rapidly and reach high molecular weight in a short time, and then terminate irreversibly. Then another chain is initiated and follows the same pathway. A diagram shows the difference between conventional and living radical polymerization on the change of molecular weight vs. the reaction time is shown in Figure 3.5. It is very obvious that by using LRP, the molecular weight can be strictly controlled by the initial monomer/initiator ratio and the conversion of the reaction. Such control is

much less effective with CRP.

The other advantage of the LRP over CRP is the ability to make copolymers with complex structures. Because the capping group on the chain end of a polymer made by LRP can be initiated again under proper conditions, the polymer made from LRP techniques can serve as a macroinitiator to trigger the formation of a second polymer on the end of the first. With such strategy, block copolymers can be easily made with well-defined molecular weight and block ratios. In addition, with multi-functionalized initiators and initiator-containing monomers, more complex structures like star-shaped polymers and graft copolymers can be made.

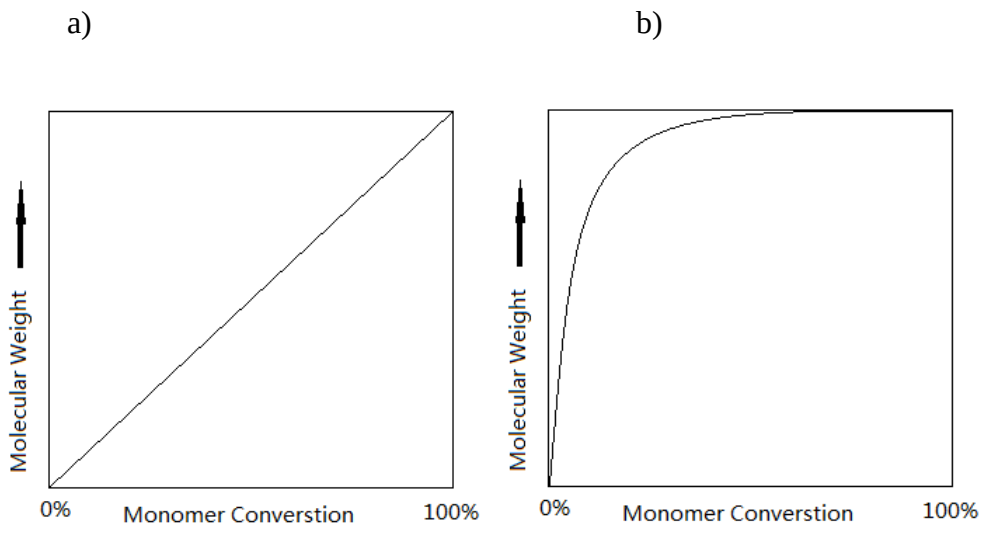

Figure 3.5 Diagram of molecular weight vs. monomer conversion of a) Living radical polymerization; b) Conventional radical polymerization.

As mentioned before, the most utilized LRP techniques currently are ATRP, RAFT and NMP. The reversible termination group employed in each technique is

different, but the principle is similar. For ATRP, the initiation, propagation and reversible termination is illustrated in Scheme 3.5. The reversible termination group employed in ATRP is usually bromide or chloride. Copper-based salts are common catalysts, although palladium and rhodium-based ATRPs have also been reported.[13]

Scheme 3.5

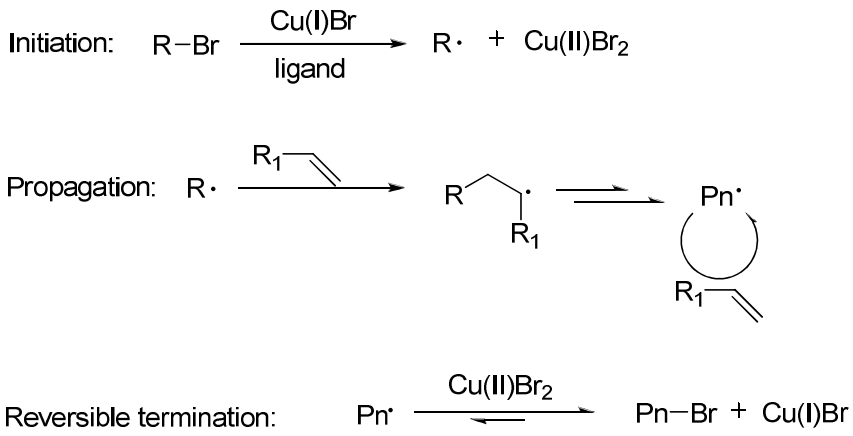

Similar to ATRP, NMP uses strategy of reversible termination with a stable nitroxide radical. (Scheme 3.6)

Scheme 3.6

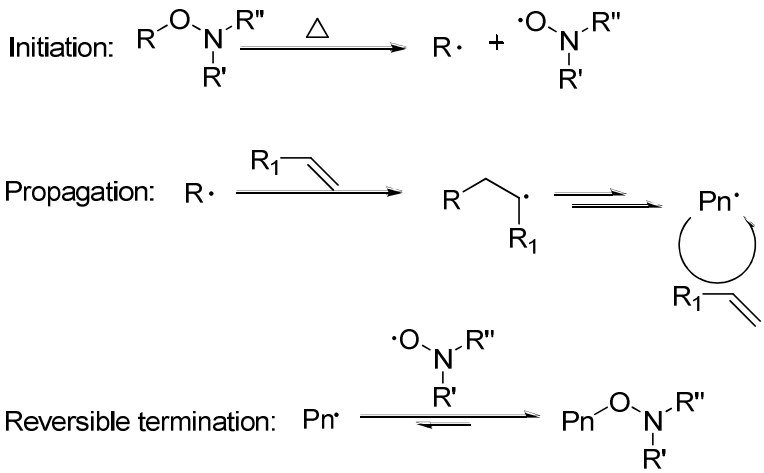

Compared to the previous two examples, the mechanism of a RAFT polymerization is somewhat different. The concept introduced by RAFT is reversible chain transfer, rather than reversible termination. In addition, RAFT polymerization needs to employ a conventional radical initiator like AIBN as a source of radicals. The mechanism of RAFT is illustrated in Scheme 3.7.

Scheme 3.7

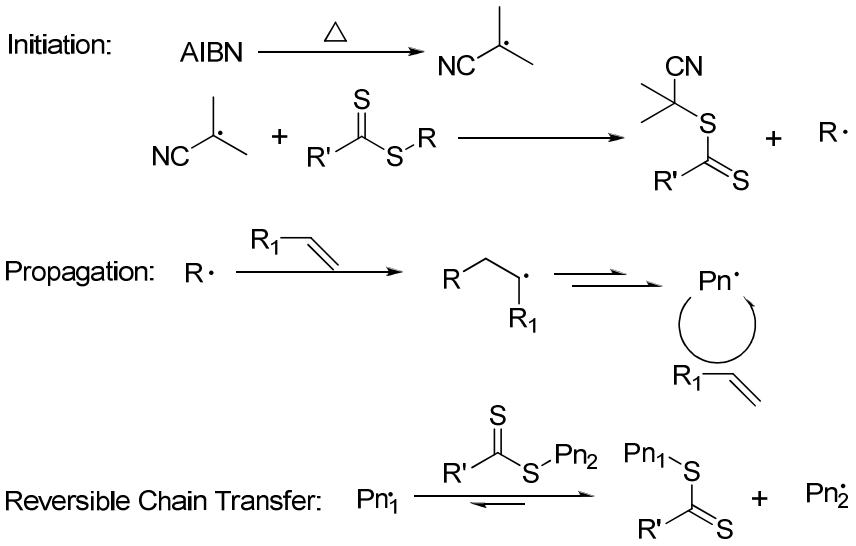

Different LRP techniques have their own advantages. For example, ATRP is easily tunable for making block copolymers. With transhalogenation, even a less reactive monomer can be used as the first block to initiate a more reactive monomer later. NMP has the advantage of simple operation, as the reaction system is comprised of a minimum number of ingredients. RAFT is known to be most tolerable of different kinds of monomers and functionalities, which makes it a suitable method of making difficult to synthesize polymers that contain functional groups like amines, alcohols, and carboxylic acids.

3.5 Initial study on the preparation of block copolymer of PBrSt and PCEMA

Since we already know that it would be easier to make the block polymer with living radical polymerization instead of anion polymerization, we decided to test whether we can use the 2-cinnamoyloxyethyl methacrylate (CEMA) monomer directly for the copolymerization instead of using HEMA and then adding the cinnamoyl group later. The idea was to save at least one reaction step, as well as the purification of the intermediate polymer. To study the possibility of using CEMA directly, styrene (St) and methyl methacrylate (MMA) were used as cheaper alternatives to 4-bromostyrene and CEMA. It is well known that MMA is a more reactive monomer than styrene, so in order to make the block copolymer, the reaction sequence polymerized MMA first. The PMMA obtained would then be used as a macroinitiator to polymerize styrene. The synthesis was conducted as illustrated in Scheme 3.8.

Scheme 3.8

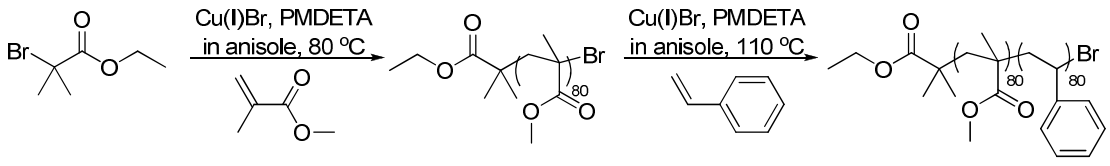

The model study proved successful, but before the chemistry could be used to build the desired substrate some concerns need to be addressed. First, different from MMA, CEMA has another double bond located on the cinnamate moiety which can potentially be polymerized. If the cinnamate undergoes polymerization during

assembly of the polystyrene block, then it will form a cross-linked network. Second, for the styrene part, 4-bromostyrene is itself a halide. Although the possibility of it undergoing a reaction to form a phenyl radical is very small, it can potentially serve as an initiator to cross-link the polymer chains.

To address these issues, a number of studies were undertaken. First, the polymerization of CEMA was performed at different temperatures (Scheme 3.9). It was found out that at approximately 80 ^{0}C the CEMA underwent polymerization without competitive polymerization of the cinnamate group. However, when the temperature was increased to 110 ^{0}C, polymerization of the cinnamate group competed well and an insoluble mass was obtained.

Scheme 3.9

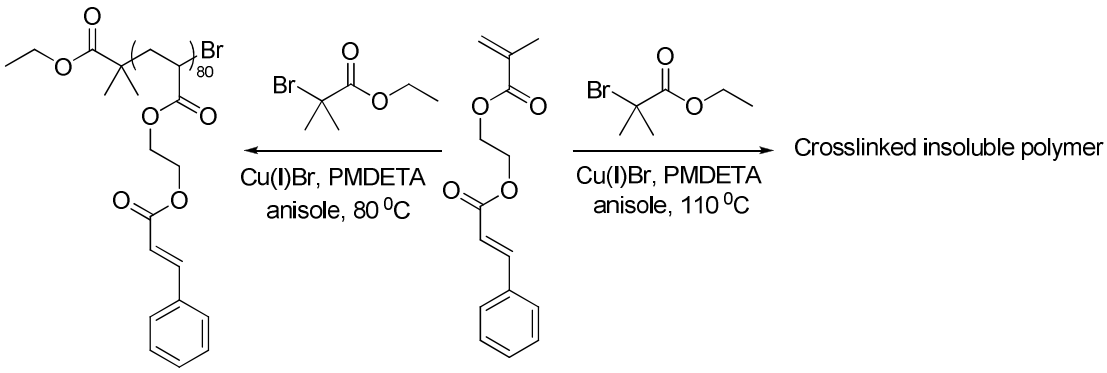

In order to make the di-block copolymer, the CEMA block should be polymerized first and then the styrene block added. In order to have efficient initiation of the second block, the more reactive monomer should always be used to construct the first block. In this way, the initiation step for the second polymerization is faster than growth of the polymer. This leads to a better size distribution for the second

block of the copolymer. Due to the slow rate of styrene polymerization at low temperatures, the polymerization of styrene was carried out at 110 ^{0}C. These conditions worked best if the styrene was diluted with a solvent. With this in mind, it was important to see if the 4-bromostyrene monomer could be polymerized at a lower temperature. If not, the conditions needed to make the styrene block might polymerize the cinnamate group in the first block. To answer this question, as well as the question asked earlier about whether 4-bromostyrne can serve as an initiator for ATRP, the polymerization of 4-bromostyrene was studied at different temperatures and different polymerization conditions (Scheme 3.10).

Scheme 3.10

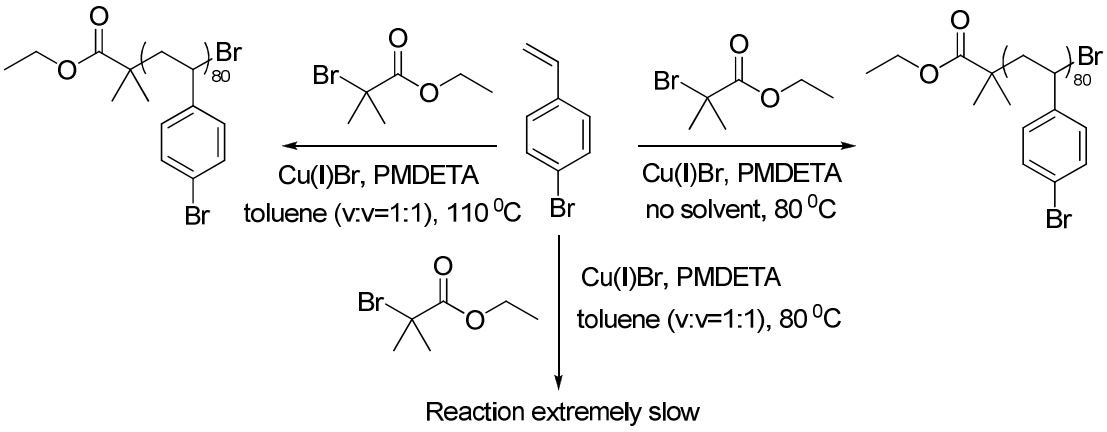

It was found that BrSt would undergo polymerization at 80 ^{0}C. The reaction worked best when conducted with no added solvent. The polymerization became very slow once solvent was used. It should be noted that the polymerization did occur when the temperature was increased to 110 ^{0}C with solvent added. However, under these conditions polymerization of the cinnamate would also occur. It is actually very

easy to understand this observation. In radical polymerization, styrene and acrylates are considered to have similar reactivity, which means that they will polymerize under similar conditions. The cinnamate group in CEMA is essentially a combination of acrylate and styrene, so the reactivity is expected to be similar as well. Under the condition that styrene would polymerize, the cinnamate group probably would polymerize as well, which means using CEMA as a monomer for the synthesis of the di-block copolymer is not a good idea. On the more positive side, we did find that 4-bromostyrene could be polymerized to provide a linear homopolymer without any side-reactions resulting from the initiation of ATRP with the bromides on the phenyl ring.

3.6 Synthesis of PBrSt-b-CEMA from PBrSt-b-HEMA

Having discovered that CEMA was not a viable monomer for the synthesis of the block copolymer, attention was turned to the use of the precursor for CEMA, 2-hydroxyethyl methacrylate (HEMA). If a block copolymer of PBrSt-b-HEMA could be made, then it could potentially be transformed into PBrSt-b-CEMA with the use of an esterification reaction (Scheme 3.11).

Scheme 3.11

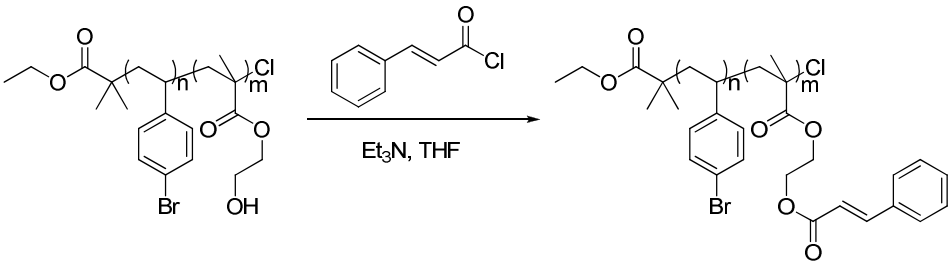

In Liu's paper[5], a TMS protected HEMA monomer HEMA-TMS was used to approach the di-block copolymer. Back then, living radical polymerization was still not widely available, so the hydroxyls had to be protected for the anionic polymerization. However, recently the polymerizations of HEMA directly under ATRP[11] and RAFT[12] conditions have been reported, so the usage of the much more expensive HEMA-TMS monomer is no longer necessary.

Due to the poor solubility of PHEMA in non-polar solvents, including styrene itself, polymerization of HEMA as the first block would not be a good choice. As a result, 4-bromostyrene was polymerized as the first block with the use of PBrSt as the macroinitiator. The block copolymerization of of HEMA onto the initial polymer was then carried out following the literature method.[11] After the PBrSt-b-HEMA was made, the block copolymer was subjected to modification with cinnamoyl chloride. The final polymer of PBrSt-b-CEMA was obtained upon precipitation from methanol (Scheme 3.12). The precipitation step was done twice in order to obtain a higher level of product purity.

Scheme 3.12

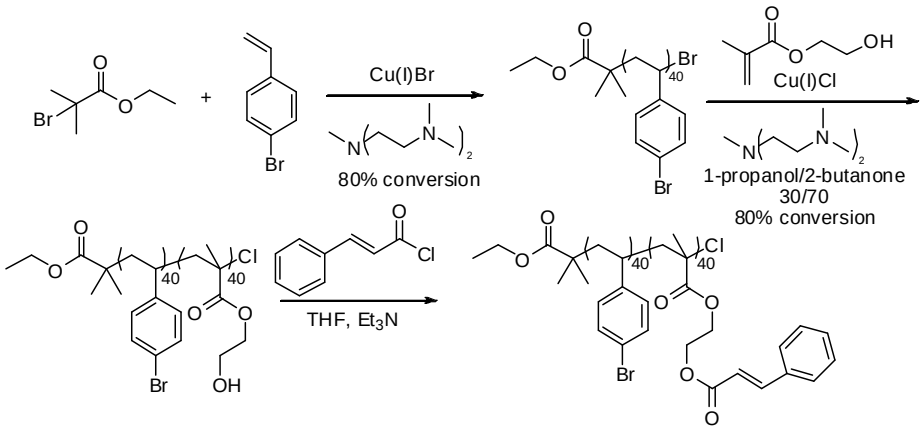

According to NMR, the block ratio of BrSt and CEMA was about 1:1. However, this did not indicate the formation of a di-block copolymer (the NMR would also be consistent with two homopolymers of equal length). Further evidence was needed to show that the molecular weight did increase from the homopolymer of PBrSt by GPC. As a result, samples of the homopolymer of PBrSt and the block copolymer PBrSt-b-CEMA were tested with GPC. The result is shown in Figure 3.6.

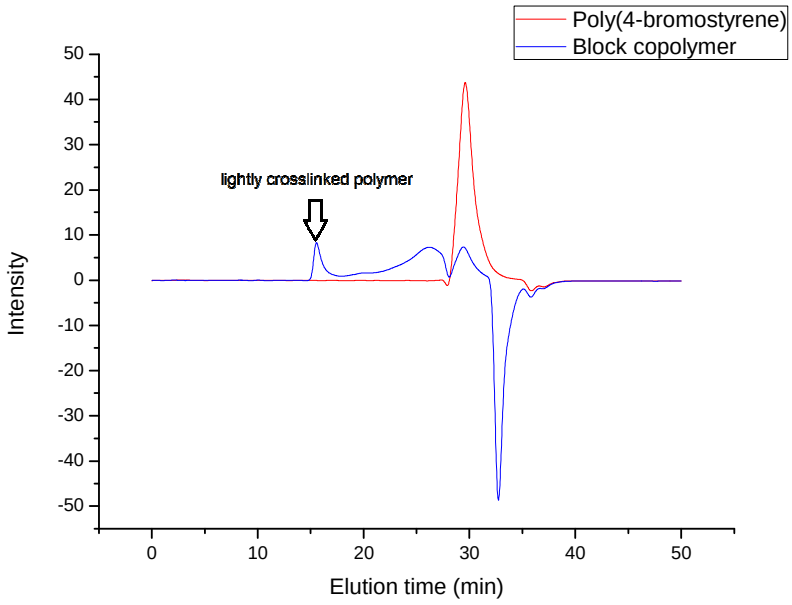

Figure 3.6 GPC data of homopolymer of PBrSt (red line) and block copolymer PBrSt-b-CEMA (blue line), methanol as internal standard.

As shown by the GPC data, the molecular weight of PBrSt-b-CEMA was larger than the molecular weight of the homopolymer of PBrSt, as shown by a shorter retention time. The negative peak was from methanol which was used as an internal standard. However, two problems also became evident from the GPC data. First, there was a considerable amount of PBrSt left uninitiated as shown by the blue peak right

under the red peak. This indicated that the initiation efficiency was not 100%. Second, the PBrSt-b-CEMA peak had a long tail, as well as another peak at the solvent front, indicating the existence of slightly cross-linked polymer, which had several times the molecular weight of a single polymer chain. To solve the first problem, the intermediate block copolymer PBrSt-b-HEMA was precipitated in a 1:1 mixture of hexane and ethyl acetate. In this solvent mixture, the homopolymer of PBrSt was able to dissolve, but the block copolymer PBrSt-b-HEMA was not. In this way, the uninitiated PBrSt was largely removed from the polymer mixture after the second polymerization, and only the block copolymer was subjected to the subsequent esterification with cinnamoyl chloride. GPC data verified that this approach was successful in removing the PBrSt homopolymer (Figure 3.7).

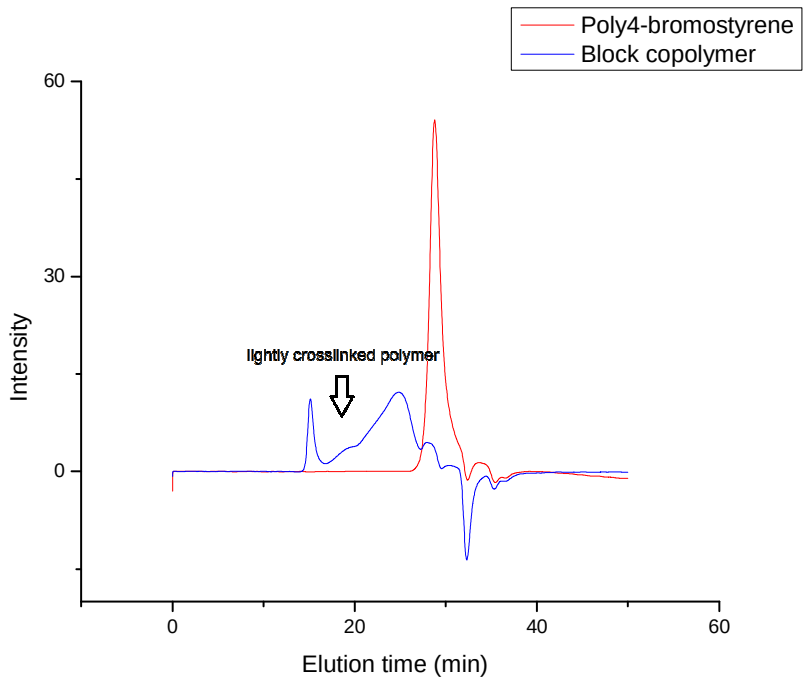

Figure 3.7 GPC data of homopolymer of PBrSt (red line) and purified block copolymer PBrSt-b-CEMA (blue line), methanol as internal standard.

For the second problem, it was decided that as long as the lightly cross-linked oligomer of single chains did not precipitate or affect our ability to coat the arrays with the polymer, it would be ignored. After all, all of the polymer chains would be cross-linked after the polymer was placed on an array.

3.7 Application of PBrSt-b-CEMA as a functional surface for the array

Once the block copolymer PBrSt-b-CEMA was made, it was tested as a coating for the microelectrode arrays. Due to the lower molecular weight as well as the much lower polarity of the copolymer compared with agarose, the solution of PBrSt-b-CEMA was much less viscous than the agarose solution. This led to problems in spin coating while applying the polymer to the surface. The usual condition for applying an agarose coating was using 0.04 g/mL agarose in 95:5 DMF/H_2O with 2000 rpm for 45 seconds. When these conditions were used for the block copolymer, the coating generated was too thin to provide enough functional groups on the surface of the electrodes. Subsequent reactions failed. As a result, the spin coating condition was optimized. It was found that the use of 0.03 g/mL copolymer in 1:1 THF/p-xylene with 1000 rpm for 40 seconds led to a better coating on the array. After that, the chip was subjected to UV irradiation with a 100 W mercury lamp for 15 minutes.

The coating was then subjected to a series of stability tests. It was examined for its stability against abrasion, washing, incubation with different solvents, etc. It was found out that the polymer coating was very stable under regular operation procedures for microelectrode array reactions. It could withstand light abrasion,

multiple washings, and could be left in a variety of solvents including DMF, although heavy washing with DMF did cause small parts of the coating to delaminate. After the initial test of stability, the polymer was examined for its compatibility with synthetic reactions on its surface. At the time, it was still unknown what the morphology of the polymer would be on the surface and whether or not the bromophenyl functionality would be accessible to the reaction solution. The Suzuki reaction was chosen for an initial test for the polymer. 1-Pyreneboronic acid was chosen as the substrate in the solution. The reaction is shown in Scheme 3.13.

Scheme 3.13

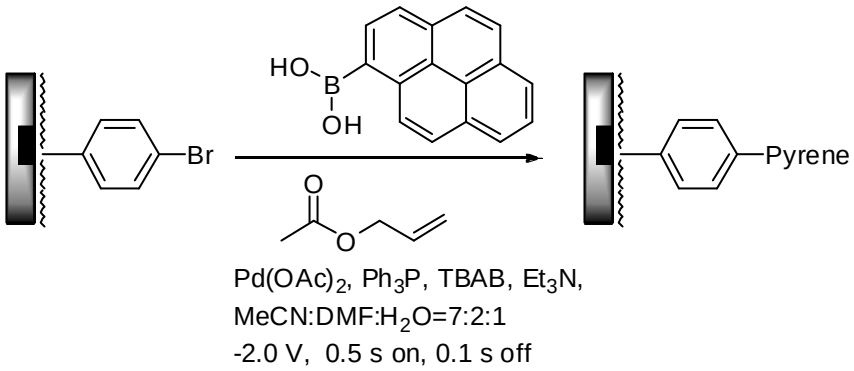

a) b)

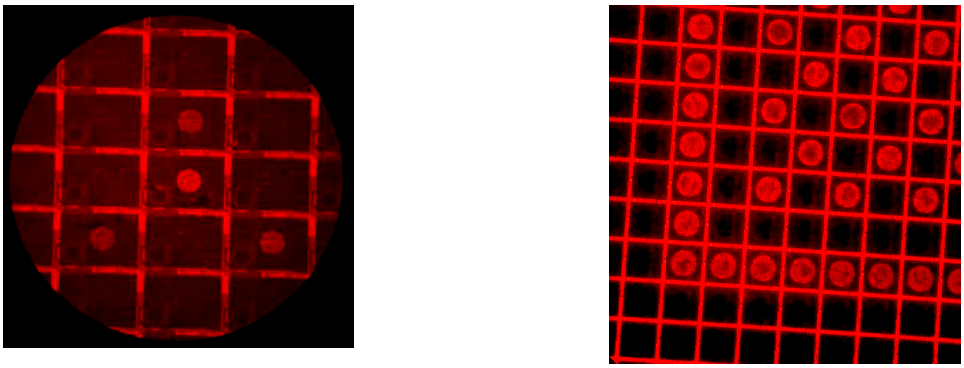

Figure 3.8 a) Suzuki reaction with PBrSt-b-CEMA as coating on 1-K array, the reaction time for each spot is respectively: lower left - 3 min; lower right -6 min; upper middle - 9 min; center – 18 min. b) Suzuki reaction with PBrSt-b-CEMA as coating on 12-K array, reaction condition: -1.7 V, 90 pause for 3 times.

Much to our delight, the block copolymer was compatible with reactions run on both 1-K and 12-K arrays (Figure 3.8). For the reaction on the 1-K array, the surface was able to withstand reaction times of 8 minutes without any problem. As a matter of fact, the surface was tested for stability against reaction conditions for more than 15 runs, each with 3 minutes reaction time. The polymer did not show any delamination from the electrode surface although the array itself stopped functioning after such intensive usage. It seems that the surface will survive past the life-expectancy of the array under these conditions. Another test was done by using an array coated three months prior to the experiment for the Suzuki reaction. Even after this extended time period, the PBrSt-b-CEMA surface was still viable and showed no difference from a freshly prepared surface in terms of stability and compatibility with reactions run on the array. This level of stability was a great improvement relative to agarose coatings on the arrays that remain viable for only a few days.

As a demonstration of the versatility of the block copolymer surface, three different reactions were run on the same chip side by side. The Suzuki reaction was run with a pattern shaped with letter “S”, the Heck reaction with a letter “H” and a copper(I) catalyzed coupling reaction between amines and aryl halides with a letter “C”. The reaction conditions were shown in Scheme 3.14 and results shown in Figure 3.9.

Scheme 3.14

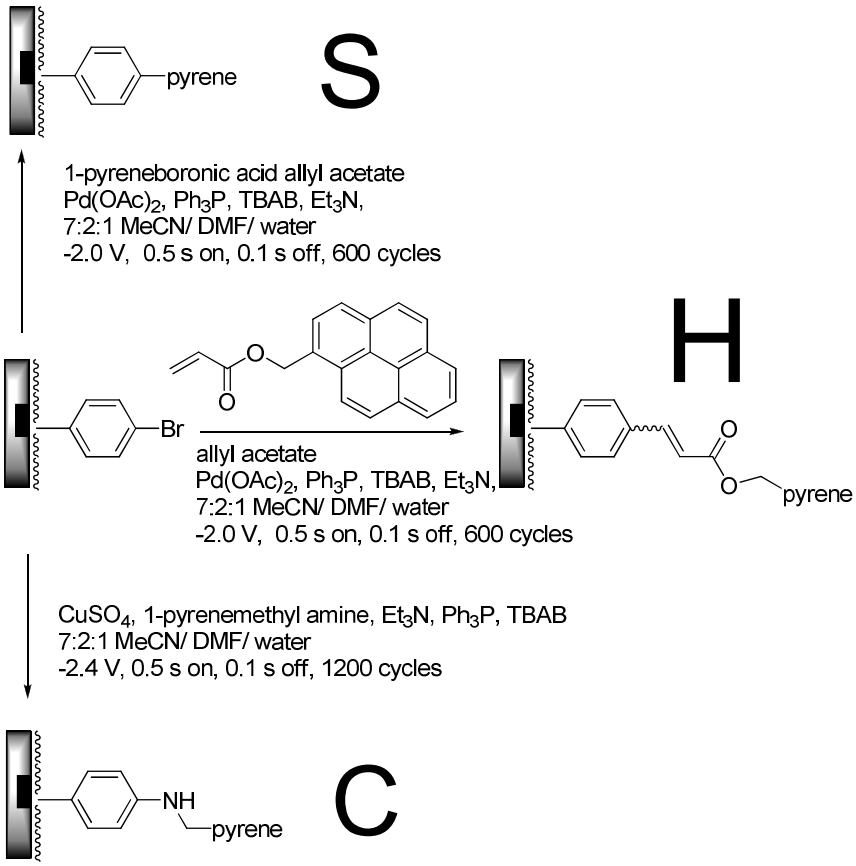

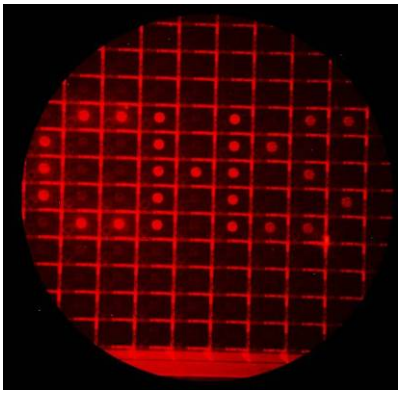

Figure 3.9 Running three different reactions on the same chip with a "CHS" pattern

The porosity of the PBrSt-b-CEMA block copolymer was also studied with AFM imaging (Figure 3.10). The average pore size was measured to be around 19.3 $\pm$ 3.0 nm, which is more than enough to let through the species in the solution to reach the electrode.

a) b)

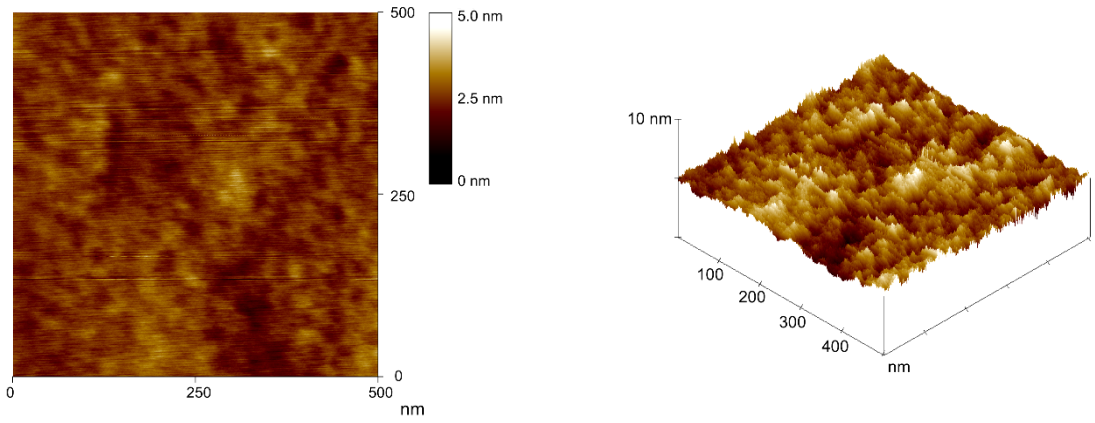

Figure 3.10 a) A blow-up image of the polymer surface showing the porous structure which allows the reactants to reach the electrodes. The size of the pores measured average at 19.3 ± 3.0 nm. b) A 3D image of the polymer surface.

3.8 Electrochemical signaling testing on PBrSt-b-CEMA surface

After verification of the compatibility of the block copolymer with synthetic experiments on the arrays, attention was turned toward its compatibility with electrochemical signaling experiments.

Although detailed information regarding signaling experiments will be discussed in Chapter 4, some of the results are important here in order to verify the overall utility of the surface developed. One of the first experiments examined the non-specific binding of bovine serum albumin (BSA) to the surface of the array (Figure 3.11). This was done in order to confirm that the block copolymer surface was compatible with measuring the current associated with iron in solution and detecting the binding of proteins to the surface of the electrodes. As can be seen in the Figure, the current for the iron could be measured, and the current measured did decrease

with increasing concentration of BSA. Taking the current intensity at 700 mV for each concentration of BSA, a binding curve could be drawn as shown in Figure 3.12.

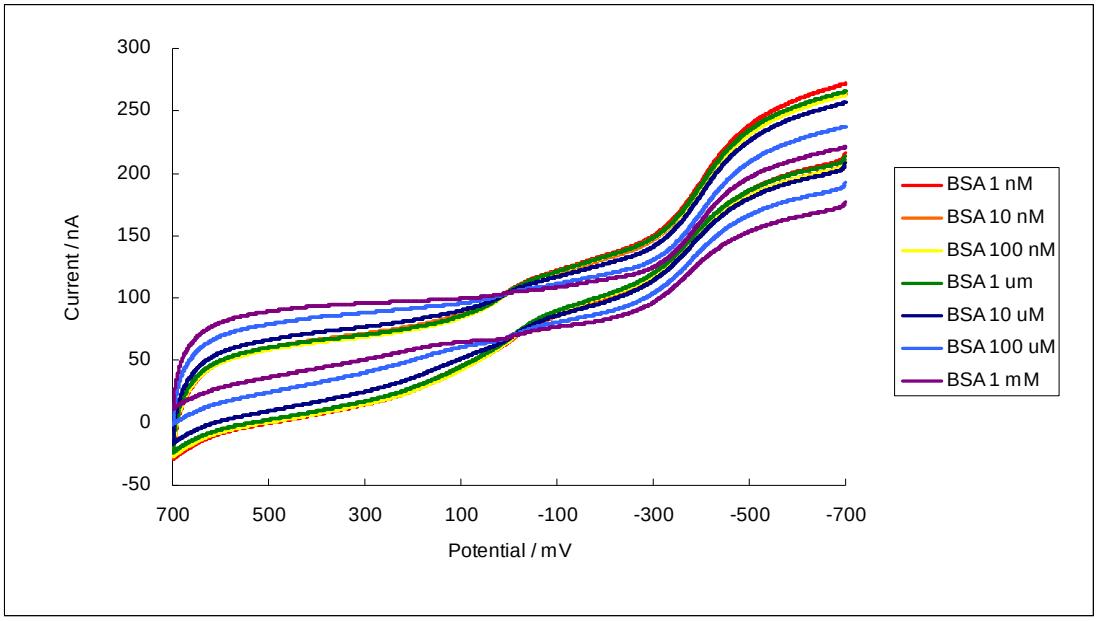

Figure 3.11 BSA non-specific binding experiment on 12-K array. Condition: 8 mM $K_3Fe(CN)_6/K_4Fe(CN)_6$ dissolved in 1x PBS solution in water, pH=7.5, BSA concentration varies from 1 nM to 1 mM.

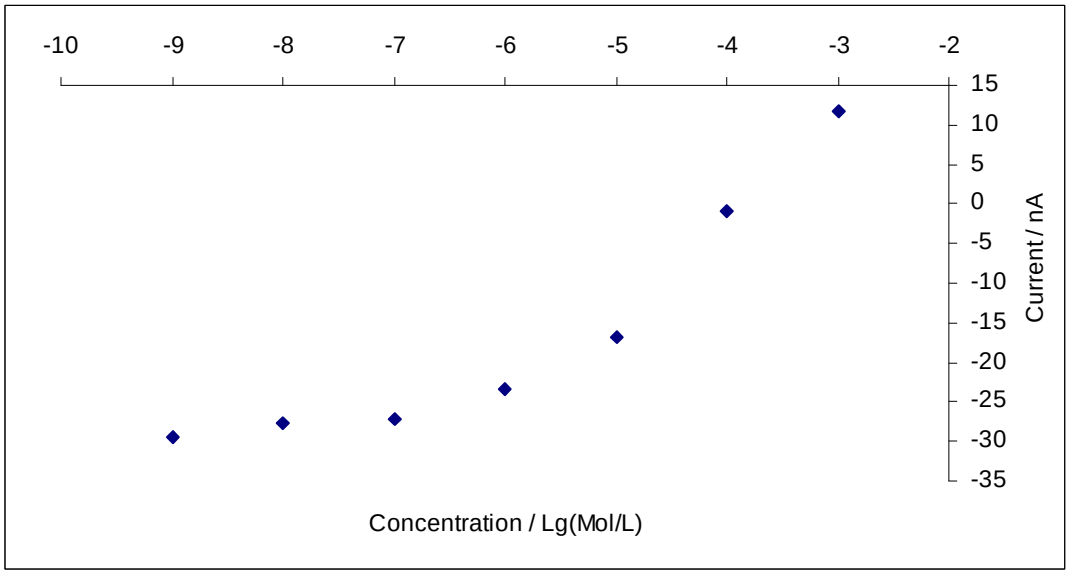

Figure 3.12 Binding curve generated for BSA non-specific binding experiment. Current spots were taken at 700 mV.

The current measured started to show an obvious drop in intensity at around 0.1 μM to 10 μM of BSA in solution. The steepest drop in current occurred between 10 μM to 0.1 mM, although the drop between 0.1 mM to 1 mM was also large. This data was also verified by doing a similar binding experiment on a regular round disk electrode with a diameter of 2 mm. Hence, the binding of BSA to the surface was a function of the polymer and not the nature of the electrode below.

In the case of the larger disk electrode the current drop associated with the coated electrode was compared to the results obtained with a bare platinum-surface. (Figure 3.13).

a)

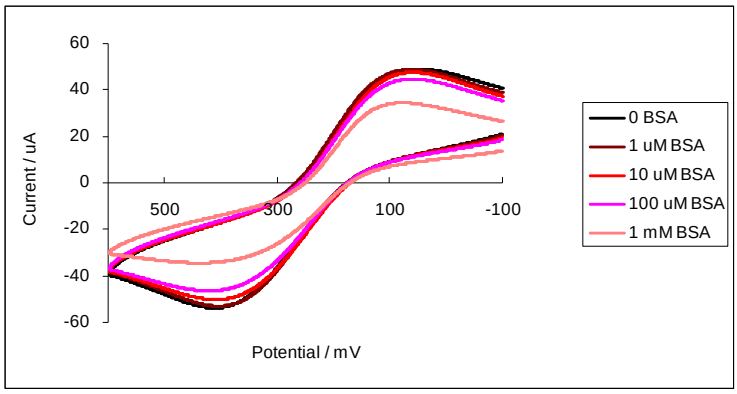

b)

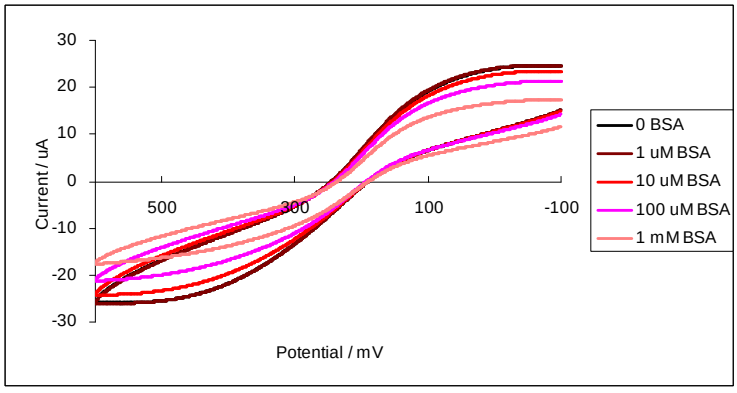

Figure 3.13 BSA non-specific binding experiment on 2 mm round disk platinum electrode. a) BSA non-specific binding on unmodified platinum surface; b) BSA non-specific binding on PBrSt-b-CEMA coated platinum surface. Condition: 8 mM $K_3Fe(CN)_6/K_4Fe(CN)_6$ dissolved in 1x PBS solution in water, pH=7.5, BSA concentration varies from 1 μM to 1 mM.

As can be seen in Figure 3.13a, BSA did bind to the bare Pt-surface. However, this binding did not occur extensively until the concentration of BSA in solution reached 1 mM. After the platinum surface was coated with PBrSt-b-CEMA block copolymer, two differences could be clearly noticed. First, the initial current associated with iron was lower even in the complete absence of protein. This current dropped from a peak value at around 55 μA for the bare platinum surface to around 26 μA for the coated surface. This indicated that the polymer coating itself did impede the iron from reaching the electrode surface. This is not surprising because of the non-conductive nature of the block copolymer. Although the polymer was proven porous enough for the ions in the solution to pass through, it still slowed the diffusion of iron to the electrode surface. The second difference between the coated and uncoated electrodes was that the polymer appeared to change the binding properties of the surface. For the coated surface, the current dropped quite evenly as the concentration of BSA increased from 10 μM to 1 mM, and showed a greater degree of total impedance relative to the bare platinum surface. Simply put, the coated surface accommodated more BSA than did the uncoated surface. This result was in accordance with the result obtained with the array.

3.9 Reducing non-specific binding of PBrSt-b-CEMA surface by PEGylation on the array with Pd(0) chemistry

While the success of the BSA non-specific binding experiment showed that the polymer-coated array was responsive to protein binding, it also brought out the problem of protein non-specific binding to the polymer. A high degree of non-specific binding has the potential to interfere with a signal on the array because it essentially increases the level of background noise. For example, if the background binding at a concentration of protein is high enough so that it prevents all of the iron from reaching the surface of the electrode, then a specific binding event cannot be observed at that concentration. For this reason, we needed the block copolymer surface to have minimal non-specific binding with any protein to be studied. This is especially important if we want to study weak interactions between ligands and receptors, as the non-specific binding will hide the actual binding interaction.

There are primarily two ways to realize this goal of reducing non-specific binding. The first one is simply by making another polymer surface that binds less to proteins. The second is to functionalize the PBrSt-b-CEMA surface with a non-binding ligand that will repel the protein from binding to the surface. This can be done in a number of ways.[15] Since the second method is much easier to carry out, it was tried first.

For the purpose of reducing non-specific binding, polyethylene glycol (PEG), or polyethylene oxide (PEO) have bee frequently utilized.[16] It was easy to propose a method of functionalizing the surface of the array with PEG. This can be done either

electrochemically or with a standard Pd(0) coupling reaction. The first attempt was done by incubating an array coated with PBrSt-b-CEMA in a reaction solution containing the reagents for Heck reaction and PEG acrylate for 1 hour (Scheme 3.15).

Scheme 3.15

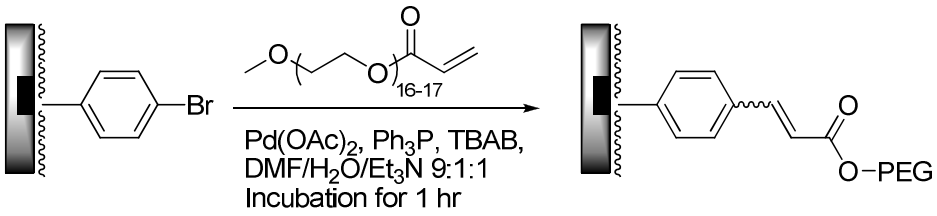

As a result of the incubation, Pd(0) precipitated out of the solution as black films on the surface which was not removable by regular washing. Since the procedure could not be performed in an inert environment except with the use of a glove box, the palladium metal in the solution which was unstable to air could easily aggregate and fell out of solution Since PEGylation could not be done non-electrochemically on the array, the electrochemical Heck reaction was used. The array based Heck reaction was performed using the same conditions employed to generate the Pd(0)-catalyst in Scheme 3.16.

Scheme 3.16

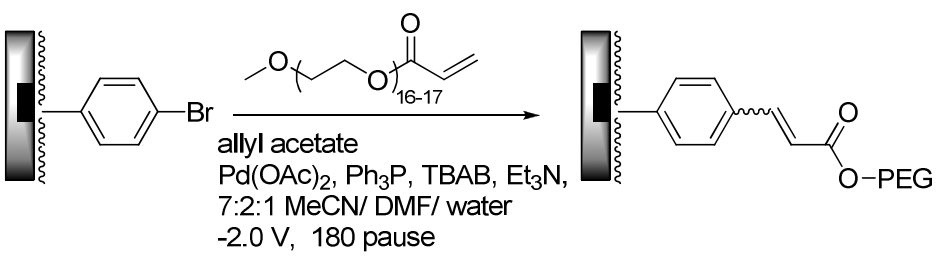

Since the Pd(0) was generated on the surface site-selectively, the PEGylation occurred on the surface site-selectively. The proof of the PEGylation could be obtained by measuring the contact angles of the surface before and after the modification. The contact angle of the unmodified block copolymer surface was measured to be around 82 $\pm$ 4 degrees, while the contact angle of the PEGylated surface was measured to be around 45 $\pm$ 4 degrees. The sharp decrease of the contact angle indicated that the surface became much more hydrophilic after the reaction, which could only be the result of PEG attaching to the surface, as PEG is highly hydrophilic and miscible with water.

With the success of PEGylation on the surface, we moved on to test whether PEGylation would reduce non-specific binding or not. A PEGylated array was subjected to the exact BSA non-specific binding experiment as shown in Figure 3.11. The result was shown in Figure 3.14. As can be seen in the cyclic voltammogram, the trend of the drop was very similar to the unmodified PBrSt-b-CEMA block copolymer surface. If following the same treatment, taking the current intensity at 700 mV, a similar plot to Figure 3.12 could be obtained (Figure 3.15).

The result of this experiment indicated that the PEGylation of the PBrSt-b-CEMA was ineffective in reducing the BSA non-specific binding. It is assumed that the BSA is binding the surface above the electrodes in order to impede the iron from reaching the electrode surface and not simply binding the regions between the electrodes. Evidence to support this assumption will be outlined below.

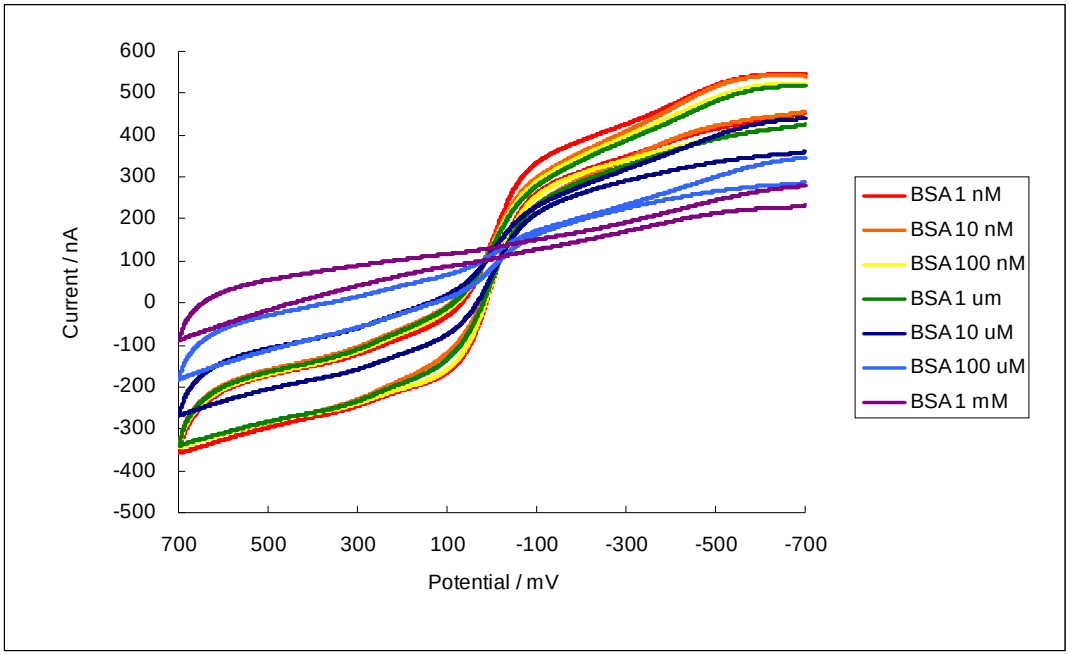

Figure 3.14 BSA non-specific binding experiment on PEGylated surface. Condition: 8 mM $K_3Fe(CN)_6/K_4Fe(CN)_6$ dissolved in 1x PBS solution in water, pH=7.5, BSA concentration varies from 1 nM to 1 mM.

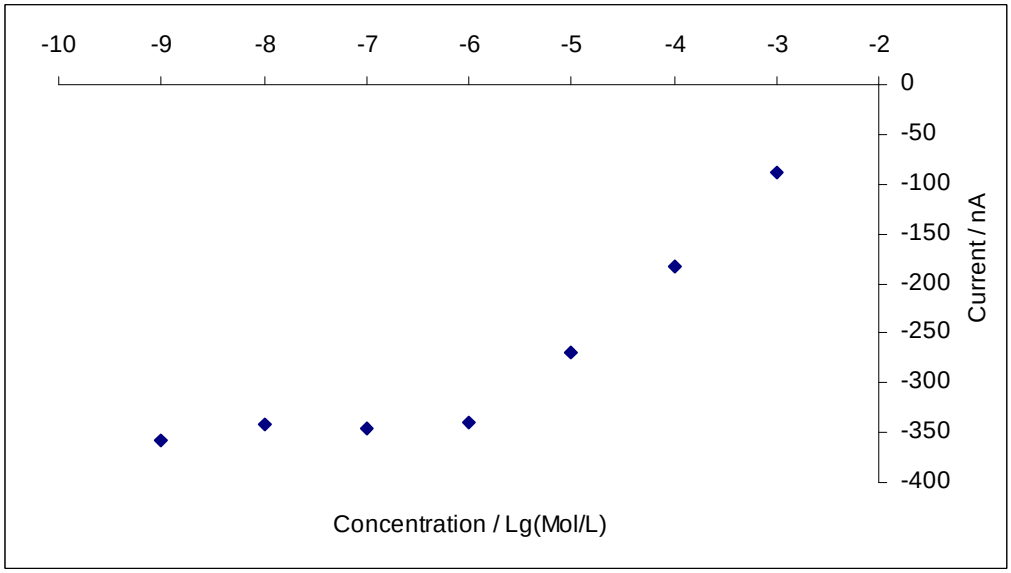

Figure 3.15 Binding curve generated for BSA non-specific binding on PEGylated surface. Current spots were taken at 700 mV.

There are two explanations that can explain why the PEG is ineffective with respect to reducing the level of BSA binding to the surface of the array. First, the

coverage of the PEG on the polymer surface may not have been sufficient to prevent the non-specific binding, especially since the PEG group was only placed by the electrodes. . Because the coverage of PEG on the surface was very difficult to characterize, this was a difficult question to address. Second, the chain length of the PEG acrylate may be too short to be effective. The PEG used was comprise of around 16 to 17 repeating units. Hence, it was more of an oligomer than polymer. Compared to the size of the protein, the chain may be too short to cover the hydrophobic surface underneath effectively. However, if a very large molecular weight PEG was used, other problems may arise such as low coupling efficiency due to the steric interaction between the PEG polymer and the surface, etc.

Evidence that the BSA really was binding to the surface of the electrode was gained by conducting a similar BSA non-specific binding experiment with the larger modified platinum disk electrode. The disk electrode was coated as described for the experiments highlighted in Figure 3.13. PEGylation of the surface was then carried out in a similar manner to the electrochemical Heck reaction on the surface. The resulting electrode surface was subjected to the same BSA non-specific binding experiment shown in Figure 3.13. The result was shown in Figure 3.16.

The result obtained from the round disk electrode was pretty much the same as the result obtained from the microelectrode arrays. This supported the conclusion that the electrochemical PEGylation of the block copolymer on the surface of the anode with the use of a Heck-reaction was ineffective in reducing BSA non-specific binding. Once again, the cause of the observation was difficult to assess

because of the challenges associated with measuring the density of the PEG on the surface. However, for our purpose it was good enough to know that PEGylation directly on the surface may not be the easiest and most efficient method for reducing the non-specific binding of proteins.

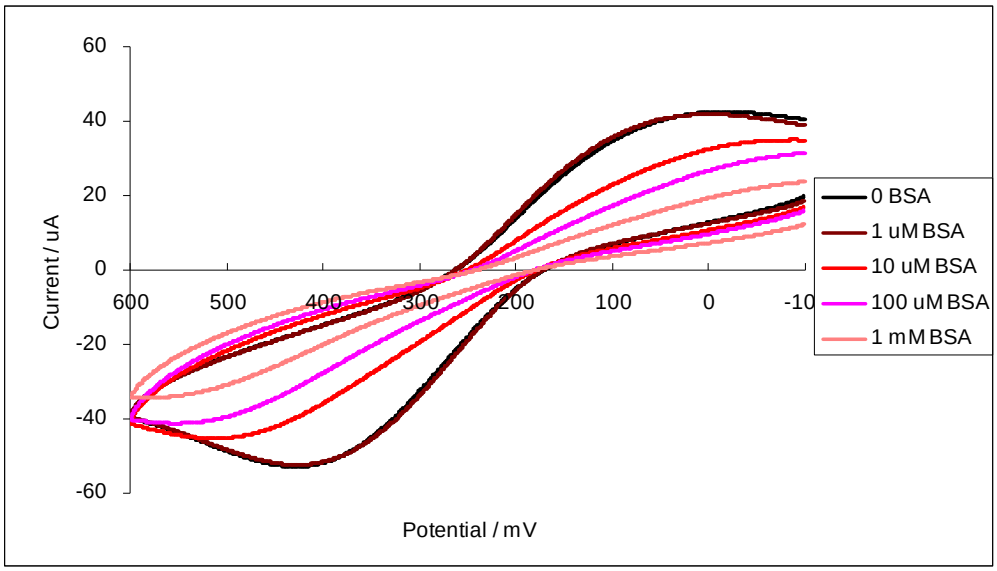

Figure 3.16 BSA non-specific binding experiment on 2 mm round disk platinum electrode modified with PBrSt-b-CEMA followed by PEGylation with PEG acrylate via Heck reaction. Condition: 8 mM $K_3Fe(CN)_6/K_4Fe(CN)_6$ dissolved in 1x PBS solution in water, pH=7.5, BSA concentration varies from 1 μM to 1 mM.

3.10 Reducing non-specific binding by synthesizing PEG-containing block copolymers

Having shown that PEGylation of the surface using a post-synthetic modification of the polymer was ineffective, attention was turned to the incorporation of the PEG into the structure of the block copolymer. As a major non-specific binding source, the polystyrene block could be switched with a poly(polyethylene glycol methacrylate) (PPEGMA) block with the other end of the PEG chain carrying the

functionality that was needed for derivatization of the surface. For this pupose, one could use a bromophenyl group, an acetylene group, and so on (Figure 3.17).

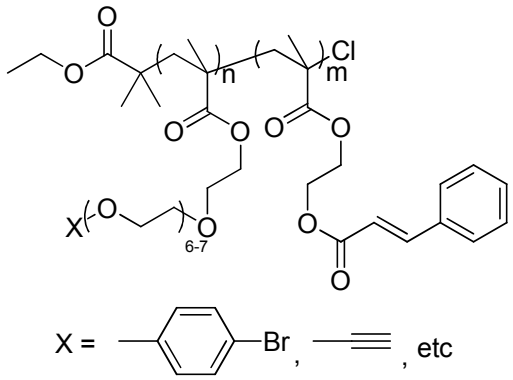

Figure 3.17 PPEGMA-b-CEMA block copolymer with the functionality on the chain end of the PEG side chain

The design of this block co-polymer was quite easy, however its synthesis presented a series of challenges. The first attempt to synthesize this polymer used PPEGMA as the first block and HEMA as the second block. The initial polymer was then post-synthetically modified in a manner identical to that used in the preparation of PBrSt-b-CEMA (Scheme 3.17). However, the polymerization of the first PPEGMA block was never successful.

Scheme 3.17

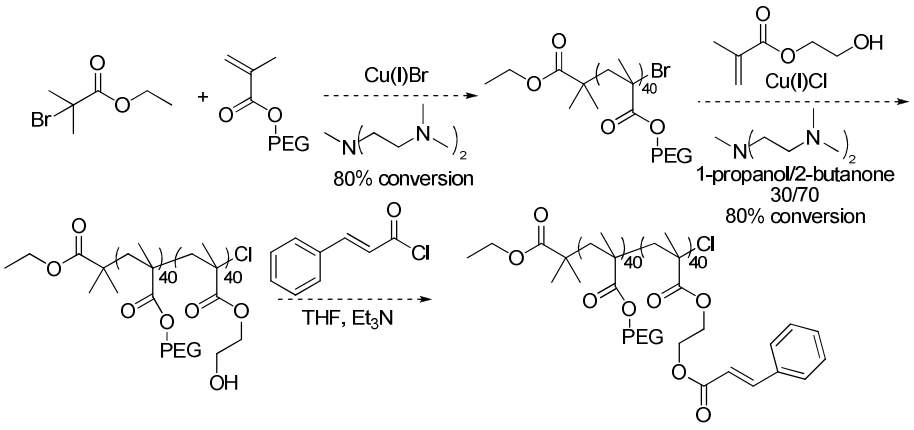

The polymerization of PPEGMA under ATRP conditions was very difficult to control. We tried several times with different solvents and reaction temperatures, some as low as 50 ^{0}C. In each case, the reaction led to an insoluble cross-linked hydrogel. Literature[16a] has reported several successful controlled polymerizations of PPEGMA. However, in most case the polymerization was carried out directly on a solid surface in order to form a layer of PEG hydrogel. It was hard to tell whether the PPEGMA on the surface was cross-linked or not. One example provided by Matyjaszewski and coworkers[17] on the polymerization of soluble PPEGMA copolymer in solution did show some success, however, in this paper, they indicated that the rate of polymerization could not be too fast. When the polymerization proceeded too quickly the reaction led to a cross-linked gel. This was especially true at high conversion of the PPEGMA monomer. In spite of the report of the successful polymerization of PEGMA, we were not able to get soluble PPEGMA homopolymer even with conditions that were identical to those used in the Matyjaszewski paper when those reactions were run to a high conversion. Homopolymer of PPEGMA could be obtained at lower conversion (less than 50%) of the PEGMA monomer. However, when PPEGMA was exposed to the radical polymerization condition for the second HEMA monomer, the PPEGMA again cross-linked to form a hydrogel. Even exposing the PPEGMA homopolymer to vacuum for prolonged time would lead to gel formation. It was quite obvious that the polymer PPEGMA was not stable under radical polymerization conditions. Since the PEG is an ether type substrate, and ethers like diethyl ether and THF are capable of reacting with radicals, which is why they

easily forms peroxides (Scheme 3.18). There are many ether units on a PEG chain, which could lead to chain transfer reactions from growing polymeric radicals easily. Possible mechanisms for the cross-linking reaction of PPEGMA are illustrated in Scheme 3.19.

Scheme 3.18

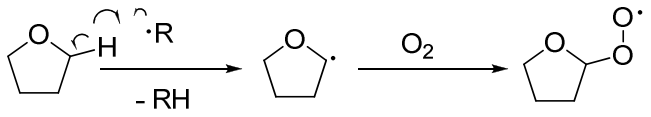

Scheme 3.19

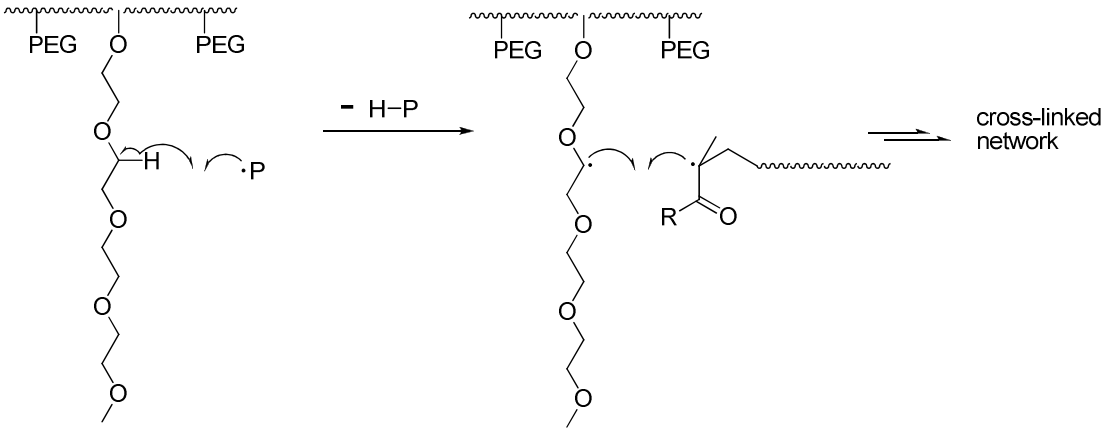

As a conclusion, the synthesis of the PPEGMA-b-CEMA block copolymer directly from PEGMA monomer was not a viable method. Since PEG was not stable in an environment with active radicals, it was best to put the PEG onto the polymer structure after all radical polymerization was done. Therefore, the synthetic route of the PPEGMA-b-CEMA was redesigned as shown in Scheme 3.20. In this plan, the CEMA would be polymerized as the first block, and HEMA polymerized as the

second block. Our previous experience has shown us that PCEMA would cross-link if the reaction temperature exceeds 80 ^{0}C. However, since the polymerization of HEMA is typically conducted at temperatures less than 50 ^{0}C, the cross-linking of PCEMA was not likely. After the polymerization was done, coupling between the PHEMA block and the PEG unit in the solution would yield the desired polymer.

Scheme 3.20

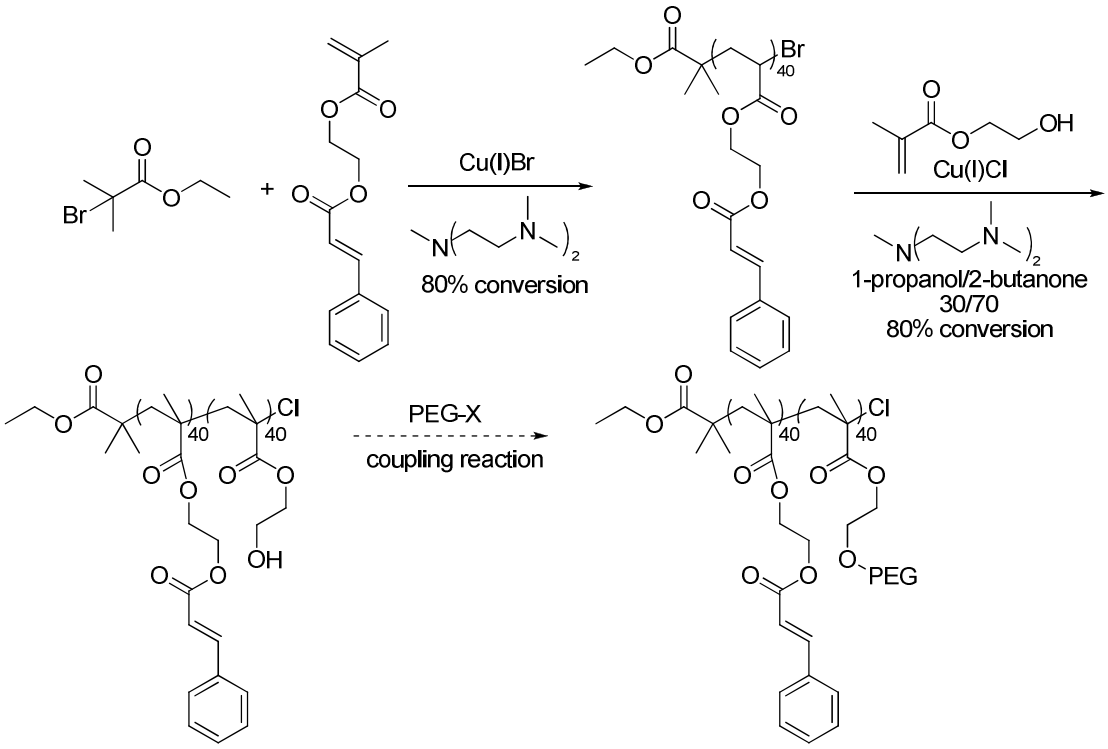

The preparation of PCEMA-b-HEMA went nicely. The polymerization of the second HEMA block did not cause any problem with the first PCEMA block. However, post-polymerization modification presented another challenge. Although the PEG substrate we used had only 6 to 7 repeating units, it still presented a serious steric challenge for the coupling reaction. Technically, the attachment of the PEG

units to the block copolymer is consistent with the formation of a graft copolymer. For making graft copolymers, usually three kinds of strategies are used: grafting from, grafting onto, and grafting through. In our case, the method was grafting onto, which couples existing polymer chains onto the backbone. It is well known that this method has the limitation of low grafting density due to the steric interactions between the polymer backbone and the side chains. Additionally, as the grafting process proceeds, this steric hindrance becomes even greater due to the side chains already grafted onto the backbone. In our case, we tried a number of methods for the coupling reaction (Scheme 3.21). Of these, only the use of a PEG substituted acid chloride showed moderate success.

Scheme 3.21

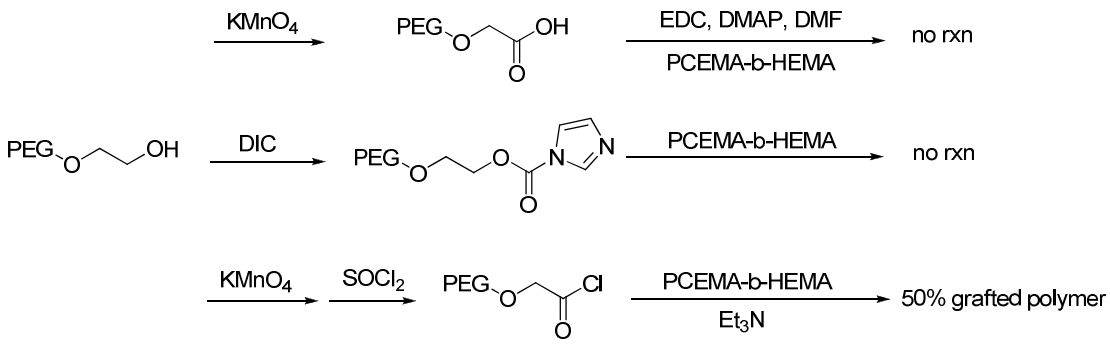

Even though only 50% of the free hydroxyls on the PHEMA block of the copolymer were functionalized with the PEG group, we felt the amount of PEG present was still sufficient to warrant testing the polymer as a coating. One notable precaution with this polymer is that with the PEG on the polymer, the polymer should not be exposed to vacuum for prolonged time. Once the PEG was completely free of

small amounts of volatile material, it was extremely difficult to dissolve in any solvent.

The PCEMA-b-(PEGMA$_{0.5}$-HEMA$_{0.5}$) polymer was tested for its stability toward synthetic reactions on the array. In order to simplify synthesis of the polymer, the PEG unit was not functionalized at the other end. It was simply capped with a methyl ether group. This did not change the method for probing the stability of the polymer to the reaction conditions needed because the surface could still be exposed to the desired reaction conditions. In this case, they would not lead to a product but they would show if the polymer was stable. As a generic testing, the polymer was dissolved in DMF as a 0.03 g/mL solution and spin-coated with different conditions ranging from 1000 rpm to 2000 rpm for 30 seconds. Then the arrays were subjected to irradiation by a 100 W mercury lamp for 20 minutes. Unfortunately, no matter how we adjusted the coating conditions, the surface always showed wrinkles after exposing to a polar solution and dried (Figure 3.18).

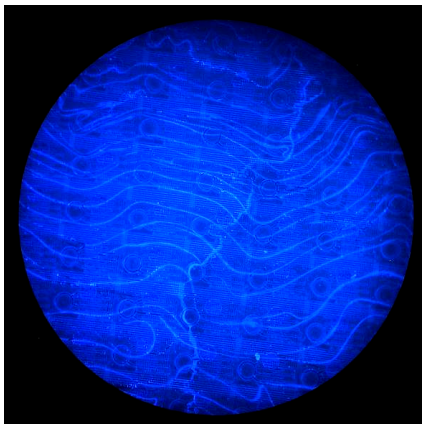

Figure 3.18 The PCEMA-b-(PEGMA$_{0.5}$-HEMA$_{0.5}$) surface showing wrinkles after exposure to a reaction solution.

This phenomenon had to do with the ability of PEG to form gels. PEGMA has been widely used as a hydrogel-forming monomer[15a] and there was no surprise that any polymer that has PEG in the structure would be ready to swell once exposed to polar solvents. We had hoped that the cross-linking of the CEMA block would limit the swelling of the PEG moieties to an acceptable degree, but it turned out that it was ineffective. Even with only 50% grafting density, the swelling and shrinking already reached an unacceptable degree. It is certain that a 100% grafted polymer would have a much more severe problem. In conclusion, although the synthesis of PEG containing block copolymer was moderately successful, the intensive hydrogelling nature of PEG precluded its candidacy as a usable coating for microelectrode array-based reactions.

3.11 Taking advantage of boronic acid functionalized polystyrene as a tunable surface for the microelectrode arrays

Brent Sumerlin's group has reported controlled radical polymerization of pinacol protected styrene boronic acid. Following the polymerization, the pinacol protected boronic acid can be deprotected to form poly(4-styrene boronic acid) (abbreviated as PBoSt) .[18] They gave this type of polymer a nick name, "sweet tooth" polymer, for the ability of the boronic acid to bind to sugars[19] and other sterically hindered 1,2-diol that let to a cyclic five-member ring boronic ester that was stable in aqueous solution.[19] Thus, a block copolymer of poly(4-styrene boronic acid) and PCEMA might provide a UV-cross-linkable surface with highly tunable properties (Scheme 3.22).

Scheme 3.22

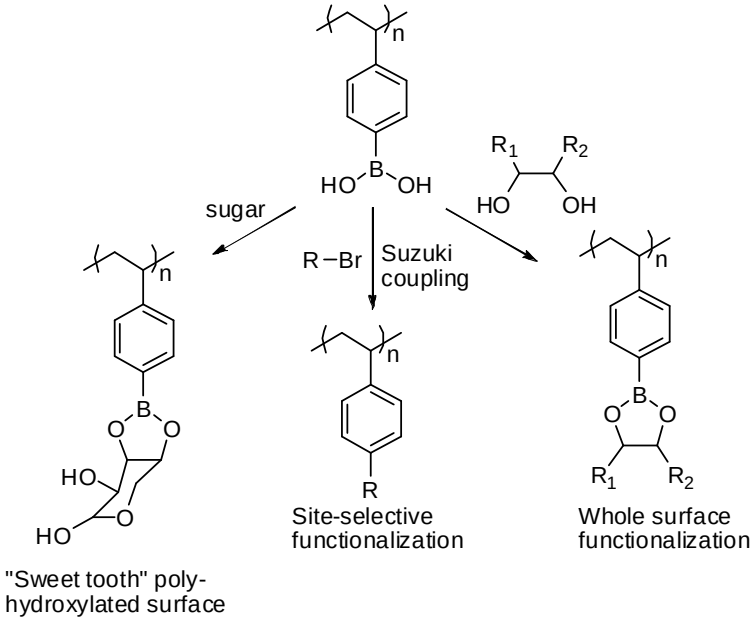

3.12 Synthesis of PCEMA-b-BoSt

According to the literature methods,[18] the pinacol protected 4-styrene boronic acid was polymerized with RAFT polymerization using a 1:1 (v:v) mixture with anisole at 70 ^{o}C. However, when using these conditions we found the polymerization to be extremely slow. Hence, the temperature of the polymerization was increased to 110^{0}C, and the polymerization completed in a couple of hours (Scheme 3.23). Once the homopolymer of the pinacol protected PBoSt (PpBoSt) was made, it was tested as the macroinitiator for the block copolymer.

Scheme 3.23

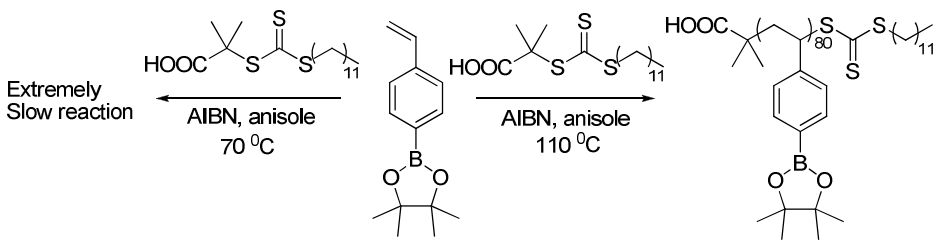

For the block copolymerization, both HEMA and CEMA had been used as the monomer for the second block. However, using polystyrene as the macroinitiator led to poor initiation efficiency. The second polymerization did not proceed at all. This phenomenon was not completely unexpected. The polymerization of styrene is much slower than reactions of methacrylates, and the homopolymer of a less reactive monomer usually has poor initiation efficiency towards a more reactive monomer.[14] Since RAFT cannot utilize the transmetallation strategy employed by ATRP, the problem can only be fixed by using a less reactive monomer for the second block or reverse the order of the blocks.

To this end, the acrylic equivalent for HEMA and CEMA (HEA and CEA) were used instead of HEMA and CEMA. Acrylates were reported to have similar reactivity towards polymerization with styrene type monomers,[14] hence a suitable choice for the polymerization of the second block. However, this strategy also did not work, as the polymerization would either not proceed or proceeded extremely slowly.

Since simply changing the reactivity of the second block did not work, the order of the polymerization of the two blocks was reversed. It is quite obvious that CEMA would not be a suitable choice as the first monomer, because the polymerization of the second block requires high temperature which would induce cross-linking in PCEMA. Therefore, HEMA was used as the first monomer and pBoSt was used as the second monomer. The polymerization was accomplished by sequential addition of the second monomer into the reaction mixture of the first block after the polymerization of the first monomer approach completion. The intermediate

homopolymer was not purified. After the conversion of the first monomer HEMA reached 90%, the second monomer pBoSt was degassed and injected into the reaction mixture. In this case, an isobutyronitrile-substituted trithiocarbonate was used as the RAFT agent instead of the isobutric acid equivalent used in the previous case to have better initiation efficiency towards the methacrylate monomer.[14] The first attempt of the polymerization was carried out in DMSO because both blocks were expected to be soluble in the solvent (Scheme3.24).

Scheme 3.24

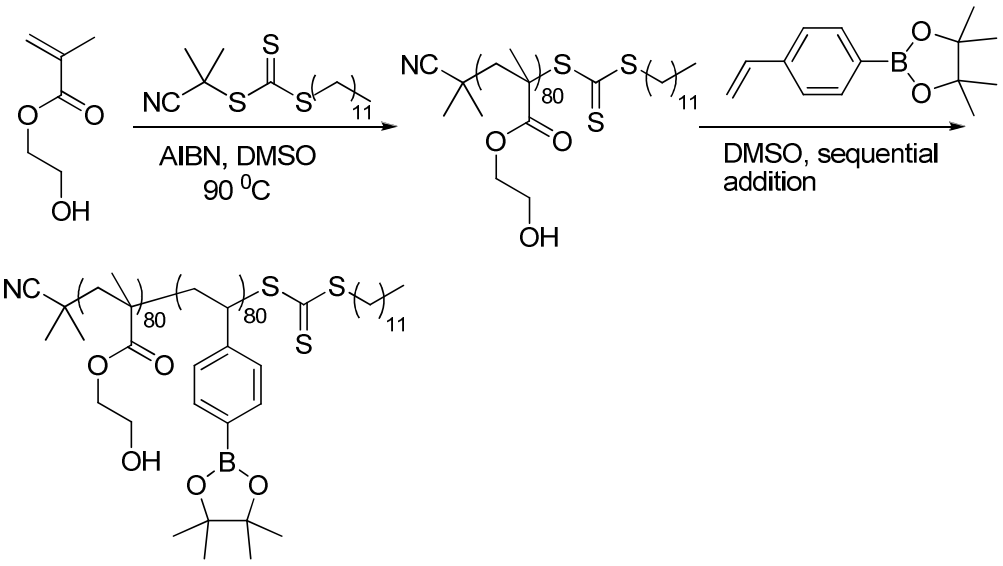

The reaction worked very well, and both monomers were consumed. The PHEMA-b-pBoSt polymer was then subjected to post-polymerization modification to make the cinnamate used for the cross-linking step to follow placement of the polymer on an array. The first attempt at this modification of the initial polymer

treated the polymer with cinnamoyl chloride and triethylamine. Surprisingly, these conditions led to a cross-linked insoluble polymer. Upon investigation of the structure of the polymer, this result was not that surprising. Under basic reaction conditions, the boronic ester could easily be attacked by the hydroxyl group on the HEMA block. This transesterification reaction cross-linked the polymer (Scheme 3.25).

Scheme 3.25

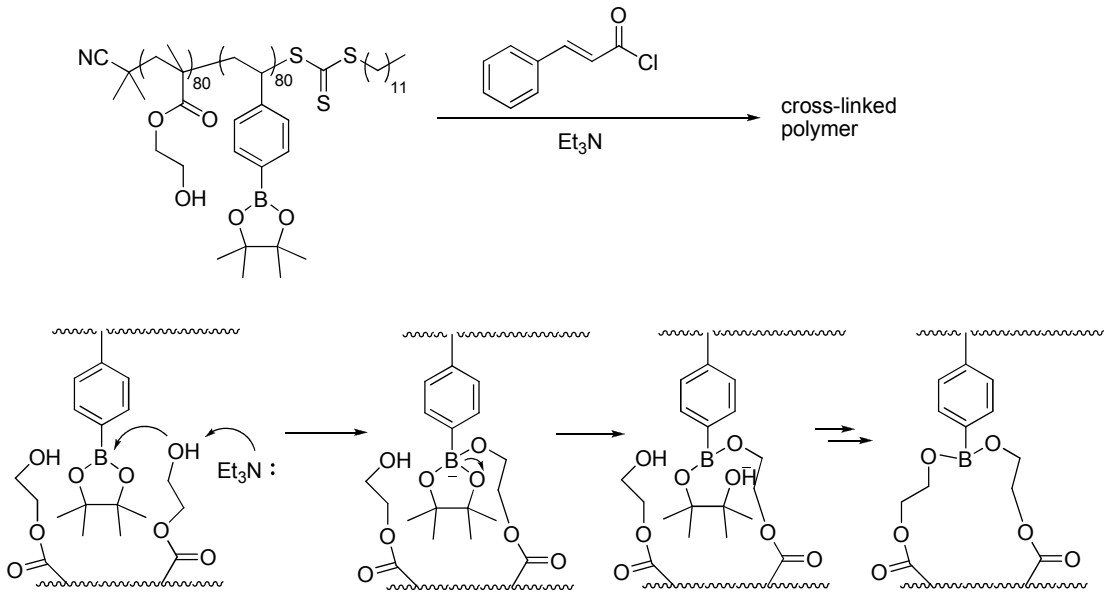

In order to avoid this sidereaction, less basic reaction conditions were needed. This was accomplished using the much milder Steglich esterification conditions.[20] To avoid the Moffat oxidation in the presence of DMSO, the whole polymerization process was conducted in DMF solvent instead of DMSO. In this way, the crude mixture after the polymerization could be directly subjected to the DCC coupling reaction without purification (Scheme 3.26).

Scheme 3.26

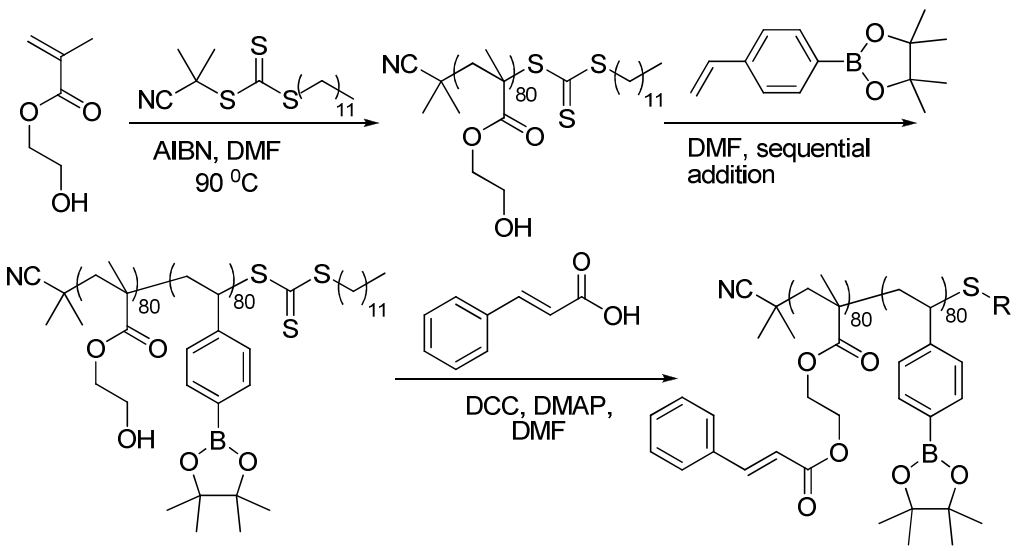

The reaction sequence worked quite well. The product was verified by NMR. The polymer was not purified until at the PCEMA-b-pBoSt stage in order to simplify the overall synthetic process. After the DCC coupling, the mixture could be filtered to remove the DCU byproduct, and precipitated into methanol to obtain the pure block copolymer.

Once the purification was accompished, the pinacol protecting group on the boronic ester needed to be removed. In the literature, hindered boronic esters are very difficult to hydrolyze.[21] Usually, the hydrolysis requires harsh conditions or a large excess of phenyl boronic acid (PBA). In the Sumerlin paper, the PpBoSt homopolymer they prepared was hydrolyzed by refluxing the polymer in an acetonitrile with 2% trifluoroacetic acid solution and a 9-fold excess of phenyl boronic acid immobilized on polystyrene resin. The identical conditions were attempted with PCEMA-b-pBoSt. Unfortunately, the reaction failed. Interestingly,

while the block copolymer hardly dissolved in acetonitrile, the deprotection of the boronic ester actually went to almost completion under these conditions (the pinacol methyl protons disappeared in the NMR). However, the protons associated with the cinnamoyl group and the ethylene group on HEMA also diminished. This indicated that the reaction conditions hydrolyzed not only the boronic ester but also the carboxylic acid derived ester as well.

Clearly, milder conditions were needed. To this end, the traditional method using excess PBA was used. Initially, the reaction was attempted using a nine-fold excess of PBA with the block copolymer in THF. The reaction was catalyzed by 2% TFA. The reaction was allowed to run at room temperature for 24 hours. By the end of the reaction, the solution had turned somewhat cloudy. After purification the polymer no longer dissolved easily in THF like its precursor before deprotection. NMR analysis showed that roughly 40% of the pinacol groups had been removed. The deprotection worked, but the reaction had not gone to completion. The reaction was then allowed to run for 48 hours. However, the longer reaction time did not lead to greater conversion. It appeared that the reaction was forming micelles in solution, a suggestion that was consistent with the reaction solution turning opaque during the deprotection. Since the deprotected PBoSt is a hydrophilic polymer, it does not dissolve in THF well. In contrast, PpBoSt and PCEMA are both hydrophobic polymers that dissolve very well in THF. As a result, PCEMA-b-pBoSt is a hydrophobic polymer and PCEMA-b-BoSt in turn is an amphiphilic polymer. As the deprotection of the pinacol ester group progressed, the PCEMA-b-pBoSt polymer

changed slowly from a hydrophobic polymer into an amphiphilic polymer. At some point, the amphiphilic property of the partially deprotected PCEMA-b-pBoSt started to force the polymers to form micelles in the THF solution. The micelles would have a hydrophobic shell (PCEMA) and hydrophilic core (partially deprotected PpBoSt). This shielded the pinacol boronic ester groups still present in the copolymer from the deprotection step.

If this was the case, then the deprotection reaction could be pushed to completion by stopping the micelle formation. This was done by adding water to the THF solution. As both the hydrophilic and hydrophobic blocks of the copolymer were solvated, micelles would not form. After using these conditions, a proton NMR of the reaction product showed that the deprotection successfully removed 90% of the pinacol groups. A Summary of the deprotection conditions is listed in Scheme 3.27.

Scheme 3.27

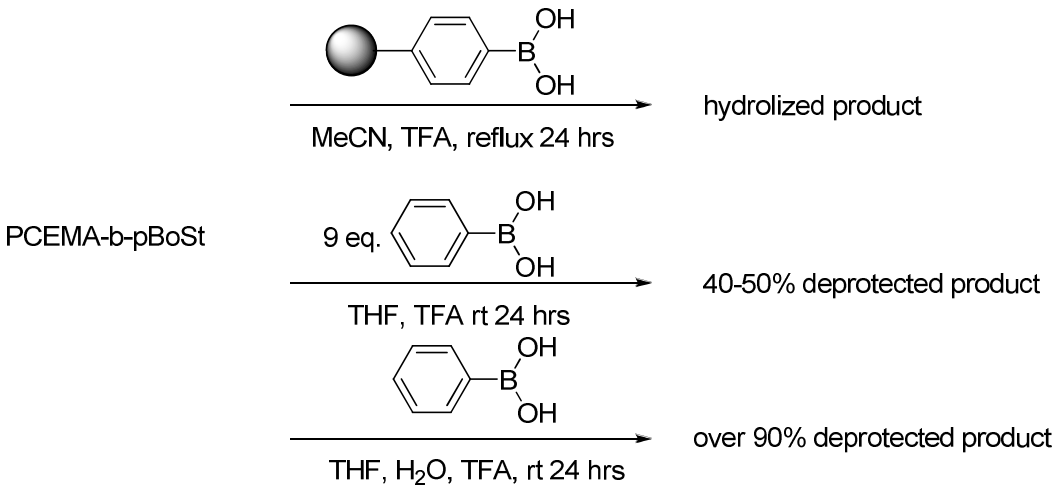

3.13 Testing PCEMA-b-BoSt for array-based reactions

After the block copolymer PCEMA-b-BoSt was obtained, it was tested for its compatibility with array-based reactions and for its stability. Due to the amphiphilic property of the block copolymer, initially it was very difficult to find the optimal conditions for coating it onto an array. The polymer was readily soluble in a THF/water 4:1 (v:v) mixture, however, this solution was not suitable for spin-coating. As the coating solution was applied, THF evaporated too fast due to its low boiling point. This caused the polymer to precipitate out of the solution before it had the chance to be evenly deposited onto the surface. The resulting coating was a whitish crispy film that would easily break upon abrasion and washing. Switching the mixture from THF to DMF alleviated the evaporation problem, but for some reason the DMF/water mixture would not form an evenly distributed coating across the array surface. There was always a dividing line in the middle of the array where one half would have more coating than the other. Eventually, the optimal coating condition was found out to be 0.03 g/mL polymer solution in 1:9 water/dioxane (v:v), mixture with a spinning rate of 1000 rpm for 40 seconds. Using these conditions, the polymer formed a clear and evenly distributed coating on the array. Due to the intrinsic amphiphilic property of the polymer, almost no single solvent can dissolve it. This made the coating very stable. After the coating was cross-linked under a 100 W mercury lamp, it was tested for its compatibility with an inverse Suzuki reaction (Scheme 3.28).

Scheme 3.28

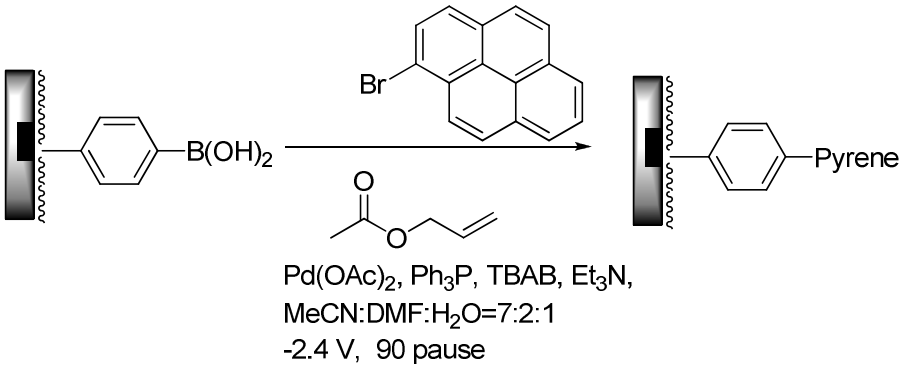

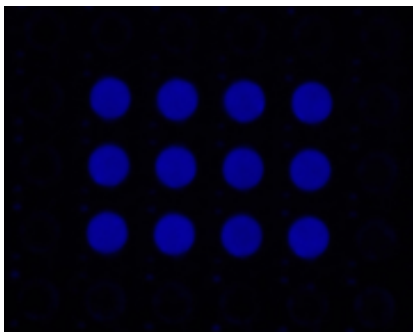

Figure 3.19 Inverse Suzuki reaction on 12-K coated with PCEMA-b-BoSt, running with 12 electrodes in a rectangle pattern. Condition: - 2.4 V vs. remote electrode, 90 pause.

As shown in Figure 3.19, the reaction worked extremely well. In fact, the intensity of fluorescence on the 12-K array rarely shows such a high level of contrast relative to the background. Additionally, the coating was able to endure potentials of -2.4 V without any problem. In this way, it was much more stable than the PBrSt-b-CEMA polymer. Additionally, same as the inverse Suzuki reaction done on the agarose surface, the Pd(II)- pyrene-bromide complex was free to migrate without the restraint from the confining agent allyl acetate. This indicated that the trapping of the Pd(II)- pyrene-bromide complex by the boronic acid was fast enough to prevent any migration. Finally, both the partially deprotected and the completely deprotected

polymers were tested for their compatibility with the Suzuki reaction. They showed no observable difference in terms of the reactions run on the array.

3.14 Testing PCEMA-b-BoSt for electrochemical signaling experiments

Although detailed signaling experiments on the PCEMA-b-BoSt polymer will be discussed in Chapter 4, a summary of the results is presented here as a conclusion for our work on the PCEMA-b-BoSt polymer.

Simply put, the boronic acid group proved to be not compatible with the signaling experiments in a way many hydrophilic polymers might be. In the signaling experiments, the CV for every protein concentration is recorded after the current becomes stabilized. If multiple CV runs are made, then the scans for the experiments should overlap. Currents swing for many reasons. The current may increase due to diffusion of the redox species into the polymer film, and may decrease due to the binding of proteins to the surface. Only until such processes reach equilibrium will the current become stabilized. Without a stable current, any record of the CV might not be a reliable indicator of the events happening on the surface. However, such cases happened frequently on a hydrophilic surface. In a previous study (details can be found in Section 4.9 of Chapter 4), a PEG-based epoxy coating on the surface was found to have constantly increasing currents over time. This observation may be due to the oxygen atoms on the polymer network binding to the iron species in solution. Regardless of the explanation, the observation of the current increase should be directly related to the fact that iron species was enriched on a hydrophilic surface. For

the PCEMA-b-BoSt surface, a similar phenomenon was observed as well (Figure 3.20). After each consecutive scan, the current kept getting larger and larger, as if the iron species that migrated toward the surface could not go back into the solution. No matter what the mechanism of this phenomenon is, the failure to obtain a stable current disqualified the deprotected PCEMA-b-BoSt block copolymer as a viable coating for the microelectrode array. Luckily, the protected polymer, PCEMA-b-pBoSt was hydrophobic and has good electrochemical properties. If deprotection of the pinacol group after the polymer is applied onto the array could be realized with good control, this problem might be fixed. Possible plans will be discussed in Section 5.3 of Chapter 5.

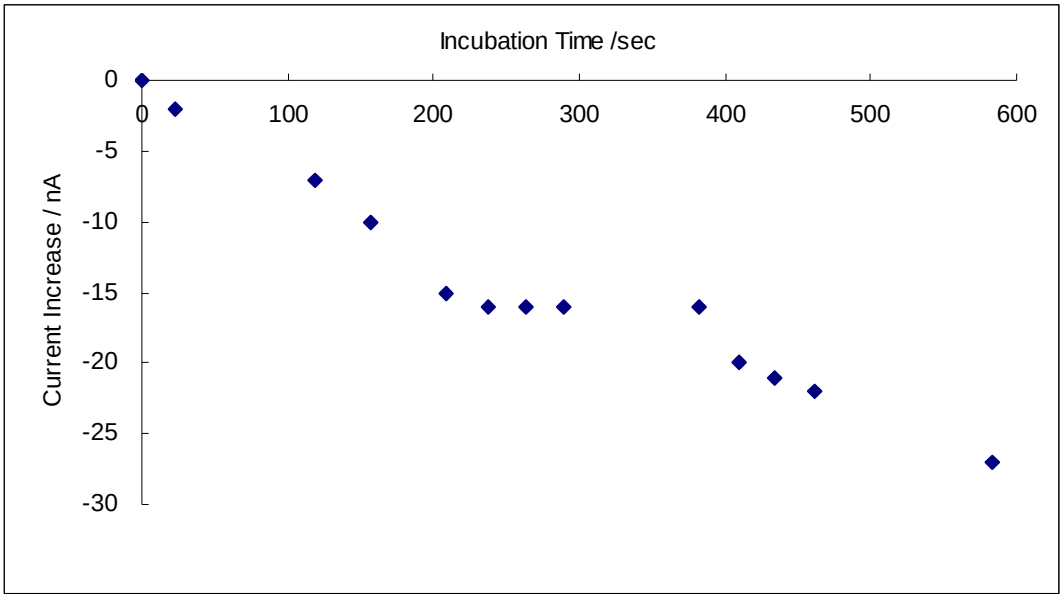

Figure 3.20 Current kept increasing as the incubation time increase on the PCEMA-b-BoSt surface. The value has been deducted with the lowest current for simplification and the current spots were taking at E = 14 mV on the oxidation wave, the more negative value means the more intense current. Condition: 8 mM $K_3Fe(CN)_6/K_4Fe(CN)_6$ dissolved in 1x PBS solution in water, pH=7.5.

3.15 Conclusion

Three different block copolymers were made to investigate the compatibility of the polymers with the array-based reactions and signaling experiments. All three polymers consisted of a PCEMA block that can be used to photochemically crosslink the polymer once it has been coated onto a surface. The other blocks varied in each polymer to achieve different purpose. The prototype polymer PBrSt-b-CEMA used 4-bromostyrene as the second block for the purpose of derivatizing the surface of the electrodes in an array. This polymer proved to be a very versatile, stable reaction layer on a chip. The surface proved to be compatible with a variety of reactions both catalyzed by Pd(0) and Cu(I). In addition, the surface was compatible with electrochemical signaling experiments. The major drawback of this polymer was its non-specific binding to proteins at higher protein concentrations. This is not a problem for the monitoring of strong binding interactions. However, in an effort to investigate weak binding interactions, a second polymer PCEMA-b-PEGMA having PEG as side chains on the second block was made in the hope that PEG would reduce non-specific binding to the surface. Unfortunately the polymer was found to swell considerably after solvated even after heavy cross-linking, which lacked the stability required as a reaction matrix. Efforts in PEGylating the PBrSt-b-CEMA surface to reduce non-specific binding was also proven to be ineffective. Finally, in an effort to make a tunable surface, a boronic acid based copolymer PCEMA-b-BoSt was chosen for the versatility of the boronic acid to easily form cyclic boronic esters. The boronic acid copolymer proved to be an improvement to the PBrSt-b-CEMA copolymer in

terms of array-based reactions. However, the PCEMA-b-BoSt polymer was found out to be incompatible with signaling experiments due to the incapability of acquiring stable currents. However, the protected PCEMA-b-pBoSt coating was hydrophobic and has good electrochemical properties. If deprotection of the pinacol group after the polymer is applied onto the array could be realized with good control, this problem might be fixed.

For future coating development, a non-binding coating with the capability to acquire stable electrochemical signals is desired. Since hydrophilic polymer tends to have unstable currents, a non-binding hydrophobic surface would be optimal. Surfaces that are highly fluorinated may be a suitable choice.

3.16 Experimental section

General experimental procedures

Materials

All materials except the monomers for polymerization were used as purchased from Aldrich without further purification unless otherwise indicated. The monomers that were used directly for polymerization were purified by passing through a short neutral alumina column. Monomers that were synthesized were purified with standard organic synthetic procedures such as column chromatography.

Characterization

Fluorescence microscopy, NMR, FT-IR, LC-MS conditions were the same as in Chapter 2.

N,N-Dimethylformamide (DMF)-based gel permeation chromatography (DMF GPC) was conducted on a Waters Chromatography, Inc. (Milford, MA) system equipped with an isocratic pump model 1515, a differential refractometer model 2414, and a three-column set of Styragel HR 4, HR 4E 5 μm DMF, and 7.8 × 300 mm columns. The system was equilibrated at 70 °C in pre-filtered DMF containing 0.05 M LiBr, which served as polymer solvent and eluent (flow rate set to 1.00 mL/min). Polymer solutions were prepared at a concentration of ca. 3 mg/mL and an injection volume of 200 μL was used. Data collection and analysis was performed with Empower Pro software. The system was calibrated with poly(ethylene glycol) standards (Polymer Laboratories, Amherst, MA) ranging from 615 to 442,800 Da.

Tapping-mode AFM measurements were conducted in air with a Nanoscope III BioScope system (Digital Instruments, Santa Barbara, CA) operated under ambient conditions with standard silicon tips [type, OTEPSA-70; length (L), 160 μm; normal spring constant, 50 N/m; resonant frequency, 246-282 kHz

Contact angles measurement with different solvent treated microelectrode surfaces

Contact angles were measured as static contact angles with the sessile drop technique with a Tantec CAM micro-contact-angle meter and the half-angle measuring method. The contact angles of water (18 MΩ·cm, nanopure) were measured on the films at 30 s after the drop application.

Surface	**Contact angle**	**Standard Dev.**
Uncoated microelectrode arrays surface	42.0	± 2.2
PBrSt-b-CEMA Coated surface without solvent treatment	82.3	± 3.5
PBrSt-b-CEMA Coated surface washed with acetone	66.2	± 3.2
PBrSt-b-CEMA Coated surface washed with THF	79.8	± 5.8
PBrSt-b-CEMA Coated surface washed with MeCN/DMF/H_20=7/2/1	76.5	± 3.6
PBrSt-b-CEMA Coated surface reacted with pyrene-1-boronic acid via Suzuki reaction	54.5	± 4.5
PBrSt-b-CEMA Coated surface reacted with PEG-acrylate (5~6 repeating units) via Heck reaction	45.2	± 3.7

Sample procedure for spin-coating arrays with the block copolymer:

The microelectrode arrays were coated with a spin-coater MODEL WS-400B-6NPP/ LITE. The chip was inserted into a socket in the spinner and adjusted to be horizontal, then three drops of 0.03 g/mL block copolymer solution (For PBrSt-b-CEMA in 1:1

p-xylene /THF; for PCEMA-b-PEGMA in DMF; for PCEMA-b-BoSt in 9:1 1,4-Dixoane /water) were added onto the chip in order to cover the entire electrode area. The chip was then spun 1000 rpm for 40 seconds. The coating was allowed to dry for 15 min and subjected to irradiation using a 100 W Hg lamp for 20 min before use.

Sample cyclic voltammetry on 12-K array:

A 12-K microelectrode array was cleaned with a 9:1 solution of 3% H_2O_2 and conc. H_2SO_4 for 30 min at 65°C and then coated with the polymer as above. The array was incubated in 200 μL of 8 mM ferrocyanide and 8 mM ferricyanide in 1x PBS solution (made by dissolving 1 Phosphate Buffered Saline tablet ordered from SIGMA® in 200 mL DI water) for 15 min and then placed in the ElectraSense reader. One 12-electrode block was activated and cyclic voltammetry performed by scanning the potential at the electrodes from -700 to 700 mV and then back again at a scan rate of 400 mV/ s. The counter electrode was a platinum plate of area of 0.75 cm^2 held 650-800 μm away from the array by an O-ring. Next, the chip was covered with 100 μL of the same solution above with the addition of 1 μM Bovine Serum Albumin (BSA). The cyclic voltammetry was repeated as above for the 12-electrode block at various time intervals.

Sample procedure for dip-coating round disk electrode with the block copolymer:

The platinum round disk electrode (2 mm diameter) was cleaned with polishing with fine grade sandpaper and wiped with acetone and allowed to dry. It was then submerged into a 0.005 g/mL PBrSt-b-CEMA polymer solution in DMF, and lifted out of the solution

vertically. The solution left on the electrode surface was allowed to dry while the electrode was subjected to irradiation under a 100 W mercury lamp for 30 minutes.

Sample cyclic voltammetry on round disk electrode:

The coated round disk electrode was inserted into 10 mL of 8 mM ferrocyanide and 8 mM ferricyanide in 1x PBS solution (made by dissolving 1 Phosphate Buffered Saline tablet ordered from SIGMA® in 200 mL DI water) with a platinum wire counter electrode and Ag/AgCl reference electrode. Cyclic voltammetry was performed by scanning the potential at the electrode from -100 to 600 mV and then back at a scan rate of 200 mV/ s. Next, the electrtode was covered with 10 mL of the same solution above with the addition of 1 μM Bovine Serum Albumin (BSA). The cyclic voltammetry was repeated as above at various time intervals.

ATRP of 4-bromostyrene

The following are typical reaction conditions. In a 25 mL round-bottom Schlenk flask, 3.66 g (20.0 mmol) of 4-bromostyrene, 78 mg (0.4 mmol) of ethyl 2-bromoisobutrate, 0.208 g (1.2 mmol) of PMDETA and solvent (toluene vs monomer v/v=1:1) were added and degassed with 2 cycles of freeze-pump-thaw. Then 57.4 mg (0.4 mmol) of CuBr was added and the mixture was further degassed with 3 more freeze-pump-thaw cycles. After the final thawing, the flask was injected with argon and was kept at 110 °C. At time intervals, samples were taken by syringe. The percent conversion was measured by proton NMR with the solvent serving as an internal standard. After the conversion reached 80%,

the reaction was stopped by freezing it in liquid nitrogen. The reaction was then opened to the atmosphere and allowed to thaw. The mixture was diluted in THF and passed through a short neutral alumina column to remove copper salt and was precipitated into methanol and filtered to afford a white powder. The polymer was subjected to GPC analysis.

Copolymerization of HEMA with poly(4-bromostyrene) as macroinitiator

Typical reaction conditions were as follows. In a 25 mL round-bottom Schlenk flask, 1.00 g of poly(4-bromostyrene), 0.89 g (6.8 mmol) of HEMA, 57 mg (0.33 mmol) of PMDETA and solvent (MEK/1-propanol v/v=70:30 6.7 mL) were added and degassed with 2 cycles of freeze-pump-thaw. Then 11 mg (0.11 mmol) of CuCl was added and the mixture was further degassed with 3 more freeze-pump-thaw cycles. After the final thawing, the flask was injected with argon and was kept at 50 °C. At time intervals, samples were taken by syringe. The percent conversion was measured by proton NMR with solvent serving as the internal standard. After the conversion reached 80%, the reaction was stopped by freezing in liquid nitrogen. The flask was opened to the atmosphere and then allowed to thaw. The mixture was poured into water and filtered. Then the solid was dissolved in THF again and precipitated into 1:1 EtOAc/hexane to remove uninitiated homopolymer of poly(4-bromostyrene). The polymer synthesized behaves like hard elastomer. It was not submitted to GPC analysis until after the next step.

Post-polymerization modification of PBrSt-b-HEMA with cinnamoyl chloride

Typical reaction conditions were as follows. In a 50 mL round-bottom flask, 1.71 g p(4-BrSt-b-HEMA) was dissolved in 20 mL of anhydrous THF, and then 2.27 g (13.6 mmol) of cinnamoyl chloride and 5 mL Et_3N added. The mixture was stirred at room temperature for 24 hrs and kept from light. After the reaction was finished, the mixture was precipitated into methanol twice to afford a white powder. According to GPC analysis the homopolymer of 4-bromostyrene was efficiently removed by precipitation in a mixture of 1:1 EtOAc/Hexane at the P(4-BrSt-b-HEMA) stage. However, some lightly cross-linked high molecular weight polymer was also present in the sample and could not be removed. Its presence did not affect the performance of the block copolymer on the microelectrode arrays.

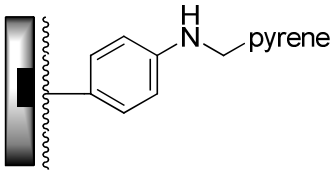

Example of the Copper(I) catalyzed coupling reaction of aryl halide and amine on the PBrSt-b-CEMA block copolymer

8.0 mg each of 1-pyrenemethylamine hydrochloride and Bu_4NBr, as well as 6 μL each of Et_3N, a 25 mM solution of $CuSO_4$ and a 50 mM solution of PPh_3, were dissolved into 100 µL of DMF in an Eppendorf tube. The DMF mixture was then dissolved into 1.5 mL of a 7:2:1 mixture of MeCN/DMF/Water. The PBrSt-b-CEMA polymer coated chip was incubated in this solution. A selected pattern was turned on and the chip was pulsed at -2.4 V relative to a remote Pt wire, cycling 0.5 sec on and 0.1 sec off for 600 cycles. The

chip was then washed with EtOH, DMF then EtOH again and let to dry. The chips were visualized with a fluorescence microscope.

Control Experiments

a) **b)**

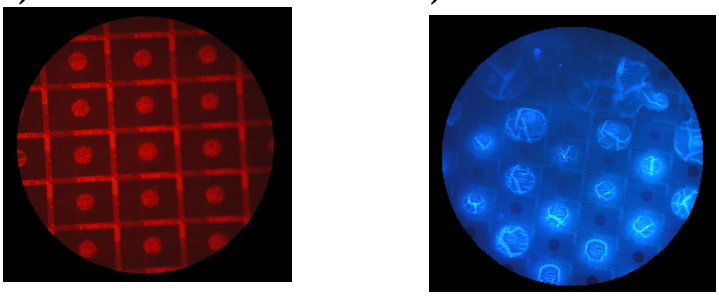

Figure S5. a) The block copolymer was stable to 15 consecutive experiments each using 300 cycles under Suzuki reaction condition. In no case, did the polymer degrade. b) The agarose polymer started to bubble and peel off after 3 consecutive experiments each using 300 cycles under the same Suzuki reaction conditions.

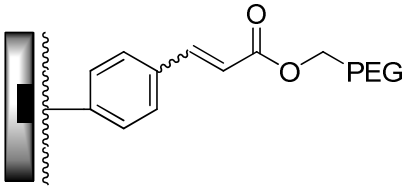

Example of the PEGylation by Heck reaction on the PBrSt-b-CEMA copolymer

A solution of 0.18 mg $Pd(OAc)_2$, 0.63 mg PPh_3, 20.0 mg Bu_4NBr, 25.0 mg PEG acrylate, 28.0μL Et_3N and 100.0 μL allyl acetate was dissolved in a 2:7:1 solution of DMF/MeCN/H_2O (1.5 mL). For the 12-K microelectrode arrays, the array was coated with the PBrSt-b-CEMA block copolymer, submerged in the solution made above, and then selected electrodes used as cathodes by pulsing them at a voltage of –1.7 V for 90 pulses for two times. The array was then repeatedly washed with acetone and DMF and

then examined using a fluorescence microscope.

ATRP of PEGMA

The following is condition that worked which did not lead to hydrogels. In a 25 mL round-bottom Schlenk flask, 2.32 g (5.0 mmol) of PEGMA benzoate, 19.5 mg (0.1 mmol) of ethyl 2-bromoisobutrate, 31.2 mg (0.2 mmol) of 2,2'-bipyridine and solvent (anisole vs monomer v/v=1:1) were added and degassed with 2 cycles of freeze-pump-thaw. Then 19.5 mg (0.1 mmol) of CuBr was added and the mixture was further degassed with 3 more freeze-pump-thaw cycles. After the final thawing, the flask was injected with argon and was kept at 50 °C. At time intervals, samples were taken by syringe. The percent conversion was measured by proton NMR with the solvent serving as an internal standard. After the conversion reached 45%, the reaction was stopped by freezing it in liquid nitrogen. The reaction was then opened to the atmosphere and allowed to thaw. The mixture was diluted in dichloromethane and passed through a short neutral alumina column to remove copper salt and was precipitated into methanol and concentrated to afford a white sticky paste. The polymer can not be dried over vacuum in which condition led to gel formation. Using of this polymer as a macroinitiator for copolymerization also led to gel formation.

ATRP of CEMA

The following are typical reaction conditions. In a 10 mL round-bottom Schlenk flask, 0.65 g (2.5 mmol) of CEMA, 9.8 mg (0.05 mmol) of ethyl 2-bromoisobutrate, 26 mg

(0.15mmol) of PMDETA and solvent (anisole vs monomer v/v=1:1) were added and degassed with 2 cycles of freeze-pump-thaw. Then 7.2 mg (0.05 mmol) of CuBr was added and the mixture was further degassed with 3 more freeze-pump-thaw cycles. After the final thawing, the flask was injected with argon and was kept at 70 °C (temperature greater than 80 °C led to cross-linking reaction). At time intervals, samples were taken by syringe. The percent conversion was measured by proton NMR with the solvent serving as an internal standard. After the conversion reached 80%, the reaction was stopped by freezing it in liquid nitrogen. The reaction was then opened to the atmosphere and allowed to thaw. The mixture was diluted in THF and passed through a short neutral alumina column to remove copper salt and was precipitated into methanol and filtered to afford a white powder.

Copolymerization of HEMA with PCEMA as macroinitiator

Procedures were the same as copolymerization of HEMA with poly(4-bromostyrene) as macroinitiator,

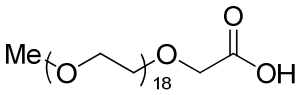

Poly(ethylene glycol) methyl ether acetic acid

To a solution of 16 g (Mw ~ 750, 0.02 mol) poly(ethylene glycol) methyl ether in 100 mL water, 6.6 g (85%, 0.1 mol) KOH was added slowly under 0 °C. After the KOH dissolved completely, 6.32 g (0.04 mol) $KMnO_4$ was added slowly over the course of 1 hour and the reaction mixture was withdrawn from ice bath and returned to RT for additional 2 hours

of stirring. The mixture was than filtered to remove the MnO^2, and acidified with 1 M HCl until pH = 3. The solution was then extracted with 30 mL of EtOAc for three times and dried over Na_2SO_4. The solvent was then removed under vacuum and the product was very clean according to NMR and was used without further purification as a white solid.

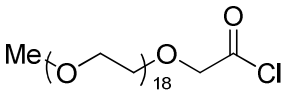

Poly(ethylene glycol) methyl ether acetyl chloride

5.41 g (7.0 mmol) poly(ethylene glycol) methyl ether acetic acid and 5 mL $SOCl_2$ was added in 30 mL benzene, and the mixture was refluxed for 3 hrs. The solvent and the unreacted $SOCl_2$ was removed under vacuum and the acid chloride was used in the coupling reaction without purification.

Post-polymerization modification of PCEMA-b-HEMA with PEG acid chloride

In a 50 mL round-bottom flask, 1.20 g PCEMA-b-HEMA was dissolved in 20 mL of anhydrous THF, and then 4.9 g (6.1 mmol, 2 equiv.) of poly(ethylene glycol) methyl ether acetyl chloride and 10 mL Et_3N added. The mixture was stirred at room temperature for 24 hrs and kept from light. After the reaction was finished, the mixture was condensed and poured into 200 mL water. The pH of the water was then adjusted to 5 and the polymer would aggregate and fall out of solution. The polymer was then filtered and dried (not in vacuum which would lead to cross-linking reaction).

RAFT polymerization of PHEMA-b-pBoSt

The following are typical reaction conditions. In a 25 mL round-bottom Schlenk flask, 1.30 g (10.0 mmol) of HEMA, 34 mg (0.1 mmol) of 2-cyano-2-propyl dodecyl trithiocarbonate, 2.8 mg (0.017 mmol) of AIBN and solvent (DMF vs monomer v/v=1:1) were added and degassed with 5 cycles of freeze-pump-thaw. After the final thawing, the flask was injected with argon and was kept at 90 °C. At time intervals, samples were taken by syringe. The percent conversion was measured by proton NMR with the solvent serving as an internal standard. After the conversion reached 80%, the second monomer pinacol protected 4-styreneboronic acid (2.30 g, 0.010 mol) was diluted in DMF (v/v=1:1) and was degassed with 5 cycles of F-P-T. The mixture was then injected into the polymerization mixture and the temperature was raised to110 °C. The reaction was stopped after the conversion of the second monomer reached 80% by cooling the reaction mixture to RT and opened to the atmosphere. The mixture was used directly for the post polymerization DCC coupling reaction without removal of the DMF solvent.

Post-polymerization modification of PHEMA-b-pBoSt with DCC coupling to cinnamic acid

In a 100 mL round-bottom flask, the reaction mixture obtained from the above procedure was diluted with 40 mL DMF, 1.64 g (0.011 mol) cinnamic acid, 2.48 g (0.012 mol) DCC, and 60 mg (5.0 mmol) DMAP was added into the solution and the mixture was protected from light and was allowed to stir under room temperature for 48 hrs. After the reaction was finished, the mixture was filtered and the polymer could be precipitated in methanol. The fluffy polymer was collected by centrifuge. The obtained polymer was dissolved in

THF and precipitated again in methanol to further purify, and was collected by centrifuge and dried over vacuum.

Deprotection of PCEMA-b-pBoSt with phenyl boronic acid on polystyrene resin

0.100 g PCEMA-b-pBoSt polymer, 0.60 g (2.6-3.2 mmol/g, ~1.8 mmol) phenyl boronic acid polystyrene resin was added into 15 mL 2% TFA/MeCN and the mixture was refluxed for 24 hrs under vigorous stirring. The mixture was then cooled down and THF was added into the mixture until the polymer dissolved. The mixture was then filtered to remove the resin and precipitated into water. NMR indicated both the boronic ester and carboxylic esters have been partially hydrolyzed.

Deprotection of PCEMA-b-pBoSt with phenyl boronic acid in THF/H_2O

1.0 g of PCEMA-b-pBoSt and 2.2 g (18 mmol) phenyl boronic acid was added into 50 mL THF with 2% TFA, and the solution was allowed to stir under room temperature for 24 hrs. If the reaction was stopped at this stage, partially deprotected (40% to 50%) could be obtained. If not stopped, water was added into the mixture slowly in small portion until the solution turned slightly cloudy, and the reaction was allowed to go until the solution turned clear again. The process was repeated until the solution no longer turned clear after the addition of water. The reaction was allowed to stir for another 2 hrs and was stopped. The polymer could be precipitate into diethyl ether to remove the PBA and be dissolved in THF/water 4:1 mixed solvent and precipitate in ether again to purify. The afforded polymer was a white powder like polymer that did not dissolve in any single solvent. A

mixture of THF/water or 1,4-dioxane/water could easily dissolve it.

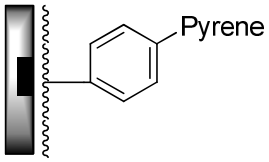

Example of the inversed Suzuki reaction on the PCEMA-b-BoSt block copolymer

A mixture of 0.18 mg $Pd(OAc)_2$, 0.63 mg PPh_3, 20.0 mg Bu_4NBr, 5.0 mg 1-bromopyrene, 28.0μL Et_3N and 100.0 μL allyl acetate was dissolved in a 2:7:1 solution of DMF/MeCN/H_2O (1.5 mL). For the 1-K microelectrode arrays, the array coated with the PCEMA-b-BoSt block copolymer was submerged in the solution and then selected electrodes used as cathodes by pulsing them at a voltage of –2.4 V for 0.5 sec on and 0.1 sec off. After 3 min, the chip was repeatedly washed with acetone and DMF and prepared for pyrene-based fluorescent analysis. For the 12-K microelectrode arrays, the array was coated with the block copolymer and then submerged in the solution prepared above. Selected electrodes were used as cathodes by pulsing them at a voltage of –2.4 V for 90 pulses. The array was then repeatedly washed with acetone and DMF before examination using a fluorescence microscope.

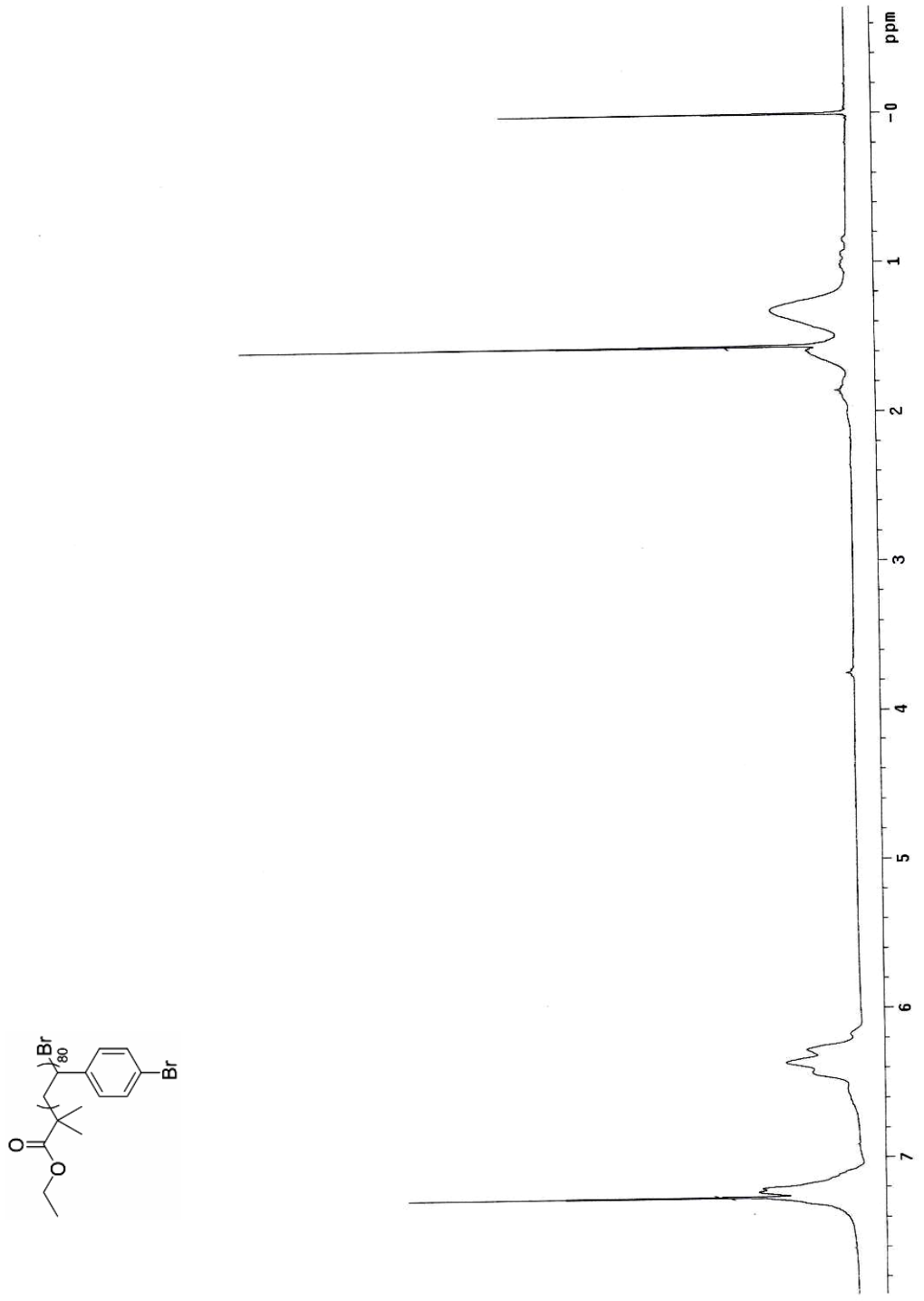
Br
80
Br
O
O
ppm
−0
1
2
3
4
5
6
7

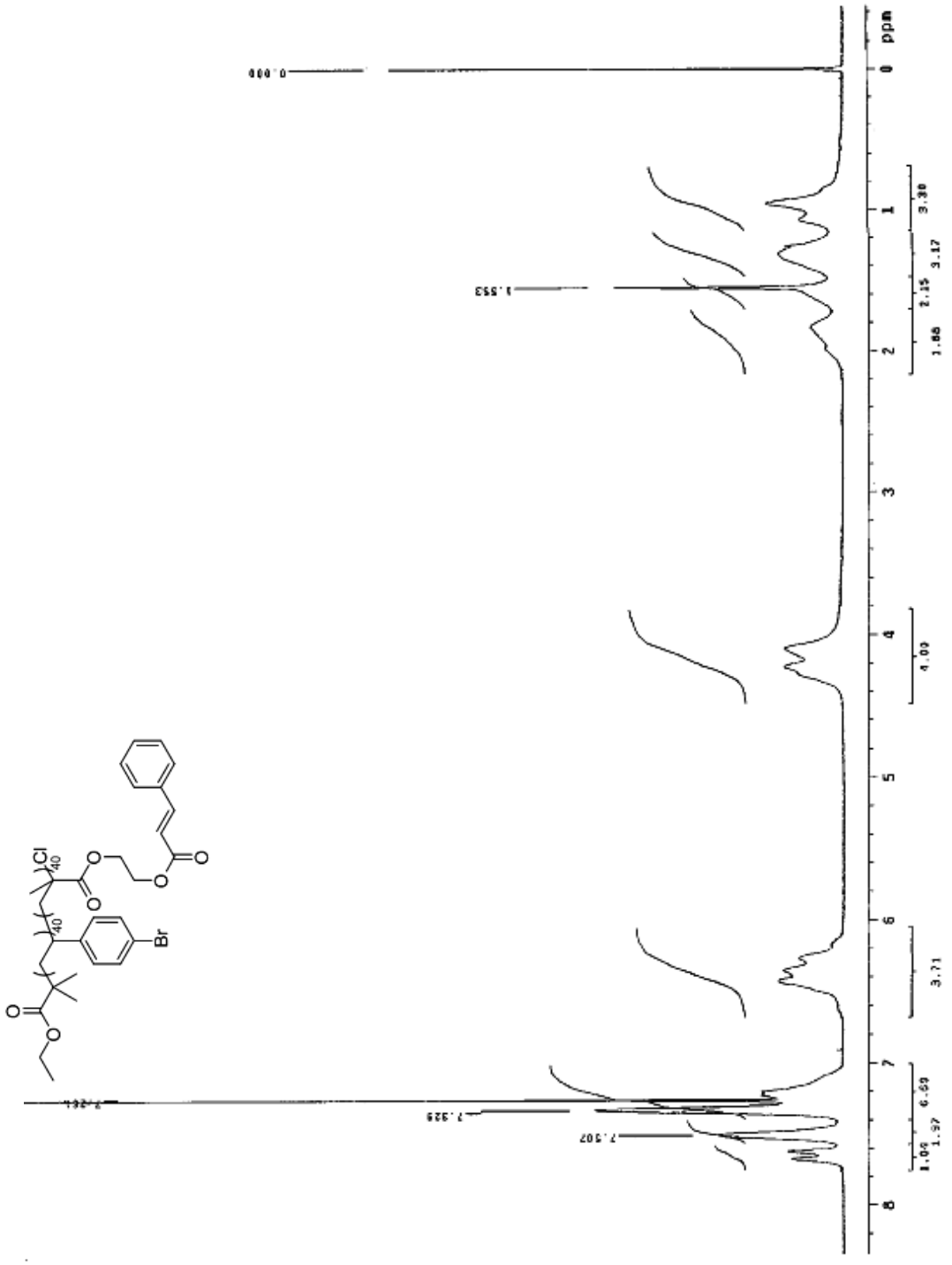
Cl
40
40
Br
O
O
O
O
O
O
0.000
1.553
7.261
7.329
7.507
ppm
0
1
2
3
4
5
6
7
8
4.00
3.71
6.69
1.97
1.00
3.30
3.17
2.15
1.88

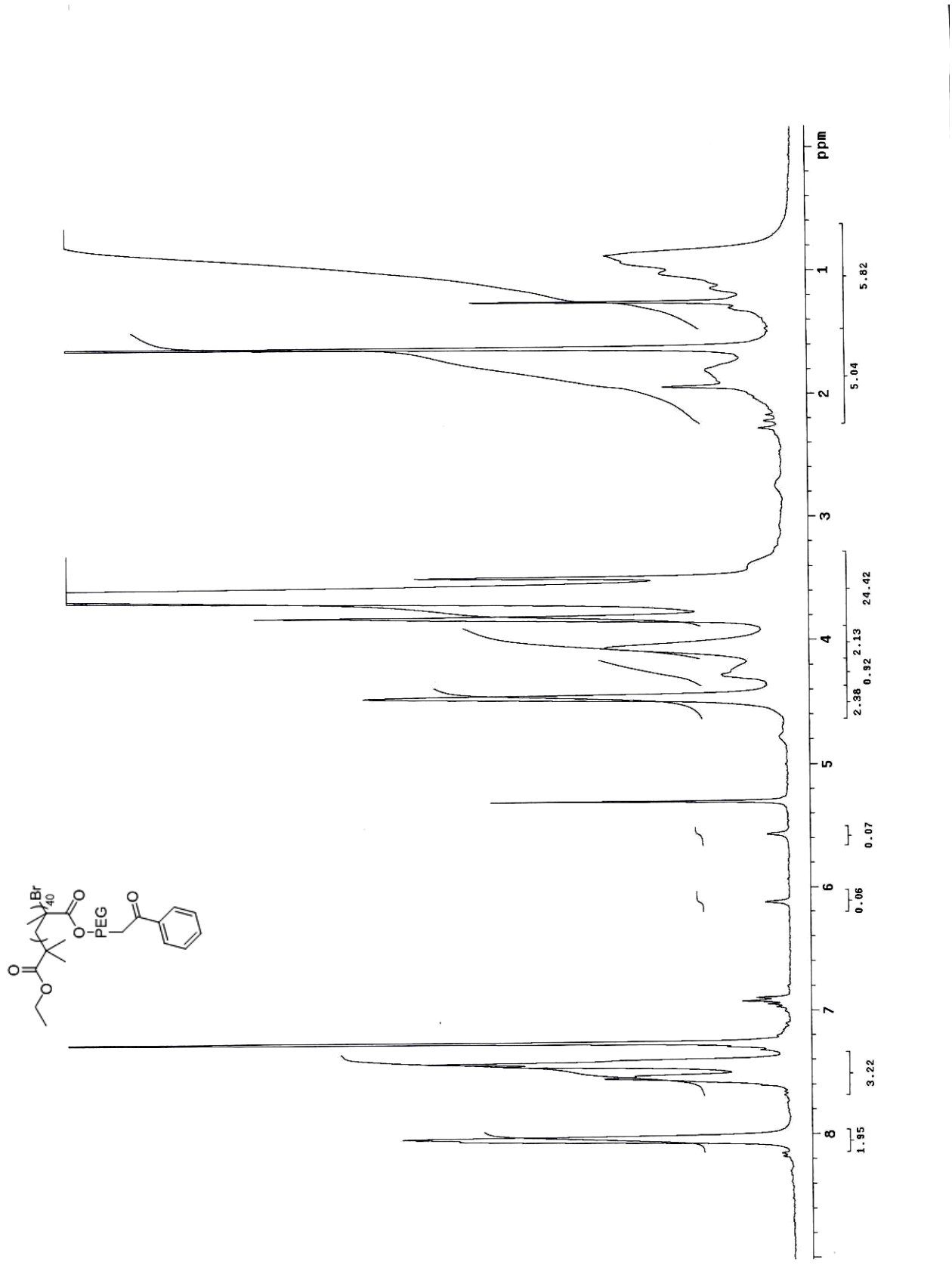
Br
40
O
O
O
PEG
O
O
ppm
1
2
3
4
5
6
7
8
5.82
5.04
24.42
2.13
0.92
2.38
0.07
0.06
3.22
1.95

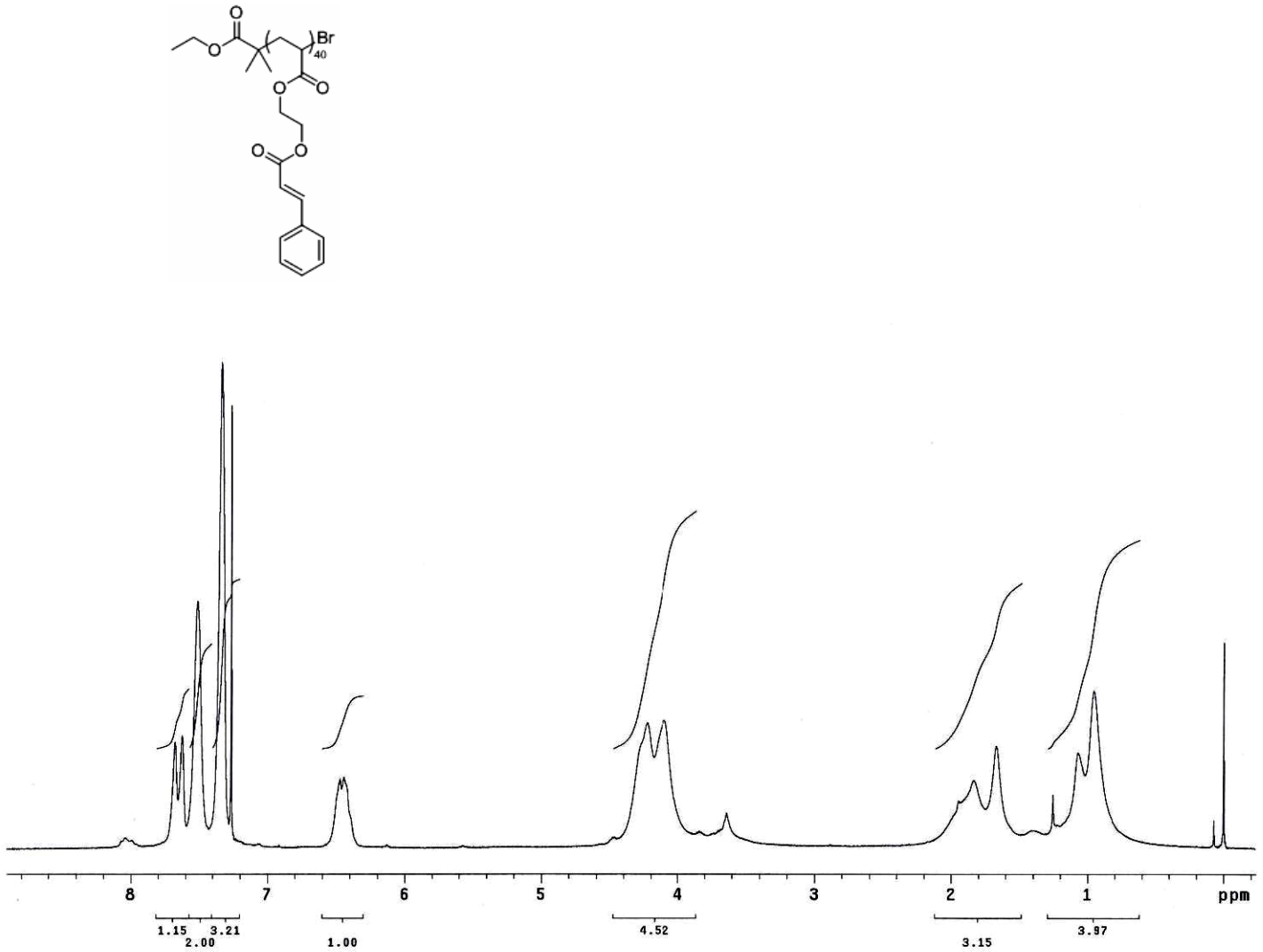
Br
40
8
7
6
5
4
3
2
1
ppm
1.15
3.21
2.00
1.00
4.52
3.15
3.97

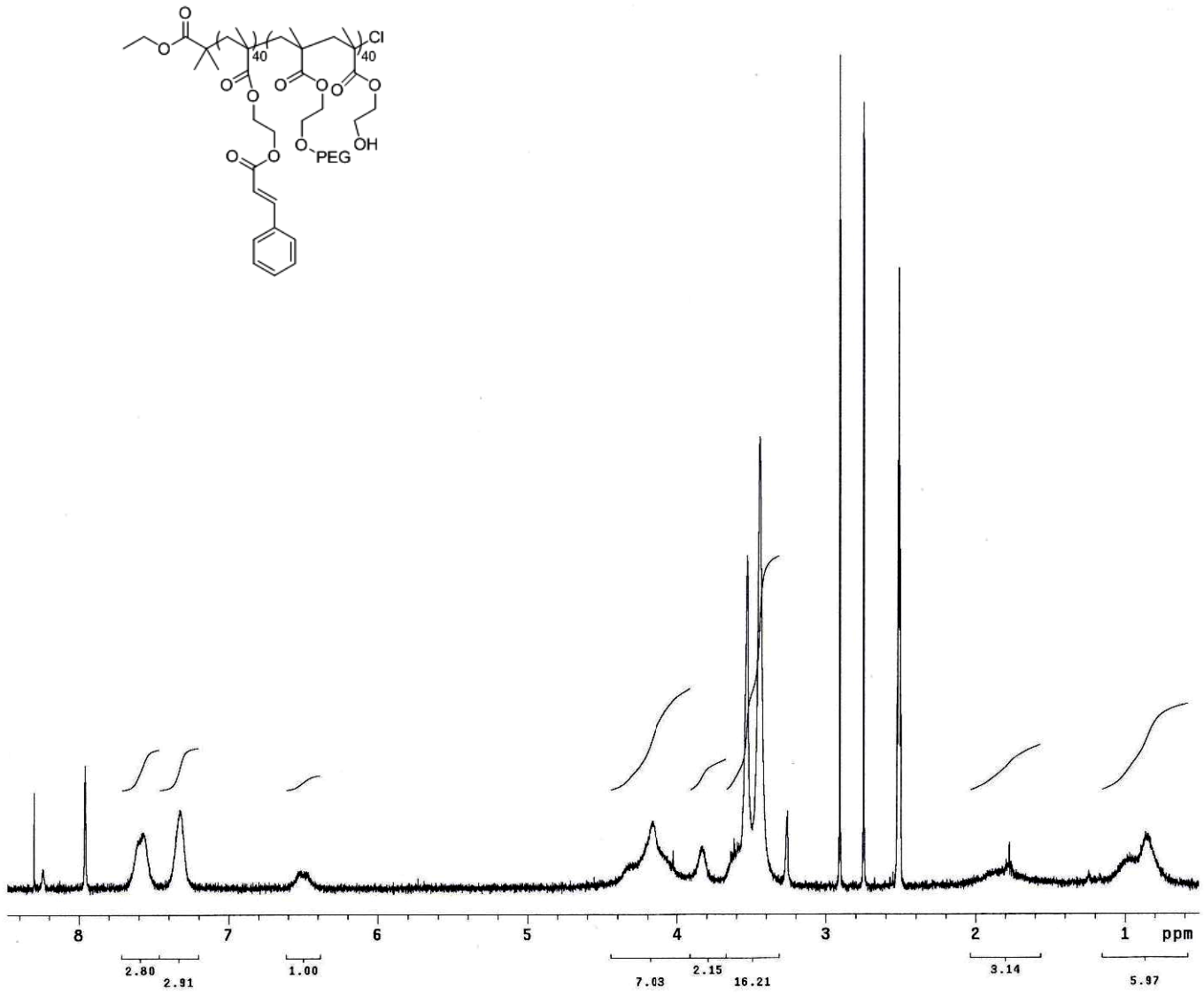
Cl
40
40
PEG
OH
8
7
6
5
4
3
2
1
ppm
2.80
2.91
1.00
7.03
2.15
16.21
3.14
5.97

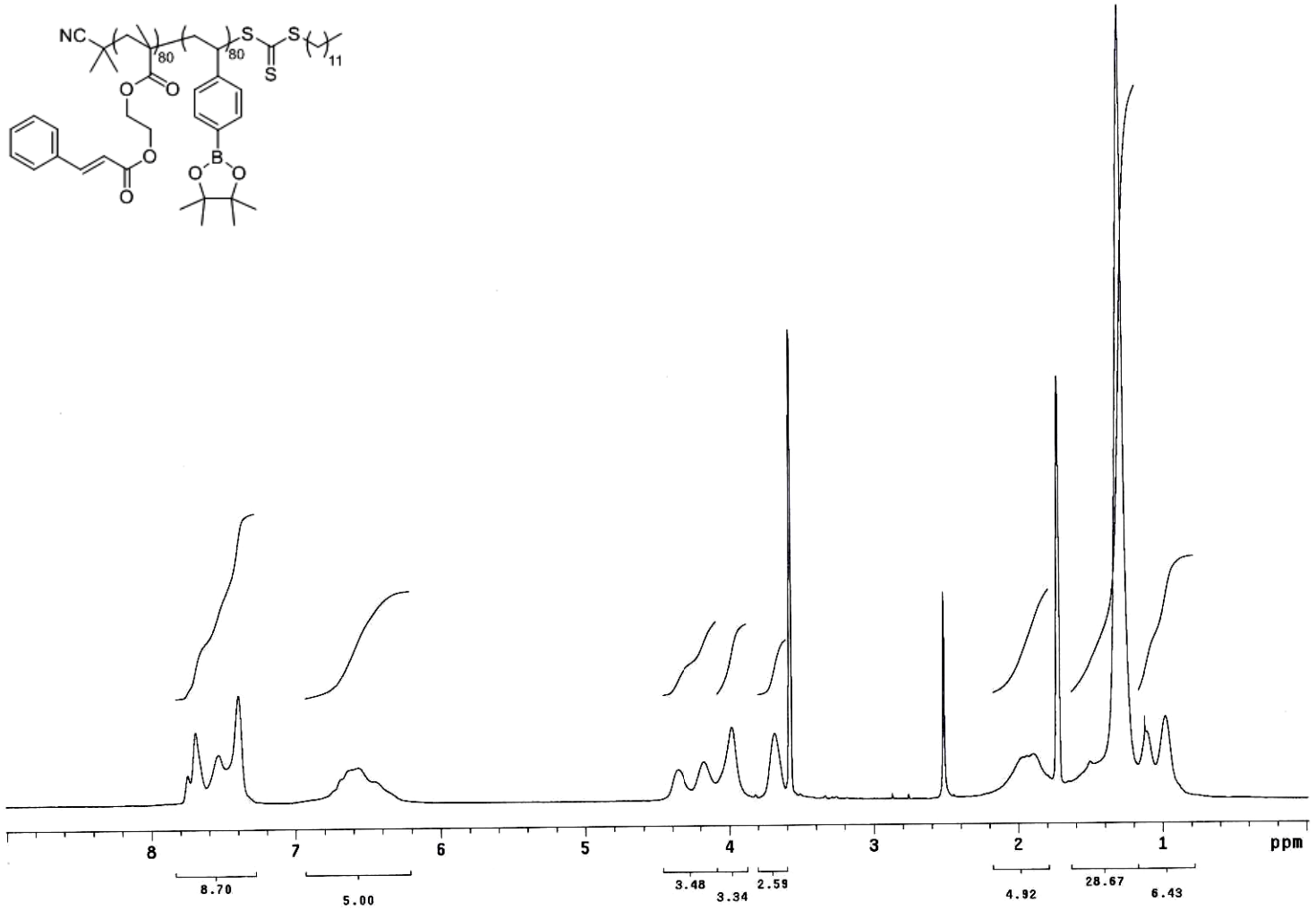
NC
80
80
S
S
S
11
O
O
O
O
B
O
O
8
7
6
5
4
3
2
1
ppm
8.70
5.00
3.48
3.34
2.59
4.92
28.67
6.43

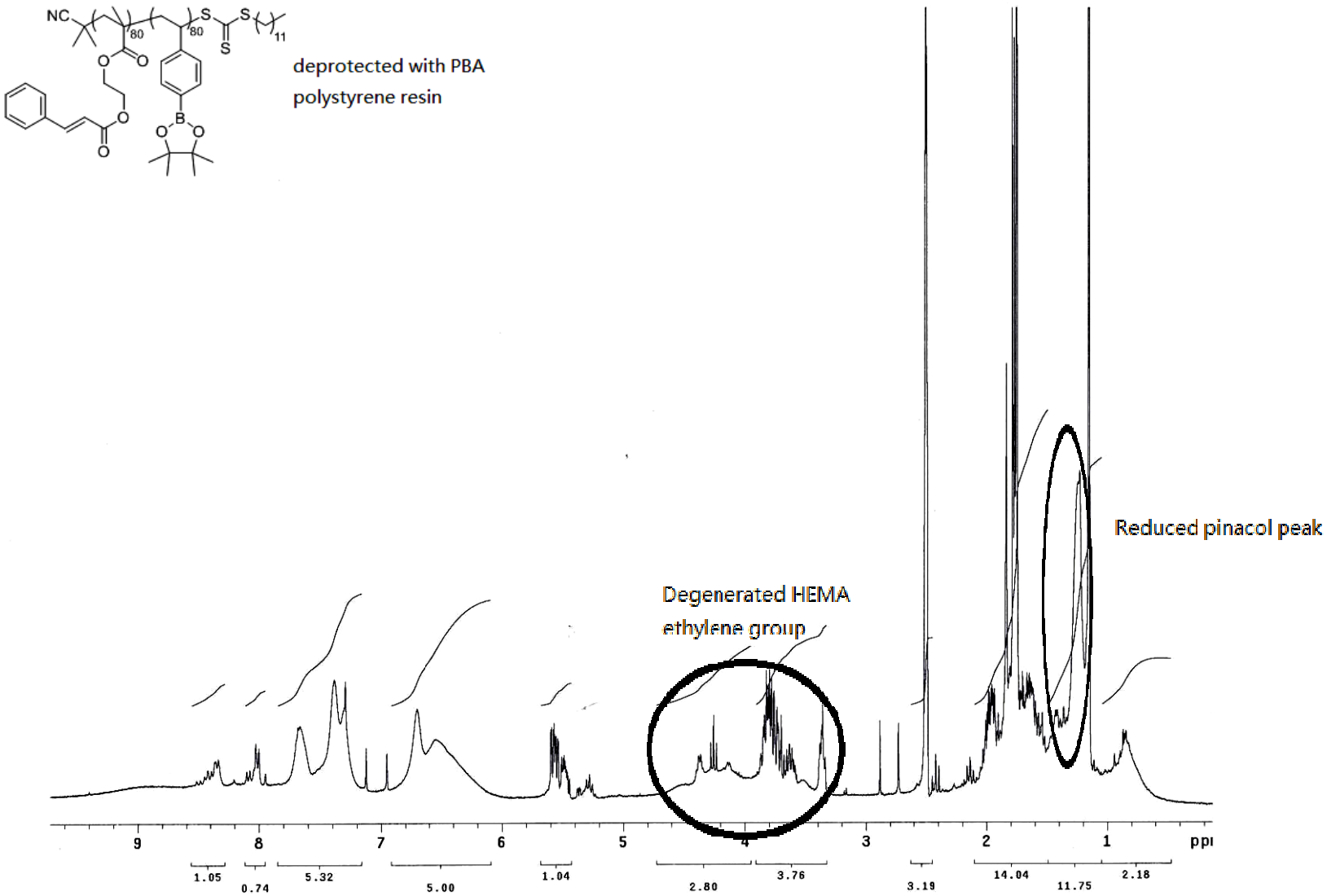
deprotected with PBA
polystyrene resin
Degenerated HEMA
ethylene group
Reduced pinacol peak
9
8
7
6
5
4
3
2
1
ppm
1.05
0.74
5.32
5.00
1.04
2.80
3.76
3.19
14.04
11.75
2.18

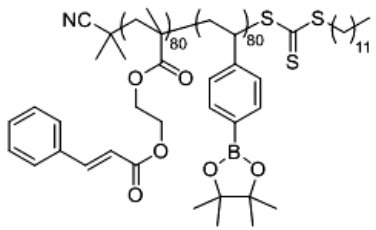

Partially deprotected with
PBA in THF/TFA

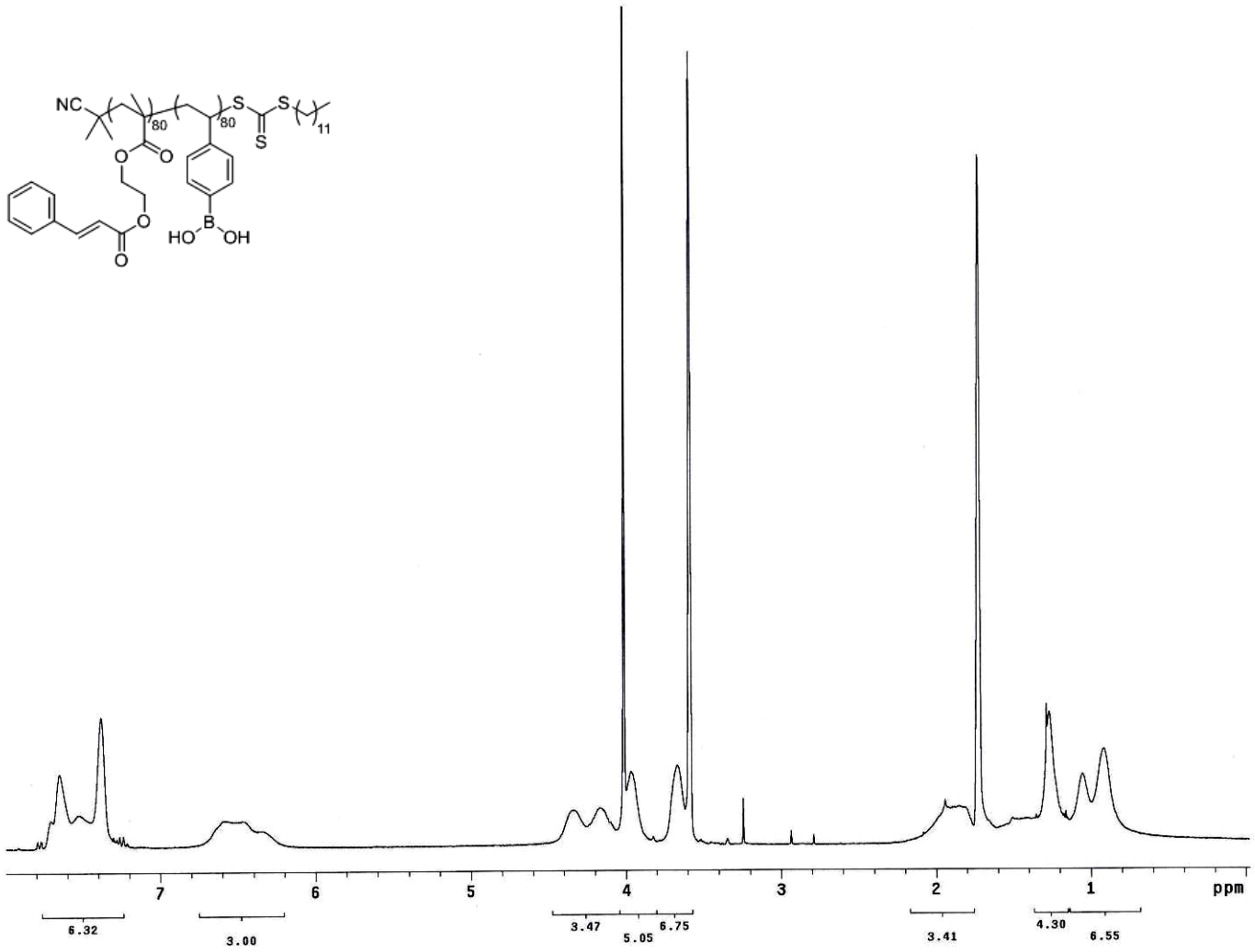
NC
80
80
S
S
S
11
O
O
O
O
B
HO
OH
7
6
5
4
3
2
1
ppm
6.32
3.00
3.47
5.05
6.75
3.41
4.30
6.55

Reference and Notes

1. For examples using agarose see: (a) Hu, L.; Maurer, K.; Moeller, K. D. *Org. Lett.* **2009**, *11*, 1273. (b) Bartels, J. L.; Lu, P.; Walker, A.; Maurer, K.; Moeller, K. D. *Chem. Commun.* **2009**, 5573.

2. For examples using sucrose see: (a) Stuart, M.; Maurer, K.; Moeller, K. D. *Bioconjugate Chem.* **2008**, *19*, 1514.(b) Maurer, K.; McShea, A.; Strathmann, M.; Dill, K. *J. Combi. Chem.* **2005**, *7*, 637.

3. For an example of agarose instability see: Kesselring, D.; Maurer, K.; Moeller, K. D. *J. Am. Chem. Soc.* **2008**, *130*, 11290.

4. Tesfu, E.; Roth, K.; Maurer, K.; Moeller, K. D. *Org. Lett.* **2006**, *8*, 709.

5. Ding, J.; Tao, J.; Guo, A.; Stewart, S.; Hu, N.; Birss, V. I.; Liu G. *Macromolecules* **1996**, *29*, 5398.

6. Liu, G. U.S. (**1995**), US 5409739 A 19950425.

7. For impedance using uncross-linked polymer see: (a) Justin, G.; Rahman, A. R. A.; Guiseppi-Elie, A. *Electroanalysis* **2009**, *21*, 1125. (b) Rahman, A. R. A.; Justin, G.; Guiseppi-Elie, A. *Electroanalysis* **2009**, *21*, 1135.

8. Bartels, J.; Lu, P.; Maurer, K.; Walker, A. V.; Moeller, K. D. *Langmuir* **2011**, *27*, 11199.

9. Wang, J.; Matyjaszewski, K. *Macromolecules* **1995**, *28*, 7901.

10. Jousset, S.; Qiu, J.; Matyjaszewski, K. *Macromolecules* **2001**, *34*, 6641.

11. Beers, K. L.; Boo, S.; Gaynor, S. G.; Matyjaszewski, K. *Macromolecules* **1999**, *32*, 5772.

12. Chiefari, J.; Chong, Y. K.; Ercole, F.; Krstina, J.; Jeffery, J.; Le, T. P. T.; Mayadunne, R. T. A.; Meijs, G. F.; Moad, C. L.; Moad, G.; Rizzardo, E.; Thang, S. H. *Macromolecules* **1998**, *31*, 5559.

13. For review of ATRP see: Matyjaszewski, K.; Xia, *J. Chem. Rev.* **2001**, *101*, 2921.

14. For review of RAFT see: (a) Moad, G.; Rizzardo, E.; Thang, S. H. *Aust. J. Chem.* **2005**, *58*, 379. (b) Perrier, S.; Takolpuckdee, P. *J. Polym. Sci. Part A: Polym. Chem.* **2005**, *43*, 5347.

15. Chen, H.; Yuan, L.; Song, W.; Wu, Z.; Li, D. *Prog. Polym. Sci.* **2008**, *33*, 1059.

16. For the usage of PEG to reduce protein non-specific binding see: (a) Tugulu, S.; Klok, H. *Macromol. Symp.* **2009**, *279*, 103. (b) Michel, R.; Pasche, S.; Textor, M.; Castner, D. G. *Langmuir*. **2005**, *21*, 12327.

17. Neugebauer, D.; Zhang, Y.; Pakula, T.; Sheiko, S. S.; Matyjaszewski, K. *Macromolecules* **2003**, *36*, 6746.

18. Cambre, J. N.; Roy, D.; Gondi, S. R.; Sumerlin, B. S. *J. Am. Chem. Soc.* **2007**, *129*, 10348.

19. Roy, D.; Cambre, J. N.; Sumerlin, B. S. *Chem. Commun.* **2008**, 2479.

20. Neises, B.; Steglich, W. *Angew. Chem., Int. Ed.* **1978**, *17*, 522.

21. Roy, C. D.; Brown, H. C. *J. Organomet. Chem.* **2007**, *692*, 784.

Chapter 4

The Study on Electrochemical Signaling Experiments

4.1 Introduction to electrochemical signaling experiments

As the advancement of biochemistry greatly progresses in recent decades, people have been seeking ways to study biological interactions more accurately and more efficiently. In this context, methods that can rapidly monitor interactions in "real-time" are particularly attractive. Because they detect interactions as they happen, real-time measurements do not require washing steps and hence can accurately account for weak binding interactions. This leads to an increase in both the amount and quality of information obtained about a biological target being examined. As mentioned in the previous chapters, microelectrode arrays hold great potential as tools for accomplishing these goals.[1-4]

The usage of microelectrode array for detecting biological interactions is not a new concept. CombiMatrix Corporation has been working to use the same microelectrode arrays used in our group for diagnostics and pathogen detection.[5] As a brief example, an electrochemical ELISA (Enzyme-Linked ImmunoSorbent Assay) technique was developed for detecting small amounts of a target antigen (Figure 4.1).[5a]

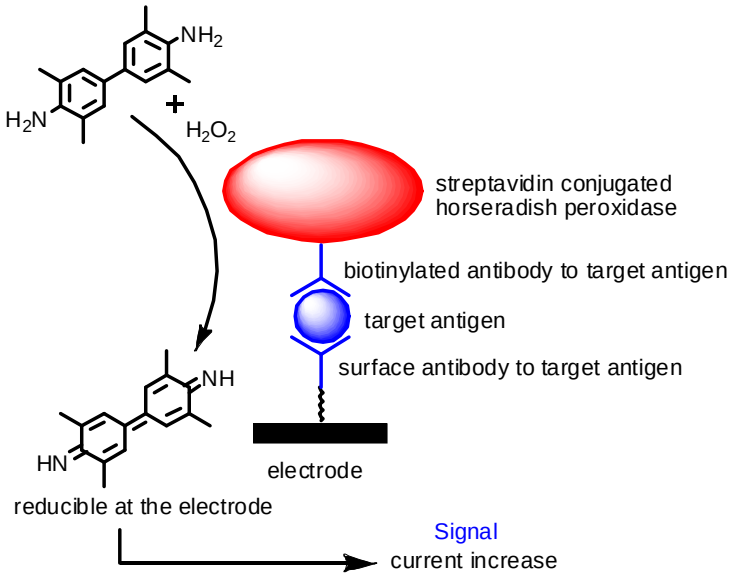

Figure 4.1 Electrochemical ELISA experiment developed by CombiMatrix.

In this experiment, several different antibodies were immobilized on different areas of the microelectrode array. Unmodified areas on the array were then blocked with bovine serum albumin (BSA) to knock down non-specific binding of other proteins. The array was then inserted into an antigen solution which was targeted by one specific antibody on the array. Then the array was washed and then incubated with another biotinylated antibody solution that would bind to the antigen. After this step, the array was washed again and placed in a solution containing streptavidin-conjugated horse radish peroxidase, an enzyme that catalyzes an oxidation reaction of a particular substrate in the solution at the presence of hydrogen peroxide. In this way, the oxidized product is formed only by electrodes in the array that are functionalized with the correct antibody for recognizing the antigen. The oxidized product then serves as a substrate for a reduction at the electrode. Hence, when the electrodes were used as cathodes, a current increase relative to the background can be observed. On electrodes modified with other antibodies no enzyme

is present and hence only background current is observed. The detection limit of this method can be as low as 10^{-9} M for the antigen concentration.[5a]

While these experiments can be very useful, our group has a different goal. We are not using the arrays to detect analytes in solution with the use of known, strong binding interactions, but rather to discover and evaluate new binding interactions. Since the binding interactions discovered may have weak binding constants, the CombiMatrix method, that takes advantage of strong binding interactions as well as multiple washing steps, is not appropriate. Instead, we need a more direct way to obtain signals from a binding event. In this context, an electrochemical impedance experiment appeared ideal (Figure 4.2).

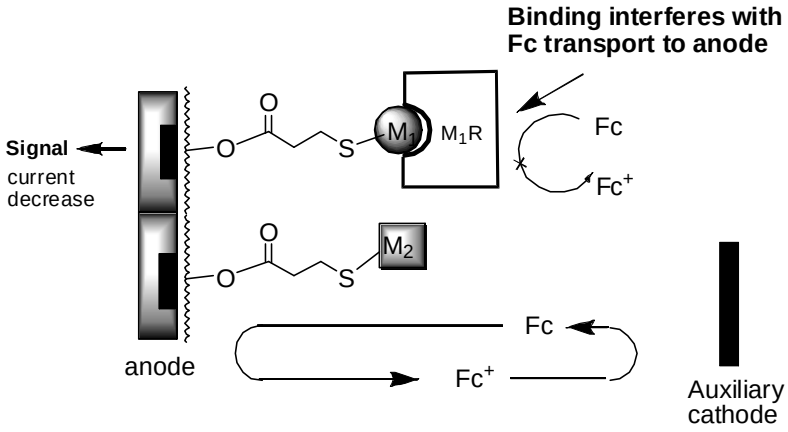

Figure 4.2 Electrochemical impedance generated by a binding event.

The proposal is analogous (although opposite) to the use of electroanalytical methods developed by the Murata group.[6] They have reported using the electrochemical impedance generated by binding of β-naphthoflavone to a dioxin receptor to serve as a biosensor for the ligand. In this experiment, a set of two gold electrodes were modified with two different receptors, and only one of them was

known to bind to the ligand. An unmodified gold electrode was also used as a negative control. Then cyclic voltammetry was run on the modified electrodes in a series of solutions containing different β-naphthoflavone concentrations. The electrode modified with the binding receptor showed extensive current drop (Figure 4.3a) as the current decreased while the electrode modified with the other receptor and the unmodified electrode did not show much drop (Figure 4.3b and 4.3c).

a) b) c)

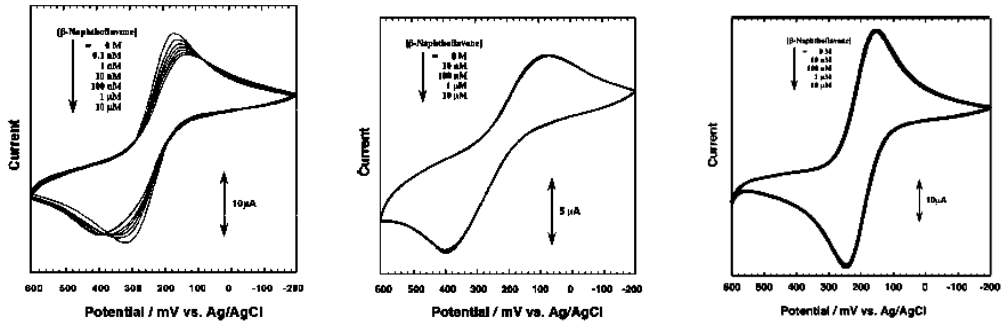

Figure 4.3 Overlapped CVs of a) the binding receptor and b) the non-binding receptor and c) bare surface with different ligand concentrations. Image courtesy of Bioorganic and Medicinal Chemistry Letters, Elsevier.

Since the microelectrode arrays we use have the intrinsic advantage of having multiple electrodes on the same surface. This provides us an opportunity to use a variant of the method developed by the Murata group to investigate the binding interactions of a receptor with multiple ligands in a very short period of time. The main variation needed is that for the studies proposed we would place the small molecule ligands on the surface of the array and the receptor in solution. Preliminary results from our group's early studies have demonstrated the viability of this variation.

The first example was a study carried out by Dr. Eden Tesfu.[7] In this study, a coumarin derivative was immobilized on the microelectrode array using the chemistry illustrated in Scheme 4.1. The array was then incubated in different antibody solutions to investigate the binding of coumarin to the antiboies. The result was shown in Figure 4.4. This preliminary result showed that the microelectrode array did not show any notable current drop when incubated in an antibody solution that was not targeted to coumarin (an anti-2,4-DNP antibody was used – red line). When incubated in the anti-coumarin antibody solution, the array was responsive to the binding event by showing a large current drop between the two CVs (green line).

Scheme 4.1

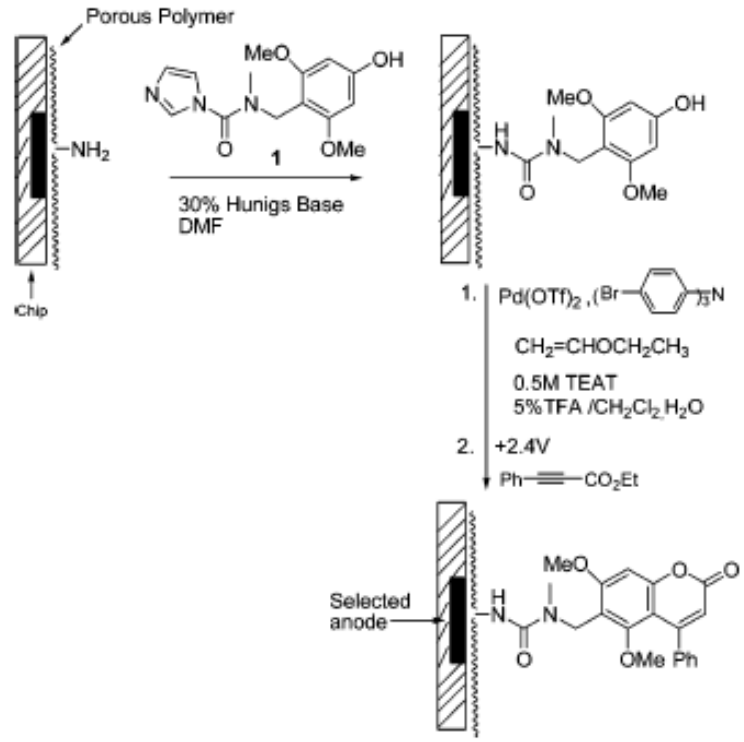

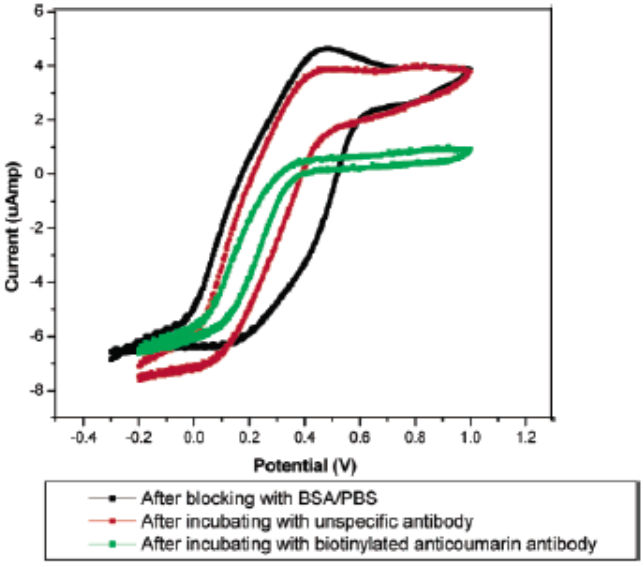

Figure 4.4 Cyclic voltammograms of the coumarin-modified electrode with different antibody solutions.

In another study carried out by Dr. Melissae Stuart, two different peptides were immobilized on the same array to compare binding properties to an integrin receptor.[8] The first was an RGD peptide known to bind tightly to the integrin receptor. The second was an RAD peptide known to have minimal binding to the receptor. In this way, the only difference between the two sites on the array was the methyl group on the alanine of RAD peptide. The array was first incubated in a solution that did not contain integrin, and background CVs were obtained for potassium ferricyanide at the electrodes modified with the two peptides (red lines in Figure 4.5). The array was then washed and incubated in the integrin solution and CVs were again obtained for the two groups of electrodes (blue lines in Figure 4.5). This experiment demonstrated the ability of the microelectrode array to signal multiple ligands on the same array by comparing relative current drops of different ligands.

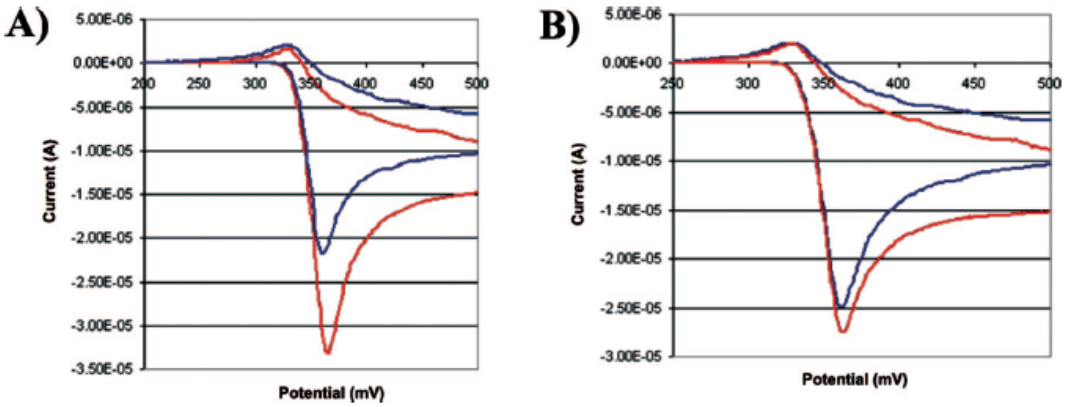

Figure 4.5 Cyclic voltammograms of a) RGD peptide b) RAD peptide. The red lines were obtained with a blank solution and show the current associated with potassium ferricyanide in the solution above the array. The blue lines were obtained with an integrin receptor in solution.[8]

Both preliminary results demonstrated the impedance experiments were possible. However, neither involved a systematic study on the signaling experiments or an examination of how receptor concentration could be used to identify relative binding constants. Such experiments were not possible because of the instability of the surface used to support the molecules on the array. With the stable surfaces developed during the efforts described in Chapter 3, this is no longer a problem. By taking advantage of a new surface, we investigated the relationship between reaction conditions and the quality of the signaling experiments. In addition, we discovered incorrect setups for the impedance experiments that will need to be avoided in the future. These studies are reported here in the hopes that they lay a foundation for future efforts in this area.

4.2 The question of non-specific binding on the block copolymer coating PBrSt-b-CMEA

The first polymer coating PBrSt-b-CEMA described in Chapter 3 serves as an excellent choice to study signaling experiments due to its stability and compatibility with array-based reactions. An initial test of whether the block copolymer PBrSt-b-CEMA is compatible with the electrochemical signaling experiment was performed by using an anti-2,4-DNP antibody to recognize a 2,4-DNP functional group placed on the surface of the array. The 2,4-DNP group was put in place by using an electrochemically mediated Heck reaction to form a ketone on the array followed by incubation of the resulting array in a solution of 0.5% 2,4-dinitrophenylhydrazine in 2N HCl for 30 min (Scheme 4.2).

Scheme 4.2

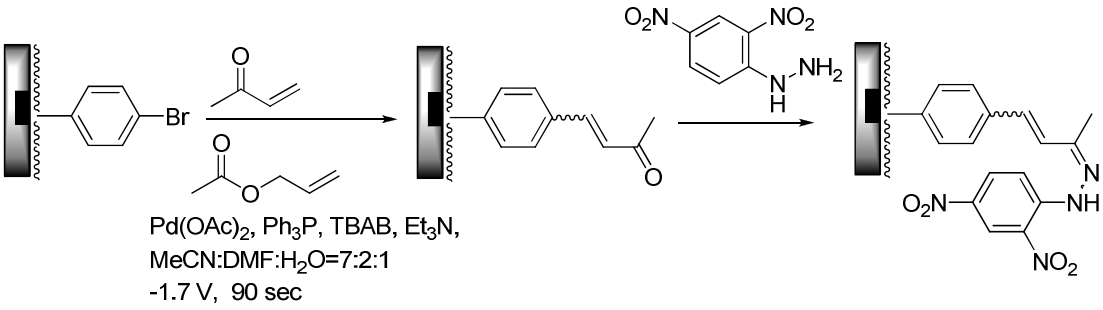

After the reaction, the array was washed with ethanol, 2N HCl, and then ethanol again. The array was then used for the electrochemical signaling experiment. For this experiment, two blocks of 10 electrodes each were selected to conduct a cyclic voltammogram (CV) of an iron species in the solution above the array. One of the electrode blocks selected was functionalized with the 2,4-DNP group and the other was a blank with no modification. The chip was incubated in a solution containing

0.13 mg/mL of the anti-2,4 DNP antibody along with solution with 8 mM ferrocyanide, 8 mM ferricyanide and 5% BSA. The solvent used was a 5x PBS buffer. The resulting CV's for the two blocks of electrodes are shown in Figure 4.6.

a)

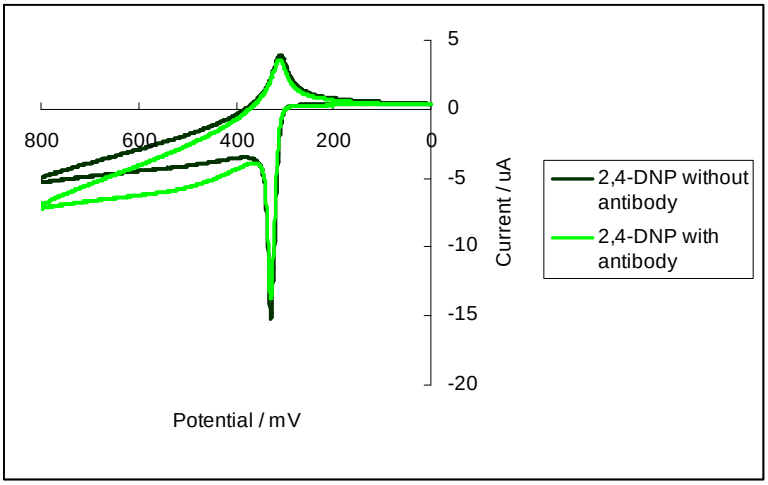

b)

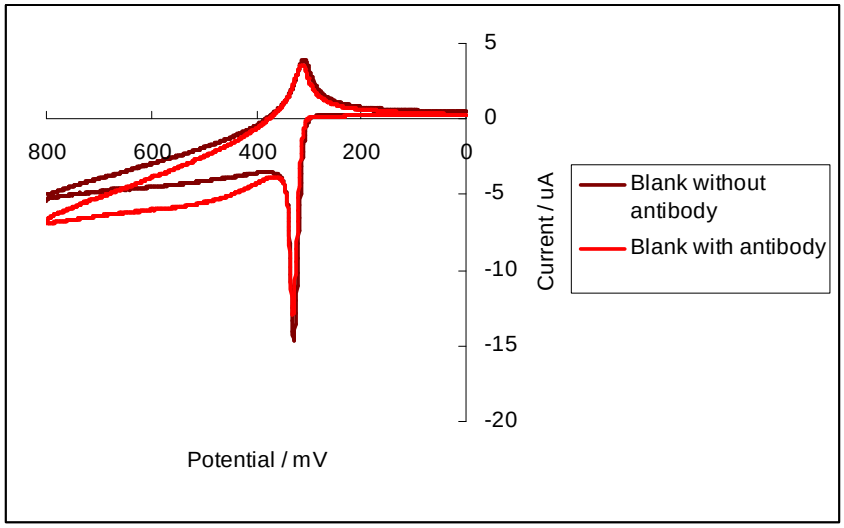

Figure 4.6 2,4-DNP binding experiment on 12K array. a) CVs run with electrodes modified with 2,4-DNP b) CVs run with unmodified electrodes. Condition: 8 mM $K_3Fe(CN)_6$ /$K_4Fe(CN)_6$ dissolved in 5x PBS solution in water, pH=7.0, anti-2,4-DNP antibody concentration ca. 10^{-5} M. Scan rate = 200 mV/s.

As shown in Figure 4.6, although the 2,4-DNP modified electrodes showed a current drop from no-antibody solution to antibody solution, the unmodified electrodes

showed an identical drop as well. When the array used in this experiment was examined with the use of a fluorescence microscope, the image showed a uniform whole board pattern rather than the selected 10 electrode pattern expected. This indicated that non-specific binding of the antibody to the block copolymer coated surface diminished the difference between the modified and unmodified electrodes.

The result of this experiment suggested a very challenging problem, the non-specific binding of proteins to the surface. To further investigate non-specific binding of proteins to the polymer surface, bovine serum albumin (BSA) was used as a cheap model protein for study. In this experiment, the $K_3Fe(CN)_6$ /$K_4Fe(CN)_6$ redox couple was selected for the cyclic voltammetry experiment. The concentration of BSA above the array was varied from 10^{-6} M to 10^{-3} M. The result was shown in Figure 4.7.

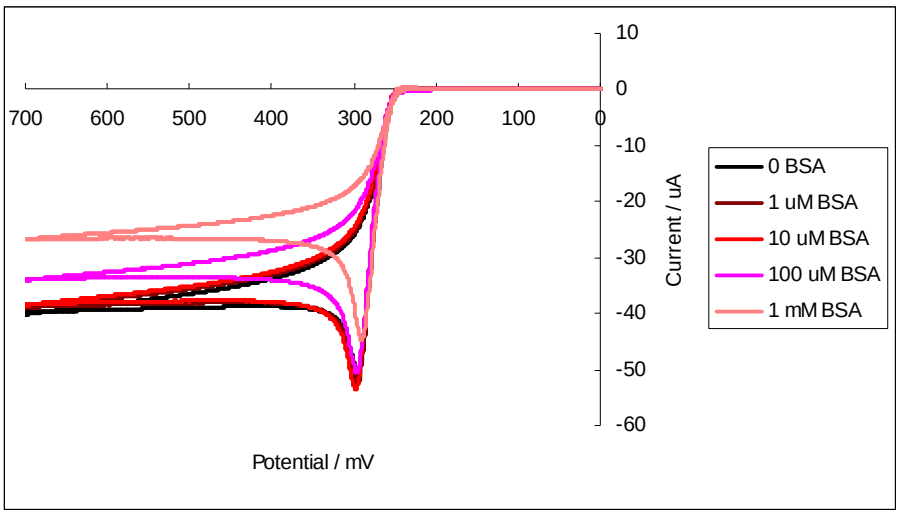

Figure 4.7 BSA non-specific binding experiment on PBrSt-b-CEMA surface. Condition: 8 mM $K_3Fe(CN)_6$ /$K_4Fe(CN)_6$ dissolved in 1x PBS solution in water, pH=7.5, BSA concentration from 10^{-6} M to 10^{-3} M. Scan rate = 200 mV/s.

The result showed that the non-specific binding of BSA to the surfaced started with a concentration of BSA of about 10^{-4} M. The non-specific binding of BSA to the surface became more extensive at 10^{-3} M. While this experiment verified the existence of non-specific binding of BSA to the polymer surface, it also raised a second question: should BSA really be used in signaling experiments to reduce the non-specific binding of other proteins to the surface of the array? In our previous studies, BSA had been used in high concentration (5% in wt, ca. 10^{-3} M) to first coat the surface of the array. The plan was to block interactions between the antibodies or integrin receptors used in these studies with the surface of the array. This idea originated from the use of BSA in ELISA studies. In an ELISA experiment, antibodies are immobilized onto plastic plates and then the plate then coated with a layer of BSA protein. The BSA prevents the binding of antigens and enzymes added to the solution above the microplate later in the experiment from binding to the microplate non-specifically. This keeps non-specific binding events involving the antigens and enzymes from giving rise to false signals that lead to a high level of background noise. In this context, the use of BSA is very effective. However, since the experiments are monitored by color change and BSA is transparent, BSA binding to the surface does not cause a false signal. However, with an impedance experiment this is not the case. BSA binding to the surface will block the iron species in solution from reaching the electrodes in the array. The CV being recorded will show this event with a large drop in current. If this is the situation, then the binding of the protein being studied to the ligands on the surface has to increase the impedance even further. If this

difference is not large enough, the signal for the protein would not be observable (Figure 4.8). Even if the new impedance can be observed, the signal to noise ratio of the experiment might be very low.

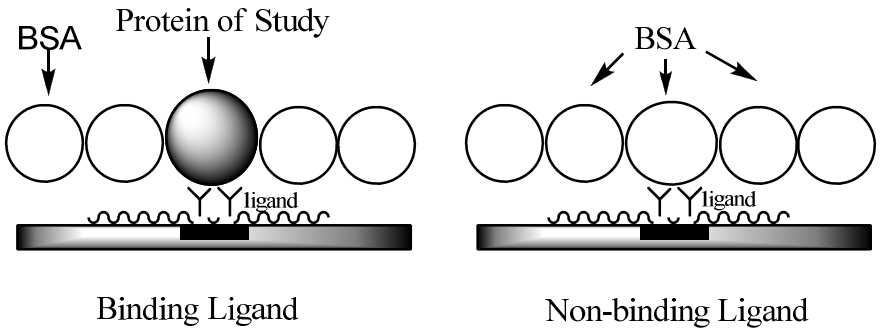

Figure 4.8 Back ground noise introduced by using BSA to block non-specific binding of protein of study to the surface.

Simply put, the BSA used in the ELISA experiments is “transparent” to the final signal generation; however, the BSA used in the electrochemical impedance experiments is not.

Now that using BSA to knock down non-specific binding was no longer a viable method, it appeared that it would be best to develop a polymer surface that underwent minimal non-specific binding with the proteins to be studied. Of course, this would only be necessary for the examination of very weak binding events. When investigating strong binding ligand-receptor interactions, the concentrations of the protein of study are so low that non-specific binding to the surface will most likely not be a problem. With moderate binding ligands on the array, the binding events are most likely still going to be strong enough so that difference data between the electrodes with the ligands and electrodes with no ligand can be used to evaluate the

ligand-protein interaction. In other words, in these cases the signal to noise for the experiments would still be expected to be sufficient for our needs. The same might be true for a weak binding interaction, but such conclusions will need to be determined on a case by case basis. Of course, the use of a minimal binding surface would be optimal (the discussion in Chapter 3).

With this in mind, we decided to use stronger binding interactions to probe the compatibility of the block copolymer with the signaling experiments and develop strategies for obtaining quantitative information from the arrays.

4.3 The correct way of connecting the 12-K instrument to the potential stat

For this work, we initially chose the binding of biotin to avidin as a model. The binding constant of biotin and avidin was reported to be approximately 10^{-15} *M*, which is one of the strongest binding interactions in nature.

In this experiment, biotin was immobilized onto the surface using the strategy illustrated in Scheme 4.3. First, the PBrSt-b-CEMA surface was functionalized with 2-hydroxyethyl methacrylate using Heck reaction. The result converted the bromophenyl of the original polymer to a free hydroxyl group by the electrodes in the array. The activated ester of biotin was then used to form an ester of this hydroxyl group. This transformation took advantage of a VB_{12}-mediated, base catalyzed esterification reaction.[9]

Scheme 4.3

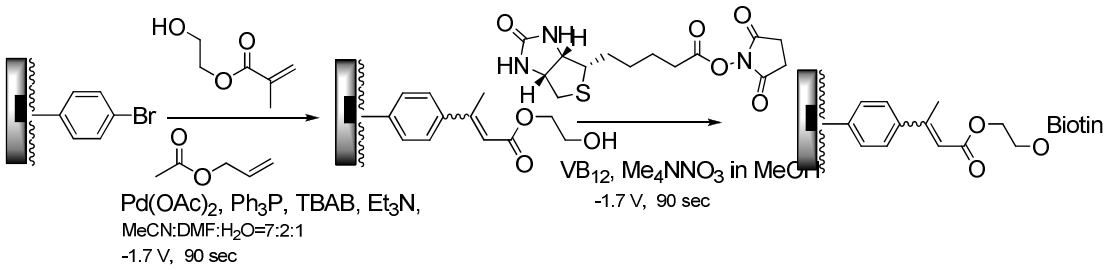

After the array was modified with biotin, it was incubated in a series of avidin solutions with each incubation being followed by a cyclic voltammogram. The cyclic voltammogram was used to monitor a $K_3Fe(CN)_6$ /$K_4Fe(CN)_6$ redox couple in the solution above the array. The avidin concentration used was varied from 10^{-18} M to 10^{-6} M in 1 order of magnitude increments. After taking the current intensity from the same potential (700 mV) of the cyclic voltammograms of each protein concentration, the result obtained from the biotin modified electrodes was shown in Figure 4.9.

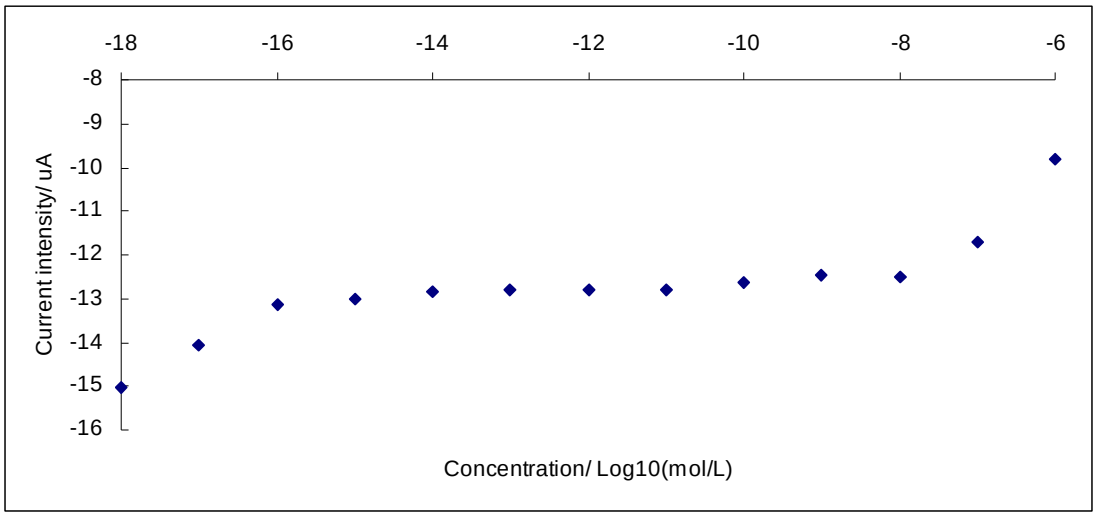

Figure 4.9 Biotin and avidin binding experiment on PBrSt-b-CEMA surface. Condition: 8 mM $K_3Fe(CN)_6$ /$K_4Fe(CN)_6$ dissolved in 1x PBS solution in water, pH=7.5, avidin concentration from 10^{-18} M to 10^{-6} M. Scan rate = 200 mV/s.

The binding curve generated showed that an initial drop in current occurred at extremely low concentration of avidin. This is consistent with the binding of avidin to the biotin on the surface. The difference between the known binding constant and the measurement here could result from errors in the concentration of protein, as well as the fact that the experiments monitor the concentration of receptor rather than the concentration of a ligand in solution. A second drop in current was observed at a concentration of 10^{-7} *M*. This drop in current was consistent with the dimerization of avidin on the surface of the array.

While this experiment showed how sensitive the experiments on the array could be, it also exposed a problem with our experimental setup. When we repeated the experiment with electrodes that were not modified with biotin on the same array, we observed an identical result (Figure 4.9). This is quite similar as the result shown in Figure 4.6. While the result shown in Figure 4.6 could be rationalized with non-specific binding of the protein to the surface, there is no way that the result in this experiment was due to non-specific binding.

After some trial and error, we found out that no matter which electrodes we chose, or how many electrodes we chose, we always got identical cyclic voltammograms from the same array in the same solution. In other words, no matter what molecules we put onto the surface, the cyclic voltammogram we obtained from them would be the same no matter what electrodes we used on the array. The molecules did not need to be near the electrodes used. We have even tried a half coated and half uncoated array, which still offered the same CV whether we used the

coated half or the uncoated half. Clearly, the CV's we were examining showed the molecule on the array but did not reflect the surface conditions of actual electrodes used for the analysis. If this problem cannot be solved, then it would be pointless to build a library on the microelectrode array because the signaling experiment could not differentiate the electrodes.

It was not until much later, after a trip to the CombiMatrix Corporation in Seattle to discuss the issue that we finally realized what the problem was. At CombiMatrix, I learned the basics of the 12K-instrument and finally understood how the original signaling experiment setup was incorrect.

As discussed in Chapter 1, a 12K-instrument has 6 terminals that are used to conduct experiments (Figure 4.10). How these terminals are connected to the working and counter electrodes determines whether oxidation or reduction happens on the microelectrode arrays.

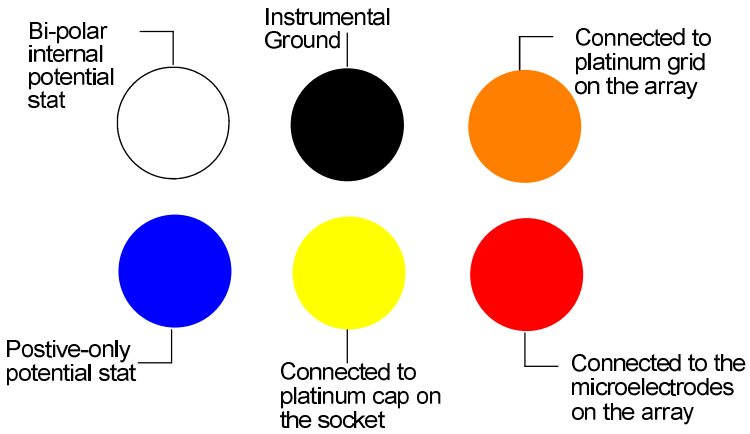

Figure 4.10 The 6 terminals on the 12 K instrument.

After gaining a better understanding of the reaction setup, it was not hard to discover the problem with our original setup (Figure 4.11a).With the original

CV-setup, the yellow terminal was connected to the working electrode clip, and the red terminal was connected to the counter and reference electrode clip. In other words, the platinum cap on the socket was used as the working electrode and the microelectrode array was used as counter and reference electrode. Hence, the current measured was being measured on the cap and not the array. The reaction setup was backwards. Since the array was only being used as the counter electrode, the experiment turned on all of the electrodes on the array. In this way, each CV-experiment conducted was identical. It did not matter which electrodes were chosen. The platinum cap never changed its size or properties. As long as the CVs were run in the same solution, we were always looking at the same experiment.

a) b)

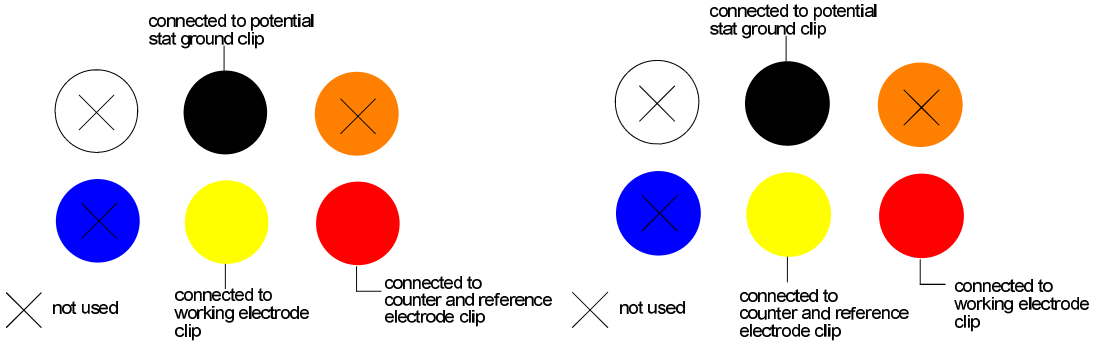

Figure 4.11 The a) wrong and b) right way to connect the 12K instrument to the external potential stat.

With the problem understood, it was easy to fix. By simply reversing the connection (Figure 4.11b), using the red terminal as the working electrode and the yellow terminal as the counter and reference electrodes, we became able to study the surface conditions on each individual microelectrode.

Once this was done, the CV's obtained from different areas of the array were no longer identical. This finally opened the door for analyzing libraries on the array and provided us with an opportunity to answer questions about the consistency and uniformity of the impedance experiments conducted at various sites on the array.

4.4 Reinvestigate the possibility of signaling experiments on microelectrode arrays

While we were glad that we finally solved the problem of the array being not able to distinguish electrodes, the CVs obtained with the correct instrumental connection looked completely different from the CVs obtained the other way (Figure 4.12).

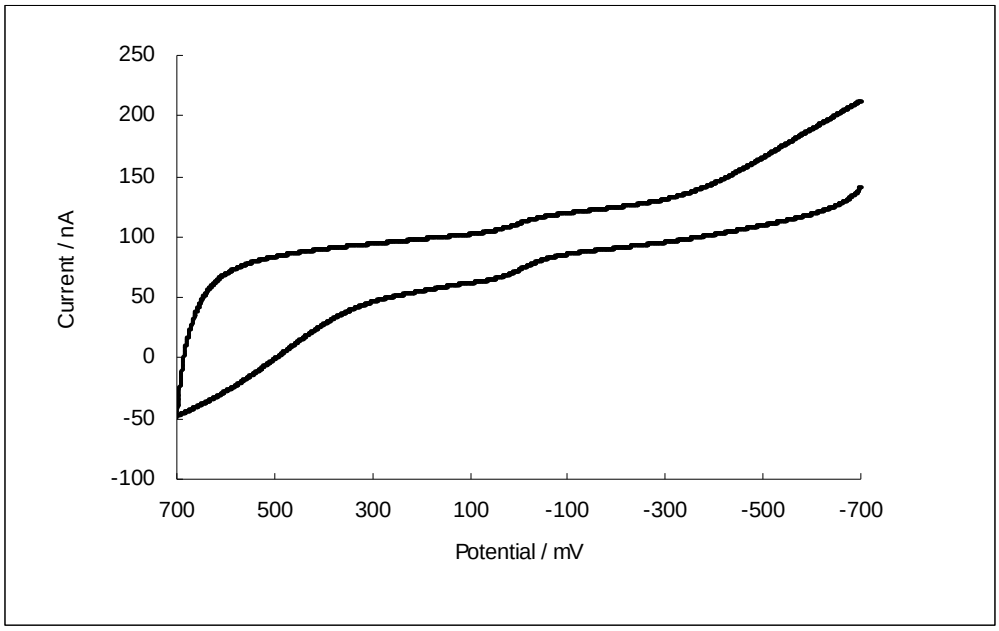

Figure 4.12 Cyclic voltammogram using a block of 12 electrodes on the 12-K arrays. Condition: 8 mM $K_3Fe(CN)_6$ /$K_4Fe(CN)_6$ dissolved in 1x PBS solution in water, pH=7.5. Scan rate = 400 mV/s.

To begin with, the shape of the CV was no longer the regular “duck-shaped” CV previously seen, the CV obtained with the correct instrumental connection was much flatter, and at times lacked the obvious peaks previously seen. This was true even at scan rates of up to 400 mV/s. This change was expected and reflects the difference between a regular bulk electrode (the cap) and a microelectrode. For bulk electrodes, the rate limiting factor during a cyclic voltammetry scan is diffusion of the redox species to the surface of the electrode. When the rate of diffusion can no longer catch up with the rate of oxidation/reduction, the current will reach the peak and start to decrease. However, with a microelectrode the rate limiting step is the electron transfer reaction between the electrode and the redox species. The rate of diffusion of the redox species to the electrode is fast. This results from the microelectrode having spherical diffusion gradients above the surface of the electrode rather than the linear diffusion gradients associated with a bulk electrode. In this case, diffusion of the redox pair to the surface of the electrode can always keep pace with the rate of electron transfer. The curve in the CV simply levels off when the maximum rate of electron-transfer possible is reached.

Secondly, the CV curve looked more reversible than the CV obtained from the wrong setup. Once again, this is very reasonable. With fast diffusion to the surface, the electrode current shows all of the species in solution. Since the solution contains a 1:1 mixture of both Fe(II) and Fe(III) species in the solution, the CV should show currents associated with each.

It is a little harder to understand why the previous reaction setup did not show

the reversible wave. However, the data obtained did offer a strong suggestion. First, when a CV experiment was run using a solution with no iron species, A CV similar to that obtained with the iron species was observed, although the magnitude of the current measured was far smaller. This CV was an artifact of the surface of the array or the cap. When iron was added to the solution, the CV increased in intensity. Such observations are consistent with catalytic currents. Catalytic currents occur when a reactive species is generated on an electrode surface and then a solution phase substrate regenerates the starting material on the surface. The result is a CV wave at a potential that reflects the artifact on the electrode surface and a current that reflects the concentration of the species in solution. Such waves are never reversible because the reactive species on the surface is recycled with the solution phase reagent and not the reversal of the electrode current. Third, the overall current obtained with the correct setup was much smaller than the current obtained with previous setup. In fact, the total current dropped from the μA level to nA level. This was again not a surprise since with the correct setup the experiments reflected the much smaller microelectrodes used as the working electrode. With the correct setup, the current recorded was proportional to the number of electrodes employed on the array, a very comforting observation. Finally, the zero current point for the CV with the correct setup drifted from the instrumental zero point by about 70 nA (higher). The reason for this phenomenon is not clear, however, as long as the zero point current stays consistent it does not matter. Since the drops in current in an impedance experiment are all relative numbers, a consistent zero point current means all of the numbers can

be normalized. With an understanding of how the correct setup changed the CV waves, we were in position to reexamine the utility of the arrays for conducting signaling experiments. The first control experiment performed examined the cyclic voltammograms obtained when different concentrations of the iron species were used. The purpose of this experiment was to verify that the current intensity obtained from the CV was indeed related to the amount of iron that reached the electrode surface. This is the foundation of the signaling experiment, because the signal measured should reflect the change of localized iron concentration proximal to the electrodes. If the current is independent from the iron concentration, then no current change would be observed and the signaling experiment would not be effective.

The experiment was done using a group of 12 electrodes with a 3x4 rectangular pattern on the array, sweeping from 1 mM $K_3Fe(CN)_6$ /$K_4Fe(CN)_6$ to 64 mM of each iron species (each increment doubled the amount of iron used in the previous experiment) in a 1 x PBS buffer solution on the PBrSt-b-CEMA block copolymer surface. The result is shown in Figure 4.13.

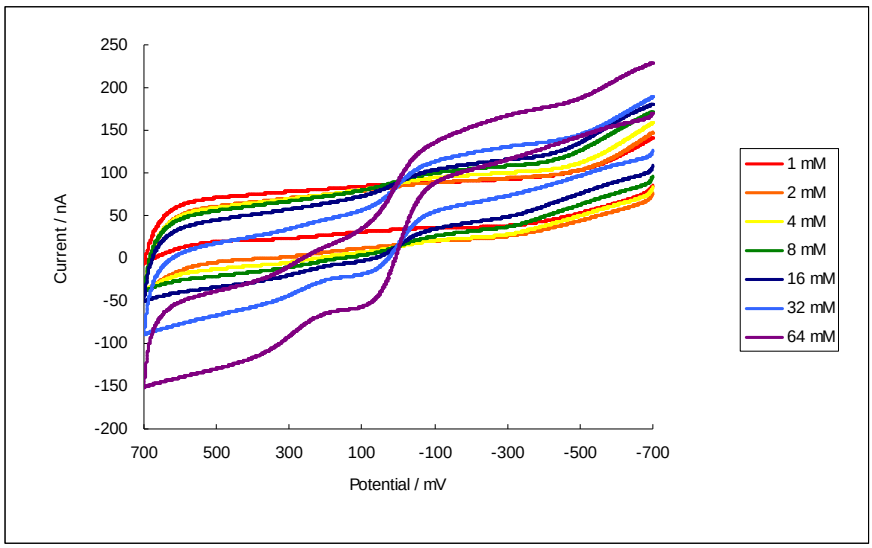

Figure 4.13 Cyclic voltammogram using a block of 12 electrodes on the PBrSt-b-CEMA surface. Condition: 1 to 64 mM $K_3Fe(CN)_6$ /$K_4Fe(CN)_6$ dissolved in 1x PBS solution in water, pH=7.5. Scan rate = 400 mV/s.

It was clear that the current intensity of the CV was directly related to the concentration of iron in solution, an observation that indicated that the binding of a receptor to the surface of the array should induce a drop in current at the electrode below. While the result of this confirmed the potential of the arrays for running the signaling experiments, it also brought up some new questions. As can be seen in Figure 4.13, the shape of the cyclic voltammograms changed as the iron concentration increased, especially after the concentration reached 32 mM and 64 mM. There was a large change in the slope of the curve at around 0 mV. This change increased dramatically as the concentration of the iron species increased. This phenomenon indicates the potential of the $K_3Fe(CN)_6$ /$K_4Fe(CN)_6$ redox pair. Since we were using the counter electrode as the reference electrode with our setup, the potential measured appears at around 0 mV vs. the reference electrode because the electrochemical reaction at the reference electrode also involves the $K_3Fe(CN)_6$ /$K_4Fe(CN)_6$ redox couple. From the experiment, it was clear that we could utilize both the wave at 0 mV and the arm of the CV to measure impedance. Both regions of the CV curve showed a nice current drop as the iron concentration decreased. However, the vertical part of the CV wave at around 0 mV may not always appear if the concentration of iron in solution is not high enough. Since $K_3Fe(CN)_6$ is an oxidant, a high concentration of this species in a protein solution is not recommended. Therefore, it was very reassuring that the impedance experiment can work even at a lower

concentrations of iron where the specific CV wave is not as apparent.

Another interesting result was observed when the experiment was repeated on a DMF-washed PBrSt-b-CEMA surface (Figure 4.14).

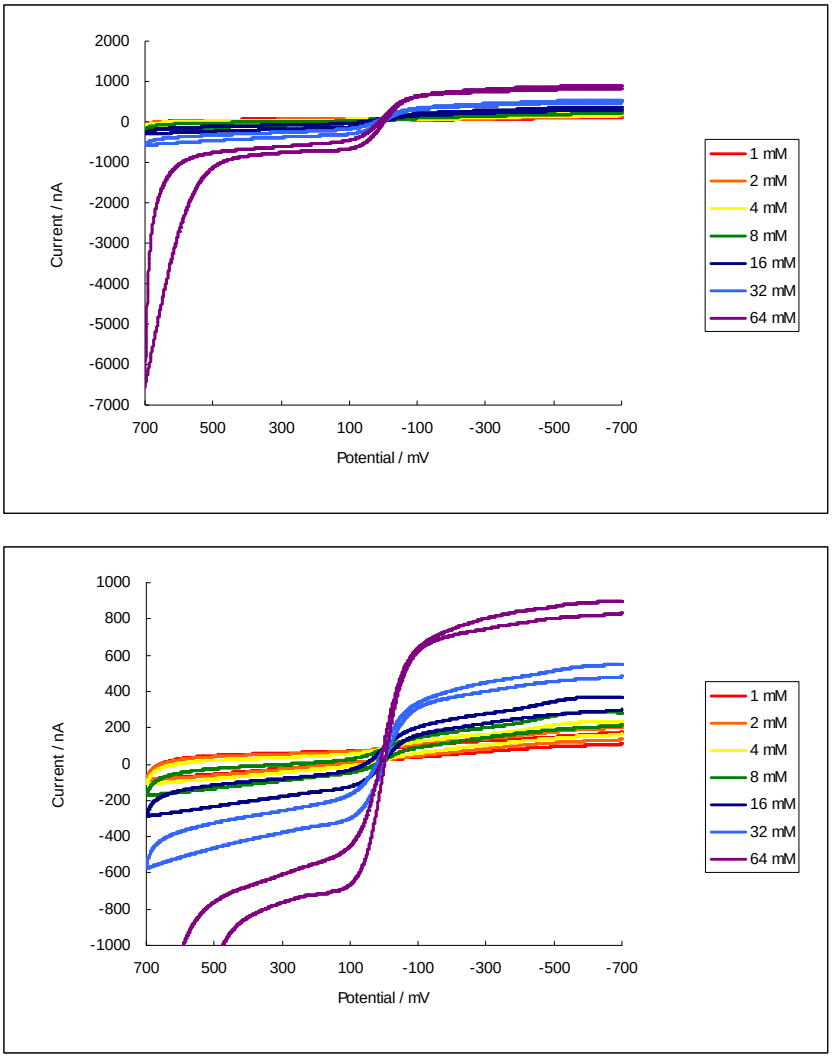

Figure 4.14 Cyclic voltammogram on DMF-washed PBrSt-b-CEMA surface. The second image is an expansion of the region between -1.0 μA to 1.0 μA. Condition: 1 to 64 mM $K_3Fe(CN)_6$ /$K_4Fe(CN)_6$ dissolved in 1x PBS solution in water, pH=7.5. Scan rate = 400 mV/s.

Washing the surface of the array with DMF caused a noticeable change in the CV. First of all, the CV wave for the iron redox couple was readily observed for each iron

concentration used, with a great increase of current intensities of each iron concentration. For example, the current intensity for the 32 mM iron solution increased from less than -100 nA at 700 mV on the unwashed surface to about -600 nA at 700 mV on the DMF-washed surface. Secondly, the change of shape of the CV happened earlier than the unwashed surface, starting from 8 mM instead of 32 mM. Last but most interestingly, a sharply increased current appeared for the 64 mM concentration on the oxidation curve, which reached all the way to around -6500 nA. The cause of this dramatic increase in current is not clear. It could be that the oxidized iron species is reacting with DMF left from the wash causing a catalytic current for the iron. All these results indicated that the polymer coating had much better ion permeability after being washed with DMF. Theoretically, this effect should be beneficial. If we start with a larger current, then there is the potential for a larger drop in current for the impedance experiment. However, whether such a phenomenon is actually beneficial for the impedance experiment still needs to be answered with an appropriate experiment.

4.5 Reexamine the BSA non-specific binding experiment with the correct setup

With the positive result of the iron concentration control experiment, we moved on to investigate signaling experiments that involve protein binding to the array surface. To this end, the BSA non-specific binding experiment was repeated with the correct wiring of the array. The experiment was selected because it was easy and because the results obtained from previous BSA non-specific binding experiments

were very questionable. They were after all measure using the incorrect wiring schematic for the array. In addition, the BSA experiment provided us with an opportunity to investigate the consistency of the surface conditions at different electrodes on the array and evaluate the deviation of the data obtained from one electrode to the next.

The BSA non-specific binding experiment was carried out in a similar manner to the BSA non-specific binding experiment conducted with the old setup. The concentrations for $K_3Fe(CN)_6$ and $K_4Fe(CN)_6$ were set at 8 mM each. The solution was made from a 1 x PBS buffer. The protein concentration varied from 10^{-9} M to 10^{-3} M for a more complete binding curve. The solutions were made by diluting a stock iron solution. For the cyclic voltammetry, the potential range was varied from -700mV to 700mV, as the oxidation/reduction of the iron species was reversible and happened around 0 mV. The scan rate also increased from 200 mV/s to 400 mV/s, due to a much weaker current passing through the small number of microelectrodes relative to the old setup. The CV was obtained from a block of 12 electrodes with a 3x4 rectangular pattern. The results obtained with various concentrations of BSA are shown in Figure 4.15. In this diagram, the CVs showed a similar drifting as the one showed in Figure 4.12, but all the CVs shared the same zero point, so it was not a matter of concern. It can be clearly seen that the currents showed minimal drop from the concentration 10^{-9} M to 10^{-7} M, and started to drop significantly from 10^{-6} M and onwards.

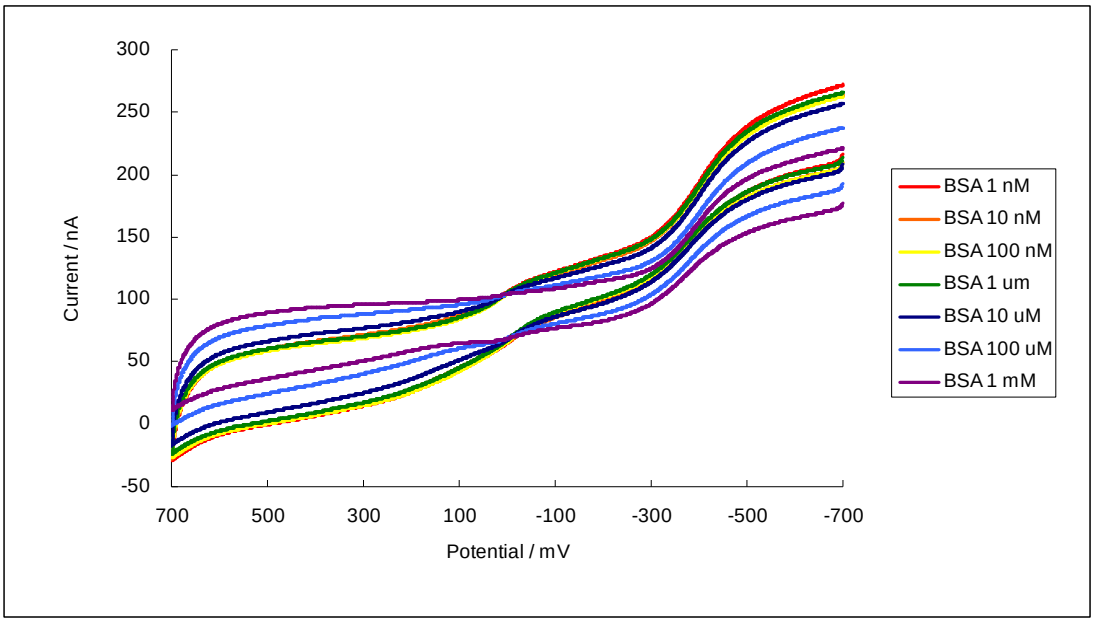

Figure 4.15 BSA non-specific binding to the unwashed PBrSt-b-CEMA surface. Condition: 8 mM $K_3Fe(CN)_6$ /$K_4Fe(CN)_6$ dissolved in 1x PBS solution in water, pH=7.5. BSA concentration varied from 10^{-9} M to 10^{-3} M. Scan rate = 400 mV/s.

With the ability to run independent CV's at each the electrodes in the array, we took advantage of non-specific BSA binding on the array to evaluate the consistency of the CV experiments across the surface of the array. For the experiment, three different groups of 12-electrodes were selected. The data is shown in Figure 4.16. The shape of the CV's looked quite different from the one illustrated in Figure 4.15, but similar to each other. The difference from the CV in Figure 4.15 was expected as the coating from array to array will have a different thickness and thus different ion permeability. Since differences in the polymer might also be expected across the same array, the current with zero protein may also differ from one site to the next on the array. Hence, it was best to normalize the current drop at each site. This was done by reporting the drop in current for any given concentration of BSA as a percentage of the maximum drop observed at that location.

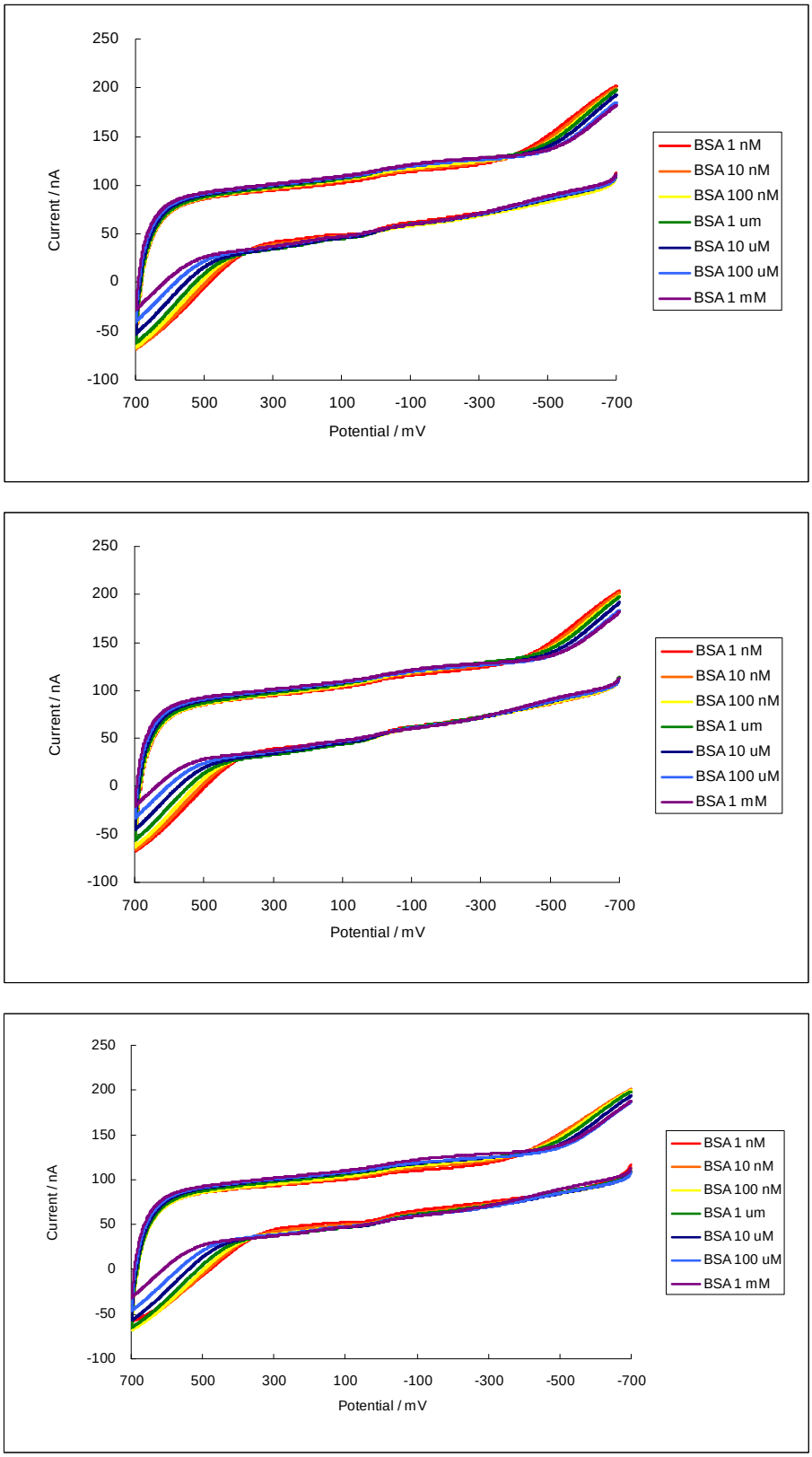

Figure 4.16 BSA non-specific binding to unwashed PBrSt-b-CEMA surface with three different groups of 12 electrodes on the same array. Condition: 8 mM $K_3Fe(CN)_6$ /$K_4Fe(CN)_6$ dissolved in 1x PBS solution in water, pH=7.5. BSA concentration varied from 10^{-9} M to 10^{-3} M. Scan rate = 400 mV/s.

The best way to understand this is to look at an example. For the data shown in Figure 4.17, the current measured at a potential value of 600 mV was recorded for each concentration of BSA obtained. The data was then plotted against the logarithm of the protein concentration. Each individual value shown represents the average value for the three blocks of electrodes shown. Error bars were then included to reflect the standard deviation of the data obtained at each concentration. The result is a binding curve for the interaction of BSA with the polymer coating on the electrodes. The error bars in the figure are quite large indicating significant variation from one site on the array to another. However, the overall drop in current was large enough to be significant relative to this error and thus provide insight into the binding event being studied. As we shall see in the additional studies shown below, this conclusion turns out to be general. There is significant variation in the signal measured at various sites on the array, but the variations are small enough so that meaningful data on a binding event can still be obtained.

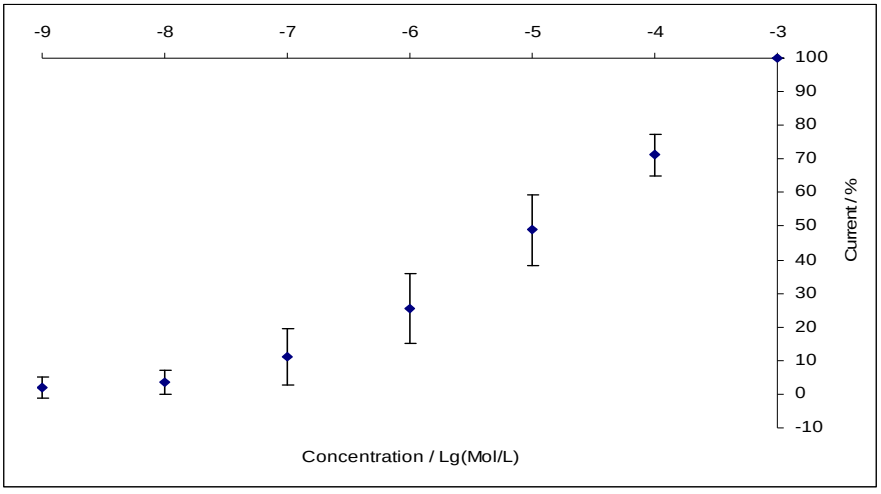

Figure 4.17 Binding curve generated for BSA non-specific binding to unwashed PBrSt-b-CEMA surface. The current was measured at 600 mV.

As stated in the iron concentration control experiment discussed in Section 4.4, washing the array with DMF changes the ion permeability of the block copolymer surface. Since the error bars generated on an unwashed block copolymer surface were quite large compared to the overall current drop, we wondered if washing the surface with DMF before making the BSA binding measurement would improve the situation by making the overall impedance measurements larger. With this in mind, the BSA non-specific binding experiment was repeated on a PBrSt-b-CEMA coated array heavily washed with DMF. The result is shown in Figure 4.18 along with an expansion of the region of the CV between 500-700mV. It can be clearly seen from this data that the current drop caused by the BSA non-specific binding is much more prominent in the DMF-washed surface. The data was gathered from different groups of electrodes, normalized and then processed in the same manner as described for Figure 4.17 in order to generate Figure 4.19.

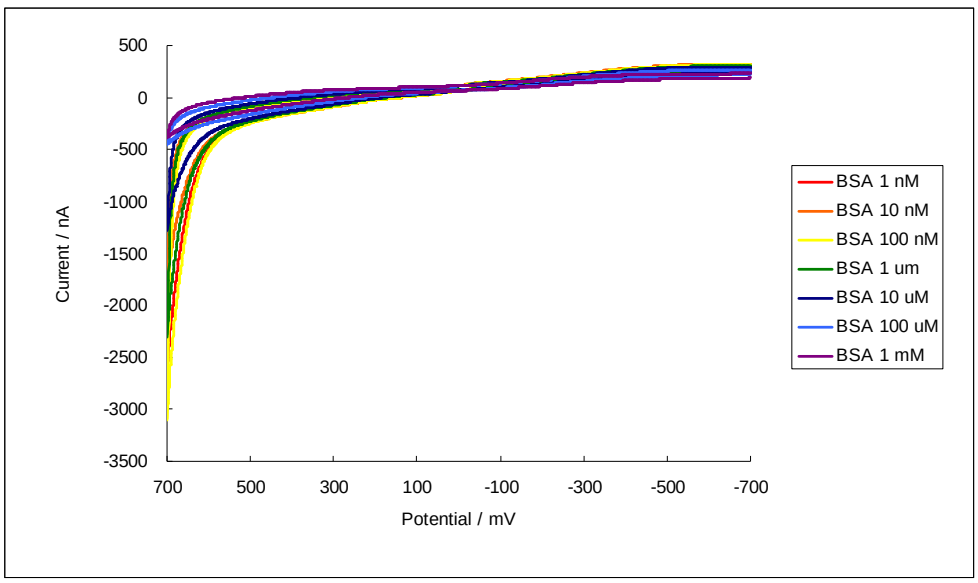

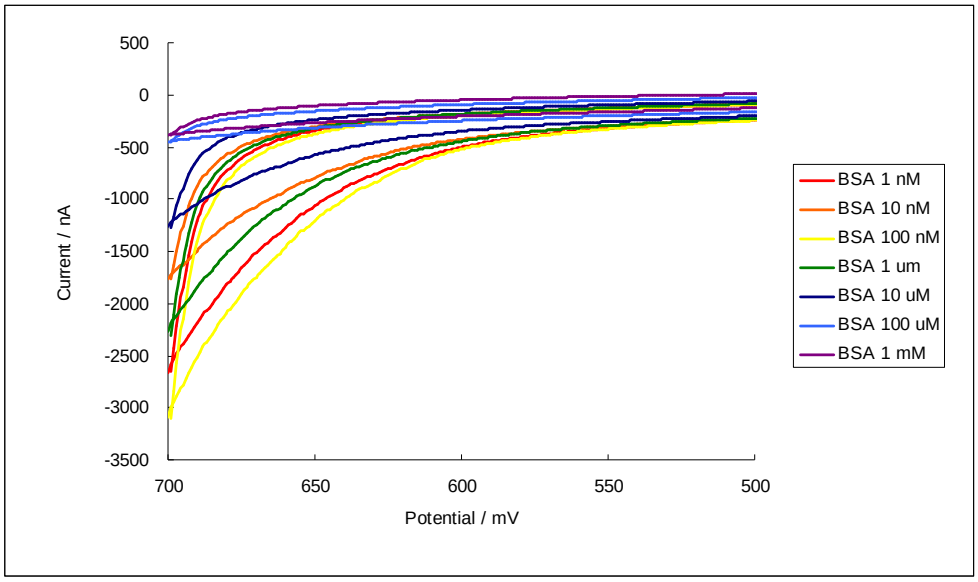

Figure 4.18 BSA non-specific binding to the DMF-washed PBrSt-b-CEMA surface. Condition: 8 mM $K_3Fe(CN)_6$ /$K_4Fe(CN)_6$ dissolved in 1x PBS solution in water, pH=7.5. BSA concentration varied from 10^{-9} M to 10^{-3} M. Scan rate = 400 mV/s.

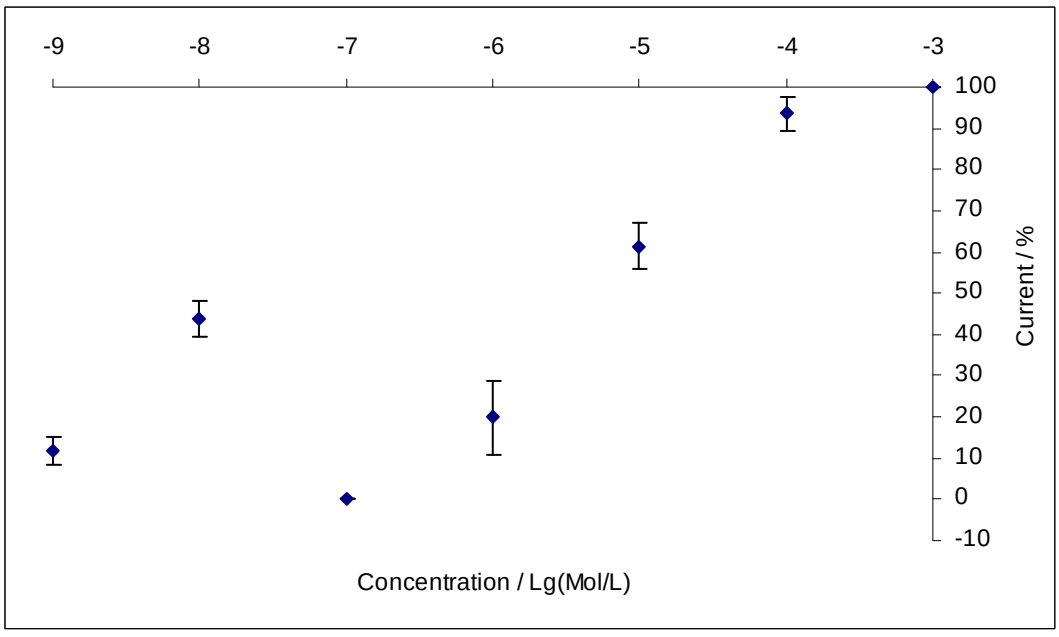

Figure 4.19 Binding curve generated for BSA non-specific binding to unwashed PBrSt-b-CEMA surface. The currents were measured at 700 mV.

Although it seemed that the error bars on the DMF-washed surface were much smaller compared to the unwashed surface, there was a significantly greater scatter in the current measured from one concentration to the next. At low protein

concentration, the currents tended to jump up and down for no obvious reason, but would get better as the protein concentration increased. It is impossible to tell if the washing of the array led to any real benefit for the experiment, as there was both an upside and downside to the procedure. In the end, the only real conclusion that could be reached is that with either the DMF washed or the unwashed surface non-specific binding of BSA occurred to a significant extent at micromolar concentrations of protein. Further refinement of the impedance experiment was conducted for experiments that observed specific binding events.

4.6 Signaling experiments on a ligand modified surface

All of the experiments reported above utilized a polymer surface that was not modified to include the incorporation of a ligand. Modification of a polymer can dramatically alter its properties. So while the results above provided a good starting point for understanding how impedance experiments can be run on the arrays, it seemed that optimization of the experiments should focus on functionalized surfaces.

To this end, the site-selective Heck reaction was used as a probe to study the effect of site-selective reactions on the cyclic voltammograms obtained on the array. In this study, two kinds of substrates were immobilized onto the surface, the first substrate was the hydrophobic 1-pyrenemethyl acrylate, and the second substrate was the hydrophilic PEG acrylate. These two substrates were put onto the microelectrode array using the typical array-based Heck reaction conditions, illustrated in Scheme 4.4. After the modification was completed, the array was subjected to the BSA

non-specific binding experiment without washing with DMF to see whether the modification changed the surface properties. Three regions of the array were examined; a region modified with pyrene, a region modified with PEG, and a region that remained unfunctionalized. The results are shown in Figure 4.20.

Scheme 4.4

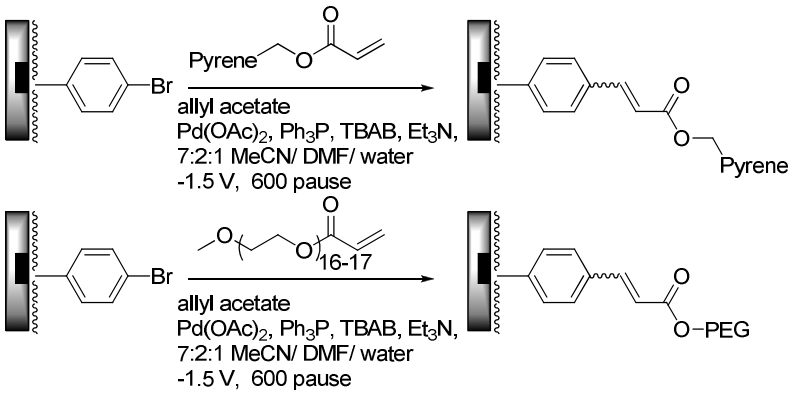

a)

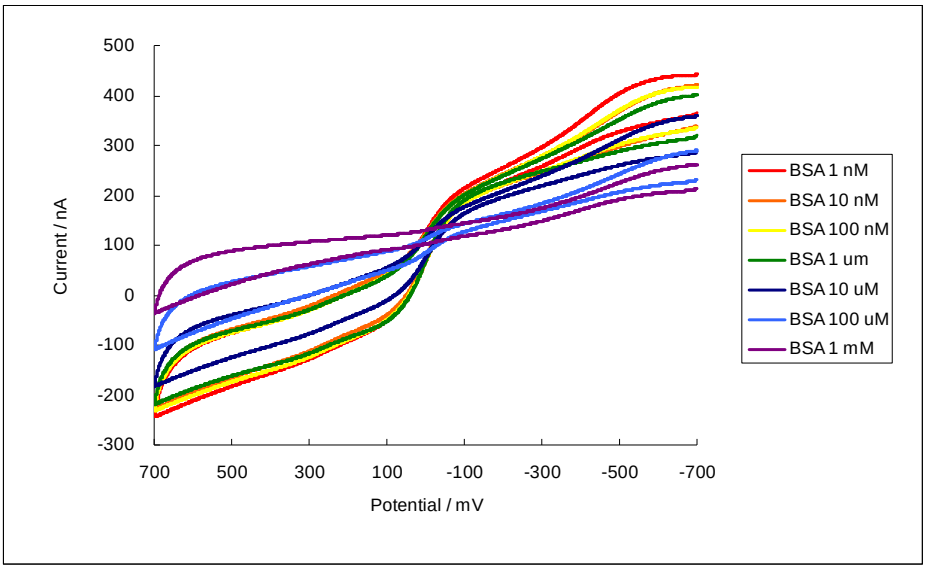

b)

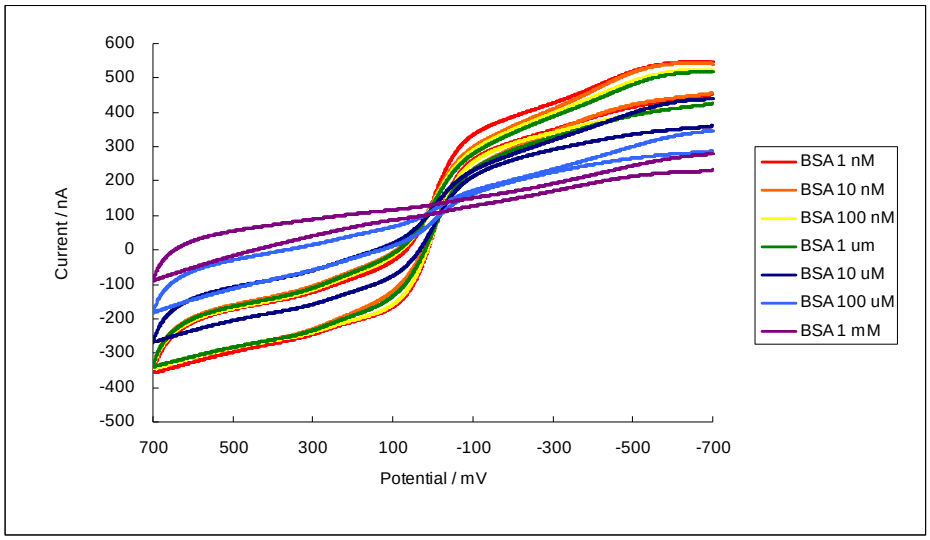

c)

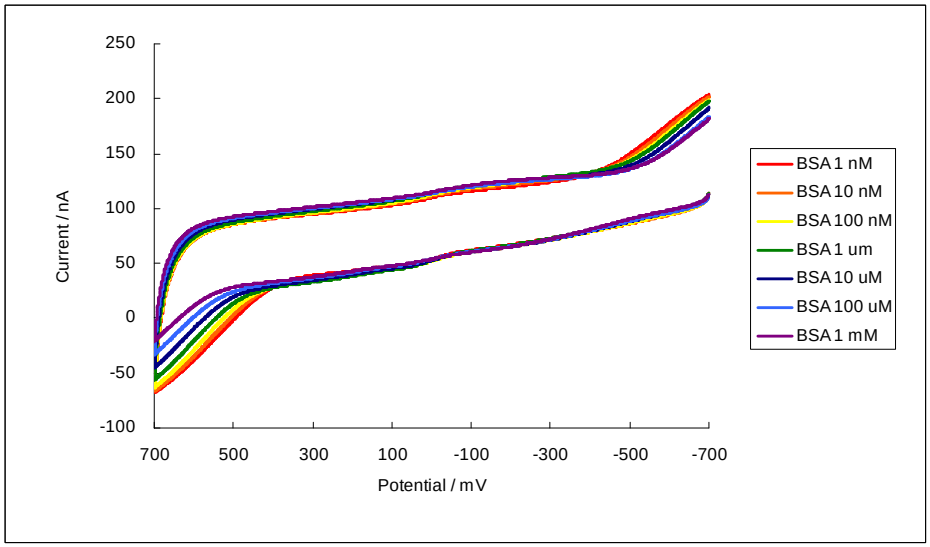

Figure 4.20 BSA non-specific binding on electrodes modified with a) 1-pyrenemethyl acrylate, b) PEG acrylate and c) unmodified PBrSt-b-CEMA surface on the same array. Condition: 8 mM $K_3Fe(CN)_6$ /$K_4Fe(CN)_6$ dissolved in 1x PBS solution in water, pH=7.5. BSA concentration varied from 10^{-9} M to 10^{-3} M. Scan rate = 400 mV/s.

The data led to several interesting observations. First, it could be clearly seen that after being exposed to the Heck-reaction conditions the CV obtained from the unmodified surface remained unchanged for the most part. It showed no significant

increase in current even though the reaction medium for the Heck reaction does use a solvent containing 20% DMF. This meant that a short exposure to DMF did not achieve the extensive change in polymer structure that was brought on by extensive washing of the surface with DMF. Second, the electrodes used for the Heck reaction showed a considerable increase of the current observed during the impedance experiments. This change occurred no matter which substrate was placed on the array. This result demonstrated that the modification of the polymer surface with small molecule ligands was capable of changing the polymer structure and making the polymer more permeable to ions. This also meant that washing with DMF may not be necessary in order to increase the current observed for impedance experiments run on a functionalized surface. Third, the increase in current that resulted from the placement of a pyrene group on the array was about 100 nA smaller than that obtained from the placement of a PEG group on the array. This makes sense since the more hydrophobic surface would have less affinity for water. The hydrophobic section of the polymer would swell less and be less permeable to ions than the section of the polymer functionalized with PEG. Finally, both ligands did not seem to change the non-specific binding of BSA to the surface. The larger overall current drop did enhance the signal for the binding event relative to the error bars associated with variations in the electrode surface (Figure 4.21). This led to an improvement in the data obtained. In terms of non-specific BSA binding, it was not a surprise that the pyrene group did not alter the surface to a great extent. However, it was disappointing that the addition of the PEG group did not help. Possible reasons for PEG not

altering non-specific binding to the surface were discussed in Section3.9 of Chapter 3.

a)

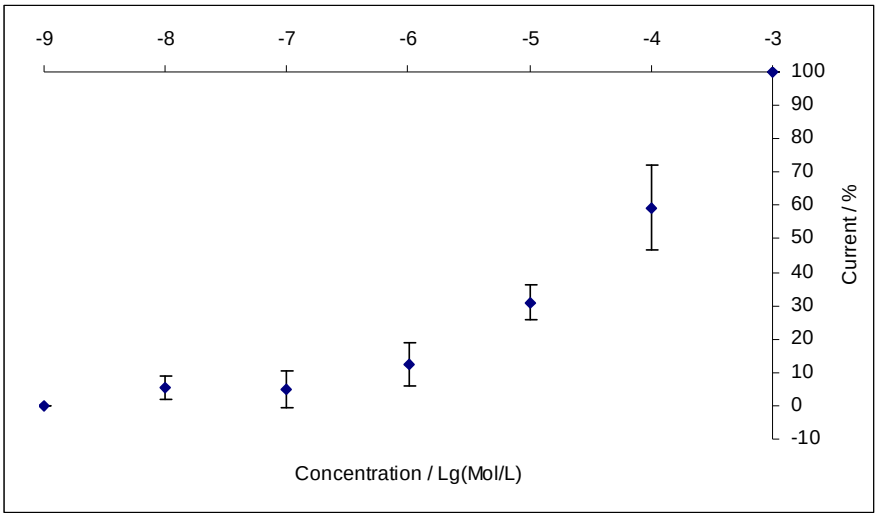

b)

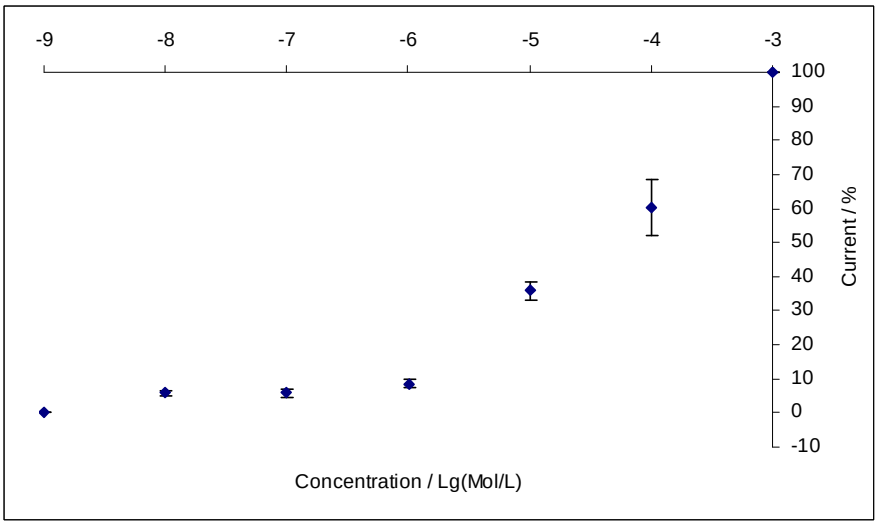

Figure 4.21 Binding curve generated for BSA non-specific binding to a) 1-pyrene-methyl acrylate and b) PEG acrylate. The current was measured at 700 mV.

In conclusion, these results continued to show us the potential of the array for monitoring binding events as they occurred. In fact, functionalizing the surface of the array with small molecules increases the permeability of the polymer coating on the

electrodes and improves the electrochemical impedance experiments used in signaling studies. It was time to examine a specific binding event on the arrays.

4.7 Study of biotin-streptavidin binding interaction using a fluorescent linker on PBrSt-b-CEMA block copolymer surface

In the previous part of this chapter, the possibility of running signaling experiment on the modified polymer surface of microelectrode array was discussed and confirmed. With all the information gathered, we moved on to examine a model interaction on the array. To this end, we turned to the binding of biotin to streptavidin for the same reasons discussed in Section 4.3.

This experiment was done in cooperation with Bo Bi and Dr. Tanabe Takamasa in our group. A fluorescent linker developed by Dr. Takamasa was used to attach the biotin to the surface of the array so that the quantity of biotin on the surface could be monitored. To this end, biotin was first linked to the fluorescent linker and then placed onto the array with the use of a Cu(I)-catalyzed coupling reaction between an aryl halide and an t-Boc protected amine (Scheme 4.5).[10] The site-selective Cu(I)-chemistry was developed by Jennifer L. Bartels in our group. The chemistry was used to place the biotin by 10 blocks of 12 electrodes each. Next, the Cu(I)-coupling reaction was used to place the methyl ester of the fluorescent linker was onto the array. Once again, 10 blocks of 12 electrodes each were used for the experiment. These electrodes were to be used as a control for the biotin signaling experiment.

Scheme 4.5

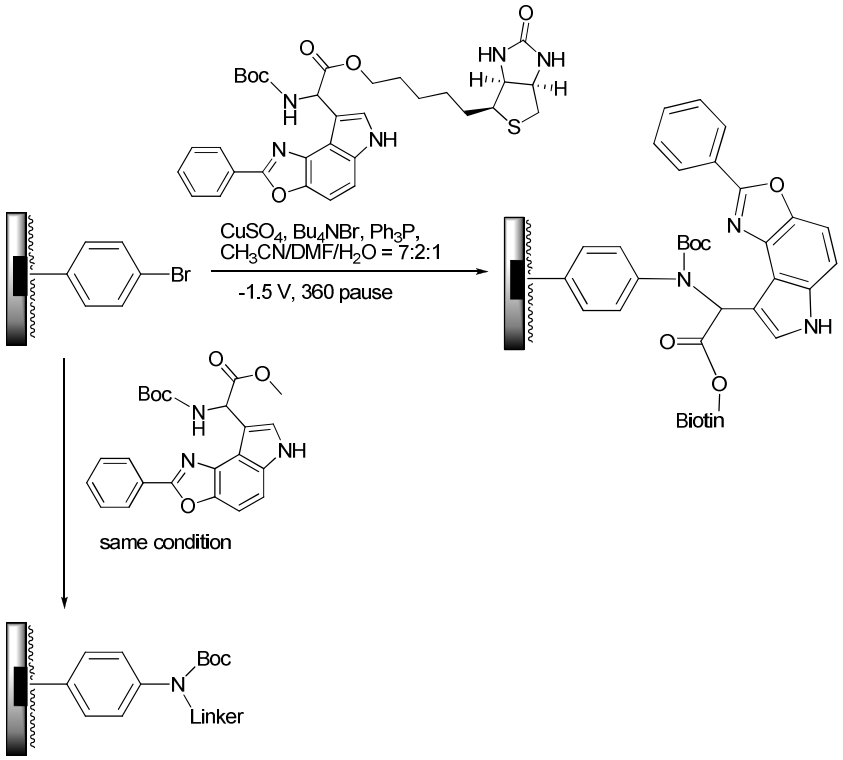

Once the array was prepared, it was incubated in a series of streptavidin solutions starting from 10^{-18} M to 10^{-6} M protein in 1 order of magnitude increments. CVs were scanned for each protein solution on three random blocks of electrodes modified with biotin plus linker, three random blocks of electrodes modified with only the linker, and three random blocks of electrodes that were not modified at all. The CV's observed at the electrodes are shown in Figure 4.22. This data is summarized in Figure 4.23.

a)

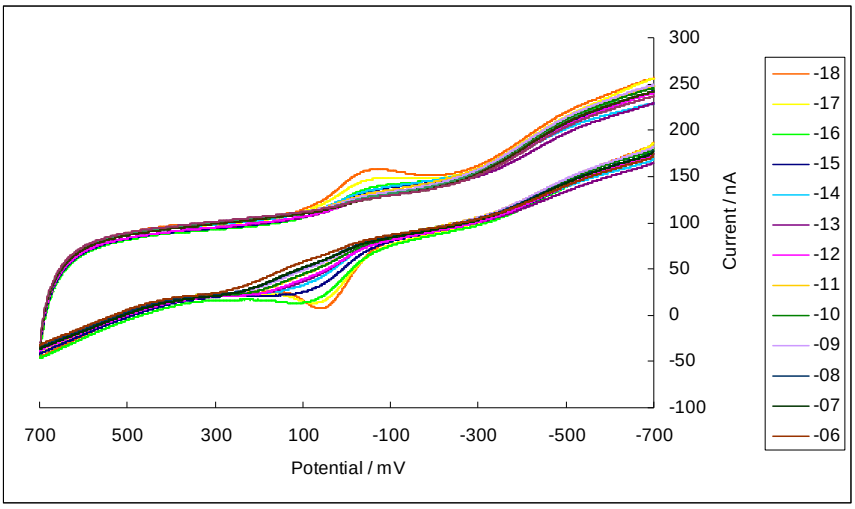
300
250
200
150
100
50
0
-50
-100
Current / nA
700
500
300
100
-100
-300
-500
-700
Potential / mV
-18
-17
-16
-15
-14
-13
-12
-11
-10
-09
-08
-07
-06

b)

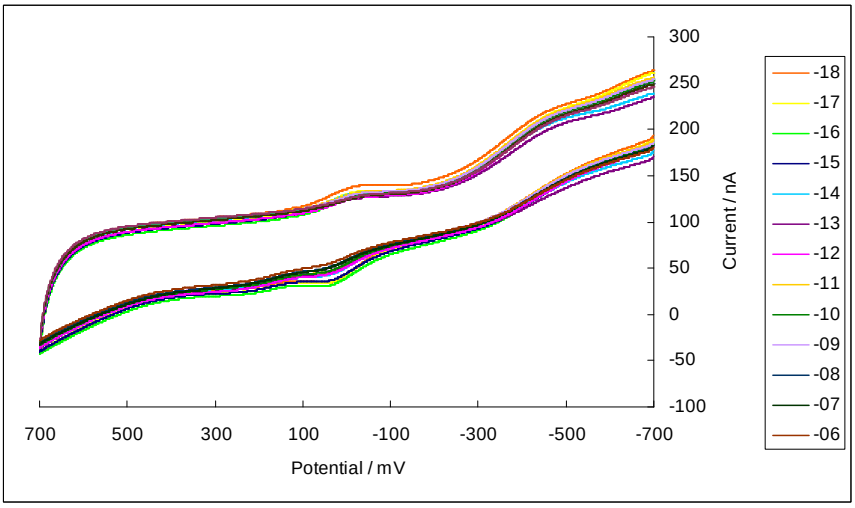
300
250
200
150
100
50
0
-50
-100
Current / nA
700
500
300
100
-100
-300
-500
-700
Potential / mV
-18
-17
-16
-15
-14
-13
-12
-11
-10
-09
-08
-07
-06

c)

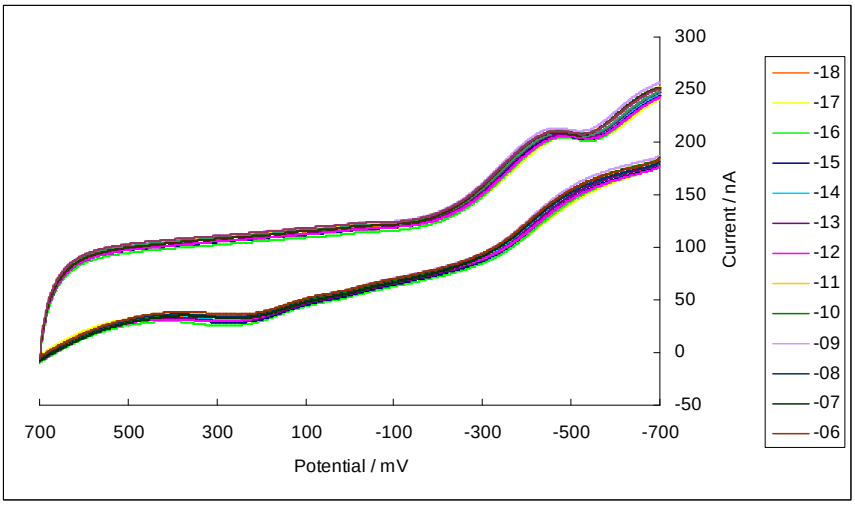
300
250
200
150
100
50
0
-50
Current / nA
700
500
300
100
-100
-300
-500
-700
Potential / mV
-18
-17
-16
-15
-14
-13
-12
-11
-10
-09
-08
-07
-06

Figure 4.22 Streptavidin binding on electrodes modified with a) biotin plus linker, b) linker only and c) unmodified PBrSt-b-CEMA surface on the same array. Condition: 8 mM $K_3Fe(CN)_6$ /$K_4Fe(CN)_6$ dissolved in 1x PBS solution in water, pH=7.5. Streptavidin concentration varied from 10^{-18} M to 10^{-6} M. Scan rate = 400 mV/s.

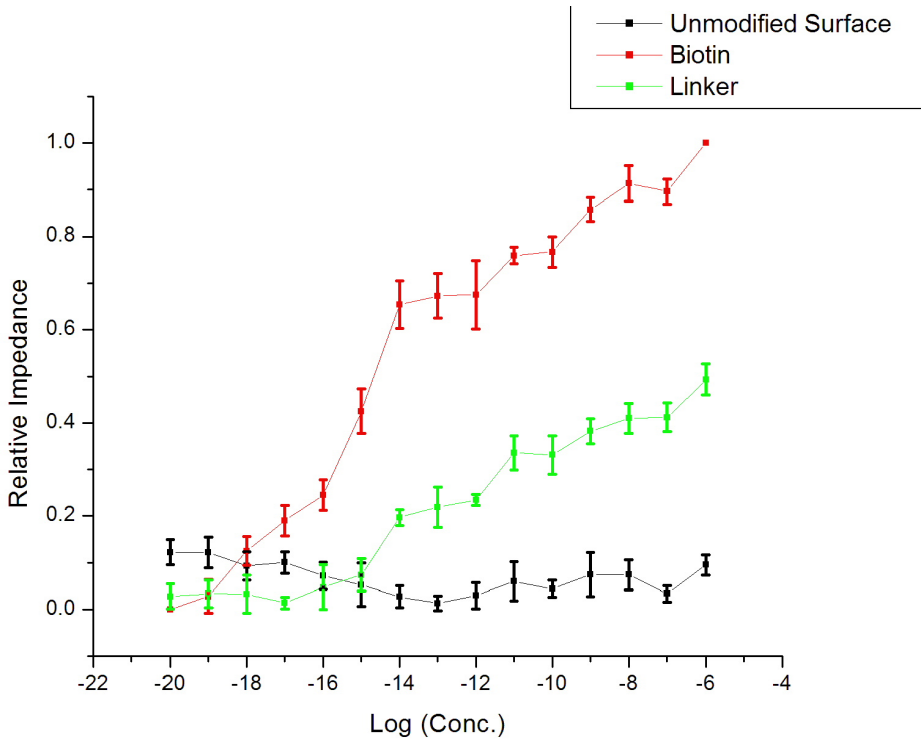

Figure 4.23 Streptavidin-biotin binding experiment. The currents reported were measured at a potential of 52 mV.

The summarized data in Figure 4.23 was prepared as described above. Each point represents an average of the three blocks of electrodes used and the error bars reflect the standard deviation in the data. The drop in current for each set of data has been normalized. This was done by setting the largest current difference observed as being 100%. In this case, the largest difference in current was measured for the electrodes modified with biotin. The remaining data is then reported as a drop in current relative to this maximum. In this way, the data directly reflects the binding of streptavidin to the surface. The larger the magnitude of the data shown, the more binding there is to

the surface. The green line in the Figure shows the binding of streptavidin to the surface containing biotin. The red line shows the binding of streptavidin to the linker, and the black line shows the non-specific binding of streptavidin to the block copolymer. What can be seen from the data is that the array can measure the binding event between streptavidin and biotin. This can be observed very nicely by subtracting the background binding to the linker from the data obtained from the blocks containing the biotin. This is done by subtracting the red line from the green line. This difference data is shown in Figure 4.24.

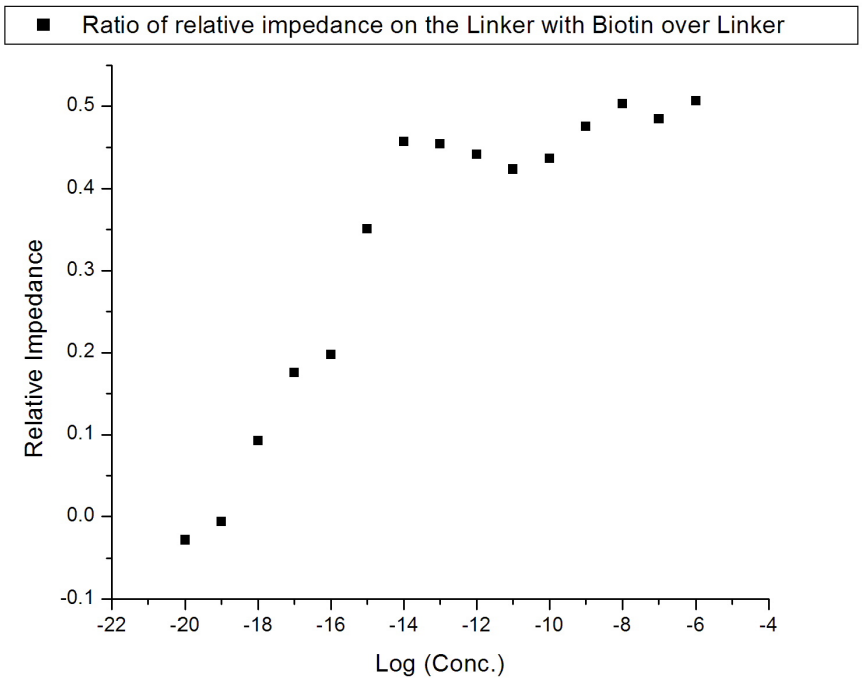

Figure 4.24 Streptavidin-biotin binding curve generated by deduction of the linker curve out of the biotin plus linker curve.

The data in Figure 4.24 represents a binding curve for the interaction of streptavidin with biotin. From this curve it appears that the major drop in current occurred from 10^{-19} M to 10^{-14} M streptavidin. The curve leveled off after 10^{-14} M and stayed mostly

flat afterward. Based on the curve, the relative dissociation constant would be around to 10^{-16}, and the theoretical value is around 10^{-14} which was very close considering the very small value.[11]. Although the "S-shape" typically associated with a binding curve would be more complete if the low concentration range was further extended, such experiments are not feasible.

The experiment nicely demonstrated the ability of the array to signal biological binding interactions between a receptor and specific ligands. Due to the very strong binding reaction between biotin and streptavidin, the change of slope on the binding curve occurred at too low of a concentration range. This made it difficult/impossible to generate good quantitative data.

4.8 Biotin-streptavidin binding interaction, a tale of two metals

While the story of biotin-streptavidin binding study seemed to complete with a perfect ending, there was another side to the story. While we were attempting to compare the binding of streptavidin to addition ligands, we used a Pd(0)-catalyzed reaction to place the ligands on the surface of the electrodes. To this end, the PBrSt-b-CEMA block copolymer was first modified with HEA (2-hydroxyethyl acrylate) to transform the bromophenyl functionality to free hydroxyls, and then the activated ester of the ligands was used to place the ligands on the surface with a base catalyzed esterification (Scheme 4.6).

Scheme 4.6

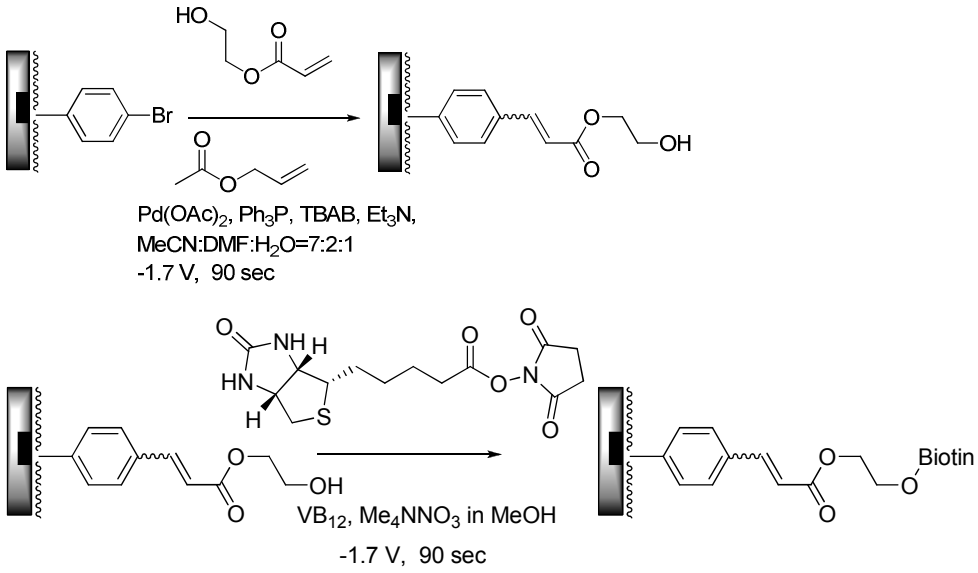

Although with this method, there would be no way for quality control due to the absence of fluorescent linker, the consistent performance of Pd(0)-catalyzed reactions was considered reliable enough to accomplish the task. Before we tried with multiple ligands, biotin was first used as a model compound to see if the result obtained in Section 4.7 could be repeated. To our great surprise, the impedance experiment conducted on this surface showed no obvious current drop at all for the electrodes modified with biotin compared with the unmodified electrodes (Figure 4.25). Don't be fooled by the presence the higher current measured at the modified electrodes. Note that the higher current does not change in intensity any more than does the lower current as the concentration of streptavidin is varied.

a)

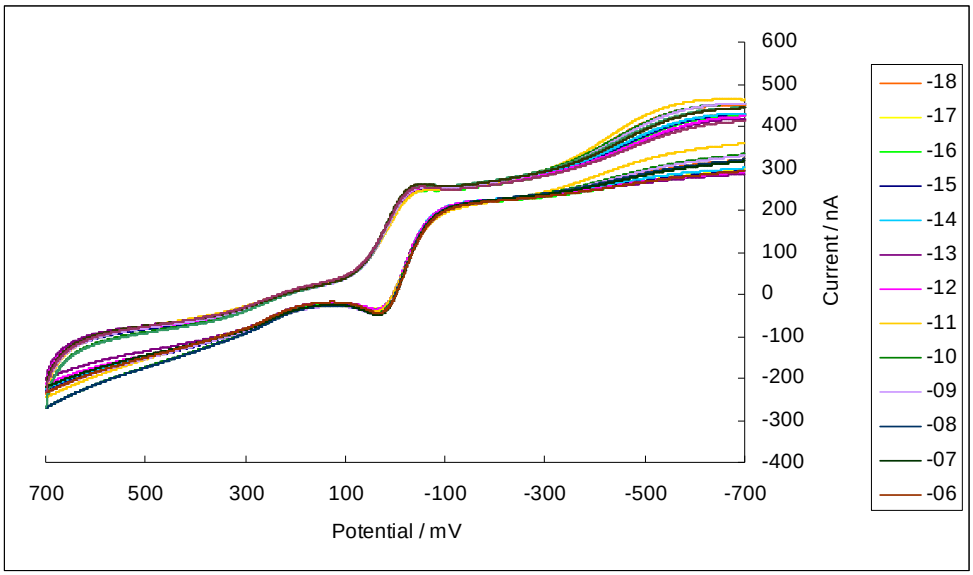

b)

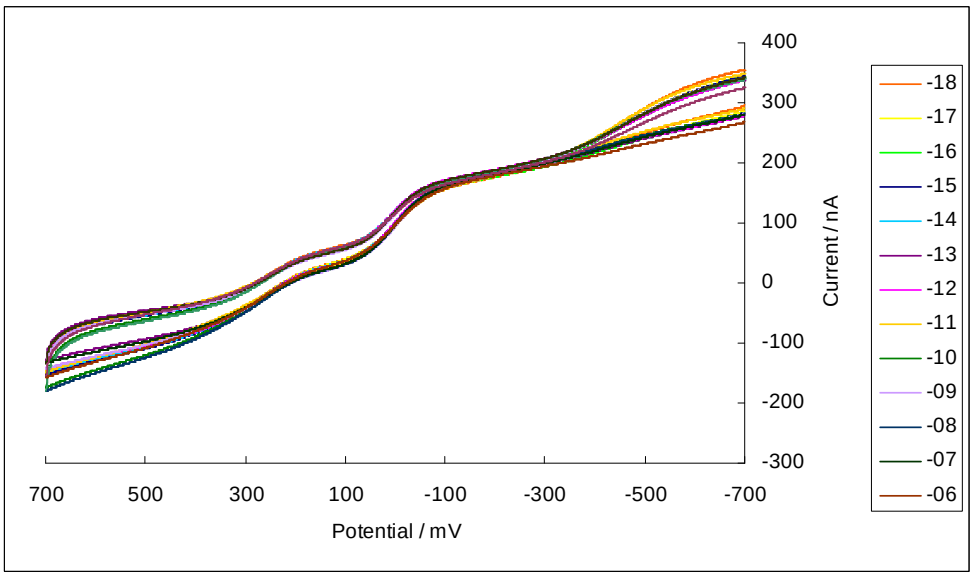

Figure 4.25 Streptavidin binding on a) electrodes modified with biotin and b) unmodified PBrSt-b-CEMA surface on the same array. Condition: 8 mM $K_3Fe(CN)_6$ /$K_4Fe(CN)_6$ dissolved in 1x PBS solution in water, pH=7.5. Streptavidin concentration varied from 10^{-18} M to 10^{-6} M. Scan rate = 400 mV/s.

Initially, our hypothesis was that we might not have put enough biotin onto the surface. Due to the fact that we did not have a fluorescent group to monitor the quantity of biotin placed on the array, it was very difficult for us to know the exact

condition on the surface. A second control experiment was conducted by placing biotin by a block of electrodes on the surface of an array with the use of the Pd(0)-chemistry and then the fluorescent-linker-tagged biotin by a second block of electrodes on the array using the Cu(I)-chemistry shown in Scheme 4.5. The impedance experiment with streptavidin was then repeated using this array.

To our surprise, in the experiment there was no current drop observed at not only the electrodes modified with the Pd(0)-reaction, but also the electrodes modified with the Cu(I)-chemistry (Figure 4.26). Since the electrodes functionalized with the Cu(I)-catalyzed reaction were modified with a fluorescently labeled biotin, we could verify that the biotin had indeed been placed by these electrodes. It appeared that something in the Pd(0)-reaction was interfering with subsequent impedance experiments on the array.

a)

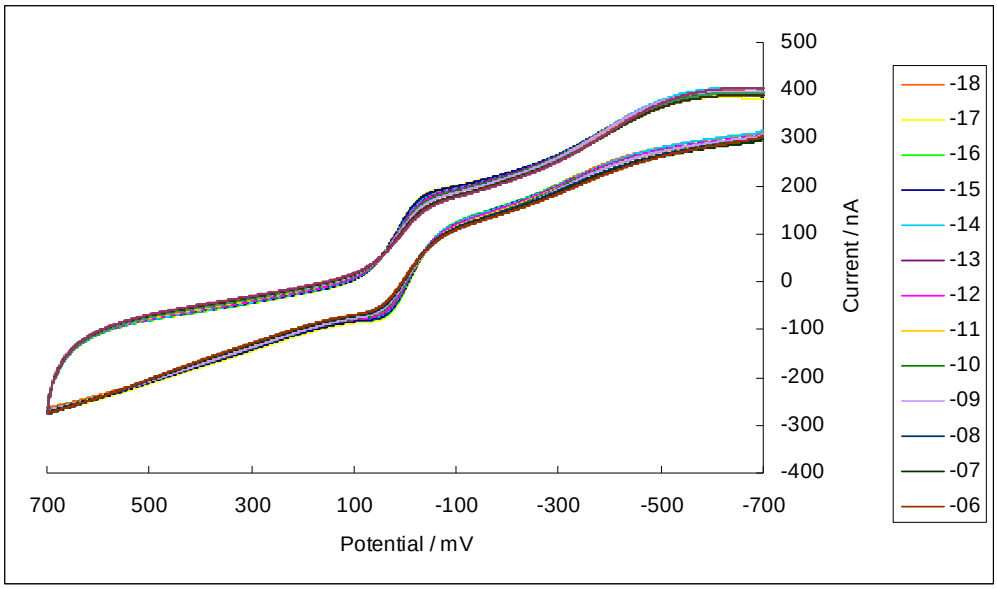

b)

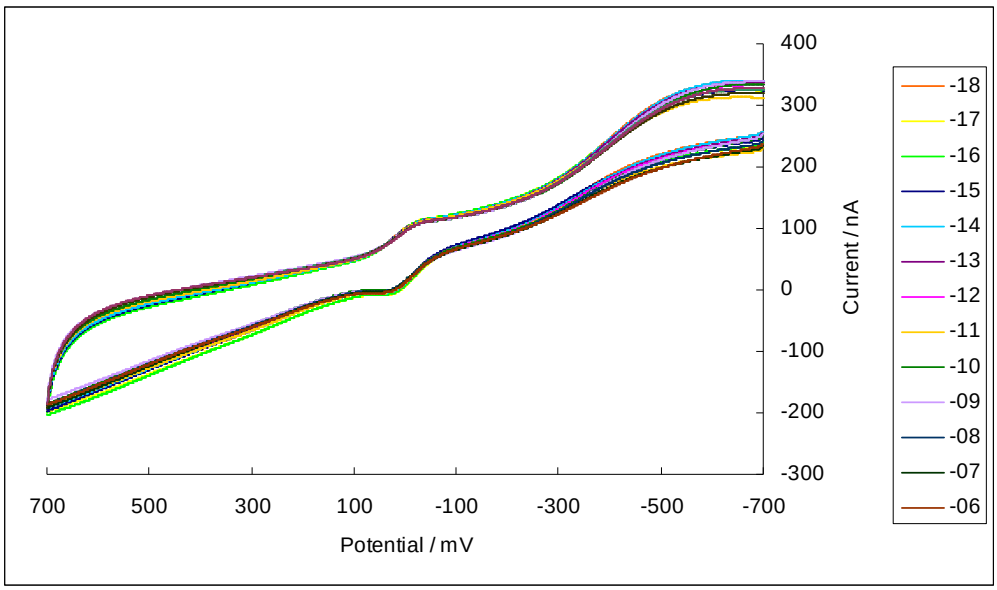

c)

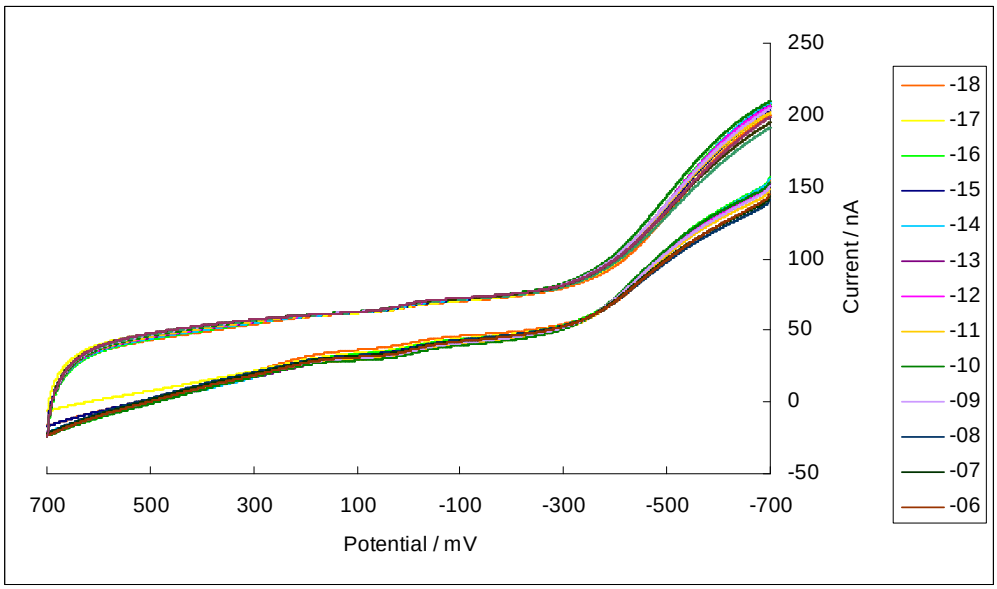

Figure 4.26 Streptavidin binding on a) electrodes modified with biotin using Pd(0) chemistry, b) electrodes modified with linker plus biotin using Cu(I) chemistry and c) unmodified PBrSt-b-CEMA surface. Condition: 8 mM $K_3Fe(CN)_6$ /$K_4Fe(CN)_6$ dissolved in 1x PBS solution in water, pH=7.5. Streptavidin concentration varied from 10^{-18} M to 10^{-6} M. Scan rate = 400 mV/s.

To verify this hypothesis, the same Cu(I)-mediated streptavidin-biotin binding experiment as shown in Figure 4.22 was repeated. This time, the modification step

was followed by incubation of the array in a Pd(0) reaction mixture for 10 min. No reaction was run. The array was then washed and subjected to the signaling experiments. The results of this experiment are shown in Figure 4.27. It is very clear that incubating the array in the solution of Pd(0) reaction mixture changed the behavior of the array in the impedance experiment. It was not clear which component in the Pd(0) solution was interfering with the signaling. However, the most probable suspect is the palladium metal itself. It was very reasonable to assume that some palladium metal may become fixed to the polymer network on the array. The multiple carbonyls in the polymer network can serve as excellent ligands for Pd. If the metal is imbedded into the polymer, then the current measured in the impedance experiment might simply reflect the presence of the Pd and not the iron in solution. No impedance would be observed with the addition of protein to the solution.

a)

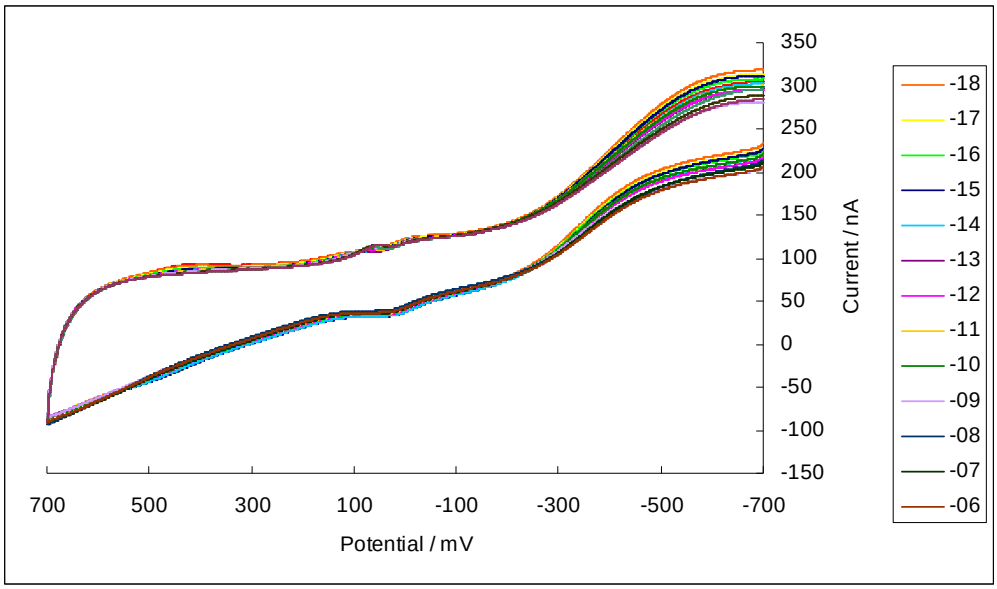

b)

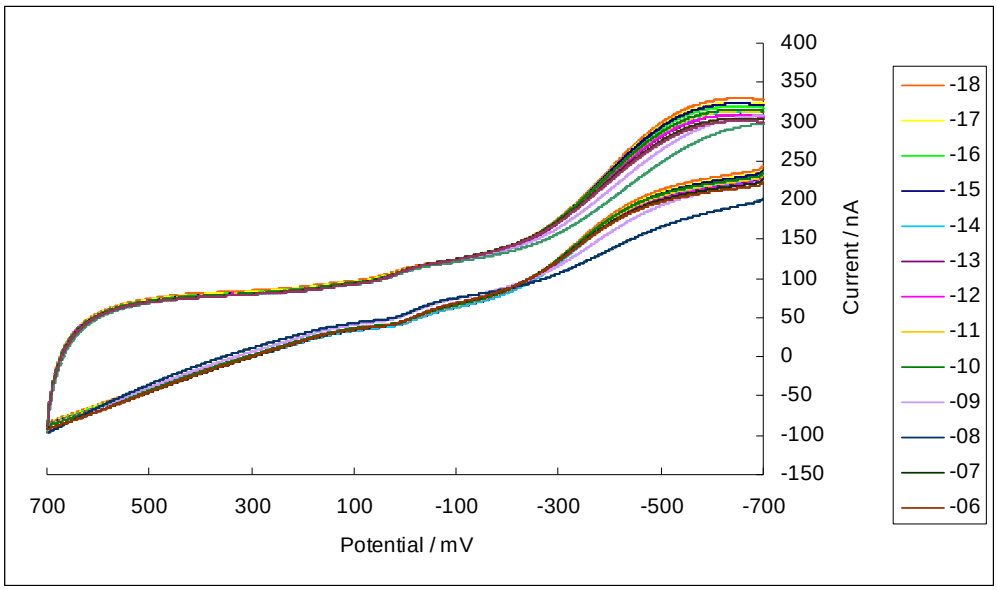

c)

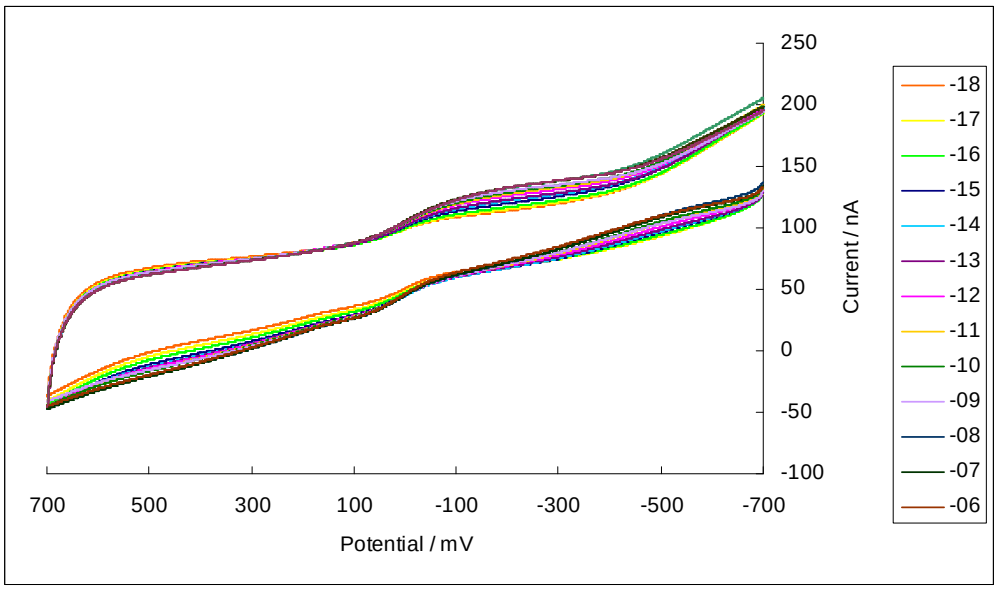

Figure 4.27 Streptavidin binding on a) electrodes modified with biotin plus linker, b) electrodes modified with linker only and c) unmodified PBrSt-b-CEMA surface. Condition: 8 mM $K_3Fe(CN)_6$ /$K_4Fe(CN)_6$ dissolved in 1x PBS solution in water, pH=7.5. Streptavidin concentration varied from 10^{-18} M to 10^{-6} M. Scan rate = 400 mV/s.

The results obtained suggest that one needs to be careful of using Pd(0) as a tool for placing molecules on the surface of the array. There must be a good method

for removing it from the surface – perhaps by washing with a phosphine ligand solution. Moreover, the results suggest that it is wise to have a number of different strategies available for immobilizing molecules onto any given surface on the array. If we do not have a large pool of reaction strategies to choose from, we may not be able to use certain surfaces. This is potentially a large issue as we continue to develop surfaces with minimal non-specific binding to a receptor of interest.

4.9 The ability to acquire stable currents, another aspect of the signaling experiment

In all the previously discussed examples, the signaling experiments were performed on the PBrSt-b-CEMA block copolymer. However, that is not the only surface we examined for its compatibility with the impedance experiments. With both the boronic acid copolymer described in Chapter 3 and the PCEMA-b-BoSt polymer we observed some really interesting phenomenon. When the cyclic voltammetry scan were run on an iron species in the solution above an array coated with the PCEMA-b-BoSt block copolymer, we found out that we could not get a stable current for a given iron concentration. The current kept climbing as the incubation time of the experiment increased (Figure 4.28).

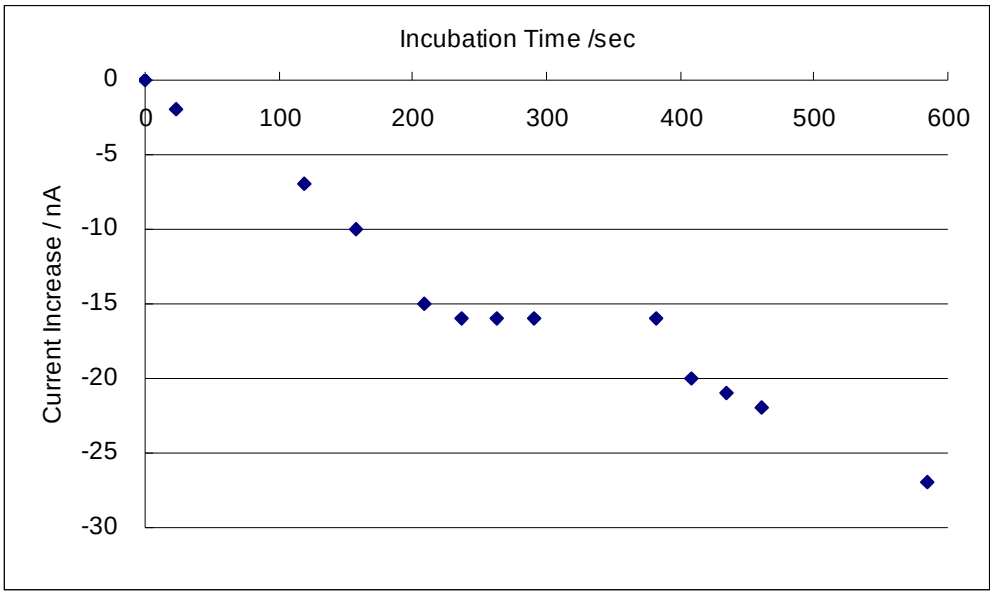

Figure 4.28 Current kept increasing as the incubation time increase on the PCEMA-b-BoSt surface. The value has been deducted with the lowest current for simplification and the current spots were taking at E = 14 mV on the oxidation wave, so the more negative value means increased current. Condition: 8 mM $K_3Fe(CN)_6$ /$K_4Fe(CN)_6$ dissolved in 1x PBS solution in water, pH=7.5.

As briefly mentioned in Chapter 3, this was not the first time we ran into this problem. We observed similar behavior on an array coated with a PEG-based photo-curable epoxy coating. In this experiment, three different types of photo-curable epoxy coatings were compared for their compatibility with the signaling experiments. All three coatings were composed of at least one of the 4 components shown in Figure 4.29. The photocuring step was triggered by a photoinitiator. The mechanism for the photo-initiated polymerization of the epoxides is shown in Scheme 4.7.

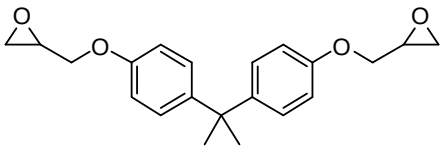

Bisphenol A diglycidyl ether

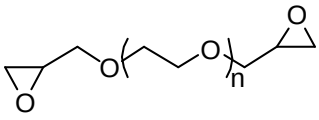

Poly(ethylene glycol) diglycidyl ether

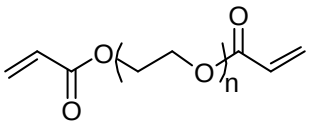

Poly(ethylene glycol) diacrylate

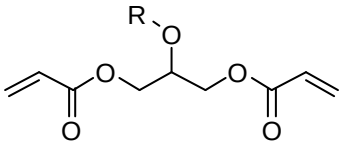

Glycerol diacrylate

Figure 4.29 The four monomers used in the photo-curable epoxy coating study.

Scheme 4.7

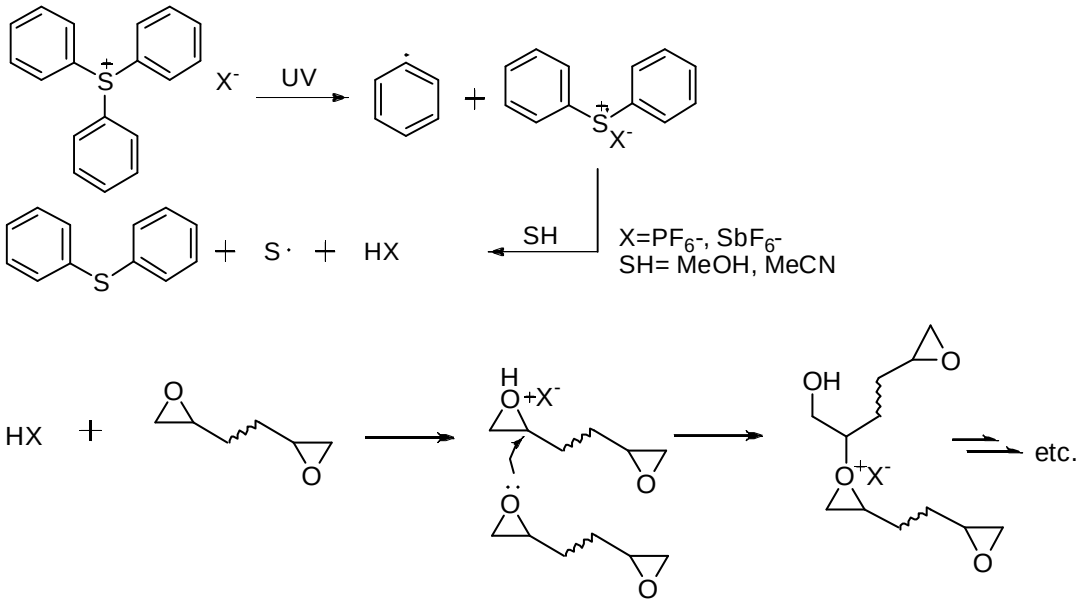

The first monomer was a derivative from bisphenol A. The structure of this monomer is rigid and compact and the resulting coating hard and crispy with a small pore size. The second monomer used was a derivative of poly(ethylene glycol). It was selected for two considerations. First, this monomer has a long chain between the two

epoxide units, so the resulting coating will be soft and elastic with a larger pore size. Second, we hoped that after adding a PEG component, the non-specific binding of protein to the surface could be alleviated. In addition to the cationic monomers, radical monomers like acrylates could also be used in these photo-curable blends to form an interpenetrating network with the addition of a radical photoinitiator. PEG diacrylate was used to form the backbone of the radical polymerization network, while the glycerol diacrylate was used to provide functionality on the secondary alcohol.

The first photo-curable coating was made by mixing 40% PEG diglycidyl ether, 20% bisphenol A diglycidyl ether, 30% glycerol diacrylate benzoate, 10% PEG diacrylate and 3% photo initiator together. The mixture was diluted 10 times by volume in THF and was spin-coated onto the array. The array was then cured under UV irradiation for 15 min. The second coating was a mixture of 80% bisphenol A diepoxide, 20% PEG diepoxide and the photoinitiator following the same treatment of dilution, spin-coating and UV irradiation as the first one. The major component of bisphenyl A diepoxide would generate a tough hydrophobic coating with smaller size pores on the surface. Finally, the third coating was 100% PEG diepoxide with photoinitiator following the same treatment. This coating should be hydrophilic and have larger pore size. The coatings were applied onto three different chips. CV's were then run in a fashion similar to the one illustrated in Figure 4.7. The result is shown in Figure 4.30.

a)

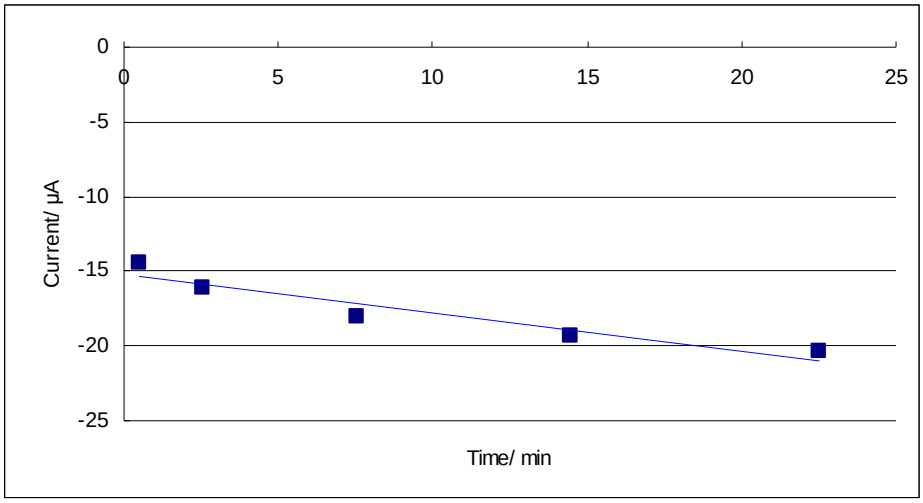
0
0
5
10
15
20
25
-5
-10
-15
-20
-25
Current/ µA
Time/ min

b)

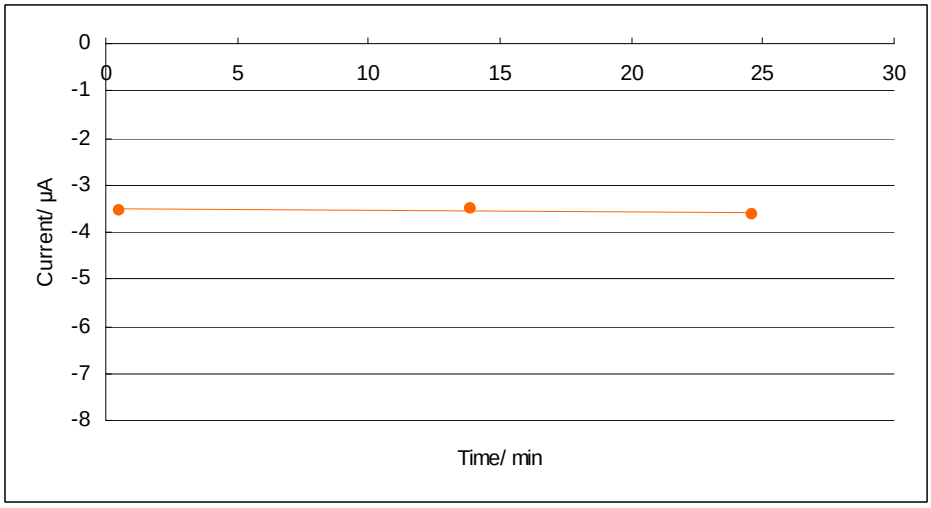
0
0
5
10
15
20
25
30
-1
-2
-3
-4
-5
-6
-7
-8
Current/ µA
Time/ min

c)

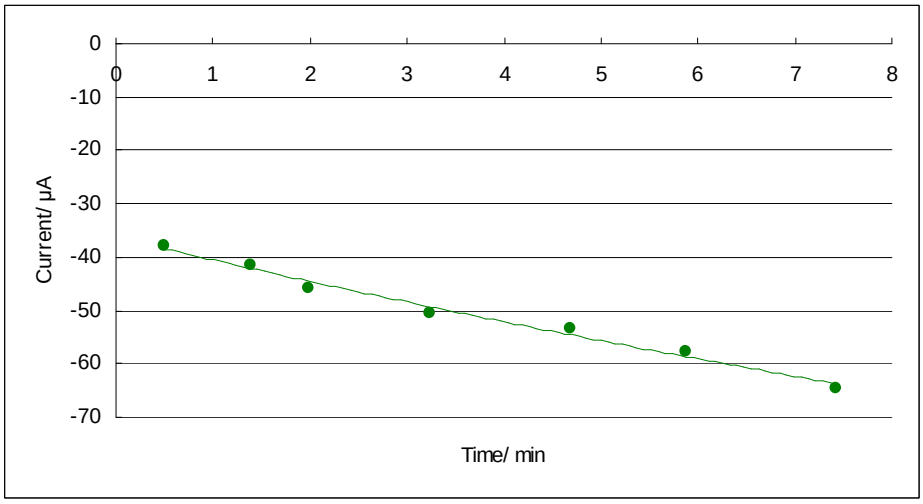
0
0
1
2
3
4
5
6
7
8
-10
-20
-30
-40
-50
-60
-70
Current/ µA
Time/ min

Figure 4.30 The current increase over time on a) the 4 monomer coating, b) the 80% bisphenyl A diepoxide coating and c) the 100% PEG diepoxide coating. Condition: 8 mM $K_3Fe(CN)_6$ /$K_4Fe(CN)_6$ dissolved in 1x PBS solution in water, pH=7.5.

The results of this experiment showed that, the hydrophobic bisphenyl A diepoxide coating was able to acquire a very stable current over a long time, and the hydrophilic PEG diepoxide coating had a rapidly increase current over short time scale. The four monomer coatings with a balanced composition fell in between: the current increased somewhat over time, but the increment was much smaller compared to the PEG diepoxide coating.

Combined with the result of the PCEMA-b-BoSt block copolymer illustrated earlier, it seemed that the coatings with hydrophilic functionalities consistently caused problems with current stability. There might be several possible explanations to this phenomenon. For one possibility, the oxygen atoms on the PEG network and the hydroxyls on the boronic acid could serve as ligands for the metal ions in the solution. In this case, the PEG network could act like a crown ether type ligand and the two hydroxyls on the boronic acid could act as a bi-dentate ligand. However, this is more likely the case for a free metal ion without any ligands. For $K_3Fe(CN)_6$ and $K_4Fe(CN)_6$, since the metals are already fully coordinated with the strong cyanide ligand, the chance of ligand exchange is low. Another possibility is that when the hydrophilic surface is exposed to an aqueous solution, it will get solvated gradually as the incubation time increases, this way, the coating will have more and more water inside the polymer network, and as a result bring more and more metal ions into the network close to the electrode. One may argue that eventually the solvation process

will stop and a stable current should be able to achieved, however, the degree of solvation may vary from electrode to electrode and from solution to solution. Hence, it may not be practical to just wait for the current to stabilize every time it changes. Additionally, we don't know if the storage of ions in the polymer network will have adverse effect on the sensitivity of the signaling experiment or not. One can easily imagine that the ions in the polymer network could serve as a redox couple that adds to the current that arises from the diffusion of ions from the solution above the array to the surface of the electrodes. The result would be a more intense current that masks a subsequent impedance experiment.

To summarize, we can not do signaling experiments without obtaining stable currents. The more hydrophilic the surface, the more this becomes a problem. This is an issue since many of the surfaces that are typically used to reduce non-specific binding events with proteins are hydrophilic.[12] There are two ways to solve this problem. One way is simply to find a hydrophobic surface with minimal non-specific binding. This is not impossible, as fluorinated surfaces have been reported to reduce protein non-specific binding.[13] One problem associated with this approach is that the coating may get too hydrophobic to pass any current and become an insulation layer. To use this method, the porosity of the coating needs to be carefully controlled. A second method for solving the problem would be to change only the outmost layer of the coating to a hydrophilic non-binding layer, and let the major part of the coating still remain hydrophobic. For example, for the PBrSt-b-CEMA block copolymer, we can do PEGylation on top of the coating; for the PCEMA-b-BoSt block copolymer,

we can deprotect the pinacol-protected polymer after it is applied to the surface using electrochemistry to just remove the pinacol protecting group on top of the surface. The draw back of this approach may be low conversion of the surface functionality such as experienced in the PEGylation case, and washing the coating with strong solvent may rearrange the structure of the coating and expose the hydrophobic moiety to the solution again. Regardless, in order for this to work, we need the pinacol protected boronic ester surface to have good electrochemical properties. To verify the possibility of obtaining stable currents on the PCEMA-b-pBoSt surface, the BSA non-specific binding experiment was repeated on an array coated with PCEMA-b-pBoSt polymer. The result was shown in Figure 4.31 and Figure 4.32.

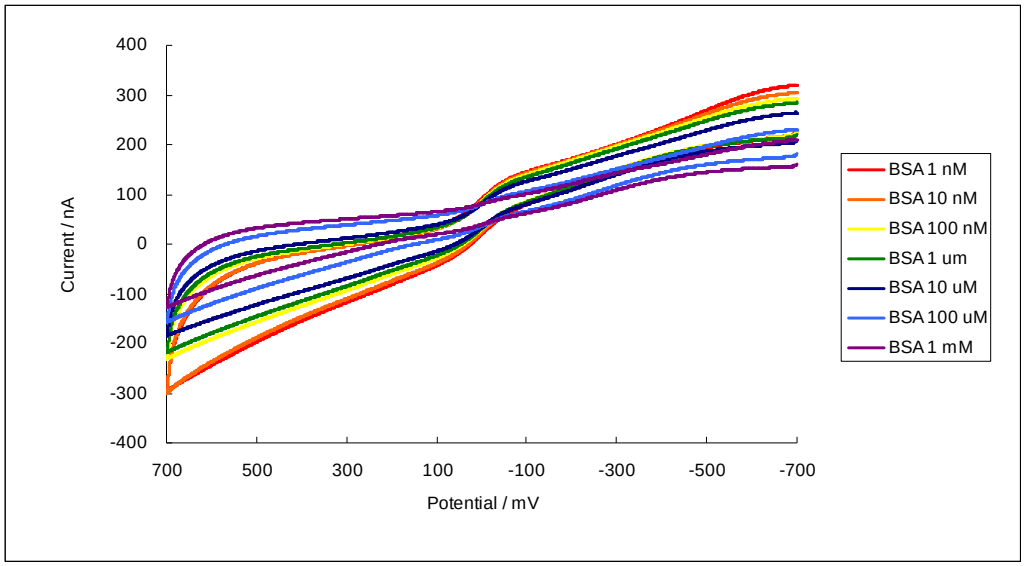

Figure 4.31 BSA non-specific binding to PCEMA-b-pBoSt surface with three different groups of 12 electrodes on the same array. Condition: 8 mM $K_3Fe(CN)_6$ /$K_4Fe(CN)_6$ dissolved in 1x PBS solution in water, pH=7.5. BSA concentration varied from 10^{-9} M to 10^{-3} M. Scan rate = 400 mV/s.

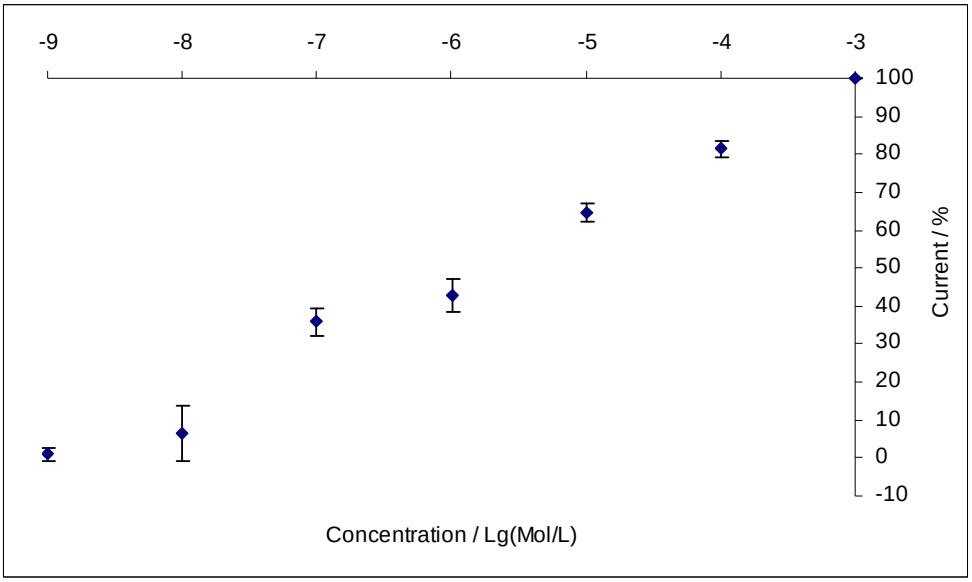

Figure 4.32 Binding curve generated for BSA non-specific binding to PCEMA-b-pBoSt surface. The current was measured at 700 mV.

Although the PCEMA-b-pBoSt showed more severe non-specific binding to the BSA protein, luckily the currents obtained from the cyclic voltammograms were very stable. It does not really matter if the binding of the surface to proteins is extensive at this stage, since the esters would be deprotected and modified with ligands later. Now that the current obtained from the protected surface is stable, the possibility of the above mentioned treatment to reduce non-specific binding to proteins while retaining good electrochemical properties may work. The details of these possibilities will be discussed in Chapter 5.

4.10 Conclusion

The possibility of running electrochemical signaling experiments on microelectrode arrays was explored systematically. Different reaction conditions were studied to find out the effect of variables on electrochemical impedance. The initial

studies on the signaling experiments were based on the wrong instrumental setup, using the platinum cap as the working electrode and the microelectrode array as the counter electrode. This led to identical CVs no matter what set of electrodes were selected using the software for running the arrays. After this problem was fixed, a series of experiments were done to explore the utility of the arrays for observing molecular interactions. An iron concentration experiment revealed that the current intensity of the CV obtained with the correct setup was related to the iron concentration Washing the array coated with PBrSt-b-CEMA surface with DMF increased the ion-permeability of the coating and resulted in a sharp current increase with high iron concentrations. This procedure has the advantage of increasing the sensitivity of the array and the disadvantage of making the overall data less consistent. Non-specific binding experiments with BSA showed that the array was responsive to protein binding by showing current drops as the protein concentration increased. Also, in this experiment it was found out that running array-based reactions could also increase the ion-permeability of the coating. This increased the sensitivity of the experiment and as a result made DMF washing of the array unnecessary. A study of streptavidin-biotin binding on the array was very successful. The arrays proved capable of not only monitoring the event but showed the potential for doing so in a quantitative manner. Repeating the same experiment with an array made using Pd(0) chemistry resulted in a complete loss of signal. It appears that the loss of signal results from Pd(0) contamination of the surface. The detail mechanism of this phenomenon remains undetermined. The result of this experiment suggested that more choices of

reaction strategies for of putting molecules down on the surface of an array are needed. Last but not the least, results from the PCEMA-b-BoSt block copolymer and photo-curable epoxy coating suggested that hydrophilic coatings are more prone to have a slowly increasing current in the signaling experiment than hydrophobic coatings. In order to run signaling experiments within a reasonable time scale, it is better to either use non-binding hydrophobic surfaces or take advantage of a modifiable hydrophobic coating to transform the outer layer of the coating into a non-binding hydrophilic surface.

4.11 Experimental section

General experimental procedures

Materials

All materials were used as purchased from Aldrich without further purification unless otherwise indicated.

Characterization

Fluorescence microscopy, NMR, FT-IR, LC-MS conditions were the same as in chapter 2.

Cyclic voltammetry was carried out on a BAS 100B Electrochemical Analyzer

potential stat, with BAS 100W Version 2.31 control software.

For array-based reactions please see the experimental section of Chapter 2 and Chapter 3.

Sample cyclic voltammetry on 12K array:

A 12K-microelectrode array was cleaned with a 9:1 solution of 3% H_2O_2 and conc. H_2SO_4 for 30 min at 65°C and then coated with the polymer as above. The array was incubated in 200 μL of 8 mM ferrocyanide and 8 mM ferricyanide in 1x PBS solution (made by dissolving 1 Phosphate Buffered Saline tablet ordered from SIGMA® in 200 mL DI water) for 15 min and then placed in the ElectraSense reader. One 12-electrode block was activated and cyclic voltammetry performed by scanning the potential at the electrodes from -700 to 700 mV and then back again at a scan rate of 400 mV/ s. The counter electrode was a platinum plate of area of 0.75 cm^2 held 650-800 μm away from the array by an O-ring. The cyclic voltammetry was repeated as above for the 12-electrode block at various time intervals.

Sample signaling experiment on 12-K array:

The cyclic voltammetry measurement in a signaling experiment is identical as the procedure illustrated above. For making the protein solutions, the protein was first dissolved in a stock solution of 8 mM ferrocyanide and 8 mM ferricyanide in 1x PBS solution to make the highest concentration protein solution (For BSA it was 10^{-3} M

and for streptavidin it was 10^{-5} M). Then 100 μL of the solution was taken and diluted with 0.9 mL stock solution of the iron solution in a 1.5 mL eppendorf tube to make the next highest protein solution. The procedure was repeated with each new solution made to have a series of protein concentration with 1 order of magnitude increment. The stock iron solution was used in all dilutions to keep the iron concentration in each protein solution constant. After all the protein solutions were made, they were kept in an ice bath and were only taken out when needed. The array was then incubated in the solutions made from the lowest concentration to run cyclic voltammetry. If the current was changing over time, usually the CV was not taken until the current finally stabilized, which usually took less than 20 minutes.

Reference and Notes

1. For a review of earlier effort on combinatorial libraries, see: Lam, K. S.; Lebl, M.; Krchňák, V. Chem. Rev. **1997**, *97*, 411.

2. For reviews of current effort on high throughput screening, see: (a) Lazo, J. S.; Brady, L. S.; Dingledine, R. *Mole. Pharmacol.* **2007**, *72*, 1. (b) Seneci, P. *Pharmacochemistry Library* **2002**, *32*, 147.

3. For reviews on microarrays, see: (a) Wu, H.; Ge, J.; Uttamchandani, M.;Yao, S. Q. *Chem. Commun.* **2011**, *47*, 5664. (b) Yarmush, M. L.; King, K. R. *Annu. Rev. Biomed. Eng.* **2009**, *11*, 235. (c) Liu, R.; Lam, K. S. *Wiley Encyclopedia of Chemical Biology* **2009**, *3*, 575. (d) Uttamchandani, M.;Yao, S. Q. *Curr. Pharm. Des.* **2008**, *14*, 2428. (e) Taipa, M. A. *Comb. Chem. High. T. Scr.* **2008**, *11*, 325. (f) Winssinger, N.; Pianowski, Z.; Debaene, F. *Top. Curr. Chem.* **2007**, *278*, 311.

4. For a review of the work done on microelectrode arrays, see: Yoshida, J.; Nagaki, A. *Angew. Chem. Int. Edit.* **2010**, *49*, 3720.

5. (a) Wojciechowski, J.; Danley, D.; Cooper, J.; Yazvenko, N.; Taitt, C. R. *Sensors* **2010**, *10*, 3351. (b) Dill, K.; Montgomery, D. D.; Ghindilis, A. L.; Schwarzkopf, K. R.; Ragsdale, S. R.; Oleinikov, A. V. *Biosens. Bioelectron.* **2004**, *20*, 736.

6. Murata, M.; Gonda, H.; Yano, K.; Kuroki, S.; Suzutani, T.; Katayama, Y. *Bioorg. Med. Chem. Lett.* **2004**, *14*, 137.

7. Tesfu, E.; Roth, K.; Maurer, K.; Moeller, K. D. *Org. Lett.* **2006**, *8*, 709.

8. Stuart, M.; Maurer, K.; Moeller, K. D. *Bioconjugate Chem.* **2008**, *19*, 1514.

9. Maurer, K.; McShea, A.; Strathmann, M.; Dill, K. *J. Comb. Chem.* **2005**, *7*, 637.

10. Bartels, J.; Lu, P.; Maurer, K.; Walker, A. V.; Moeller, K. D. *Langmuir* **2011**, *27*, 11199.

11. Green, N. M. *Adv. Protein Chem.* **1975**, 29, 85.

12. For a review on using PEG(PEO) and PC to reduce non-specific binding, see: Chen, H.; Yuan, L.; Song, W.; Wu, Z.; Li, D. *Prog. Polym. Sci.* **2008**, *33*, 1059.

13. Chen, H.; Sung, W.; Liang, S.; Chen, S. *Anal. Chem.* **2010**, *82*, 7804.

Chapter 5

Future Directions for Coating Development and Surface Modification on Microelectrode Arrays

5.1 Summarization of previous experiences

As discussed in Chapter 4, the fact that we are measuring impedance in our signaling experiments prevents us from using BSA to knock down the non-specific binding of a target protein to the surface of the array. As a result, we have to minimize the non-specific binding properties of the surface in order to maximize signal-to-noise in the experiments. When studying strong binding interactions, the problem is relatively easy because non-specific binding usually only happens at high protein concentration. However, if we want to study weak binding interactions, then non-specific binding can be large enough to interfere with the measurement. We need a surface with minimal non-specific binding to the target protein being studied. This inertness of the surface to protein binding must be balances with the need for the surface to have stable electrochemical properties. Key to this issue is the compatibility of the surface with impedance experiments that require stable currents when running multiple cyclic voltammograms. If the current does not stabilize or needs an extremely long time to stabilize, it becomes either impossible or impractical to obtain meaningful data from the desired analytical experiments. These two requirements serve as the key guidelines for the future development of microelectrode array coatings.

In the conclusion of Chapter 3 and Chapter 4, we stated that through our observation, hydrophilic surfaces are more prone to lead to unstable currents in an impedance experiment than hydrophobic surfaces. However, many of the non-binding surfaces typically employed are hydrophilic.[1,2] As these two factors compete with each other, the solution to our problem becomes more complex. As proposed at the end of Chapter 4, there are at least two possible ways to solve the problem. The first is to find hydrophobic yet non-binding surfaces. This is potentially difficult due to the contradictory nature of the plan. The second is to use a modifiable hydrophobic coating. After the coating is applied, the outmost layer of the polymer can then be transformed into a non-binding hydrophilic film of sorts that reduces non-specific binding. The majority of the polymer network would still remain hydrophobic and hopefully would not solvate extensively in aqueous solutions and preserve the stability of an electrochemical current. In this chapter, these two possibilities will be discussed.

5.2 Possibility of a hydrophobic and non-binding coating

While most of the coatings with minimal protein binding are hydrophilic polymers, some fluorinated surfaces are very hydrophobic and are resistant to non-specific binding with many proteins as well.[3-5] For example, Kramer and coworkers reported a block copolymer of polystyrene and poly(ethylene oxide) with doped perfluorinated side chain to have antifouling properties.[3] The fluorinated side chains reduce protein binding to the surface. In another study, Chen and coworkers

reported using a functional fluorinated surface to immobilize G-proteins on a substrate microarray. The arrays were then used to detect antibodies.[4] The surface utilized the acrylic acid terminals for attachment of the G-protein and the fluorinated terminals to repel non-specific binding of the antibodies to the surface. The coating was also reported to have long-term stability and better sensitivity relative to PEG-based coatings. These findings suggest that fluorinated surfaces maybe a promising target as the coatings for microelectrode arrays. However, before the idea of fluorinated surface is fully embraced, there are some concerns that will need to be addressed. First, while the fluorinated surfaces are hydrophobic and desirable with respect to non-specific binding, they may end up being so hydrophobic that they prove impermeable to ions. This would interfere with the passage of current in the impedance experiment.[6] For example, some perfluorinated surfaces are called super-hydrophobic surfaces for their extremely hydrophobic nature. If the coating on an array was so hydrophobic that is was not wettable at all, then no ions in the solution above the coating would be able to pass through the polymer and reach the electrode. The result would be no current and hence no impedance experiment. Second, due to the non-sticking nature of fluorinated surface, it might become hard to attach the coating to the array. Third, fluorinated surfaces are not able to repel all proteins. For proteins with non-specific binding via hydrophobic interactions, the fluorinated surface may actually increase the level of non-specific binding.[7] Last but not the least, fluorinated compounds are potential carcinogens as well. They do not present acute toxicity, but their extremely long half life still presents long term health

concerns.[8]

To resolve the first problem, a copolymer of fluorinated monomer with other non-fluorinated monomers may be needed to reduce the hydrophobicity to an acceptable degree. For example, based on the previous block copolymer design, a styrene monomer with pentafluorinated benzene ring could be used to copolymerize with the 4-bromostyrene to make the polymer illustrated in Figure 5.1.

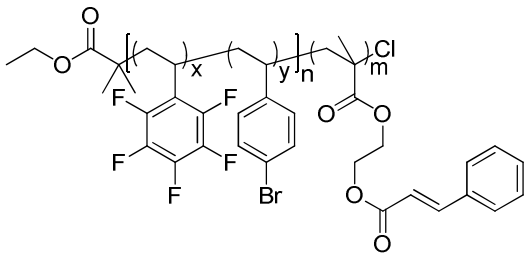

Figure 5.1 Incorporating fluorinated functionality into the block copolymer structure

In this way, the fluorinated groups will be doped into the block of the polymer used to functionalize the surface. Of course, there are many other ways to incorporate the fluoride into the polymer structure. All are fine if they can achieve the goal of reducing non-specific binding while retaining enough porosity and hydrophilicity so that they do not serve as an insulator for the electrode below. One can also think about matching such a surface with a modified redox couple. For example, the ligands on a copper complex can potentially be fluorinated so that they improve the solubility of the complex in a fluorinated polymer that is being used to coat the array. Of course the nature of such a ligand would need to be tuned so that an appropriate balance between the solubility of the complex in the polymer and a stable current is obtained.

To respond to the second concern, whatever polymer is used will need to retain blocks that allow it stick to the surface of the array. Since the fluorinated monomers will only be a small part of the overall polymer, this may not be a large problem. However, if it is, then the "stickiness" of the polymer can be increased by modifying the methacrylate block of the polymer. Monomers such as acrylic acid and acrylonitrile are known to lead to polymers that adhere to surfaces tightly (Figure 5.2).[9] These monomers can be incorporated into the polymer structure by copolymerization with the methacrylate block.

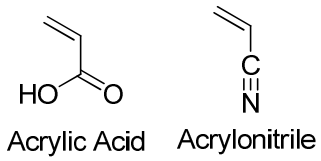

Figure 5.2 Monomers that promote adhesion.

With regard to the third problem (non-generality of the solution), any polymer used will need to be tested for its compatibility with a protein targeted for study. It is expected that no one surface will be compatible with every protein studied. For this reason, our approach to building the surfaces must be as flexible as possible. This gives rise to the idea of making coatings that have tunable surfaces (see below).

As for health concerns associated with the fluorinated surfaces, this is a matter of awareness as much as anything else. The lab has the proper safety equipment necessary to handle the materials, but we must make sure that group protocols carefully specify their proper use.

5.3 Post-synthetic modification of microelectrode array coatings

As an alternative, potentially more flexible approach to the methods discussed in Section 5.2, we can also coat the surface of an array with a polymer known to have stable electrochemical properties and then tune its surface to try and reduce non-specific binding events. In this manner, it may be possible to minimize non-specific binding while maintaining the overall electrochemical properties of the surface.

For example, we can modify the PBrSt-b-CEMA block copolymer coating electrochemically with a substrate that repels protein binding, like PEG.

Scheme 5.1

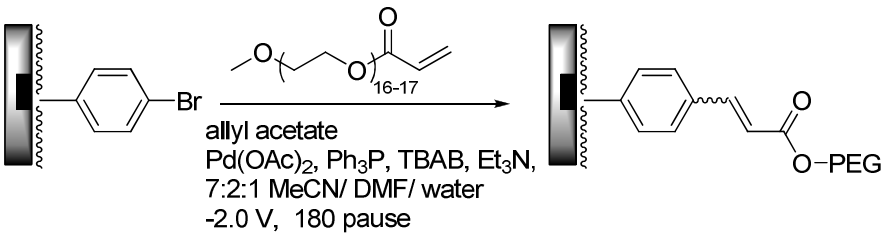

However, from our previous experience, modification with short chain PEG was ineffective in reducing protein binding to a satisfactory degree. Regardless, other potential substrates can also be used, like the fluorinated substrates discussed earlier (Scheme 5.2), longer PEG groups,[1] and groups that add a charge to the surface of the array.[2] For this last suggestion, it is important to remember that the electrodes on the array are insulated from groups tied to the surface of the polymer. Hence, the charged groups will not interact directly with the electrodes.

Scheme 5.2

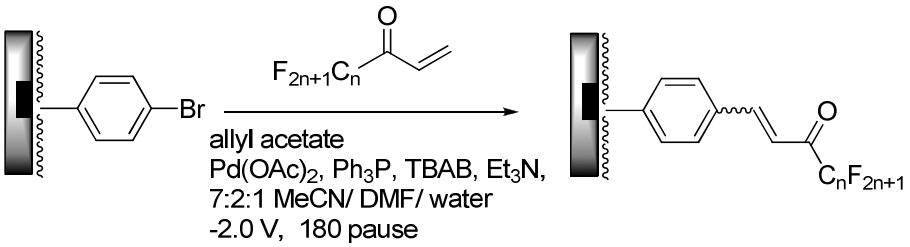

For the PCEMA-b-BoSt polymer coating discussed in Chapter 3, the deprotected polymer was not compatible with the acquisition of stable currents on the array. To take advantage of this polymer, the pinacol-protected copolymer can be applied to the array, and then the deprotection of selected boronic acid groups accomplished as needed. Since the deprotection of the boronic acid uses aqueous acid, the transformation can be conducted in a site-selective fashion on an array[10] as illustrated in Scheme 5.3 (preliminary results with Mr. Matt Graaf).

Scheme 5.3

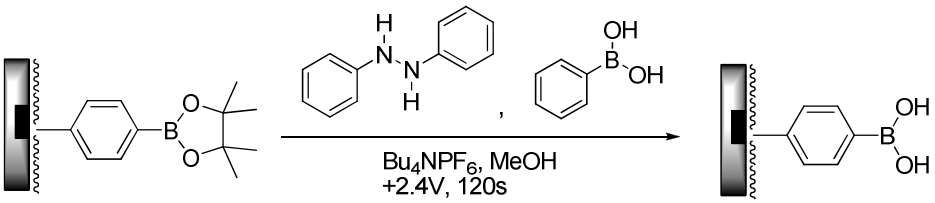

Once deprotected, site-selective Suzuki reactions can be with the boronic acid groups (the protected surface is inert to the Suzuki conditions) or the electrodes modified with solution-phase substrates by incubation.[11] Signaling studies would then involve mainly the protected surface – a surface that was known to have excellent electrochemical properties as demonstrated at the end of Chapter 4 (Scheme 5.4).

Scheme 5.4

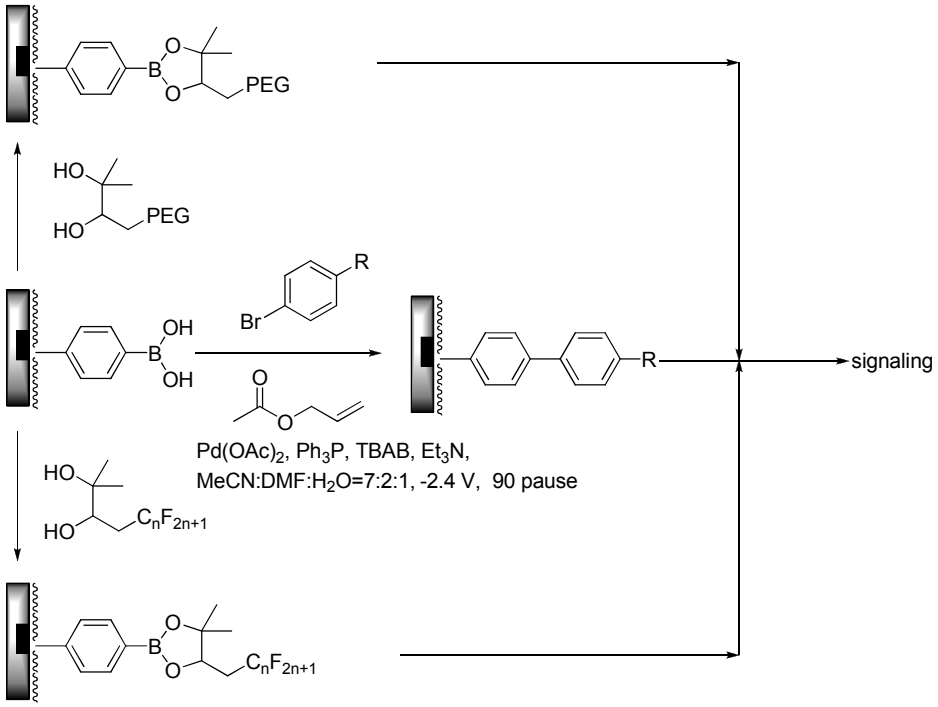

The advantage of this approach is that we can take advantage of the coatings we have already developed. Of course, there are drawbacks with this approach compared with the other method discussed in Section 5.2. First, we may encounter low conversion of the surface functionality or low covering density, just like we saw when the PEGylation of PBrSt-b-CEMA was attempted. Second, the morphology of the polymer surface may change extensively after washing with a solvent. This could alter the nature of the modified polymer surface so that the new groups added to repel a protein are no longer on the surface and unmodified sections of the polymer exposed to the reaction solution. Such an event might render the modification effort ineffective. If this phenomenon does happen, it will raise questions as to whether a block copolymer strategy is the best platform for building coating for the microelectrode

arrays.

5.4 Strategies that do not use a block copolymer

As an alternative to the use of a di-block copolymer for coating the array, either a multiple-block copolymer or a random copolymer might prove useful (Figure 5.3). With the different monomers more evenly distributed in the bulk polymer, the polymer network created will have more uniform properties (like hydrophilicity for example). This will make the coating less likely to change its morphology after exposure to a solvent. In addition, the coating may show better consistency across the array in terms of the currents obtained from cyclic voltammetry.

Of course, there may also be drawbacks associated with these types of polymers. As the UV-cross-linkable repeating unit is more evenly distributed across the polymer network, the pores generated in these types of coatings can be much smaller than those generated in a di-block copolymer. This can result in greatly reduced electrochemical currents. For this reason, the degree of cross-linking will need to be carefully controlled in order to retain good porosity of the surface. Second, since more of the bromostyrene units are hidden within the cross-linking network, the number of available sites on the surface of the polymer for functionalization may be far fewer than that encountered with the di-block copolymer coatings. Finally, the possibility of making these polymer structures depends on the polymerization kinetics of the monomer used. If the monomers initially selected for building the polymers are not compatible with the syntheses, then their structures will be altered.

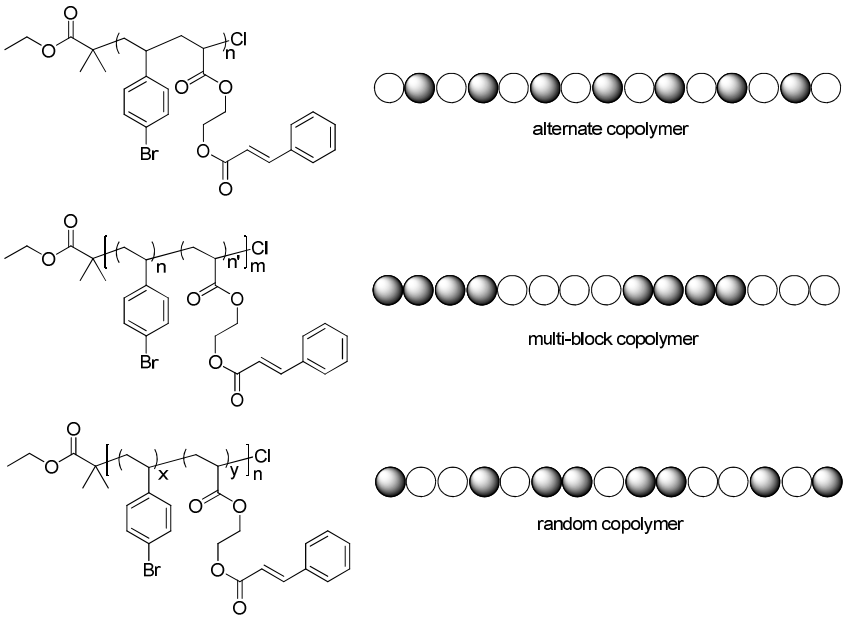

Figure 5.3 Other possible polymer structures for coatings of microelectrode arrays

Reference and Notes

1. For examples using PEG to reduce protein non-specific binding, see: (a) Tugulu, S.; Klok, H. *Macromol. Symp.* **2009,** *279,* 103. (b) Michel, R.; Pasche, S.; Textor, M.; Castner, D. G. *Langmuir* **2005**, *21*, 12327.

2. For example using phosphorylcholine to reduce protein non-specific binding, see: Katsuyuki, M.; Aya, H.; Kenichi, S.; Kazuyuki, M. *J. Chromatogr. Sci.* **2011,** *49,* 148.

3. Dimitriou, M. D.; Zhou, Z. K.; Yoo, H.; Killops, K. L.; Finlay, J. A.; Cone, G.; Sundaram, H.; Lynd, N. A.; Barteau, K. P.; Campos, L. M.; Fischer, D. A.; Callow, M. E.; Callow, J. A.; Ober, C. K.; Hawker, C. J.; Kramer, E. J. *Langmuir* **2011**, ASAP.

4. Chen, H.; Sung, W.; Liang, S.; Chen, S. *Anal. Chem.* **2010**, *82*, 7804.

5. Haddad, L. C.; Swenson, B. C.; Bothof, C. A.; Raghavachari, M. U.S. (**2005**), US 0142563.

6. Cunha, A. G.; Freire, C. S. R.; Silvestre, A. J. D.; Neto, C. P.; Gandini, A.; Orblin, E.; Fardim, P. *Biomacromolecules* **2007**, *8*, 1347.

7. For examples of fluorinated surface increasing protein binding, see: (a) Kiaei, D.; Hoffman, A. S.; Horbett, T. A. *Radiat. Phys. Chem.* **1995**, 46, 191. (b) Valdes, T. I.; Ciridon, W.; Ratner, B. D.; Bryers, J. D. *Biomaterials* **2008**, 29, 1356.

8. Kleszczynski, K.; Gardzielewski, P.; Mulkiewicz, E.; Stepnowski, P.; Skladanowski, A. C. *Toxicol. In Vitro* **2007,** *21,* 1206.

9. Ward, P. M. G.B. (**1972**), GB 1176204.

10. For site-selective generation of acid, see: Kesselring, D.; Maurer, K.; Moeller, K. D. *Org. Lett.* **2008**, 10, 2501

11. Roy, D.; Cambre, J. N.; Sumerlin, B. S. *Chem. Commun.* **2008**, 2479.

Appendix A

Operation Manual for 1-K Arrays and Instruments

A.1 1-K array preparation before running a reaction

The new unused 1-K array has the metal wiring exposed, which is very fragile and can be easily damaged. The first thing to do with a 1-K array is to coat the wiring area with a heat-curable epoxy coating. The liquid form of epoxy is spread across the wiring area and the coated array is carefully placed into an oven with 200 ^{0}C to bake overnight. The array is then taken out to cool down to room temperature and is ready to use.

a) b)

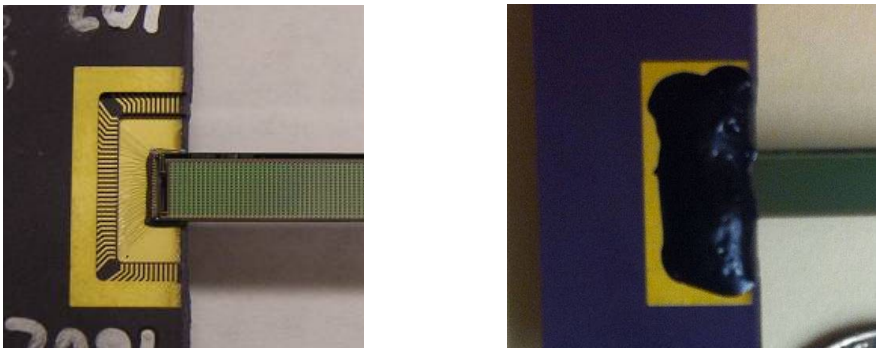

Figure A.1 1-K array (a) before and (b) after coating with epoxy

A.2 Connection of the circuit and the instrument

The way to connect the equipment depends on whether an oxidation or a reduction is run on the array. First of all, there are 12 pins (3 x 4) next to the socket to insert the 1-K array, which are used to connect with an ampere meter and the counter

electrode (Figure A.2). The four rows stand for number 0, 1, 2, 3 from top to bottom in the map editing of 1-K array. For one particular reaction, only one row of pins is used. If one certain row is used, for example, the second row is used, then in the excel file of the map, the grids in the table marked as 1 represent the electrodes turned on, and the grids marked as other numbers (either 0, 2 or 3) are electrodes turned off. If the first row is used, then the electrodes marked with 0 will be turned on and all other numbers are turned off. Different users can edit the map to make their own patterns. Each grid in the excel table corresponds to each electrode on the array and there are a total of 1,024 grids/electrodes.

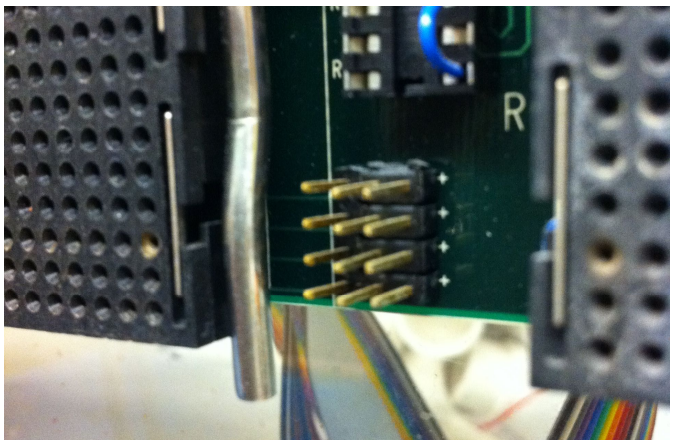

Figure A.2 The 12 pins on the 1-K instrument

To connect the pins for a reduction reaction, the rightmost pin is connected with the counter electrode and the two pins on the left are connected to the ampere meter (Figure A.3a); to do an oxidation reaction, the leftmost pin is connected with the counter electrode and the other two pins are connected to the ampere meter (Figure A.3b). If no ampere meter is available, the two pins can be simply covered

with a “bridge” which simply short-circuits the two pins. After the circuits are connected, the coated 1-K array (follow the spin-coating instruction in each chapter’s experimental section) could be inserted into the socket and the microelectrodes on the array as well as the counter electrode can be inserted into the reaction solution, as illustrated in Figure 1.6 in Chapter 1. One thing needs to be mentioned is that when inserting the 1-K array into the socket, the third row of pins from the bottom on the back of the chip needs to be bent downward so that the array is easier to be inserted.

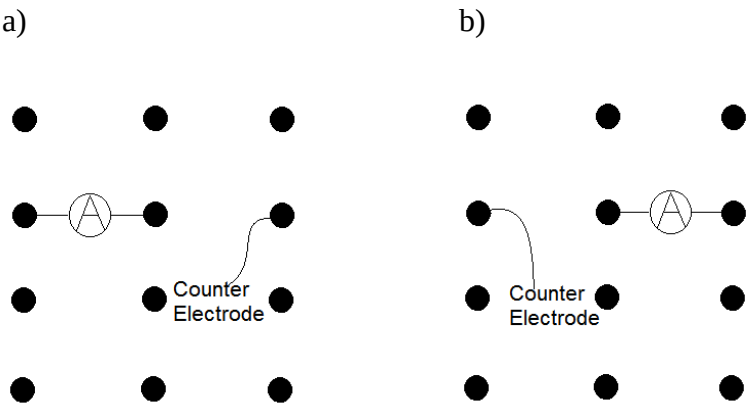

Figure A.3 Pin connections for a) reduction and b) oxidation reactions.

A.3 Software control of the 1-K array

When the experimental setup is in place, the reaction can be initiated with the computer program. To begin with, open the software “Chemprog V1.36” on the desktop. When the window appears, open the “Functions” menu and select “Chip Control Functions” and a new window will appear. If this is the first time to run the program since a reboot, one needs to go to the “Functions” menu in this window and click on “Set Num of Mirrored Chambers” and set the value to be 0. If the window is

already opened, this step can be skipped. Whenever restarting the program, this step needs to be done again; otherwise the program won't run correctly. After that, click "Test Chip" in the "Functions" menu. A small window will appear, and click "Test" to test how many electrodes are good to operate on the array inserted into the socket. Usually, one or two electrodes may fail. In more severe cases, parts of the array like a row or a block or even half of the array may not work. The computer program will deem the test fail when the pass rate is less than 99%. However, for our purpose, it does not really matter as long as there are good electrodes that are usable. For example, for an array with half of its electrodes not working, one can still run a reaction with a checkerboard pattern on it and see if the reaction worked.

Once these previous testing and setting up steps are done, click "Add or Change Layers" in the "Functions" menu to run a particular experiment. In the newly appeared window, click "Insert", and a new window which allows the user to input the voltage, number of cycles, time on and time off (in seconds) will appear. Input all information as desired, and click the "Find File" button on the lower left to load a map. After choosing the desired map, click "Save File" to exit the window and "Done" to go back to the "Chip Control Functions" window. Finally, click "Start Running Sequence" to initiate a reaction. At this point, the pattern in this window will change to show the map loaded. The red color represents electrodes that are not working, while other colors represent the numbers chosen for each electrode according to the map. The ampere meter could be turned on at this point to the μA level to monitor the reaction. The intensity of the current depends on how many

electrodes are turned on and what exact reaction is being run. Generally as a rule of thumb, running a reaction with a whole board pattern has the maximum current intensity around 300-600 μA and with a checkerboard pattern around 200-300 μA.

A.4 After-reaction cleanup

After the reaction is finished, the eppendorf tube containing the reaction mixture is lowered to reveal the array, and the array can be taken off the socket to be cleaned off the residues of the reaction mixture. Depending on the experiment run, the array can be washed with a solvent from ethanol to dichloromethane. The counter electrode also needs to be washed between each reaction to prevent contamination. After all the characterization is done, the chip can be cleaned and reused. For general cleaning, the chip is incubated in concentrated nitric acid for 30 seconds and washed with water. After that, it can be incubated in DMF overnight and cleaned with a Q-tip to remove any coating residue. The array is finally washed with DI water and acetone and is ready to be reused.

Appendix B

Operation Manual for 12-K Arrays and Instruments

B.1 12-K array preparation before running a reaction

Since the basic experimental setup, instrumental connection as well as experimental procedures have been discussed in detail in Chapter 1 and in the experimental sections of each chapter, in this appendix only the software program for controlling 12-K reactions and signaling experiments will be discussed.

To prepare a 12-K array for any experiment, the array needs to be cleaned first. All the "new" arrays from CombiMatrix are actually used array which failed their commercial quality control, thus almost all of them have sucrose coating on them. Before any experiment can be run on the array, the sucrose residue needs to be cleaned so that a new coating, either agarose or a synthesized coating can be applied onto the array surface.

The 12-K array has different cleaning method from the 1-K array. Since the array is immobilized onto a slide and the electronic circuits lay right next to the microelectrodes, a cleaning instrument made specifically for 12-K arrays is used to clean the arrays while protecting the circuits (Figure B.1). Eight slides of 12-K arrays are inserted into the sockets with the electrodes side facing out and the spring-loaded switches in the back are pulled up to have the arrays in tight contact with the chambers in the front. Then, Nano-strip^{TM} (Cyantek Corp., Fremont, CA), a non-explosive form of piranha solution (mixture of conc. H_2SO_4 and H_2O_2), is

injected into the incubation chambers with a screw-head syringe to dissolve the coating residues on the arrays. The arrays are then incubated in this mixture for 20 minutes and the mixture is then pulled out by the same syringe. After that, the arrays are washed with DI water for 3 times using the syringe to remove the corrosive Nano-strip solution. Then the arrays are taken out and rinsed with acetone and should be ready to use. The array can be washed many times until it is no longer usable (too many dead electrodes) eventually. The old type 12-K array lasts shorter than the new type 12-K array, which is made of higher quality materials.

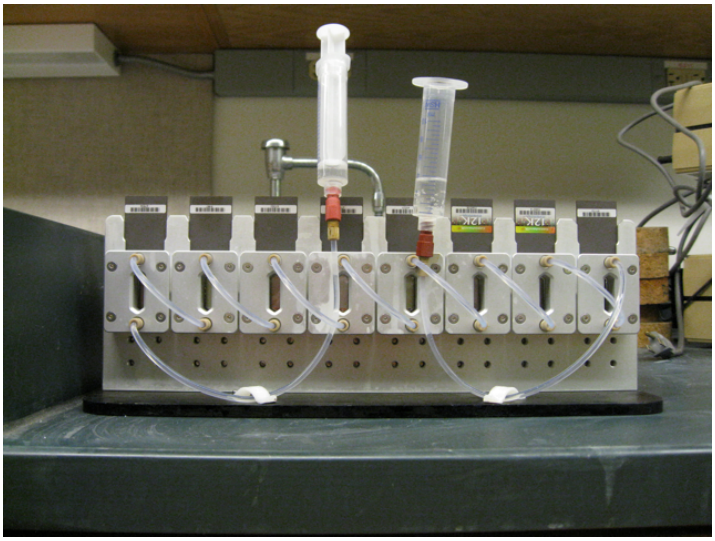

Figure B.1 Instrument for 12-K array cleaning

B.2 Software control for 12-K array-based reactions

Although the experimental setup for the 12-K array reactions are more complicated than 1-K, the software used for 12-K is actually easier to use. Of course, before using the software, the user needs to prepare for the experiment by spin-coating the array, making the reaction solution, making the array-socket complex

and inserting it to the instrument. The terminals also need to be connected properly depending on the reaction done on the array. Since these steps are all explained in Chapter 1, no addition comments shall be given here. Once the instrument setup is ready, the user will need to open the 12-K array program on the computer, **ElectraSense-Instrumental W 71-5.7.0**. Once the window is open, click on “Initiate” to turn the instrument into working mode. Then, the user will need to load the reaction protocol file which is in text file form. The protocol files are located in the reaction protocol file folder in C drive. Since most reactions use similar protocols, people tend to modify one particular file each time they do a new experiment instead of creating a new file for each new experiment. As a result, most people choose the file “VB12 coupling” to modify their reaction protocol, but anyone can make their own protocol files. Taking the VB12 coupling protocol file as an example, when opening the text file, the following input will show up in the text window:

```
MainBlock Begin
        InitChipSystem (5, 1)
        testchipmap (4, 5)
        groundv1 ()
        # setgridvoltage (1.5)
        SetOffChipElectrodeVoltage (1.7)
        applyexactmapfromfile(C:\Maps\Small Checker 1)
        pause (90)
        GroundGrid ()
        SetOffChipElectrodeVoltage (0)
MainBlock End
```

While these commands look complicated, only three of them need to be changed to accommodate a specific reaction. The first parameter to be changed is the "SetOffChipElectrodeVoltage" in the sixth row. The number in the parentheses represents the voltage applied between the array and the counter electrode in the unit of volts. Since whether reduction or oxidation is running on the array is controlled by the connection of the terminals, only positive number is input here. The second parameter is the "applyexactmapfromfile" command, which allows the user to change the map applied onto the array. The user needs to copy the file path into the parentheses, which needs to be exactly correct from the root directory, otherwise the program will not recognize it. One thing to mention here is that the users can also make their own maps by editing a map file in Excel. When the map file is opened in Excel, it will show a table of numbers corresponding to each individual electrode on the array. The electrode marked with 4 are turned off and marked with 2 are turned on. The user only needs to change the numbers to make the desired pattern. Once the editing is done, the file should be still saved as a text file to be recognizable by the protocol file. After the desired map is in place, the third parameter to be changed is the reaction time. To do so, change the number in the parentheses next to the "pause" command. The total reaction time equals to the number input in seconds. After all the editing is done, save the text file and exit the window (can be left open for further editing if more than one reaction needs to be done). At this stage, click "Change Protocol File" in the ElectraSense window, and load the protocol file just edited. After

that, click “Run” to initiate the reaction.

After the reaction is finished, open the instrument and take the array-socket complex out. Drain the reaction solution with a pipette first and disassemble the array from the socket. Wash the array with any solvent of desire and let dry before rendering to any characterization instrument.

B.3 Software control for cyclic voltammetry

To run a cyclic voltammetry experiment on the 12-K array, two computers are needed to control the 12-K instrument as well as the external potential stat. For the 12-K instrument, the controlling is pretty much the same except a few minor differences. The first difference is the terminal connections discussed in Chapter 1, as external potential stat is used to provide potential difference between the working electrode and the counter/reference electrode. Secondly, the protocol used for cyclic voltammetry is also a little different from the reaction protocol. The cyclic voltammetry protocol is in the file “cvtest”. When this file is open in a text file, the following commands are shown in the window:

```
MainBlock Begin
    InitChipSystem (5, 1)
    testchipmap (4, 5)
    groundv1 ()
    applyexactmapfromfile(C:\Maps\Small Checker 1)
    pause (90)
    GroundGrid ()
```

MainBlock End

In this protocol, the commands that set the potential difference in a reaction protocol have been removed. Only the map file and the reaction time need to be changed. Interestingly, it seems that once this protocol is initiated in the program, one can run cyclic voltammetry as many times as they want as long as the 12-K instrument is not opened, even if the reaction time is finished. So the reaction time in this CV protocol is actually not important, the user can make it as short as 10 seconds, which will not make any difference from setting it to be 10 minutes. The map file used should match the map file used in the reaction protocol, so that the CV is run on desired electrodes.

For the program to control the BAS potential stat, open the program BAS 100W on the computer which is used to run CVs. For a first time run after a reboot, open the “Control” menu and click “Self Test Hardware” to test the potential stat. If everything works well, open the “Method” menu and click “Select Mode”. Here a new window will open to let the user choose the desired electrochemical methods. To run cyclic voltammetry, click “1. Sweeping Techniques” and choose “CV = Cyclic Voltammetry”. Once the method is selected, click “General Parameter” also in the “Method” menu to input the CV parameters. There are seven parameters can be changed. The “Initial E” parameter stands for the initial potential the scan begins with. The “High E” and “Low E” parameters stand for the highest and lowest potential of the scan. The “Scan Rate” let the user to choose the scan rate in mV/s. The “Initial Direction” determines whether the scan begins with positive direction (oxidation) or

negative direction (reduction). The “Number of Segments” let the user to decide how many cycles of CV to be run. One segment is only half the cycle, so always use at least two segments. Finally, the “Sensitivity” parameter allows the user to choose the current intensity window of the scan. If the sensitivity is too high, the current may exceed the measurable limits; if the sensitivity is too low, then the curve obtained will be very bumpy, less smooth, and may lose a lot of details. How to adjust the sensitivity is a try-and-error procedure which may need a couple of tries. Some example parameters used for signaling experiments with a pattern of 12 electrodes on the 12-K array with 8 mM $K_3Fe(CN)_6/K_4Fe(CN)_6$ as the solution are listed below:

Initial E: -700 mV
High E: 700 mV
Low E: -700 mV
Scan Rate: 400 mV /s
Initial direction: positive
Number of Segments: 2
Sensitivity: 100 nA

The user can change these parameters to his/her best judgment, as there is no uniform parameter for different kinds of experiments. Once the parameters are set, open the “Control” menu and click “Start Run”, or simply click “F2” on the keyboard to initiate a scan.

Once the scan is complete, open the “File” menu and click “Save Data” to save the cyclic voltammogram. Also in this menu the user can load previously

obtained data using the “Load Data” command. To observe an overlapped diagram of several CVs, open the “Graph” menu and click “Multi-Graph” to choose the files to be overlapped.

After all the desired data are obtained, open the “File” menu and use the “Convert Files” command to convert the bin file format of the CV files into text files. The files can then be opened with Excel or Origin to plot the CV diagrams. When imported into Excel, remember to choose “dividing the data by comma”, as this will help divide the potential data and the current intensity data into different columns.